

**SOIL STRUCTURE INTERACTION ANALYSIS OF
LATERALLY LOADED PILES IN SHIP BERTHING STRUCTURES**

Thesis Submitted to
Cochin University of Science and Technology
In fulfillment of the requirements for the award of the degree of
Doctor of Philosophy

By

KAVITHA P. E.
Register No 3487 (2008 Admission)

Under the supervision of

Dr. K. P. NARAYANAN
Associate Professor (Retd.)
Department of Ship Technology
Cochin University of Science and Technology
Kochi-682022, Kerala, India

and

Dr. K. S. BEENA
Professor of Civil Engineering
School of Engineering
Cochin University of Science and Technology
Kochi-682022, Kerala, India



DEPARTMENT OF SHIP TECHNOLOGY
COCHIN UNIVERSITY OF SCIENCE AND TECHNOLOGY
KOCHI-682022, KERALA, INDIA

August 2016

Dedicated to my teachers, colleagues, friends and family

Certificate

This is to certify that the thesis entitled “**Soil Structure Interaction Analysis of Laterally Loaded Piles in Ship Berthing Structures**” submitted by Kavitha P. E. to the Cochin University of Science of Technology, Kochi for the award of Doctor of Philosophy is a bonafide record of research work carried out by her under our joint supervision and guidance. The contents of this thesis, in full or in parts have not been submitted to any other institute or University for the award of any degree or diploma.

Kochi – 22
31-08-2016

Dr. K. P. Narayanan
(Research Guide)
Associate Professor (Retd.)
Department of Ship Technology
Cochin University of Science and Technology
Kochi-682022, Kerala, India

Dr. K. S. Beena
(Co-Guide)
Professor of Civil Engineering
School of Engineering
Cochin University of Science and Technology
Kochi-682022, Kerala, India

Declaration

I, hereby declare that the thesis entitled “**Soil Structure Interaction Analysis of Laterally Loaded Piles in Ship Berthing Structures**” is based on the original work done by me under the supervision of Dr. K.P. Narayanan, Associate Professor (Retd.), Department of Ship Technology, Cochin University of Science and Technology, Kochi and Dr. K. S. Beena, Professor of Civil Engineering, School of engineering, Cochin University of Science and Technology, Kochi. No part of this thesis has been presented for any degree from any other university or institutions.

Kochi-22

Date: 31/08/2016

Kavitha P. E.

Acknowledgement

I take the opportunity to express my heartfelt gratitude to my research guide, **Dr. K.P. Narayanan**, Associate Professor (Retd.), Department of Ship Technology, Cochin University of Science and Technology for his unreserved guidance, constructive suggestions and inspiration in nurturing this research work.

I am thankful to my research co-guide, **Dr. K. S. Beena**, Professor of Civil Engineering, Cochin University of Science and Technology for her invaluable guidance, continuous support and encouragement during the entire course of my research work.

I am grateful to the doctoral committee member, **Dr. C.G. Nandakumar**, Head of the Department, Department of Ship Technology, Cochin University of Science and Technology for providing me invaluable suggestions during the study.

I am deeply obliged to **Prof. (Dr.) G. R. Dodagaudar**, Professor, IIT (Madras) for his valuable suggestions in the formulation of the present work. I would like to express my sincere gratitude to **Dr. Job Thomas**, Assistant Professor, Division of Civil Engineering, SOE, CUSAT for his cooperation and guidance in conducting the experimental works.

I would like to express my gratitude to **Prof. S. Usha**, Professor and head, Department of Civil Engineering, SNGCE, Kadayiruppu for her support and valuable suggestions. I would like to thank **Ms. Ranjini S. Menon**, Faculty Member, SOE, CUSAT for associating with me in learning the software PLAXIS 3D.

The cooperation of the all the staff members of Department of Ship Technology - CUSAT, School of Engineering, Division of Civil Engineering- CUSAT and Department of Civil Engineering - SNGCE, Kadayiruppu are acknowledged with sincere thanks.

I owe a lot to my Husband **Dr. Shajan P. X.**, my loving kids **Shaun & Evan** and my beloved parents for their constant support and encouragement. I would not have been able to undertake this work without their support.

Above all, I express my indebtedness to the "**ALMIGHTY**" for all His blessing and kindness.

Kavitha P.E.

Abstract

The soil found in most of the coastal region is soft marine clay which is usually under- consolidated with low shear strength. Most of the coast line have surface which are sloping towards water front. The method of foundation normally adopted under such soil condition is a pile foundation. Such vertical piles are often subjected to a significant amount of lateral loads in addition to the axial loads. The critical lateral loads applied at the head of the pile in a sloping ground are due to earth pressure from the soil in the sloping surroundings, wind acting on the superstructure, mooring pull from the ship in berthing structures etc.. The analysis of this problem is complex due to the high nonlinearity of the stress-strain behaviour of soil. The response of piles under lateral loading also nonlinear even for low levels of applied loads. The proper assessment of the lateral displacement and internal forces for the design of structures is of paramount importance.

Under the above circumstances a study on the influence of bed slope of soil and slenderness ratio of pile is carried out using a series of laboratory model tests, analytical investigations and numerical studies for the optimum design of piles in sloping ground. Laboratory tests are carried out on laterally loaded aluminium model piles embedded in sloping clay bed. The pile top deflection and the strain along the length of the pile are measured and studied. The study has been conducted for different diameters and length of pile and also for different bed slope. The model test results are compared with the results obtained from the program developed in MATLAB, based on the classical analytical formulations.

Laboratory tests are also modeled in finite element software PLAXIS-3D and the results are validated. The work is further extended for various bed slopes and the variation in bending moment, depth of fixity and deflection of pile top are studied. A set of multivariable regression equations are also developed to

predict the maximum bending moment, depth of fixity of pile and deflection of pile top with the change in diameter of pile, length of pile and the bed slope.

The influence of pile diameter and the soil modulus in the structural behaviour of pile under dynamic loading was also investigated. The study has been conducted using a MATLAB program developed based on the classical theories and by developing a numeric model in PLAXIS-3D.

The findings are also extended to predict the behaviour of piles in berthing structures under lateral load. A series of numerical analyses has been conducted in PLAXIS-3D on a typical frame of a ship berthing structure and the influence of pile diameter, soil modulus and bed slope on the structural behaviour of the piles are studied. A set of multivariable regression equations are also developed to understand the contributions of pile diameter, soil modulus and bed slope in predicting the maximum bending moment, depth of fixity of pile and deflection of the pile top.

Keywords: Soil-Structure Interaction, Laterally Loaded Pile, Ship Berthing Structure

Contents

Chapter 1

INTRODUCTION	01- 09
1.1 General	01
1.2 Scope of the Present Study	06
1.3 Objectives	06
1.4 Methodology.....	07
1.5 Organization of the Report	08

Chapter 2

LITERATURE REVIEW	10 - 38
2.1 Introduction.....	10
2.2 Types of Investigations	11
2.2.1 Theoretical Investigation	11
2.2.2 Numerical Investigation.....	16
2.2.3 Experimental Investigation	22
2.3 Factors Influencing Soil Structure Interaction of Laterally Loaded Pile	24
2.3.1 Characteristics of Soil	24
2.3.1.1 Soil Properties	25
2.3.1.2 Vertical Soil Profile	25
2.3.1.3 Alignment of Ground Surface	26
2.3.2 Characteristics of Pile	27
2.3.2.1 Flexibility of Pile.....	28
2.3.2.2 Stiffness of Pile.....	28
2.3.2.3 Arrangement of Pile	29
2.3.3 Type of Loading.....	31
2.3.3.1 Static Loading.....	31
2.3.3.2 Dynamic Loading	32
2.4 Review on Analysis of Ship Berthing Structures.....	34
2.5 Summary.....	36

Chapter 3

EXPERIMENTAL INVESTIGATION	39 - 71
3.1 Introduction.....	39
3.2 Derivation of Scale Factors	39
3.2.1 Buckingham's π - theorem.....	40
3.2.2 Rayleigh Method.....	43
3.2.3 Scale Factors for the Present Study	45
3.3 Feasibility Study of Model Test.....	49
3.3.1 Experimental Setup	49
3.3.2 Results	50

3.3.3	Inference based on Feasibility Study.....	51
3.4	Materials and Instrumentation	51
3.4.1	Preparation of Soil Sample	51
3.4.2	Specifications of Strain Gauge.....	52
3.4.3	Model Pile Instrumentation with Strain Gauge.....	53
3.4.4	Calibration of Strain Gauge	54
3.4.5	Working of Datalogger	56
3.5	Test Setup and Procedure	57
3.6	Plotting the Results	60
3.6.1	Load Deflection Diagrams	60
3.6.2	Bending Moment Diagrams.....	62
3.7	Observations from the Experimental Investigations.....	67
3.7.1	Variation of Bending Moment with the Change in Embedment Depth of Pile	67
3.7.2	Variation of Bending Moment with the Change in Bed Slope.....	68
3.7.3	Variation of Bending Moment with the Change in Diameter of Pile	69
3.8	Summary.....	70

Chapter4

ANALYTICAL INVESTIGATION	72–82	
4.1	Introduction.....	72
4.2	Analytical Formulation.....	72
4.3	Validation of the Formulation.....	76
4.4	Analysis of Model Tests.....	79
4.5	Summary.....	82

Chapter5

NUMERICAL INVESTIGATION	83-110	
5.1	Introduction.....	83
5.2	Soil-Pile Modeling in PLAXIS-3D.....	83
5.2.1	Soil-Pile Interaction Modeling using Mohr-Coulomb Model.....	84
5.2.1.1	Formulation of Mohr-Coulomb Soil Mode.....	84
5.2.1.2	Basic Parameters of Mohr-Coulomb Soil Model.....	85
5.2.2	Soil-Pile Interaction Modeling using Embedded Pile Element.....	85
5.3	Modeling of a Laterally Loaded Single Pile in Sloping Bed.....	87
5.4	Analysis of Results from Parametric Studies	88
5.4.1	Load Deflection Curves.....	88
5.4.2	Bending Moment Diagrams	93
5.4.3	Tabulated Results	102
5.5	Multivariable Regression Equations	106
5.6	Summary.....	109

Chapter 6

NUMERICAL ANALYSIS OF SHIP BERTHING

STRUCTURE	111-131
6.1 Introduction.....	111
6.2 Modeling and Analysis of a Berthing Structure	112
6.3 Parameters of Soil and Structure.....	113
6.4 Parametric Study	114
6.5 Influence of Pile Diameter on Depth of Fixity	115
6.6 Influence of Soil Modulus on Depth of Fixity.....	117
6.7 Influence of Bed Slope on Depth of Fixity	118
6.7.1 Influence of Soil in the Upper Part of Bed Slope.....	119
6.7.2 Influence of Soil in the Lower Part of Bed Slope	119
6.8 Regression Equations to Predict Depth of Fixity.....	121
6.9 Influence of Pile Diameter on Bending Moment.....	123
6.10 Influence of Soil Modulus on Bending Moment	124
6.11 Influence of Bed Slope on Bending Moment	124
6.11.1 Influence of Soil in the Upper Part of Bed Slope.....	125
6.11.2 Influence of Soil in the Lower Part of Bed Slope	125
6.12 Regression Equations to Predict Bending Moment	126
6.13 Influence of Pile Diameter on Maximum Deflection.....	128
6.14 Influence of Soil Modulus on Maximum Deflection	128
6.15 Influence of Bed Slope on Maximum Deflection.....	129
6.16 Regression Equation to Predict Maximum Deflection.....	129
6.17 Summary.....	129

Chapter 7

SUMMARY AND CONCLUSIONS..... 132-139

7.1 Summary.....	132
7.2 Conclusions.....	134
7.2.1 Review of Literature.....	134
7.2.2 Model Investigation.....	134
7.2.3 Analytical Investigation.....	135
7.2.4 Numerical Investigation.....	135
7.2.5 Numerical Analysis of ship Berthing Structure	136
7.2.6 Multivariable Regression Equations.....	138
7.3 Scope of Future Work	139

REFERENCES

APPENDICES..... 154-247

Appendix A Experimental Investigation of Soil Sample	154-157
--	---------

Appendix B	Model Tests	158-165
Appendix C	MATLAB Coding for the Analysis of Single Pile	166-181
Appendix D	Parametric Study based on Analytical and Numerical Investigation	182-194
Appendix E	Review on Soil Constitutive Models	195-204
Appendix F	Validation of PLAXIS-3D Model	205-211
Appendix G	Parametric Study of a Single Pile Using PLAXIS-3D	212-225
Appendix H	Parametric Study of a Typical Berthing Structure Using PLAXIS-3D.....	226-235
Appendix I	Multivariable Regression Analysis.....	236-237
Appendix J	Design Chart for the Analysis of Ship Berthing Structure.....	238-247

PUBLICATIONS248

CURRICULUM VITAE..... 249 - 250

List of Tables

	Page No
Table 3.1	Derivation of π -terms 42
Table 3.2	Length of Prototype Piles used in the Present Model Tests..... 46
Table 3.3	Diameter of Prototype Piles used in the Present Model Tests 46
Table 3.4	Height of Prototype Pile above the Ground Level..... 47
Table 3.5	Scale factors to calculate Load on Prototype Pile 47
Table 3.6	Load on Prototype Pile..... 47
Table 3.7	Comparison of Deflection of Prototype Piles used using Model Analysis and Analysis of PLAXIS-3D Model 48
Table 3.8	Strain Gauge Calibration Data..... 55
Table 3.9	Details of Model Tests Conducted and Test Results 66
Table 4.1	Recommended Values of soil modulus as per IS 2911 (Part 1/Section 2) – 2010..... 80
Table 4.2	Comparison of Maximum Bending Moment on Pile..... 81
Table 4.3	Comparison of Deflection at Pile Top 81
Table 5.1.a	Numerical Investigation Results of Model Piles (D=19 mm, L=600 mm) 102
Table 5.1.b	Numerical Investigation Results of Model Piles (D=19 mm, L=700 mm) 102
Table 5.1.c	Numerical Investigation Results of Model Piles (D=19 mm, L=800 mm) 103
Table 5.1.d	Numerical Investigation Results of Model Piles (D= 25.4 mm, L=600 mm)..... 103
Table 5.1.e	Numerical Investigation Results of Model Piles (D= 25.4mm, L=700 mm) 104
Table 5.1.f	Numerical Investigation Results of Model Piles (D= 25.4 mm, L=800 mm)..... 104
Table 5.1.g	Numerical Investigation Results of Model Piles (D= 30 mm, L=600 mm) 105
Table 5.1.h	Numerical Investigation Results of Model Piles (D= 30 mm, L=700 mm) 105
Table 5.1.i	Numerical Investigation Results of Model Piles (D= 30 mm, L=800 mm) 106
Table 5.2	Variation of Depth of Fixity as per the Suggested Equation and the Conventional Method..... 109
Table 6.1	Parameters of Pile and Beam..... 113
Table 6.2	Parameters of Soil..... 114

List of Figures

	Page No
Figure 1.1 A Ship Berthing Structure	02
Figure 1.2 Fenders in a Ship Berthing Structure	03
Figure 1.3 Bollards in a Ship Berthing Structure	03
Figure 1.4 Failure Mechanism in a Laterally Loaded Pile.....	04
Figure 1.5 Behaviour of a Laterally Loaded Long Pile	05
Figure 1.6 Active and Passive Wedge of Soil in a Soil-Pile System.....	05
Figure 2.1 General Beam Column Element	11
Figure 2.2 Behaviour of Laterally Loaded Pile.....	12
Figure 2.3 Basic Strain Wedge Model.....	12
Figure 2.4 Reissner Type Simplified Elastic Continuum Applied to Laterally Loaded Pile	14
Figure 2.5 Degradation Curve of Shear Modulus of Soil	15
Figure 2.6 Free-body Diagram Showing the Forces in a Soil-Pile- Structure System.....	16
Figure 2.7 Simple structure-pile-soil system connected to free-field ground	18
Figure 2.8 Building Pile System Supported by the Free-Field Ground through Winkler Type Soil Model	19
Figure 2.9 Sketch of Bending Moment Distribution in Fixed Head Pile Group	20
Figure 2.10 Shadow Stress Zone and Gap Formation in LLP Group.....	30
Figure 2.11 Lateral Load and Components of Resistance offered by Soil- Pile System.....	32
Figure 2.12 Schematic Diagram of Dynamic <i>p-y</i> Analysis Model.....	33
Figure 3.1 Schematic Diagram of the Experimental setup	49
Figure 3.2 Experimental Setup.....	50
Figure 3.3 Lateral Load Vs Deflection Curve.....	51
Figure 3.4 Sundrying and powering of soil sample.....	52
Figure 3.5 Strain Gauges.....	53
Figure 3.6 Typical Strain Gauge Bonding Method and Damp-proofing Treatment	53
Figure 3.7 Typical Installation with Bonding to Metal Surface in Wet Condition.....	54
Figure 3.8 Model Pile instrumented with Strain Gauge	54

Figure 3.9	Bending Test Setup	55
Figure 3.10	Strain Gauge Calibration Curve for 25.4 mm Diameter Model Pile	56
Figure 3.11	Data Logger Arrangement in Test Setup.....	57
Figure 3.12	Weighing and Placing soil in the tank.....	58
Figure 3.13	Packing of soil in 10 cm layers	58
Figure 3.14	Soil Packed in the Tank.....	59
Figure 3.15	Dial Gauges fixed at top of the pile and at the ground level.....	59
Figure 3.16.a	Load Deflection Curve of Model Piles with Length 600 mm.....	60
Figure 3.16.b	Load Deflection Curve of Model Piles with Length 700 mm	61
Figure 3.16.c	Load Deflection Curve of Model Piles with Length 800 mm	61
Figure 3.17.a	Bending Moment Variation in Model Piles (D= 25.4 mm & S= 1:1.5)	62
Figure 3.17.b	Bending Moment Variation in Model Piles (D= 19 mm & S= 1:1.5)	63
Figure 3.17.c	Bending Moment Variation in Model Piles (D= 25.4 mm & S= 1:2)	64
Figure 3.17.d	Bending Moment Variation in Model Piles (D= 19 mm & S= 1:2)	65
Figure 3.18	Variation of Bending Moment with the Change in Embedment Depth of Pile	67
Figure 3.19	Variation in Depth of fixity with Change in Length of Pile.....	68
Figure 3.20	Change in Passive Earth Presssure with Bed Slope	68
Figure 3.21	Variation in Bending Moment with Pile Diameter	69
Figure 4.1	Element of a Beam-Column.....	73
Figure 4.2	Finite Element Discretisation of the Pile.....	75
Figure 4.3	Computed Values of Deflection and Bending Moment of the Validating Problem	77
Figure 4.4	Deflection Variation along the Length of the Pile	78
Figure 4.5	Bending Moment Variation along the Length of the Pile	79
Figure 5.1	Illustration of Stress Path in Mohr-Coulomb Soil Model	84
Figure 5.2	Embedded Pile inside Soil Volume.....	86
Figure 5.3	Embedded Pile with Interface	86
Figure 5.4	Embedded Pile in PLAXIS-3D	86
Figure 5.5	PLAXIS-3D Model of a Single LLP in Sloping Bed.....	87
Figure 5.6.a	Load-Deflection Curve for 19 mm Diameter Model Pile with 550 mm Embedment Depth	88

Figure 5.6.b Load-Deflection Curve for 25.4 mm Diameter Model Pile with 550 mm Embedment Depth	89
Figure 5.6.c Load-Deflection Curve for 30 mm Diameter Model Pile with 550 mm Embedment Depth	89
Figure 5.6.d Load-Deflection Curve for 19 mm Diameter Model Pile with 650 mm Embedment Depth	90
Figure 5.6.e Load-Deflection Curve for 25.4 mm Diameter Model Pile with 650 mm Embedment Depth	90
Figure 5.6.f Load-Deflection Curve for 30 mm Diameter Model Pile with 650 mm Embedment Depth	91
Figure 5.6.g Load-Deflection Curve for 19 mm Diameter Model Pile with 750 mm Embedment Depth	91
Figure 5.6.h Load-Deflection Curve for 25.4 mm Diameter Model Pile with 750 mm Embedment Depth	92
Figure 5.6.i Load-Deflection Curve for 19 mm Diameter Model Pile with 750 mm Embedment Depth	92
Figure 5.7.a Bending Moment Diagram for 19 mm Diameter Model Pile with 550 mm Embedment Depth	93
Figure 5.7.b Bending Moment Diagram for 25.4 mm Diameter Model Pile with 550 mm Embedment Depth	94
Figure 5.7.c Bending Moment Diagram for 30 mm Diameter Model Pile with 550 mm Embedment Depth	95
Figure 5.7.d Bending Moment Diagram for 19 mm Diameter Model Pile with 650 mm Embedment Depth	96
Figure 5.7.e Bending Moment Diagram for 25.4 mm Diameter Model Pile with 650 mm Embedment Depth	97
Figure 5.7.f Bending Moment Diagram for 30 mm Diameter Model Pile with 650 mm Embedment Depth	98
Figure 5.7.g Bending Moment Diagram for 19 mm Diameter Model Pile with 750 mm Embedment Depth	99
Figure 5.7.h Bending Moment Diagram for 25.4 mm Diameter Model Pile with 750 mm Embedment Depth	100
Figure 5.7.i Bending Moment Diagram for 30 mm Diameter Model Pile with 750 mm Embedment Depth	101
Figure 6.1 Typical Frame of a Berthing Structure Considered for the Present Study	112
Figure 6.2 Meshed model and Deflection Pattern of the Typical Berthing Structure Considered	113
Figure 6.3 Bed Slope Variation Adopted for Parametric Study	115

Figure 6.4	Variation of Depth of Fixity with Diameter of Pile ($E_s = 1000 \text{ kN/m}^2$).....	116
Figure 6.5	Passive Earth Pressure Acting on Piles in the Berthing Structure	116
Figure 6.6	Variation of Depth of Fixity with Soil Modulus	118
Figure 6.7	Influence of Soil in the Upper Part of Bed Slope in Depth of Fixity	119
Figure 6.8	Influence of Soil in the Lower Part of Bed Slope in Depth of Fixity	120
Figure 6.9	Actual Value of Depth of Fixity Vs Calculated Value of Depth of Fixity	122
Figure 6.10	Variation of Bending Moment with Change in Diameter and Soil Modulus	123
Figure 6.11	Variation of Bending Moment with Change in Bed Slope By Removing Soil from the Upper Part of the Slope	125
Figure 6.12	Variation of Bending Moment with Change in Bed Slope By Removing Soil from the Lower Part of the Slope	126
Figure 6.13	Actual Value of Bending Moment Vs Calculated Value of Bending Moment.....	127
Figure 6.14	Variation of maximum deflection with pile diameter and soilmodulus	128
Figure 6.15	Actual Value Vs Calculated Value of Deflection of the Frame.....	129

List of Abbreviations

A_b	Cross Sectional area of Beam
c	Soil Cohesion
C	Bending Constant
C_u	Undrained Shear Strength
D	Outside Pile Diameter
D_f	Depth of Fixity
E	Young's Modulus of Concrete
EI	Pile Stiffness
E_s	Soil Modulus
F_{max}	Base Resistance
h	Height of Applied Load from the Ground Surface
I	Moment of Inertia of the Cross Section
L	Pile Length
L_s	Lower Part of Bed Slope
L_e	Embedment Depth
m	Mass at Pile Top
M	Bending Moment
M_{max}	Maximum Bending Moment
p	Soil Reaction
P	Applied Lateral Load
P_x	Force Acting in x- direction
S	Bed slope
SHM	Simple Harmonic Motion
SSI	Soil Structure Interaction
T_{max}	Skin Resistance
U_s	Upper Part of Bed Slope
ν_c	Poisson's ratio of concrete
ν_s	Poisson's ratio of soil

y	Pile Deflection
y_{\max}	Maximum Deflection
γ_c	Density of Concrete
γ_{sat}	Saturated Unit Weight of Soil
γ_{unsat}	Unsaturated Unit Weight of Soil
ε	Micro Strain
λ	Scale Factor
ψ	Dilatancy Angle

.....କେଉଁ.....

- 1.1 *General*
- 1.2 *Scope of the Present Study*
- 1.3 *Objectives*
- 1.4 *Methodology*
- 1.5 *Organization of the Report*

1.1 General

Soil structure interaction (SSI) analysis is the study on the influence of the behaviour of soil in the structural response and vice versa. To predict the behaviour of a structure, it is necessary to consider the properties of structure as well as properties of surrounding soil, especially when the structure is founded in a weak soil stratum. Traditional methods of structural analysis and design neglect the SSI effects. The effect of SSI will be prominent for structures resting on relatively soft soils. Most of the coastal and offshore structures such as bridge abutment on river shore, open type berthing structures etc., are heavy concrete structures founded on piles in soft soil and these structures are subjected to significant amount of lateral loads due to wind, mooring pull, lateral soil movement and earthquake forces.

The present study focuses on the soil structure interaction analysis of laterally loaded piles in ship berthing structures. Berthing structures are constructed to facilitate berthing and mooring of ships. Berthing structures are of two types namely vertical face structures and open type structures. Open type

berthing structures which are commonly adopted in Cochin Port area is considered in this study.



Fig. 1.1 A Ship Berthing Structure
(courtesy: <http://www.thehindubusinessline.com>)

Berthing structures are subjected to considerable amount of lateral loads in addition to vertical loads. The vertical loads on the structure include the self-weight of the structure and the weight of the cargo and machinery operating on the deck of the structure. The lateral loads on the structure are the berthing force, mooring force, wave force, current force, seismic force, active earth pressure and differential water pressure.

The lateral loads acting on berthing structures are primarily resisted by fenders and bollards (Fig.1.2 and Fig.1.3). Fenders provided on the berthing structures transfers the berthing forces from the ship to the structure as a reaction force. The mooring force from the ship is transferred to the structure using the bollards provided on the berthing structure. The wave force, current force and the differential water pressure enhances the berthing and mooring forces on the structure. The active earth pressure from the shore side of the berthing structure may cause additional load on the piles of berthing structure. The dynamic lateral load like earthquake, changes the soil structure interaction behaviour and hence it

causes changes in the structural response. The nonlinear behaviour of soil and the interaction of the soil-structure system necessitate the need of a thorough analysis.



Fig. 1.2 Fenders in a Ship Berthing Structure
(courtesy: <http://www.portfenders.com>)



Fig. 1.3 Bollards in a Ship Berthing Structure
(courtesy: <http://www.popularmechanics.com>)

Pile foundations are adopted to construct heavy structures like berthing structures since in most of the cases they are founded in soft soil stratum. Based on the load transfer mechanism, pile foundations can be classified into axially loaded piles and laterally loaded piles. Load carrying capacity of axially loaded pile is due to the frictional resistance developed at the surface of pile as well as due to the bearing capacity of end bearing stratum. Load carrying capacity of a laterally loaded pile depends on the stiffness of the pile as well as the depth of fixity of the pile. The stiffness of pile depends on the material of pile and the diameter of pile. The depth of fixity of pile depends on the soil

structure interaction effect. The behaviour of soil being highly nonlinear in nature, a detailed investigation on the soil structure interaction analysis is required for the better understanding of the structural behaviour of laterally loaded pile.

The failure pattern of laterally loaded pile foundations are of two types, failure by rotation and failure by bending. Short piles fails by rotation at the point of rotation and long piles (flexible piles) fail by bending at the depth of fixity where the maximum bending moment acts (Fig.1.4).

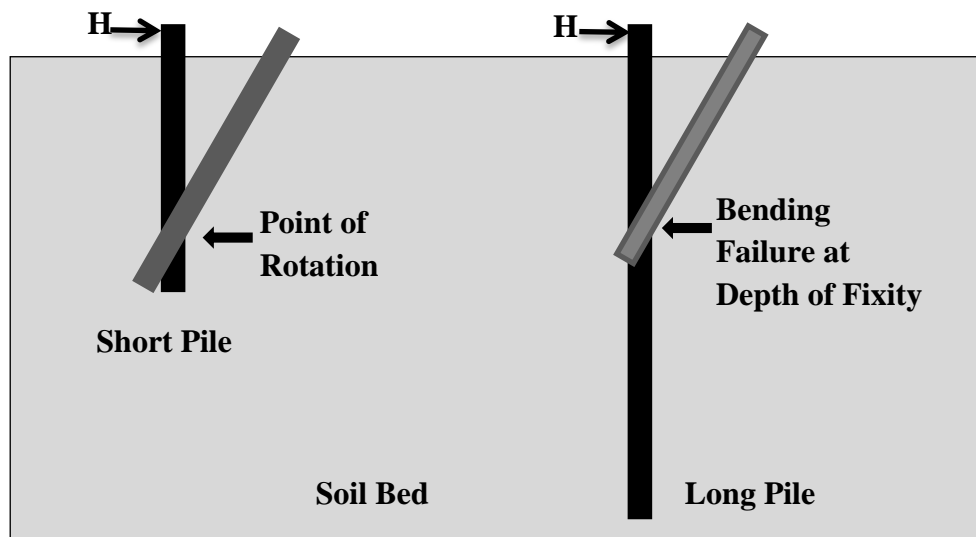


Fig. 1.4 Failure Mechanism in a Laterally Loaded Pile (Tomlinson, 1987)

The load carrying capacities of short piles are less compared to those of long piles. Hence when a heavy structure is to be built in a weak soil stratum long piles are preferred over short piles. The structural behaviour of a long pile is shown in Fig.1.5.

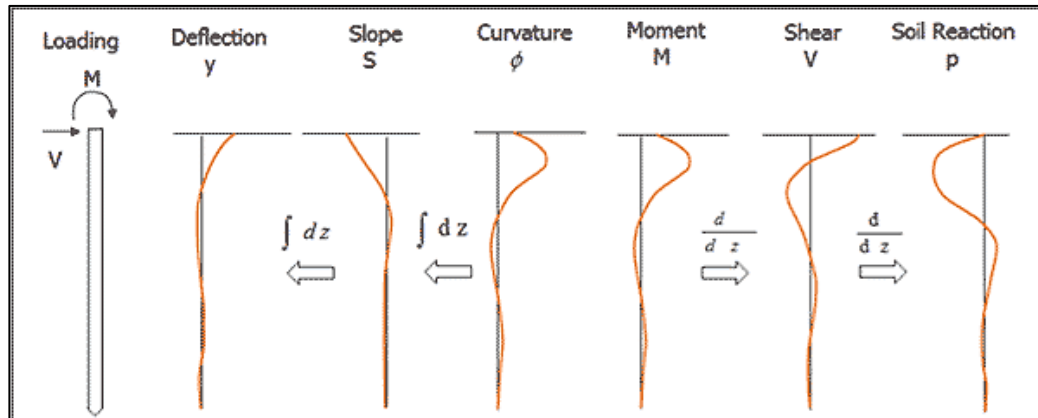


Fig. 1.5 Behaviour of a Laterally Loaded Long Pile [71]

In a laterally loaded pile the depth of fixity is decided by the passive wedge of soil offering resistance to the external lateral load as shown in Fig.1.6. The problem of laterally loaded piles becomes critical when it is founded in sloping ground. It is due to the fact that as the bed slope increases the volume passive wedge decreases. It is a complex soil-structure interaction problem and needs to be investigated in detail.

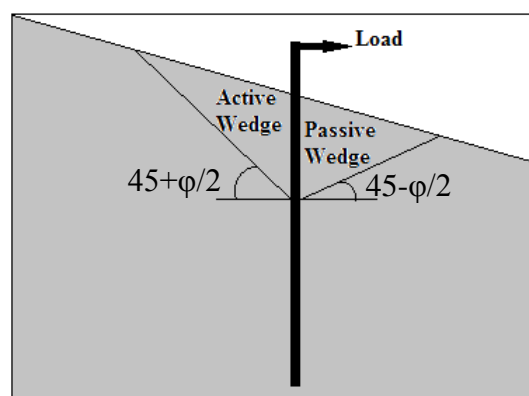


Fig. 1.6 Active and Passive Wedge of Soil in a Soil-Pile System [134]

1.2 Scope of the Present Study

The soil found in most of the coastal region is soft marine clay which is usually under-consolidated with low shear strength. Most of the coast line have surface which are sloping towards water front. The method of foundation normally adopted under such soil condition is a pile foundation. Such vertical piles are often subjected to a significant amount of lateral loads in addition to the axial loads. The critical lateral loads applied at the head of the pile in a sloping ground are due to earth pressure from the soil in the sloping surroundings, wind acting on the superstructure, mooring pull from the ship in berthing structures etc.. The analysis of this problem is complex due to the high nonlinearity of the soil stress strain behavior. The lateral pile response is also nonlinear even for low levels of applied loads. The proper assessment of the lateral displacement and internal forces for the design of structures is of paramount importance. Under the above circumstances soil-structure interaction of laterally loaded piles is intent to study the influence of bed slope of soil and slenderness ratio of pile on the structural behavior of a laterally loaded pile. This can be carried out using a series of model tests, analytical investigations and numerical studies for the optimum design of pile in sloping ground. The analyses are extended to predict the behaviour of piles in berthing structures also.

1.3 Objectives

The main objectives are:

- 1) To study the soil-structure interaction effect and the significance of laterally loaded piles in ship berthing structures by conducting a detailed literature survey.
- 2) To analyze the soil pile behaviour in a sloping ground for different diameters and lengths of pile and in different bed slopes by conducting model tests.
- 3) To develop a MATLAB code for a laterally loaded pile in sloping bed using classical theories and compare the results with the model test results.

- 4) To simulate the model tests in PLAXIS 3D and extend the analysis for various bed slopes.
- 5) To conduct numeric analysis of a typical ship berthing structures with laterally loaded piles in sloping ground by considering the mooring pull on piles. The diameter of pile, soil modulus and bed slope are to be varied and its influence are to be studied.
- 6) To develop a set of multivariable regression equations based on numerical analysis of laterally loaded piles for both single pile and a typical frame in a berthing structure.

1.4 Methodology

The analysis of a laterally loaded pile becomes critical when it is embedded in sloping clay ground. The present study addresses the problem using model investigation, analytical investigation and numerical investigation. The study has been done to analyze the effect of static lateral loading on a pile in sloping clay bed. As an appendix, the conceptual behavior of the soil-pile system under dynamic loading is also studied.

An extensive literature review has been conducted to understand the present scenario of the problem considered. Initially a single pile in sloping clay bed has been analyzed for a static lateral load at the pile top. Since prototype study is tedious and costly, model investigations are adopted for the present study. The structural behaviour of laterally loaded piles with change in pile diameter, pile length and bed slope are studied.

An analytical solution of the problem has been derived from the governing equation suggested by Reese *et al.* [71] The solution of the finite difference equations is very tedious for manual calculations and hence MATLAB coding is adopted for the same. The analytical solution is also validated by an onsite pile load test results. Model Tests are also simulated using analytical formulations and the results are compared.

Numerical models of the above problem is also created in PLAXIS-3D and validated with the model test results. A detailed parametric study of the laterally loaded pile is conducted by varying the bed slopes. The influence of change in bed slope in the structural behaviour of pile is studied. A set of multivariable regression equations are also developed to predict the maximum bending moment, depth of fixity and deflection at the pile top.

The study is then extended to the lateral behaviour of a berthing structure under static loading. Numerical investigations are suggested for the solution of the problem. The finite element software PLAXIS-3D which can be used for solving SSI problems is adopted for the present study. PLAXIS-3D models created for the study is validated with the experiments in the literatures as well as with the present model investigations and analytical investigations. A typical berthing structure has been modeled with the dimensions, soil conditions and loading details adopted from the berthing structure details of Cochin Port Trust. A detailed parametric study has been done and multivariate regression analysis has been adopted to generate a set of design equations to represent the analysis results.

1.5 Organization of the Report

The present work deals with the static and dynamic analysis of laterally loaded pile embedded in sloping clay bed. The organization of the chapters is as follows.

The first chapter is an introduction to the problem, scope and objectives of the present study and the methodology adopted in the study.

The second chapter is a detailed review of the related works carried out so far. Around hundred literatures from national and international journals/proceedings are critically reviewed.

The third chapter contains the details of model investigation carried out on laterally loaded single piles on sloping clay bed. A set of model tests on laterally

loaded pile are carried out by varying the pile diameter, embedment depth of pile and bed slope. The variations in pile top deflection and bending moment on the piles are studied.

The fourth chapter discusses the analytical formulation and the solution of the governing equation. Since the procedure being lengthy and tedious, MATLAB coding is adopted to solve the governing equation.

The fifth chapter presents the numerical simulation of the problem using PLAXIS-3D, finite element software. A detailed parametric study has also been done to study the structural behaviour of the soil-pile system.

The sixth chapter describes the extension of the above work to the analysis of ship berthing structures embedded in sloping clay bed. It explains the behaviour of berthing structures under static lateral loading. A detailed parametric study and a multivariable regression analysis are done for the better representation of the analysis results.

The seventh chapter gives the summary and conclusions based on the present study and the scope of further study.

.....❧❧.....

Literature Review

Contents	2.1 <i>Introduction</i>
	2.2 <i>Types of Investigations</i>
	2.3 <i>Factors Influencing Soil Structure Interaction of Laterally Loaded Pile</i>
	2.4 <i>Review on Analysis of Ship Berthing Structures</i>
	2.5 <i>Summary</i>

2.1 Introduction

The pile foundations are adopted to transfer the load from the structure to soil when the structure is embedded in a weak soil stratum. In an axially loaded pile the load is transferred to the soil through the side friction at the soil pile interface and base resistance offered by the soil bed. Pile foundations are subjected to significant amount of lateral forces in addition to the vertical forces. The lateral forces are due to the wind, wave, earthquake, dredging and impact loads [25, 41, 80, 83,88]. When the pile is subjected to lateral loads the load carrying mechanism changes. The lateral load is resisted by the soil pile interaction effect [125], which in turn depends on pile material, pile diameter, soil properties and bed slope of ground. Studies showed that the influence of vertical load on the lateral response is not so significant when the vertical load is applied simultaneously with the lateral load [68]. The current design practices consider the influence of these two loadings independently and hence pile designs are carried out separately for vertical and lateral loads. The effects of vertical loads on the piles are well established through these years whereas studies on vertical piles under lateral loads are limited and are continuing to establish a well-defined method of analysis considering the effect of all the influencing parameters [33]. The present study focuses on the significant factors affecting the soil structure interaction of

laterally loaded pile foundation (LLP). For better understanding, the literatures have been grouped into different categories based on: type of investigations, characteristics of soil, characteristics of pile and type of loading.

2.2 Types of Investigations

Reviewing the available literatures it was observed that, the studies on laterally loaded piles (LLP) are generally carried out by conducting the theoretical, numerical and experimental investigation of soil-pile system. For better understanding of the literatures, they are grouped based on the type of investigation carried out to study the behaviour of laterally loaded piles.

2.2.1 Theoretical Investigation

Theoretical investigations are the basis of numerical formulations. The theoretical formulations are to be studied for the advanced modifications in the numerical formulations. Earlier developments in the theoretical formulations are also discussed here. Lateral loads on piles causes deflection and rotation of pile caps. To calculate the pile cap deflection and rotation the pile has been idealized as a beam. Laterally loaded pile analysis had been conducted by considering a cantilever action with tip load. Further the soil structure interaction can be incorporated by considering the effect of soil parameters. Such an attempt was done by Mazurenko *et al.* to analyze the behaviour of a laterally loaded pile [75].

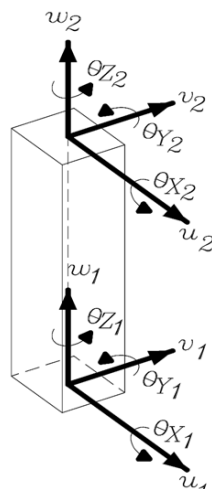


Fig. 2.1 General Beam Column Element [23, 25]

In a laterally loaded pile the point of zero deflection or the point of maximum bending moment is considered to be the point at which failure of the soil-pile system occurs. An analytical method to calculate the point of zero deflection and the point of maximum bending moment was suggested by Mironov [76]. To develop this general method the factors considered are, flexural rigidity of the pile, nature of variation of stiffness of soil mass with depth and the ratio between the deflections and soil reactions. Better understanding on the behaviour of laterally loaded piles can be obtained from the soil reaction – pile deflection (p - y) curves of the soil. Reese *et al.* [115] have developed non-dimensional curves from the numerical solution of the differential equation describing the pile behaviour and it can be used to estimate the p - y curves. He had further suggested p - y method of analysis for laterally loaded piles by taking into account, the nonlinear and in-elastic characteristics of soil [117].

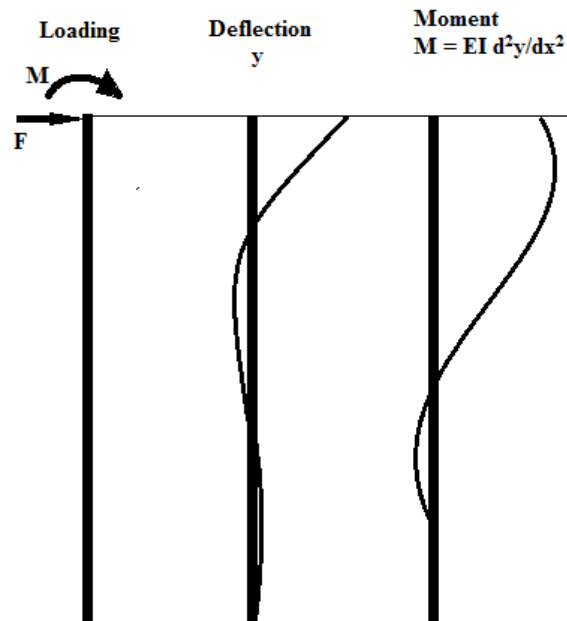


Fig. 2.2 Behaviour of Laterally Loaded Pile [152]

Later p - y analysis method was modified by Duncan *et al.* and is referred as the characteristic load method [31]. It is simpler than p - y analyses initially developed by Reese *et al.* The method used dimensional analysis to characterize the nonlinear behaviour of laterally loaded piles and drilled shafts by means of

relationships among dimensionless variables. The characteristic load method has been found to be in good agreement with values measured in field load test also. More advancement in this was suggested by Brown *et al.* and his analytical method proves a rigorous and reliable method of interpreting lateral load tests on piles or drilled shafts using inclinometer data [20]. The method utilizes a least square regression technique that will converge to a solution for analytical p - y curves which produce minimum error between the predicted and measured deflection versus depth profile over a range of loading.

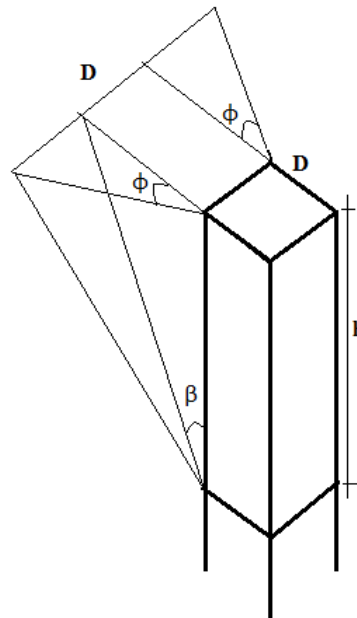


Fig. 2.3 Basic Strain Wedge Model [55]

Further, the strain wedge (SW) model was suggested and was found to have advantages over p - y curve method [5, 6]. SW model analysis predicts the response of laterally loaded piles and had shown very good agreement with actual field tests in sand, clay and layered soils. The advantage of the SW model is that it is capable of taking into account the effect of changes in soil and pile properties on the resulting p - y curves.

The studies on laterally loaded single pile were extended to pile groups also. Reese *et al.* who have already developed p - y method for laterally loaded single pile have presented the analysis of a cluster of piles [118]. The importance

of various parameters involved in the solution is studied using different analytical approaches. A modification of this has been suggested by Poulos-Focht-Koch in which the pile group has been considered as a large diameter pile. Later, Chore *et al.* have extended the work of Reese and derived finite element formulation for the non-linear analysis of pile groups subjected to lateral loads using p - y curves [25,26, 129]. In the study, pile was idealized as one dimensional beam element, pile cap as two dimensional plate element and soil as non-linear elastic springs using modified p - y curves [37]. It was observed in the study that the nonlinearity of the soil is found to increase the top displacement of the pile group and decrease the fixed moments and positive moments. Kim *et al.* have conducted studies on pile-soil system subjected to lateral loads in clay soil by improved wedge failure model and hyperbolic p - y criteria [58]. The proposed p - y curves with an improved wedge model are more appropriate and realistic for representing a pile-soil interaction for LLP in clay than the existing p - y method.

The behaviour of soil becomes complex when the change in its property along the vertical profile is considered. In a simplified analysis the vertical soil profile was considered uniform as suggested by Reissner. It was modified by Horwath [47] with additional case of Young's modulus varying with depth for layer of finite thickness.

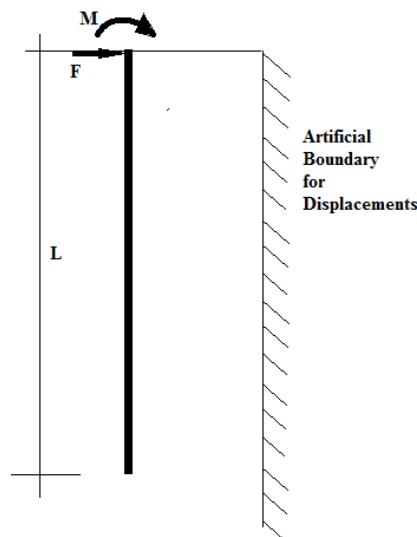


Fig. 2.4 Reissner Type Simplified Elastic Continuum Applied to Laterally Loaded Pile [47]

The response of single pile subjected to lateral load in layered soil was further studied by Rongqing *et al.* and developed an analytical method which uses fundamental basis of structural mechanics to obtain the governing equation of the soil-pile system [69]. Both free head and fixed head methods are considered here. The pile deflection, bending moment and soil reaction can be calculated using this method.

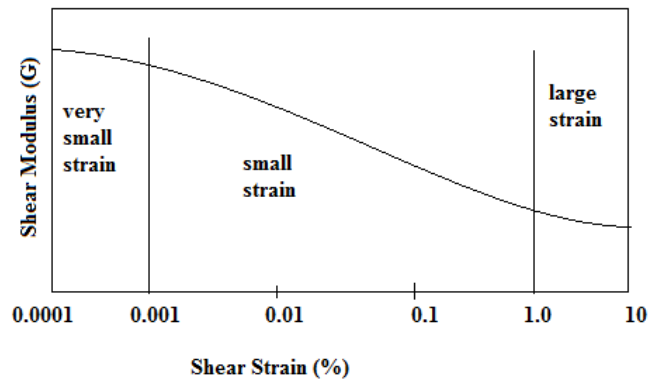


Fig. 2.5 Degradation Curve of Shear Modulus of Soil [38]

The modulus of soil resistance was further modified as an exponential function with depth and derived a new γ parameter to predict the pile response [56]. The direct shear test was used to determine modulus of soil resistance and ultimate soil resistance. The existing methods were later modified considering the nonlinear elastic properties and modulus degradation characteristics of soil [154]. The stress strain behaviour of most geo-materials is highly nonlinear at all phases of loading and s-shaped degradation curve as shown in Fig. 2.5 is commonly found. Further, certain studies suggest two dimensional mapped infinite elements and non-linear stress-strain behaviour of the soil using hyperbolic fit [40].

Later, a detailed investigation by Banerjee *et al.* incorporated layering effect of soil in finite element method (FEM) and boundary element method (BEM). Studies presents inelastic pile-soil-structure interaction under static loading with piles modeled using linear beam column finite elements and soil was modeled using nonlinear springs [13]. Researchers have developed finite

element formulations and its MATLAB coding by considering modulus of subgrade reaction approach to analyze fixed head and free head single piles in cohesion-less soil [82, 101, 102, 129, 144]. Solutions are obtained for pile response with various cohesionless soils taking into account the short pile and long pile behavior.

Through these years theoretical investigations have developed solutions for laterally loaded piles and pile groups embedded in homogeneous as well as layered soil. Even though the incorporation of soil layering in the theoretical formulation of laterally loaded pile makes the solution more complicated, adopting finite element analysis techniques as well as computational power of latest computers can produce accurate results.

2.2.2 Numerical Investigation

A set of numerical formulations for advanced analysis of soil structure interaction are developed by many researchers [59, 60, 63, 140, 141]. A new frequency domain method for evaluating the earthquake input energy to a structure-pile system or a superstructure alone subjected to horizontal ground motion was developed by Takewaki *et al.* [141].

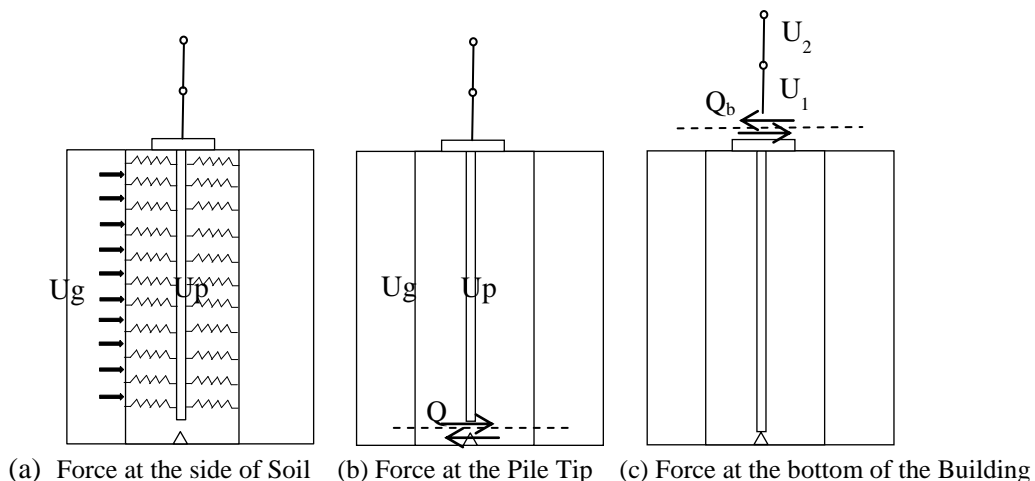


Fig. 2.6 Free-body Diagram Showing the Forces in a Soil-Pile-Structure System [141]

The soil-pile-structure system is idealized as shown in Fig. 2.6 and derived the energy transfer function, which plays a key role in the input energy calculation. Input energy was expressed in time domain as,

$$E_I^A = \int_{-\infty}^{\infty} F_A(\omega) |A(\omega)|^2 d\omega \text{ and } E_I^S = \int_{-\infty}^{\infty} F_S(\omega) |A(\omega)|^2 d\omega \dots\dots\dots (2.1)$$

Where $F_A(\omega)$ and $F_S(\omega)$ are called the energy transfer function for the soil-pile system and the energy transfer function for the structure respectively. The method was developed in frequency domain approach and hence has the advantage of being able to include directly the frequency dependent characteristics such as stiffness and damping of the soil considered. Takewaki *et al.* [140] have also incorporated the effect of pile group on the seismic stiffness and strength design of buildings. Pile group effect is taken into account through the influence coefficients among piles which are defined for inter-story drifts and pile head bending moments. It has been shown that pile group effect reduces the inter-story drift of buildings and increases the bending moment of pile at the top.

Takewaki *et al.* [59] have further extended the method to analyze the earthquake energy input in soil pile structure system with uncertain soil parameters. Taking the advantage of frequency domain approach the earthquake input energy to the structure can be obtained in a compact form. The method was further modified as a unified response spectrum method incorporating the kinematic and inertial effects [60, 63]. The equilibrium equation is derived for the structure-pile-soil system and is represented in eq. 2.2. Where m and k are the mass and stiffness of the system considered.

$$\sum_{i=0}^1 m_i (\ddot{u}_G + \ddot{u}_i) + k_i (u_0^{(I)} + u_0^{(k)} - u_G) + k_p (u_0^{(I)} + u_0^{(k)}) = 0 \dots\dots\dots (2.2)$$

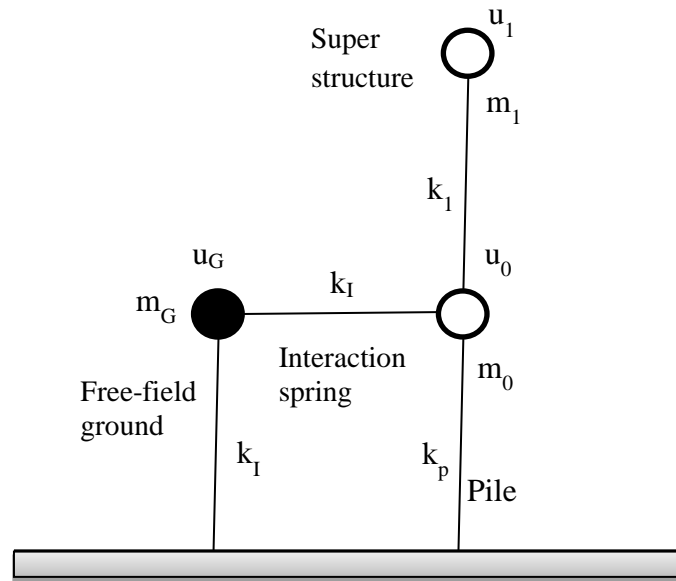


Fig. 2.7 Simple structure-pile-soil system connected to free-field ground [63]

In order to verify the numerical model with winkler type soil model, Takewaki *et al.* have considered an onsite building pile system in Yokohama, Japan. The building consist of 12 storied steel frame structure supported by 20 cast in situ concrete piles of 35 m long and 1.7 m in diameter. The numerical model adopted for the analysis is as shown in Fig. 2.7. The bending strains at the top of the pile were compared and it was found that the strain values obtained using continuum model with winkler type soil element was in good agreement with the measured values of stains.

A newly developed updated reference point (URP) method was used by Okada *et al.* [95], to study the seismic pile response of a structure pile soil system with uncertain soil and concrete properties. A ten storied building was modeled and the pile head bending moments were compared in URP and NURP methods. It was confirmed in the studies that the NURP method can be applied to the seismic pile response in terms of the structure pile soil system with an acceptable accuracy and the worst variation for weak soil parameter are to be clarified. It was also found that the variability of equivalent shear wave velocities of soil, even at a deep underground influences the bending moment at the pile head.

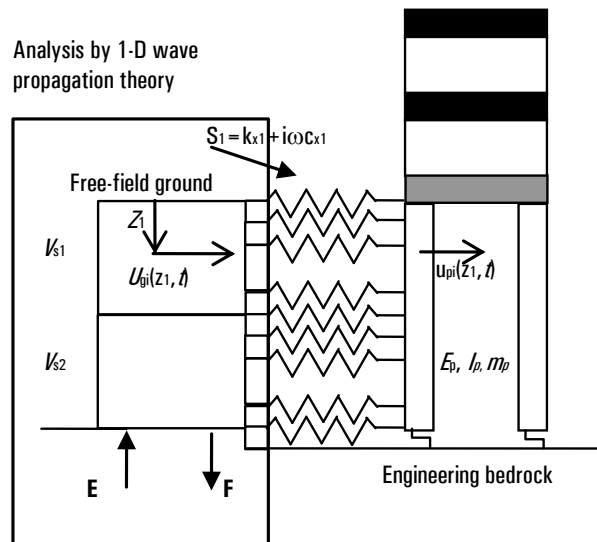


Fig. 2.8 Building Pile System Supported by the Free-Field Ground through Winkler Type Soil Model [50]

Seismic soil structure interaction of a pile group was studied using equivalent pier method (EPM) by Badry *et al.* [12]. The study was conducted on an axisymmetric multistoried building and the peak response of the building under fixed base condition and flexible base condition were studied. It was observed that the response of flexible base structure was more, about 15-20% compared to fixed base structures. Also it was concluded that EPM approach reduces the analysis time by 68%, since in this method, equivalent piers gives rise to larger elements during meshing, which facilitates to take larger time steps and hence less duration of analysis.

Increased computational power of computers has made the numerical investigations the most cost effective and accurate method of investigation. Most of the numerical investigations reported, include the analysis based on the finite element method using software such as ABAQUS [27], ANSYS [137], FLAC [73], FLIPER [152], GROUP [126], LPILE [77], PLAXIS Foundation 1.1 [11,24,87, 144], PLAXIS 3D [133] etc.

Studies on the coupled bridge foundation-superstructure finite-element was conducted by Zhang *et al.* [152] using the finite element code FLPIER to predict

the lateral response of the single piles and pile groups (3X3 to 3X7 pile groups) founded in both loose and medium dense sands. FLIPER incorporates Reese *et al.*'s p-y curves, Brown *et al.*'s p-multiplier approach and Mc Way *et al.*'s p-multiplier factor for large pile groups [20]. The studies involved the predictions of lateral load versus lateral deflection of the group, the shears and bending moments developed in the individual piles, and the distributions of the lateral loads in each pile row, which were all in good agreement with the measured results. The suggested variation of bending moment in a fixed head pile group is shown in Fig. 2.9.

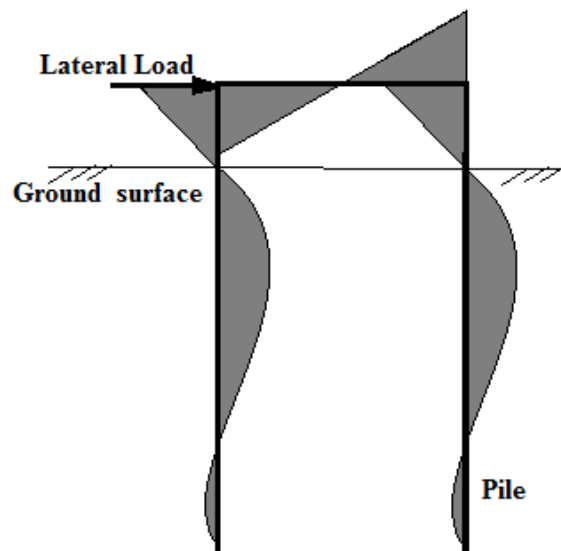


Fig. 2.9 Sketch of Bending Moment Distribution in Fixed Head Pile Group [152]

The effect of pile-soil interaction was effectively represented using CONTACT 49 element (5 node, 3 DOF) element in ANSYS in a set of analyses conducted by Soltani *et al.* [137] and the results were compared with linear method of Hetenyi, non-linear method of Matlock and finite element program of Bowles. The 3D pile-soil interaction effect was incorporated in ANSYS model and it lead to the difference in maximum bending moment and pile top deflection in comparison to the others methods. Many researchers have performed the finite element analysis using the software PLAXIS- 3D FOUNDATION using embedded

pile element and the analysis results are in good agreement with the pile load test conducted by various researchers such as Ismael *et al.* [50] and Y. EI-Mossallamy [150].

Piles in cohesive soil were analysed by a series of numerical analysis conducted by Moayed *et al.* [77] using the LPILE software. Broms (1964) proposed graphs to obtain ultimate lateral bearing capacity of such piles. Broms solution does not consider the effect of vertical loading on lateral bearing capacity of piles. This study incorporates the effect of vertical load also in predicting the lateral capacity of pile. Avaei *et al.* [8] have investigated the effects of different parameters such as pile properties, soil stress-strain behaviour, pile-soil interaction etc. on the behaviour of pile subjected to lateral load. A comparison has been made between the results derived from finite difference and equivalent spring methods. Finite difference program has been developed in Turbo Pascal and the equivalent spring method is solved using SAP 2000 package. The results obtained using both the methods are found to be in good agreement. Parametric study on a laterally loaded pile with length 15m and diameter 1m subjected to a lateral load of 300 kN showed that the properties of soil near the pile head greatly influence the pile head displacement. It was also noticed that the pile end displacement was influenced by the pile length and after a particular length (9m in this case) the influence of pile length decreases and this length is called the depth of fixity.

The lateral behaviour of single pile in cohesionless soil subjected to both vertical and horizontal loads were studied by Chik *et al.* [149] by conducting numerical analysis using the software PLAXIS 3D FOUNDATION 1.1. The verification of the model is done by comparing the results with the pile load test conducted by Jamaludun & Hussein, 1998. Babaei [11] performed numerical investigation on axial bearing capacity of piles embedded in sloping sandy ground, using PLAXIS 3D FOUNDATION. The verification of the model is done by comparing with the field test data conducted by Ismael *et al.* [50] and Y.

EI-Mossallamy [150]. The results have shown that the pile axial capacity increases with increase in upward slope and decreases with increase in downward slope. Nonlinear finite element modeling using PLAXIS 3D Foundation was done by Kim *et al.* [58] to investigate numerically pile deflection, bending moment and p - y curves along the length of the pile. Based on the findings of this study it was found that pile elastic modulus (E_p), interface property (R_{inter}), and pile toe condition exerts no significant influence on the p - y characteristics.

Conte *et al.* [27] have used the finite element code ABAQUS to predict the response of reinforced concrete pile to horizontal loading. Finite element codes are supplied with several constitutive models. However, the choice of a constitutive model is generally influenced by the material parameters that are available for the case study. Sophisticated soil models could not be justified if all the material properties related to the model are not available. Hence, the present study uses a linear elastic perfectly plastic soil model with Mohr-Coulomb failure criteria which uses five soil parameters such as shear modulus (G), poisson's ratio (ν'), shearing resistance angle (ϕ'), effective cohesion (c') and angle of dilatancy (ψ).

2.2.3 Experimental Investigation

Experimental investigations were conducted either on full scale field piles or on model piles. Though the full scale test results are considered to be more reliable, the costs of full scale tests being very high, properly engineered model tests were usually adopted for the studies. Even though the experimental investigations are costly and difficult, the most commonly adopted numerical investigation results are validated with properly conducted experimental results. Some of the widely used experimental results are also discussed here. Rollins *et al.* [122-125] and Gandhi *et al.* [35] have conducted a number of full scale tests on LLP and the same has been adopted for many researchers for the verification of other studies. Experimental model tests are also conducted to

study the behaviour of laterally loaded piles by researchers like Gandhi, Mostafa, Rao, Cox etc. [28, 33, 34, 100, 113,131, 135].

Full scale field tests conducted by a number of researchers had studied the behaviour of group piles in comparison to single pile with the intension of predicting the group effect from the behaviour of a single pile. The pile group deflection and the maximum bending moment under the same average load per pile are reported to be almost twice as that of a single pile. Similar investigations were conducted using model piles also by applying laws of similitude and experiments were carried out similar to that of field tests. Laws of similitude are adopted to model the piles from the available field piles. Field piles are generally concrete or steel. A suitable material capable of predicting the deflection and bending moment is adopted for a model pile. Model piles can be made using aluminium [33, 81, 135], mild steel [28, 113, 131] or PVC [62].

It was observed from the studies that for a particular load aluminium pipe piles showed more deformation at the top of the pile and strains along the length of the pile, compared to steel pipe piles [127]. Considering the above facts aluminium pipes piles are more suited for model studies since it can give strain readings even for a small variation of load. Model tests were conducted to plot the load deflection curve as well as the bending moment variation along the depth of pile. Based on the studies it was observed that individual pile efficiency can be increased by increasing the spacing between the piles. Researchers have suggested that at a spacing of eight to nine times the pile diameter the individual piles attain 100% efficiency [28]. A similar study revealed that the optimum spacing between piles for maximum resistance to be about two times relative stiffness factor T [33].

$$T = \left(\frac{EI}{n_h}\right)^{1/5} \dots\dots\dots (2.3)$$

Where EI is the flexural rigidity of the pile material and n_h is the coefficient of modulus variation (possible range values of n_h from 2.5MN/m³ to 20MN/m³)

(Terzaghi 1955)) [14, 29]. Studies have also inferred that the pile group efficiency decreases with increase in the number of piles in the group even for same spacing between the piles. Piles embedded in slopes showed a decreased load carrying capacity in comparison to piles in level ground. Model studies on sloping ground have found that the effect of slope on the strength reduction of the pile soil system could be neglected for piles located beyond five pile diameters from the crest of the slope [135].

The pile cap imparts fixity to the pile head. Experiments show that fixed head pile exhibit 40% reduction in pile head deflection in comparison to free head pile [35]. The influence of pile cap on the lateral load carrying capacity of piles were also studied by Nath *et al.* [93] and it was found that an increase in embedment depth of pile cap increase the lateral resistance offered by the pile cap to the pile group.

2.3 Factors Influencing Soil Structure Interaction Analysis of Laterally Loaded Pile

From the detailed review of the different investigation methods, it was understood that, proper assessment of the characteristics of soil and pile, loading details etc. are essential in the accurate modeling of the soil-pile system. Hence a brief review on the characteristics of soil, characteristics of pile and type of loading are also incorporated in the present study.

2.3.1 Characteristics of Soil

In soil structure interaction analysis the distribution of load from the structure to the soil is investigated. In this load transfer mechanism, the characteristics of soil has very important role. The behaviour of soil is predicted based on the engineering properties of soil, vertical soil profile and the alignment of ground surface.

2.3.1.1 Soil Properties

The behavior of soil is anisotropic, nonlinear and time dependent [38]. However, the soil parameters such as unit weight (γ), shear modulus (E_s), poisson's ratio (ν), shearing resistance angle (ϕ), effective cohesion (c) and angle of dilatancy (ψ) plays a very important role in representing the soil behaviour. Soil properties vary from very soft to very stiff consistency, based on which there will be changes in the soil-structure interaction. Most of the studies on LLP are conducted with piles embedded sandy soil [5, 29, 33, 34, 109]. Only a very few studies are available for LLP embedded in clay [112, 135, 140].

The engineering properties of soil could be found out using the standard test methods like ASTM, BIS methods [135]. Proper assessment of the properties of the soil is required for the prediction of the behaviour of the structure under external loading. It is also required for the accurate modeling of soil during numerical analysis. It was observed in certain studies that reduction in soil moisture content causes an increase the lateral soil resistance [66]. In clayey soil, studies revealed that drying the soil sample for affects the index properties and on the compressibility and the shear strength behaviour especially for clays in which Kaolinite is the major constituent [99,114].

The improvement of lateral capacity of pile can be achieved by compaction of surrounding soil and thereby reducing the number of piles and hence saving the cost [29, 101, 102]. This is true only upto a certain depth and it was found that when the thickness of densified soil increases beyond a certain height there is not much increase in lateral load.

2.3.1.2 Vertical Soil Profile

In the actual ground surface the vertical soil profile is always layered and the properties vary from layer to layer though it is considered to remain constant for a particular layer for the purpose of analysis [10]. For example in the

Winkler approach which considers the soil as a layered system to study the lateral resistance of piles, the soil pressure p is related to lateral deflection y through the modulus of subgrade reaction k_h of the particular layer,

$$p = k_h y \dots\dots\dots (2.4)$$

Various geotechnical engineers such as Terzaghi, Broms, Poulos, Matlock and Reese have suggested an equation for subgrade reaction in terms of E_s , the soil modulus and D , the diameter of the pile [108].

$$k_h = (0.48 \text{ to } 1.8) E_s / D \dots\dots\dots (2.5)$$

2.3.1.3 Alignment of Ground Surface

Generally a level ground surface is assumed in a soil structure system. But when the ground surface is sloping or when the slope of the ground is varying with time, it is found that the surface profile of the ground affects the structural behaviour of the pile. Hence if there is a sloping ground surface that should be taken into consideration while analyzing a soil-pile system.

Prediction of the behaviour of a laterally loaded pile could be obtained from the theoretical solution derived based on the force-equilibrium model of rigid piers embedded in cohesionless and $c-\phi$ soil profiles in sloping ground surfaces [32]. A parametric study indicated that the amount of reduction in load carrying capacity due to the slope is dependent on the value of the surface slope angle θ and soil strength properties. Later operating charts were developed using finite element method for estimating behaviour the slopes under different submergence conditions under complex geometries and properties of slope stability problems [67]. The charts developed using finite element method are claimed to be superior to the traditional charts of Morgenstern, used for the same purpose.

The load carrying capacity of a laterally loaded pile decreases as the bed slope increases [135]. The decrease in the load carrying capacity is due to the decrease in the resistance offered by soil at the top portion of the soil mass, as there is a reduction in soil mass due to the formation of sloping bed. It was found that as the slope increases there is an increase in the magnitude of maximum bending moment [14]. The increase in relative density is found to be significant for piles embedded in sloping ground [52]. The relative stiffness between the pile and soil has an importance in determining the failure mode of the pile [73]. It was also found that in a pile groups, with the increase in the pile spacing, the critical slip surface becomes deeper [149]. Scour can also cause reduction in lateral load carrying capacity [61, 62].

Researchers have developed relationships to predict the pile top displacement and the maximum bending moment of a laterally loaded pile in sloping ground based on the corresponding values for the piles embedded in horizontal ground [130]. Based on the experimental results it was concluded that slope reinforcement significantly increases the lateral capacity of pile groups. Geo-grid layer provided with sufficient length and breadth beyond the potential failure surface could improve the slope stability [131].

Sleeving can also be provided to minimize the transfer of lateral loads from the buildings to shallow depths of slopes [23]. The load transfer mechanism from the laterally loaded sleeved pile to sloping ground is through a shear load transfer mechanism in the vertical plane. Under large lateral loads, the influence of the sleeving on pile performance appears to diminish because of the wide spread plastic zone developed around the pile.

2.3.2 Characteristics of Pile

The characteristics of pile also play a very important role in determining the behaviour of pile under external loading. The characteristics of pile include the length of pile, stiffness of pile, and the arrangement of pile.

2.3.2.1 Flexibility of Pile

Based on the flexibility condition, piles can be categorized into short and long piles. The influence of pile length in the variation of bending moment was studied and it was concluded that short piles behave linearly and long piles behave nonlinearly [9]. Unlike long piles, in short piles maximum bending moment is affected by the length of the pile. It is also observed that in the displacement plots, the pile length could have a substantial influence on the maximum displacement at the pile end. However this influence decreases from a particular length. Beyond that length the pile is considered to be a long pile. Thus for a long pile the changes in the length of the pile will not considerably affect the displacement as well as bending moment.

2.3.2.2 Stiffness of Pile

Stiffness properties of a pile depend on the Young's modulus of the material of the pile and the cross sectional area or moment of inertia of the pile. The generally adopted material properties for pile foundations are concrete, steel and timber [109]. Depending upon the availability, cost and the strength requirements, a suitable material will be selected. In India concrete piles are widely used as onsite piles. Young's modulus of concrete is $E_c = 500(f_{ck})^{1/2}$.

Circular and square are the generally adopted cross sectional shapes of pile. Square shape is adopted for precast piles. Most of the cast in situ piles are circular in shape. Certain researchers has made a serendipitous finding that there is a significant shape factor affecting the ability of pile to mobilize soil resistance to lateral loads [39]. Under a given lateral load applied to free head piles having approximately equal moment of inertia, those having circular cross sections were more resistant to lateral movements than square or H-beam cross section. Investigations were also done to study the effect of pile shape for both circular and square cross section on pile response. In a particular study, the 1.2 m circular piles (M.I. = 0.03 m⁴) and 1.2 m sided square piles (M. I. = 0.05 m⁴) were

considered and it was concluded that square pile is more resistant to lateral load than a circular pile due to high contact surface area between the pile and the surrounding soil and due to high bending resistance [52].

2.3.2.3 Arrangement of Pile

Single pile arrangement or group pile arrangement can be adopted to transfer the structural load to the ground depending on the load to be transferred and the type of soil. Researches show that the average pile group response was softer than the single pile response. However the single pile test can be a good indicator of the pile group behaviour. It was also found that the p multipliers work well to account for the group effect [125,126].

Studies have already established the influence of pile group rigidity of laterally loaded pile in marine clay. The group efficiency under lateral loading is estimated from the ultimate lateral capacity of the pile group, Q_g and ultimate lateral capacity of single pile, Q_s for a group of 'n' number of piles using the formula,

$$\text{Lateral group efficiency} = \frac{Q_g}{nQ_s} \dots\dots\dots (2.6)$$

It was also concluded that short and rigid piles are more resistant to lateral loads when they are arranged in a parallel configuration than in a series, whereas the reverse is true in cases of long and flexible piles [88].

Researchers have developed p -multiplier concept which provides a reasonable means of accounting for the reduction in capacity produced by group effects and the resulting lateral group effect by considering the shadow stress zone and soil gapping as shown in Fig. 2.10 [48, 124, 125]. The studies show that p -multiplier is unity for pile spacing greater than 5D to 6D spacing.

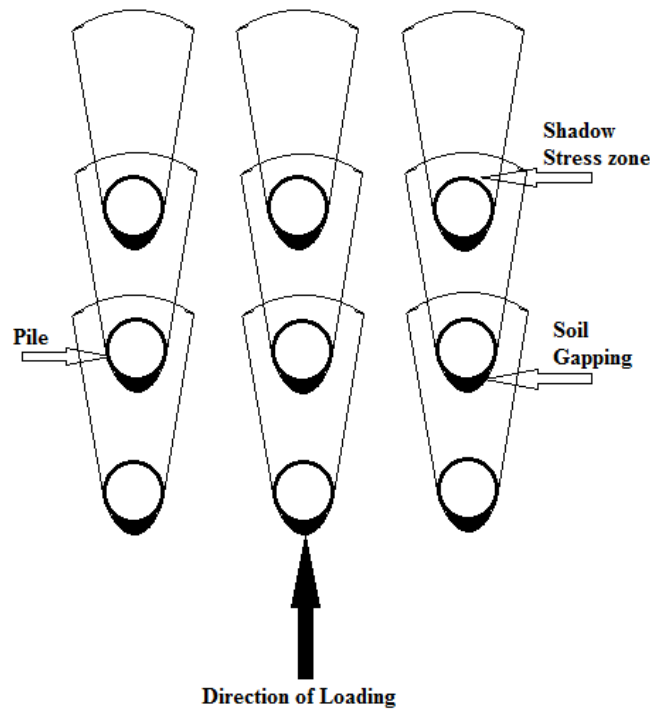


Fig. 2.10 Shadow Stress Zone and Gap Formation in LLP Group [124]

Certain studies show that the ultimate lateral capacity of pile group depends on the length to diameter ratio of pile, pile friction angle, pile group geometry, spacing of piles in a group and the sand placement density [93, 109]. The pile group deflection and the maximum bending moment under the same average load per pile were investigated to be twice as that of a single pile [124]. Experiments showed that in a pile group, trailing rows of piles carried less loads in comparison to leading rows of piles [1, 2]. Back calculated *p-multipliers* were 0.8 for front rows and 0.4 for trailing rows [123]. It is interesting to note that group interaction effects vanish after liquefaction [52]. Pile groups with pile cap showed more lateral resistance in comparison to free head piles and it was observed that pile cap contributed 40% of the total resistance [35, 125].

2.3.3 Type of Loading

The structure is designed to resist the external loads acting on it. The structure may be subjected to static or dynamic loading. The behaviour of the structure will be different under different loading conditions.

2.3.3.1 Static Loading

The magnitude and direction of the static loading on the structure are given the prime consideration while designing the pile foundations and the structure as a whole. Even though the pile material is considered to be linearly elastic, the nonlinear behaviour of soil is to be incorporated in the load-deflection analysis of piles.

The governing equation to represent pile under lateral static loading incorporating the bending stiffness of the pile (EI), subgrade modulus of soil (k) and deflection of the pile element considered (y) is expressed as [8, 20, 128],

$$EI \frac{\partial^4 y}{\partial x^4} - ky = 0 \dots\dots\dots (2.7)$$

Researchers have conducted full scale and model tests on laterally loaded piles subjected to static loading. The basic arrangement of a laterally loaded pile and soil resistance is shown in Fig. 2.11. Load will be applied at the pile top at regular intervals of time and the pile top deflections were noted [134,135]. Corresponding to each load the dial gauge reading at the top of the pile and the strain gauge readings along the length of the pile were studied. The bending moment (M) is proportional to strain gauge reading (ϵ) and hence the constant of proportionality 'C' is obtained from simple bending test. The relation thus obtained can be expressed as, [14]

$$M = C * \epsilon \dots\dots\dots (2.8)$$

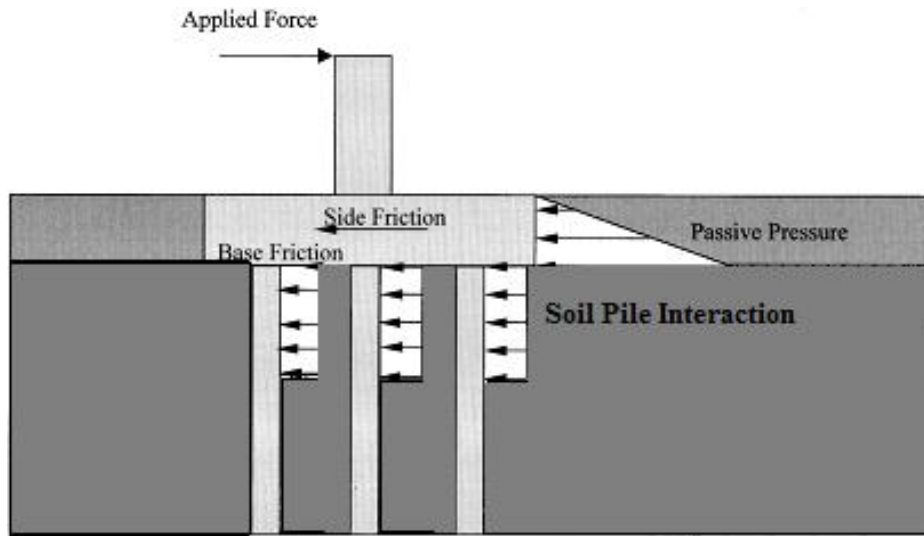


Fig. 2.11 Lateral Load and Components of Resistance offered by Soil-Pile System [125]

The influence of axial loads on the lateral response of piles was studied and it was found that the lateral deflection and the bending moment of the pile increased with the increase in axial load [53]. The influence of combined loading on lateral capacity decreases as the L/D ratio of the pile increases. The study was extended in layered soil and the variation of displacement along the depth of pile is studied. It was found that when a sand layer is present within a clay deposit, there is reduction in displacement and when a clay layer is present within a sand deposit there is increase in displacement [151].

2.3.3.2 Dynamic Loading

Dynamic loadings are time dependent in nature. The behaviour of structure under dynamic loading depends on the natural frequency of the structure. Hence the possible changes in the natural frequency of the structure with the changes in the soil and the structure are to be studied. The dynamic flexural differential equation of the pile under free vibration condition can be written as [36],

$$m_p \frac{\partial^2 y}{\partial t^2} + C_p \frac{\partial y}{\partial t} + K_{ds} Dy + E_p J_p \frac{\partial^4 y}{\partial x^4} + N_p \frac{\partial^2 y}{\partial x^2} = 0 \dots\dots\dots (2.9)$$

- Where, m_p - mass of the pile per unit length
 C_p - structural damping coefficient of the pile
 K_{ds} - dynamic stiffness of the soil
 E_p - young's modulus of pile
 J_p - polar moment of inertia of the pile
 N_p - axial load on pile
 y - lateral deflection of the pile.

The fundamental natural frequency of the pile for the first mode is,

$$f_1 = \frac{ak_1^2}{2\pi} \dots\dots\dots (2.10)$$

Where, $a = \frac{E_p J_p}{m_p}^{1/2}$, $k_1 = \frac{1.875}{l_e}$, l_e is the effective length of pile.

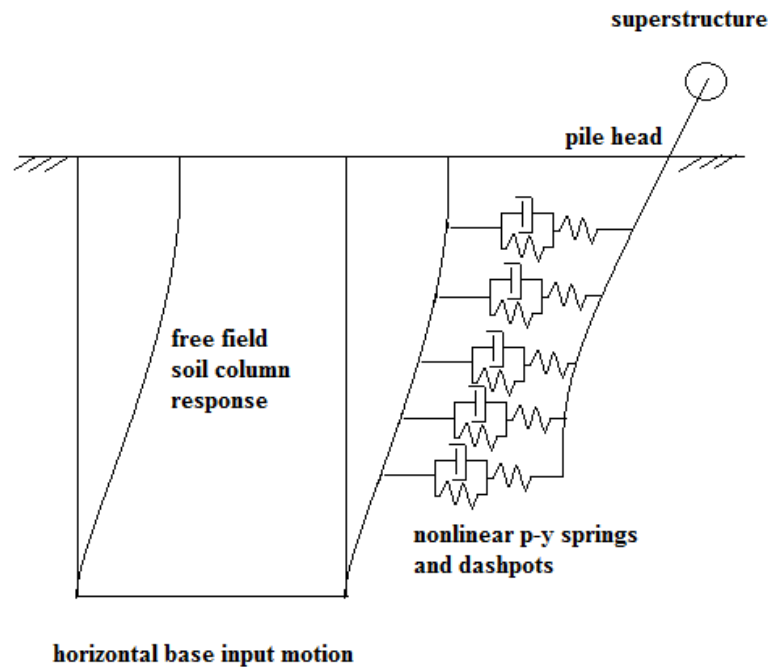


Fig. 2.12 Schematic Diagram of Dynamic *p-y* Analysis Model [18]

Dynamic *p-y* analysis was suggested for analyzing seismic soil-pile-structure interaction [18]. A simplified analytical model for the lateral harmonic response of single pile and pile group in layered soil was developed by Mylonakis

et al. [89]. The predictions of the model are in agreement with the earlier results, while its simplicity offers a versatile alternative to rigorous solutions. The governing equation for the vertical elastic pile embedded in winkler medium is,

$$\frac{d^4y}{dx^4} + 4\lambda^4y = \frac{q}{EI} \dots\dots\dots (2.11)$$

Where EI is the flexural rigidity of the pile, q is the distributed force along the pile and λ is the complex wave number associated with the propagation of flexural waves along the pile.

The soil pile system behaves predominantly in a nonlinear fashion close to the resonance region under dynamic loads [9, 10, 17]. The maximum dynamic BM is magnified by about 1.5 times the maximum static BM for model piles in clay. The maximum dynamic BM occurs at a depth of about 1.5 times the depth of maximum static BM for model piles, which indicates an increase of active length under dynamic load [17,22].

A new approach to model the material nonlinearity of soil media for the dynamic analysis of pile foundations is proposed by Maheshwari *et al.* [72]. They incorporated the effects of material nonlinearity of soil on the free field response which depend very much on the frequency of excitation [139]. Due to the material nonlinearity of the soil, at low frequencies (as compared to the natural frequency of the soil pile system) the seismic response increases as much as 30% and at higher frequencies the reverse is true.

2.4 Review on Analysis of Ship Berthing Structures

Muthukkumaran *et al.* have developed a numerical model for plain strain analysis of a berthing structure to simulate the effect of dredging and it was concluded that the numerical model developed in PLAXIS agree well with full scale field data [83]. Muthukkumaran *et al.* (2007) in another paper, have addressed the problem of generating lateral forces by the lateral soil movement due to dredging [84]. It was observed that lateral deflection of the berthing

structure increases due to dredging and it was also found to increase further during a course of three months. Hence it was concluded that the change in bed slope due to dredging causes an increase in lateral deflection of the berthing structure. Premalatha *et al.* have studied the influence of tie rod in reducing the lateral deflection of a berthing structure. The study was conducted using a two dimensional finite element program PLAXIS-2D, in which pile was modeled as a 5 node beam column element, soil as a 15 node element which incorporates Mohr-Coulomb's soil model and the structure was considered as a plane strain model. The studies optimize the length of tie rod for an optimum deflection of the structure [106]. Muthukkumaran *et al.* have analysed the influence of change in bed slope of Kandla port which was observed to change from 1V:3 H to 1V to 1.5H during a course of time. The influence of large forces due to mud slide during a course of earthquake was studied. It was observed that the magnitude of bending moment increases considerably when the bed slope increases from 1V:3 H to 1V to 1.5H. It was also concluded that the bending moment during earthquake condition is 58% higher than that of a pre-earthquake condition [87]. Premalatha *et al.* have studied the influence of tie rod in a berthing structure under lateral load by conducting a series of model tests. It was commented that mooring pull is much critical compared to other lateral loads in a berthing structure. The studies have concluded that the tie rods can carry a significant amount of lateral loads when the structure was embedded in sloping bed than in the case of a horizontal bed [105]. Mostofi *et al.* have studied the response of fixed and floating piers to ship berthing impact. The studies have developed a new approach for evaluating the berthing force in floating piers. In traditional methods for fixed piers the reaction force corresponding to energy absorption in fender is calculated as in references of design of piers, eg. Tsinker (1989, 2004), OCDI2009, PIANC2002, EAU2004 and etc.. It was concluded that the ratio of total static equivalent force to new method for floating piers to traditional method for fixed piers was around 2 to 2.5 [80]. Kelesoglu *et al.* have analysed full height bridge abutments on pile foundations installed through soft soils, with commercially available finite element software

PLAXIS 3D Foundation and the results were compared with the available centrifuge test results. The studies showed that even though the results were comparable, numerical results were lower than the measured values. Numerical findings revealed that arching of soil has a significant effect on the lateral loading of the abutment wall. The bending moment results obtained for front and rear rows of piles are found to be comparable in both the methods of analysis.

2.5 Summary

Based on the literature review following conclusions can be made:

- Properties of soil and pile, type of loading, analysis methods etc., play important roles in predicting the behavior of a soil-structure system.
- The five significant soil parameters are identified such as, unit weight (γ), shear modulus (E_s), poisson's ratio (ν), shearing resistance angle (ϕ), effective cohesion (c) and angle of dilatancy (ψ) which can contribute to soil behavior in a soil-structure system. Standard methods such as ASTM, BIS etc. should be adopted to quantify the above properties for the accurate analysis of the soil behavior.
- The vertical profile of soil is also very important in predicting the soil-pile behaviour. However, for simplicity in conducting various studies, soil profile may be considered to be either homogeneous or layered.
- The gradient of the ground surface is also significant in predicting the soil-pile behaviour under lateral load.
- Pile stiffness contributes towards the lateral load carrying capacity of pile. Stiffness of pile is mainly governed by the material property (E) and the moment of inertia of cross section (I) of the pile. Hence pile characteristics such as cross sectional shape, cross sectional area and material properties are also significant in the structural behaviour of laterally loaded piles.

- Seismic loads are considered to be the most complex dynamic loading condition. It could be studied in a simplified manner using sinusoidal loading condition. During the dynamic analysis of soil pile system, the variations in the natural frequency of the system with the variation in soil properties are to be studied and accounted.
- A softer soil consistency causes an increase in the depth of fixity of the pile which in turn decreases the natural frequency of the soil pile system.
- The method of analysis to study laterally loaded pile can be analytical, experimental or numerical investigation of soil-pile system. Each of the methods has its own advantages and disadvantages. Analytical formulations are much developed now-a-days which demands computer programs for the formulation and solution of the problem.
- Experimental investigations on field pile are found to be superior to all the other analysis methods. But it is found to be costly and time consuming. Experimental investigations using model test set up is a good alternative to study the present problem, if all the parameters involved in the study could be modeled using the laws of similitude.
- Numerical simulation and analysis of the problem solved using finite element or finite difference methods are becoming popular with the increasing computational power of computers and the availability of reliable software particularly designed by considering the influence of soil-structure interaction. Proper validation of model created in the numerical software could ensure better results.

Based on the classical theories, the failure of a flexible pile occurs when the moment at the depth of fixity of the pile exceeds the moment of resistance of the pile. According to the findings in the recent literatures it is found that only a few researchers have studied the effect of slopes on maximum bending moment

as well as the depth of fixity of laterally loaded piles embedded in clayey soil. Hence detailed analyses based on experimental, analytical and numerical investigations are needed to be carried out to study the variations in the structural behaviour of laterally loaded piles with the change in bed slope.

.....✂.....

Experimental Investigation

Contents	3.1 <i>Introduction</i>
	3.2 <i>Derivation of Scale Factors</i>
	3.3 <i>Feasibility Study of Model Test</i>
	3.4 <i>Materials and Instrumentation</i>
	3.5 <i>Test Setup and Procedure</i>
	3.6 <i>Plotting the Results</i>
	3.7 <i>Observations from the Experimental Investigation</i>
	3.8 <i>Summary</i>

3.1 Introduction

An extensive literature survey conducted in Chapter 2 recommends a detailed analysis of laterally loaded piles in sloping clay bed. Based on the previous studies of Gandhi *et al.* [29, 33, 35, 134, 135], it is decided to adopt 1g model tests in line with the procedure suggested in literature. The load-deflection curves and the bending moment diagrams are plotted and studied. Using appropriate scaling laws, the observed and measured parameters can be extrapolated to that of a prototype.

3.2 Derivation of Scale Factors

Dimensional analysis is essential to 1g modeling in geotechnical engineering. The basic principle is that any particular phenomenon can be described by a dimensionless group of the principal variables. Similarity between the model and the prototype is ensured when the dimensionless group has the same value in the model and prototype.

Model analysis is done using the principle of similitude so that a model pile considered represents a realistic prototype. Premalatha *et al.* [106] have also adopted this method for modeling the test setup similar to the present investigation. Dimensional analysis can be done using Buckingham's π - theorem or using Rayleigh method. Both the methods derives the same relation among the physical quantities as follows,

$$\frac{y}{D} = f\left(\left(\frac{PD^2}{EI}\right), \left(\frac{L}{D}\right), \left(\frac{cD^4}{EI}\right), \left(\frac{h}{D}\right)\right) \dots \dots \dots (3.1)$$

The detailed procedure is as follows.

3.2.1 Buckingham's π - theorem

The Buckingham's π - theorem states that if there are n dimensional variables involved in a phenomenon which can be completely described by m fundamental quantities or dimensions (such as mass, length, time etc.) and are related by a dimensionally homogeneous equation then the relationship among n quantities can always be expressed in terms of exactly $(n-m)$ dimensionless and independent π terms. The method is now illustrated in the present case study.

Step 1:

The physical quantities involved in the study are,

y = pile deflection (L)

P = applied lateral load (F)

D = outside pile diameter (L)

L = pile length (L)

EI = flexural rigidity (FL^2)

c = soil cohesion (F/L^2)

h = height of applied load from the ground surface (L)

It can be written in general form as,

$$f_1(y, P, D, L, EI, c, h) = C \dots\dots\dots (3.2)$$

Thus the total number of variables is seven and these variables may be completely described by the two fundamental dimensions F and L in F-L-T system. Since there are seven variables (n) and two fundamental dimensions (m), there should be five ($n-m=5$) dimensionless π terms. Hence,

$$f_2(\pi_1, \pi_2, \pi_3, \pi_4, \pi_5) = C_1 \dots\dots\dots (3.3)$$

Step 2:

In order to form these π -terms, we have to choose two repeating variables since in this case $m=2$. As stated earlier these variables should be such that they, among them, contain all the fundamental dimensions and they themselves do not form a dimensionless parameter. Thus let us choose EI (FL^2) and D (L) as repeating variables, since the above noted requirements are fulfilled by these variables.

Step 3:

Since the physical quantities of dissimilar dimensions can neither be added nor subtracted the terms are expressed as a product as follows.

$$\pi_1 = EI^{a_1} D^{b_1} y \dots\dots\dots (3.4a)$$

$$\pi_2 = EI^{a_2} D^{b_2} P \dots\dots\dots (3.4b)$$

$$\pi_3 = EI^{a_3} D^{b_3} L \dots\dots\dots (3.4c)$$

$$\pi_4 = EI^{a_4} D^{b_4} c \dots\dots\dots (3.4d)$$

$$\pi_5 = EI^{a_5} D^{b_5} h \dots\dots\dots (3.4e)$$

Step 4:

Expressing π dimensionally in F-L-T system, $\pi = F^0 L^0$. Expressing equation numbers (3a) -3(e) in F-L-T system and equating the exponents of F and L of equation and solving,

Table 3.1 Derivation of π -terms

$\pi_1 = EI^{a1} D^{b1} y$	$F^0 L^0 = (FL^2)^{a1} L^{b1} L$	$a1 = 0$ $2a1 + b1 + 1 = 0$	$a1 = 0$ $b1 = -1$	$\pi_1 = EI^0 D^{-1} y$ $\pi_1 = \frac{y}{D}$
$\pi_2 = EI^{a2} D^{b2} P$	$F^0 L^0 = (FL^2)^{a2} (L)^{b2} (F)$	$a2 + 1 = 0$ $2a2 + b2 = 0$	$a2 = -1$ $b2 = 2$	$\pi_2 = EI^{-1} D^2 P$ $\pi_2 = \frac{PD^2}{EI}$
$\pi_3 = EI^{a3} D^{b3} L$	$F^0 L^0 = (FL^2)^{a3} (L)^{b3} (L)$	$a3 = 0$ $2a3 + b3 + 1 = 0$	$a3 = 0$ $b3 = -1$	$\pi_3 = EI^0 D^{-1} L$ $\pi_3 = \frac{y}{D}$
$\pi_4 = EI^{a4} D^{b4} c$	$F^0 L^0 = (FL^2)^{a4} (L)^{b4} \left(\frac{F}{L^2}\right)$	$a4 + 1 = 0$ $2a4 + b4 - 2 = 0$	$a4 = -1$ $b4 = 4$	$\pi_4 = EI^{-1} D^4 c$ $\pi_4 = \frac{cD^4}{EI}$
$\pi_5 = EI^{a5} D^{b5} h$	$F^0 L^0 = (FL^2)^{a5} (L)^{b5} (L)$	$a5 = 0$ $2a5 + b5 + 1 = 0$	$a5 = 0$ $b5 = -1$	$\pi_5 = EI^0 D^{-1} h$ $\pi_5 = \frac{h}{D}$

Step 5:

Since, $f_2(\pi_1, \pi_2, \pi_3, \pi_4, \pi_5, \pi_6, \pi_7) = C_1$

Substituting the π terms in the above equation,

$$f_2\left(\frac{y}{D}, \frac{PD^2}{EI}, \frac{L}{D}, \frac{cD^4}{EI}, \frac{h}{D}\right) = C_1$$

OR

$$\frac{y}{D} = f\left(\left(\frac{PD^2}{EI}\right), \left(\frac{L}{D}\right), \left(\frac{cD^4}{EI}\right), \left(\frac{h}{D}\right)\right) \dots\dots\dots (3.5)$$

3.2.2 Rayleigh Method

It is proposed by Lord Rayleigh in 1899. In this method a functional relationship of some variables is expressed in the form of an exponential equation which must be dimensionally homogeneous. Thus if X is some function of variables x_1, x_2, \dots, x_n then the functional equation can be written in the following general form,

$$X = f(x_1, x_2, \dots, x_n) \dots \dots \dots (3.6)$$

In this equation X is a dependent variable while x_1, x_2, \dots, x_n are independent variables. A dependent variable is the one about which information is required while independent variables are those which govern the variation of dependent variables. The above equation can be expressed as,

$$X = K(x_1^a x_2^b x_3^c \dots x_n^n) \dots \dots \dots (3.7)$$

Where, K is a dimensionless constant which may be determined from the physical characteristics of the problem or from experimental measurements. The exponents a, b, c, \dots, n are then evaluated on the basis that the equation is dimensionally homogeneous. The dimensionless parameters are then formed by grouping together the variables with like powers.

The method is now adopted in the present case study and the physical properties involved in the study are,

y = pile deflection (L)

P = applied lateral load (F)

D = outside pile diameter (L)

L = pile length (L)

EI = Flexural rigidity (FL^2)

c = soil cohesion (F/L^2)

h = height of applied load from the ground surface (L)

The functional relationship in this method can be expressed as follows,

$$y = K(P^a D^b L^c (EI)^d c^e h^f) \dots\dots\dots (3.8)$$

Where, K is a dimensionless quantity. Substituting the proper dimensions for each variable in the exponential equation in F-L-T system,

$$(L) = F^0 L^0 \left((F)^a (L)^b (L)^c (FL^2)^d \left(\frac{F}{L^2}\right)^e (L)^f \right) \dots\dots\dots (3.9)$$

For dimensional homogeneity the exponents of each dimension on both sides of the equation must be identical. Thus, from equation no. (3.9)

$$\text{For F: } 0 = a + d + e \dots\dots\dots (3.10)$$

$$\text{For L: } 1 = b + c + 2d - 2e + f \dots\dots\dots (3.11)$$

Since there are seven unknown constants and two equations, two of the unknown constants must be expressed in terms of the other five unknown constants. From equation no. (3.10) and (3.11),

$$d = -(a + e) \dots\dots\dots (3.12)$$

$$1 = b + c + 2[-(a + e)] - 2e + f \dots\dots\dots (3.13)$$

Hence,

$$b = 1 + 2a + c + 4e - f \dots\dots\dots (3.14)$$

Substituting equation no. (3.12) and (3.14) in (3.8),

$$y = K(P^a D^{(1+2a+c+4e-f)} L^c (EI)^{-(a+e)} c^e h^f)$$

$$y = K \left(D^1 \left(\frac{PD^2}{EI}\right)^a \left(\frac{L}{D}\right)^c \left(\frac{cD^4}{EI}\right)^e \left(\frac{h}{D}\right)^f \right)$$

OR

$$\frac{y}{D} = f \left(\left(\frac{PD^2}{EI}\right), \left(\frac{L}{D}\right), \left(\frac{cD^4}{EI}\right), \left(\frac{h}{D}\right) \right) \dots\dots\dots (3.15)$$

3.2.3 Scale Factors for the Present Study

Considering the above two methods of model analysis the π -terms are,

$$\pi_1 = \frac{y}{D} \dots \dots \dots (3.16 \text{ a})$$

$$\pi_2 = \frac{PD^2}{EI} \dots \dots \dots (3.16 \text{ b})$$

$$\pi_3 = \frac{L}{D} \dots \dots \dots (3.16 \text{ c})$$

$$\pi_4 = \frac{cD^4}{EI} \dots \dots \dots (3.16 \text{ d})$$

$$\pi_5 = \frac{h}{D} \dots \dots \dots (3.16 \text{ e})$$

The scale factors (λ) are established by equating the model π -terms with the prototype π -terms (*ie.* $\lambda = (L/D)_p / (L/D)_m$). Since cohesion is not a function of soil stress, it need not be scaled and hence the test soil is same as the prototype soil.

For the present study model piles are selected with two different diameters (19 mm, 25.4 mm) and three different lengths (600 mm, 700 mm, 800 mm). The π -terms will be same for both model and prototype. Considering equation no. (3.16c),

$$\left(\frac{L}{D}\right)^m = \left(\frac{L}{D}\right)^p \dots \dots \dots (3.17)$$

Where, $\left(\frac{L}{D}\right)^m$ is the length to diameter ratio of model and $\left(\frac{L}{D}\right)^p$ is the length to diameter ratio of prototype. Assuming a prototype pile diameter of 1000 mm and a concrete mix of grade M30, the following dimensions of prototype pile can be modeled using the model analysis of the present study.

$$\begin{aligned}
 \text{Consider } L_m = 600 \text{ mm and } D_m = 19 \text{ mm then } \left(\frac{L}{D}\right)^m &= \frac{600}{19} \\
 &= 31.58, \text{ since } \left(\frac{L}{D}\right)^m \\
 &= \left(\frac{L}{D}\right)^p \text{ and considering a field pile with diameter } D_p \\
 &= 1000 \text{ mm, } L_p \text{ is calculated as } 31580 \text{ mm} = 31.58 \text{ m}
 \end{aligned}$$

Table 3.2 Length of Prototype Piles used in the Present Model Tests

L_m (mm)	D_m (mm)	$\left(\frac{L}{D}\right)^m$	D_p (mm)	L_p (mm) = $\left(\frac{L}{D}\right)^m * D_p$
600	19.00	31.58	1000	31.58e3
700	19.00	36.84	1000	36.84e3
800	19.00	42.10	1000	42.10e3

Keeping the length corresponding to 600 mm, 700 mm and 800 mm as 31.58 m, 36.84 m and 42 m the diameter of the field pile corresponding to 25.4 mm is calculated as 1337 mm.

Table 3.3 Diameter of Prototype Piles used in the Present Model Tests

L_m (mm)	D_m (mm)	L_p (mm)	$\left(\frac{L}{D}\right)^m$	D_p (mm) = $L_p / \left(\frac{L}{D}\right)^m$
600	25.40	31.58e3	23.62	1337
700	25.40	36.84e3	27.56	1337
800	25.40	42.10e3	31.50	1337

Similarly, considering equation no. (3.16.e),

$$\left(\frac{h}{D}\right)^m = \left(\frac{h}{D}\right)^p \dots \dots \dots (3.18)$$

Table 3.4 Height of Prototype Pile above the Ground Level

h_m (mm)	D_m (mm)	$\left(\frac{h}{D}\right)^m = \left(\frac{h}{D}\right)^p$	h_p (mm)	D_p (mm)
50	19.00	2.63	2.63e3	1000
50	25.40	1.97	2.63e3	1337

Considering equation no. (3.16.e),

$$\left(\frac{PD^2}{EI}\right)^m = \left(\frac{PD^2}{EI}\right)^p \dots \dots \dots (3.19)$$

Table 3.5 Scale factors to calculate Load on Prototype Pile

P_m (N)	D_m (mm)	E_m (N/mm ²)	I_m (mm ⁴)	$\left(\frac{PD^2}{EI}\right)^m = \left(\frac{PD^2}{EI}\right)^p$
10 N	19.00	70e3	2298.21	2.24e-5
150 N	19.00	70e3	2298.21	33.66e-5
10 N	25.40	70e3	5716.54	0.90e-5
150 N	25.40	70e3	5716.54	13.53e-5

$$E_p = E_c = 5000\sqrt{f_{ck}}(IS\ 456\ code) = 5000\sqrt{30} = 25743 = 26000$$

Table 3.6 Load on Prototype Pile

$\left(\frac{PD^2}{EI}\right)^m = \left(\frac{PD^2}{EI}\right)^p$	D_p (mm)	E_p (N/mm ²)	I_p (mm ⁴)	P_p (N)
2.24e-5	1000	26000	4.91e10	28.6e3
33.66e-5	1000	26000	4.91e10	429.7e3
0.90e-5	1337	26000	15.69e10	20.5e3
13.53e-5	1337	26000	15.69e10	308.8e3

By performing a lateral load analyses of the prototype pile and correlating it with the model test, scale factors for the output deflection could be obtained

[i.e. $\lambda_y = (y/D)_p / (y/D)_m$) In the present study, the prototype analyses is done in PLAXIS-3D and the use of scale factor is verified.

To verify the model analysis three model tests and three prototype tests are done in PLAXIS-3D with the following specifications. Model pile is having 19 mm diameter, 600 mm length, 50 mm height above the ground level subjected to 50N, 100 N and 200 N lateral loads. The corresponding prototype pile is having 1000 mm diameter, 31500 mm length and 2630 mm height above the ground level subjected to 143 N, 286 N and 572 N lateral loads. Dimensions in model pile are converted to prototype pile dimensions as per the similitude obtained.

The analysis was done in PLAXIS-3D and the scale factor is obtained by keeping the model pile with 100 N as the reference.

$$\text{The scale factor } \lambda_y = (y/D)_p / (y/D)_m = \left(\frac{6.8}{1000} \right) / \left(\frac{3.455}{19} \right) = 0.037 \dots (3.20)$$

Table 3.7 Comparison of Deflection of Prototype Piles used using Model Analysis and Analysis of PLAXIS-3D Model

$y_m, \text{ mm}$ ($P_m \text{ N}$)	$D_m (\text{mm})$	$D_p (\text{mm})$	Predicted $y_p (\text{mm})$	$y_p, \text{ mm}$ ($P_p \text{ kN}$) (PLAXIS-3D)
1.5 (50 N)	19.0	1000	2.9	3.6(143 kN)
3.455 (100 N)	19.0	1000	-	6.8(286 kN)
7.763 (200 N)	19.0	1000	15.1	14.4(572 kN)

A strict parallelism may not be maintained between the model pile and the prototype pile, because the results of the model pile tests will be compared to the predictions made by the finite element SSI analysis software PLAXIS-3D. Once the software is validated for the experiments conducted, it can be used for further extension of present study.

3.3 Feasibility Study of Model Test

An experimental study on model pile in sloping sandy soil bed is conducted to understand the behaviour of a laterally loaded pile as well as to verify the feasibility of a model test.

3.3.1 Experimental Setup

The arrangement of test setup used for the feasibility study of the model test is shown in Fig.3.1. To maintain a uniform density all through the tank depth, sand was placed in the tank from a constant height of about 0.5 m. Natural slope of sand (1V:1.456 H) was maintained. Model pile was placed after filling a base layer of 15cm height. Sand was placed in such a way that pile comes at the crest of the slope. After filling the tank, the upper surface of sand was leveled. The lateral load was applied to the pile top through a pulley arrangement with flexible wire. The other end of the wire was attached to the loading apron. Load was applied by dead weight over the loading pan starting from the smallest with gradual increase in steps. To measure the lateral and vertical deflection dial gauges with a sensitivity of 0.01 mm were used. When step by step lateral loads were applied on the pile it was deflected in the direction of the lateral load and the dial gauge readings and the corresponding loads were recorded.

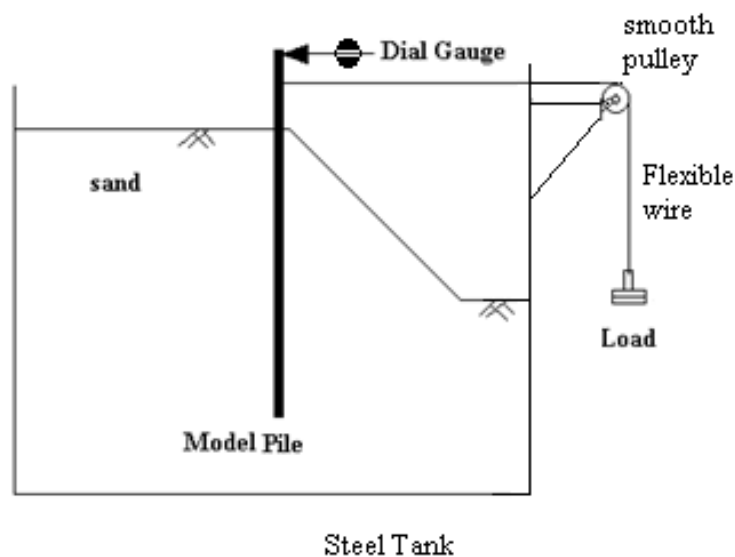


Fig. 3.1 Schematic Diagram of the Experimental setup

The model pile was a steel hollow pipe of 25.4 mm outer diameter and 2mm thickness. The experiment was done with an L/D ratio of 25. The embedded length of pile was 635mm. The lateral load was applied at a height of 75 mm above the ground level. The soil sample used was river sand with a placement density of 1.575 g/cc and specific gravity 2.63. Since the embedded length 635 mm is more than 15 times the diameter (25.4 mm) of the pile, it is a long pile. A natural slope was formed in the tank.



Fig. 3.2 Experimental Setup

3.3.2 Results

The ultimate lateral resistance of the pile was found out by plotting the lateral load Vs deflection curve (Fig.3.3). At the ultimate resistance, pile showed some deflection without any increase in load and this load was taken as ultimate load for the pile. The curve obtained follows the standard pattern of load deflection curve for a pile subjected to lateral load. At 109 N lateral load the pile was showed a large deflection and it was taken as the ultimate load.

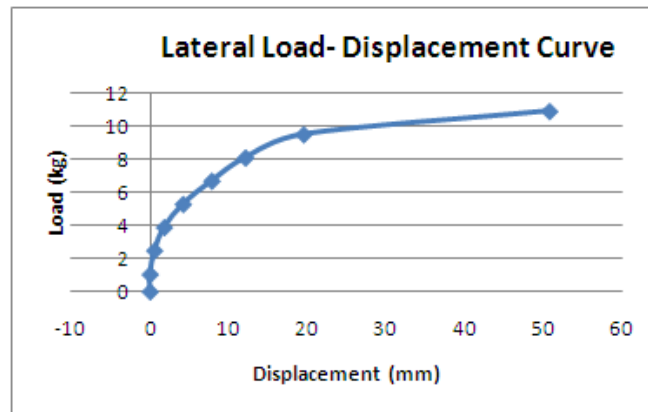


Fig. 3.3 Lateral Load Vs Deflection Curve

3.3.3 Inference based on Feasibility Study

The behaviour of a single laterally loaded pile in sloping ground was observed through a model study. Load-Displacement curve is in good agreement with the same obtained in literatures. Hence it is decided to continue the work in clayey soil sample for a detailed investigation of soil structure interaction analysis of laterally loaded piles.

3.4 Materials and Instrumentation

The experimental investigation is carried out in model test piles embedded in sloping clay bed. The model test piles are instrumented with strain gauges to measure the strain variation along the length of the pile. Preparation of soil sample and calibration of the strain gauges are to be done prior to the conduct of experiments.

3.4.1 Preparation of Soil Sample

Dredged clayey soil is collected from Vallarpadam near Cochin Port. It was sundried and powdered. The presence of large sized particles may adversely affect the model test results. Hence the soil was sieved through 500 micron sieve and used for the test.



Fig. 3.4 Sundrying and powdering of soil sample

Laboratory tests were conducted on soil sample to determine the Atterberg limits, specific gravity and other properties as per Indian standards IS 2720 and is included in Appendix-A.

3.4.2 Specifications of Strain Gauge

Electrical resistance type strain gauges were used for the study. It consists of a grid of very fine wire that is bonded to a surface. The overall size of the strain gauge is about 2 cm long. The image below shows an example of strain gauge used for the present model study. The strain gauge has two terminals that are the ends of the long piece of wire. The material that the strain gauge is mounted to is called the backing or carrier matrix. This material is flexible like a thin piece of plastic tape but durable so that it can hold the strain gauge wire in its proper position. The backing also is the material that the adhesive is applied to so that the strain gauge can be glued into place. On loading, the strain gauge stretches along with the surface and the resistance of the wire changes. It was measured and the change in resistance is converted to strain along the material on which strain gauge is pasted.

The strain gauges used for the present model study were having gauge length 5mm, gauge factor 2 and resistance 120 Ω . Strain gauges were always pasted on the tension side of the pile to exhibit the maximum elongation on

loading. They were pasted with the axis of the strain gauge parallel to the axis of the pile.

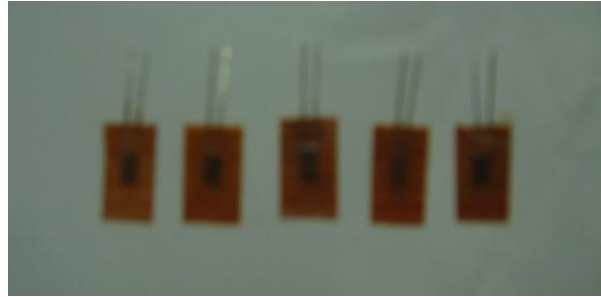


Fig. 3.5 Strain Gauges

3.4.3 Model Pile Instrumentation with Strain Gauge

Aluminium pipes having outer diameter 25.4 mm and 19 mm with 1 mm wall thickness were used as model piles. Both the ends of the pile were closed with wooden cap to prevent soil to enter into the pile. The surface of the pile was cleaned and the strain gauges were pasted at the tension side of the pile with the axis of strain gauge parallel to the axis of pile. Special epoxy cyanoacrylate super glue, Fevikwik was used to paste the stain gauge to the surface of aluminium pile. The lead wires of strain gauges were then soldered to the wire, which is to be connected to the channel of data logger. Strain gauges were well insulated to prevent the entrance of moisture into it.

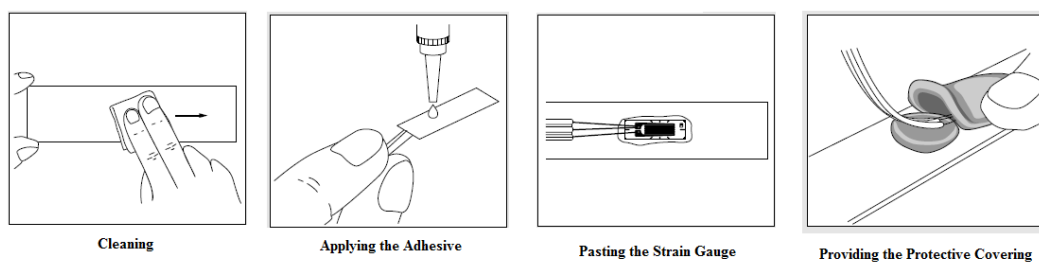


Fig. 3.6 Typical Strain Gauge Bonding Method and Damp-proofing Treatment

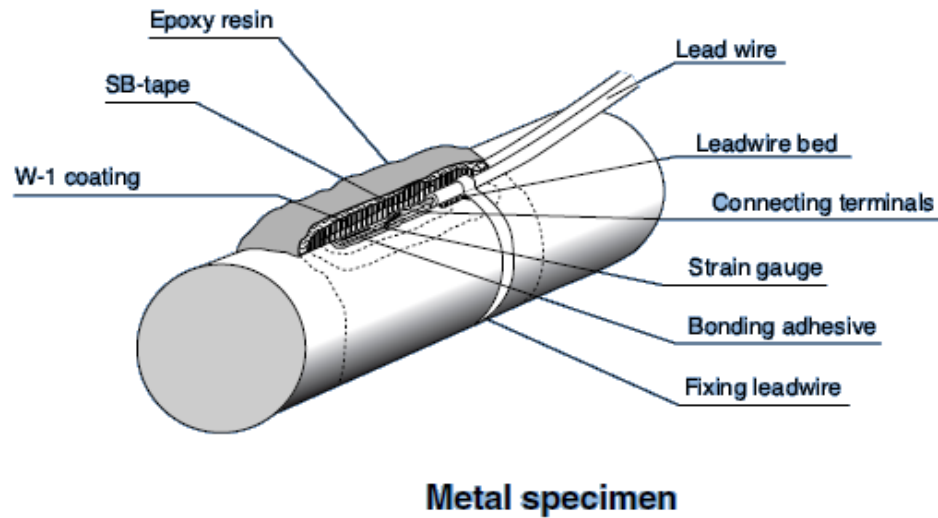


Fig. 3.7 Typical Installation with Bonding to Metal Surface in Wet Condition



Fig. 3.8 Model Pile instrumented with Strain Gauge

3.4.4 Calibration of Strain Gauge

Strain gauges were calibrated using a two point bending test for the calculation of bending moment along the pile length. The details of bending test for 25.4 mm diameter and 1000 mm length aluminium pile are described below. The pile is arranged with two points loading at quarter span from both the

support of the pile. Strain gauges were pasted on the tension side of the pile with the axis of the strain gauge parallel to the axis of the pile.



Fig. 3.9 Bending Test Setup

For each load increment the corresponding reading on the data logger and the deflection at the centre of the pile were recorded. Data logger reading gives the micro strains on the pile. The readings are tabulated in Table 3.8. A typical bending moment – strain curve is plotted in Fig.3.10 and it is found that the strain response is linear with the bending moments for the applied loads. The bending constant is obtained from the slope of the calibration curve and is equal to 35.7 Nmm per microstrain.

Table 3.8 Strain Gauge Calibration Data

Load, W (N)	Strain (10e-6 mm/mm)	Bending Moment, $\frac{WLe}{4}$ (Nmm)
0.00	0	0
0.74	2	178.752
2.12	14	508.032
3.49	25	837.312
4.88	33	1171.296
6.27	39	1505.28

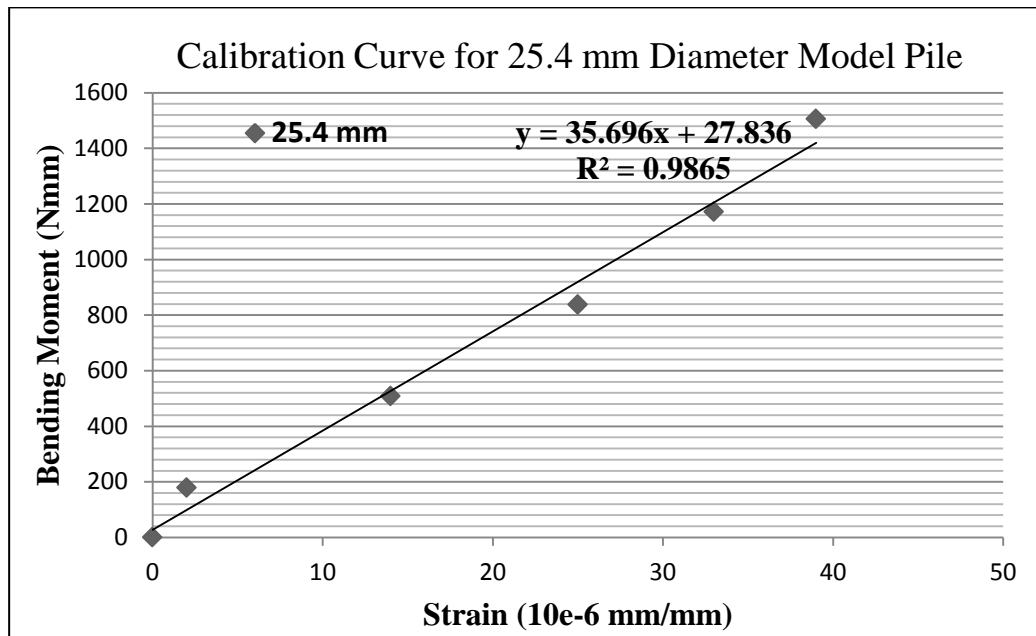


Fig. 3.10 Strain Gauge Calibration Curve for 25.4 mm Diameter Model Pile

Hence to calculate bending moment from the strain gauge reading the following equation is adopted.

$$M = C\varepsilon \dots\dots\dots (3.21)$$

Where, M = bending moment at various depths (Nmm)

C = bending constant (Nmm per microstrain)

ε = microstrain (10e-6 mm/mm)

The bending constant for 25.4 mm pile is calculated to be 35.7 Nmm per microstrain and that of 19 mm pile is calculated to be 20.1 Nmm per microstrain. (Appendix-B.1)

3.4.5 Working of Data Logger

Model piles instrumented with strain gauges are subjected to lateral loads. As a result the pile gets deflected and the deflection of piles causes elongation of strain gauges pasted in the tension side of the pile. As the strain gauges get elongated the resistance of the strain gauge wire increases. A data logger is an

electronic device used to convert the change in resistance in strain gauges into micro strains.

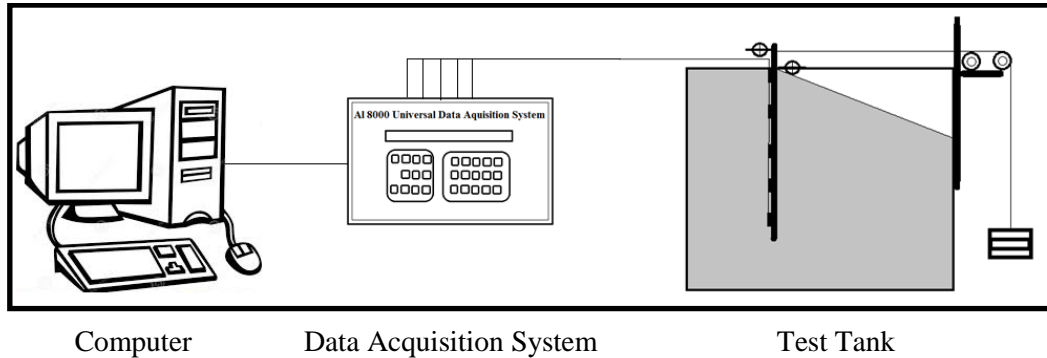


Fig. 3.11 Data Logger Arrangement in Test Setup

3.5 Test Setup and Procedure

A test tank with dimensions 1 m X 1 m X 0.6 m is used for the model test. It is made with mild steel sections and plate. One of the sides of the tank is kept transparent by using 10 mm thick acrylic sheet, to allow visibility of soil packed inside the tank. The uniform packing of soil can be seen in Fig.3.14. Soil bed is prepared with unit weight of 1.778 g/cc [65].



Fig. 3.12 Weighing and Placing soil in the tank



Fig. 3.13 Packing of soil in 10 cm layers



Fig. 3.14 Soil Packed in the Tank

Soil required for filling 10 cm height of test tank was weighed and placed inside the tank. It was then packed to the required height of 10 cm. Similarly the subsequent layers were also filled. The soil-pile was completely removed after each test and the tank was refilled as per the specifications.

The model piles preinstalled with strain gauges were placed in the tank with a minimum bottom clearance of four times the pile diameter [68]. The loading pulley was placed 50 mm above the level soil surface. The pulley was greased properly to avoid frictional loss of the lateral load. Lateral load was applied using static weight at free end of the flexible wire starting from the pile top. Each load increment was maintained for 15 minute time interval to stabilize the displacement without any movement. The horizontal displacement of the pile top and the point at the level ground were measured using mechanical dial gauges of 0.01mm sensitivity.



Fig. 3.15 Dial Gauges fixed at top of the pile and at the ground level

A static lateral loads of 10 N was applied and maintained for 15 minutes. The corresponding dial gauge reading and the strain gauge readings were noted. The load was applied in increments of 10 N. The details are included in Appendix-B.2.

3.6 Plotting the Results

Based on twelve model tests on model piles of three different lengths, two different diameters and two different bed slopes, the bending moment variation along the length of the pile and load-deflection curves were plotted and studied (Fig. 3.16 and Fig.3.17).

The twelve model tests consist of model piles with length 600 mm, 700 mm, and 800 mm with 50 mm projection above the ground level having two different diameters 19 mm and 25.4 mm embedded in two different bed slope of 1:2 and 1:1.5.

3.6.1 Load Deflection Diagrams

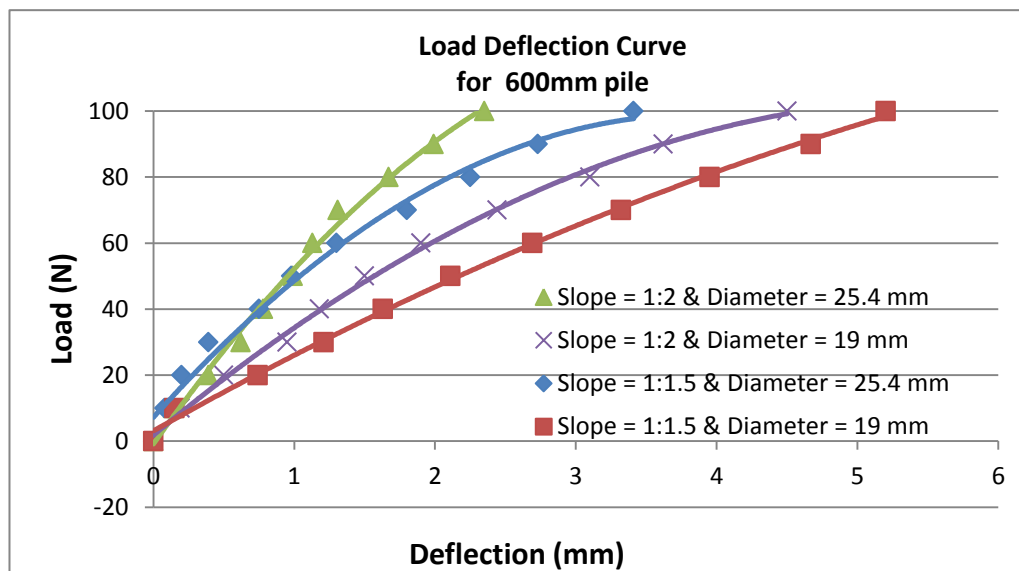


Fig. 3.16.a Load Deflection Curve of Model Piles with Length 600 mm

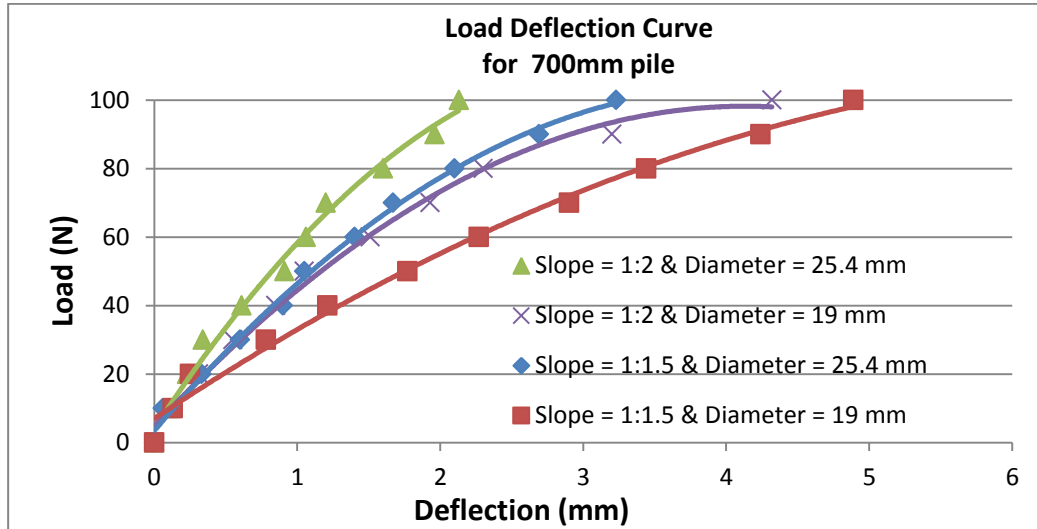


Fig. 3.16.b Load Deflection Curve of Model Piles with Length 700 mm

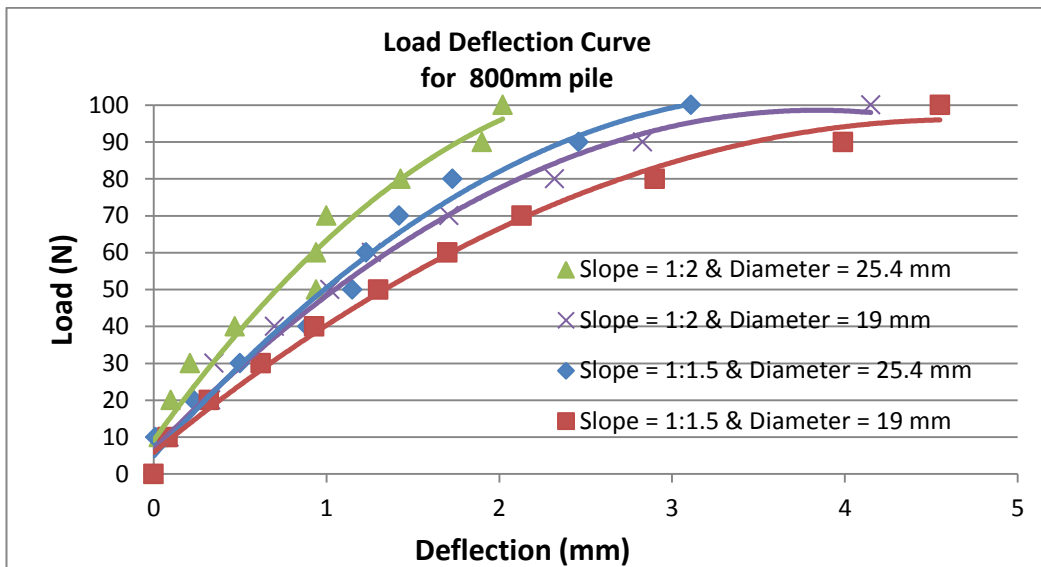


Fig. 3.16.c Load Deflection Curve of Model Piles with Length 800 mm

3.6.2 Bending Moment Diagrams

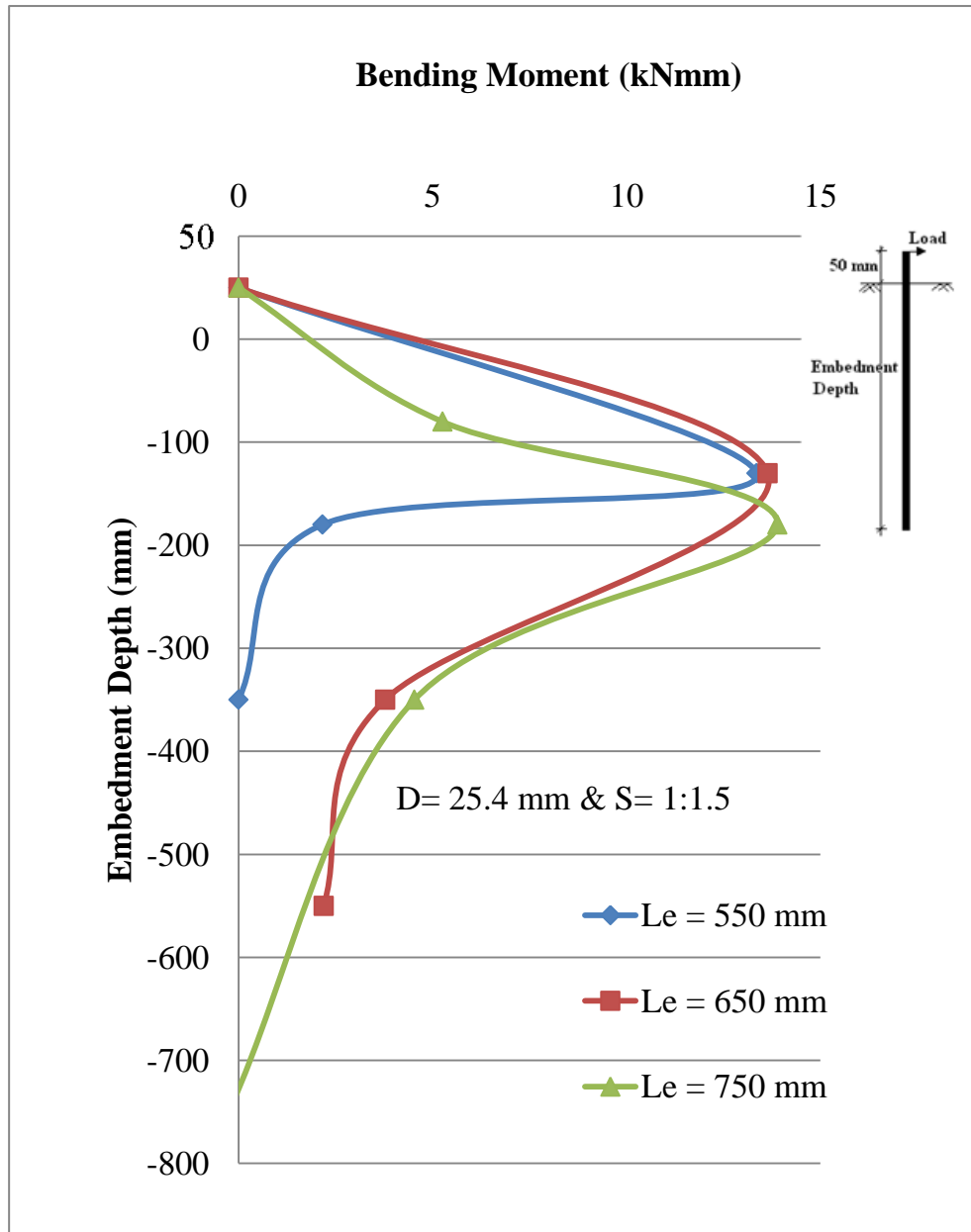


Fig. 3.17.a Bending Moment Variation in Model Piles (D= 25.4 mm & S= 1:1.5)

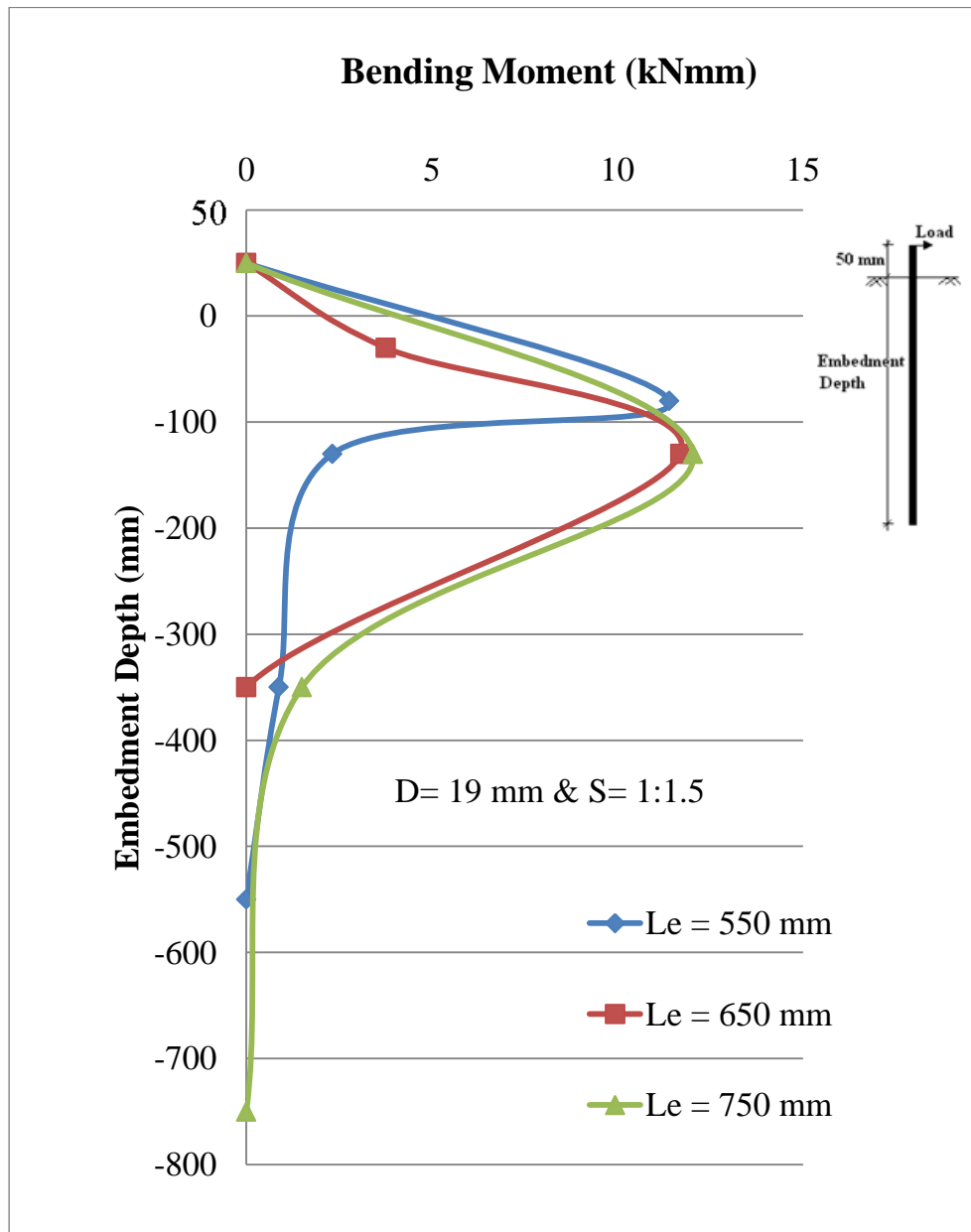


Fig. 3.17.b Bending Moment Variation in Model Piles (D= 19 mm & S= 1:1.5)

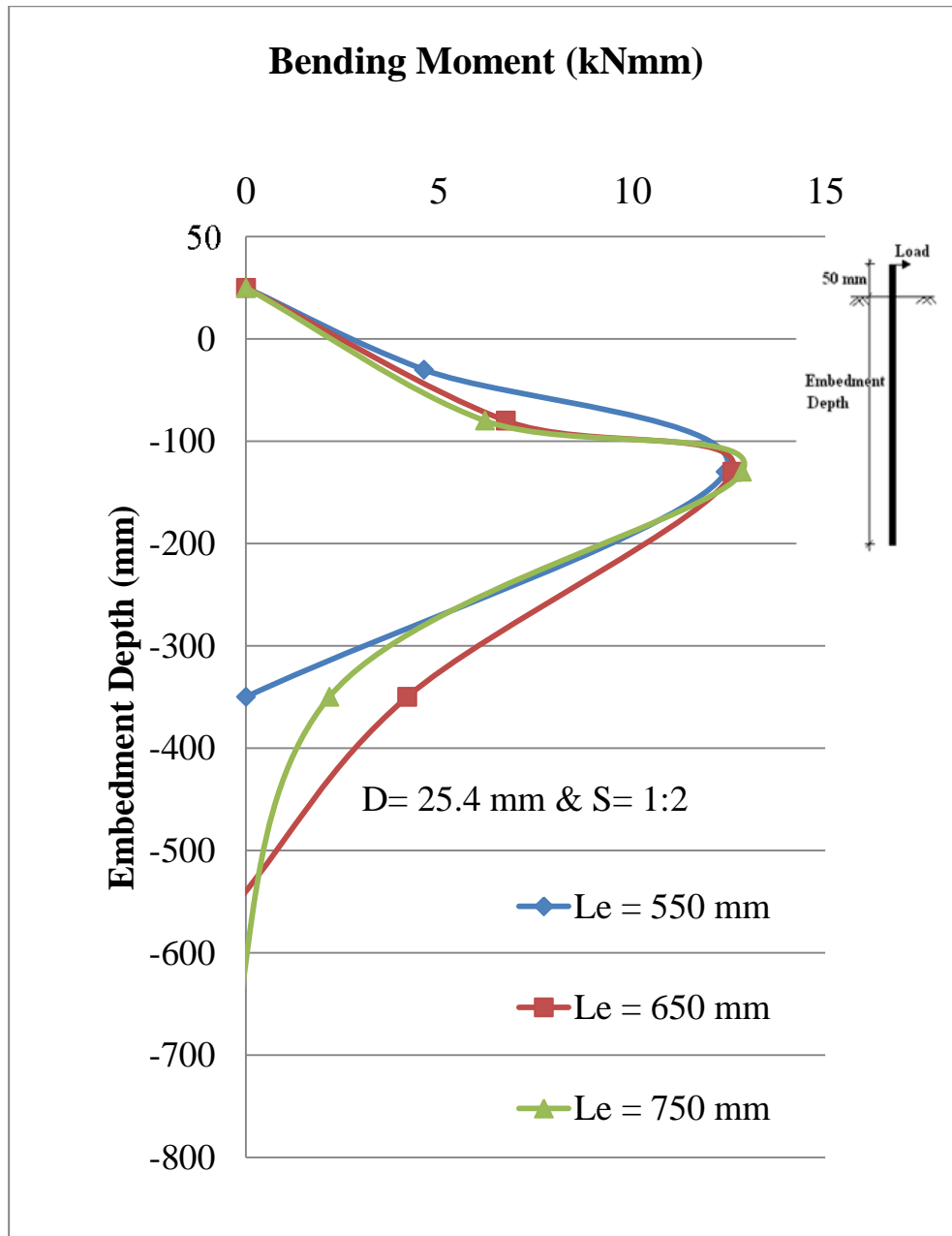


Fig. 3.17.c Bending Moment Variation in Model Piles (D= 25.4 mm & S= 1:2)

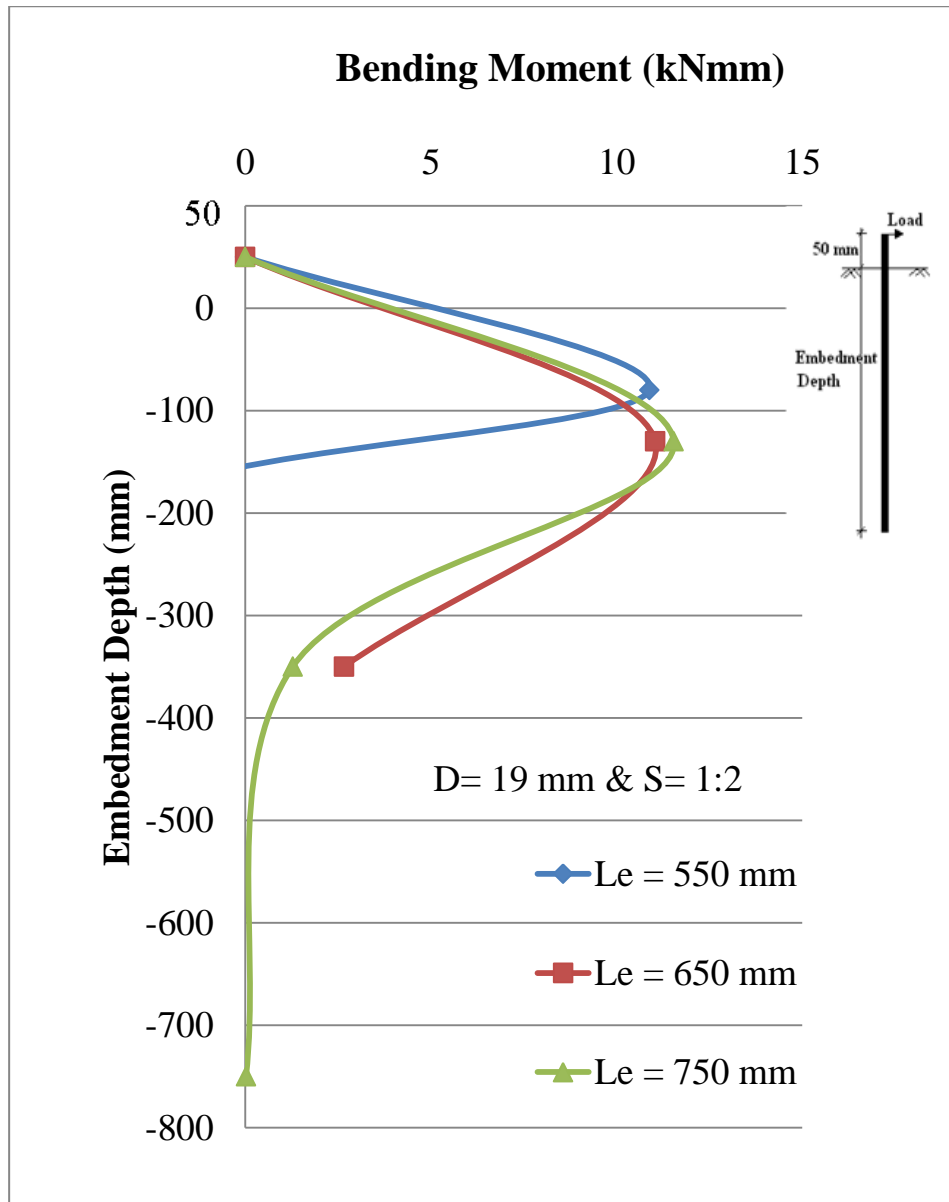


Fig. 3.17.d Bending Moment Variation in Model Piles (D= 19 mm & S= 1:2)

Table 3.9 Details of Model Tests Conducted and Test Results

Sl. No.	Embedment Depth of Pile (mm)	Diameter of Pile (mm)	Slope of Soil Bed (1:S)	Maximum Bending Moment (kNmm)	Maximum Deflection (mm)
1	550	19	1:2	10.9	4.5
2	650	19	1:2	11.1	4.32
3	750	19	1:2	11.6	4.15
4	550	25.4	1:2	12.3	2.35
5	650	25.4	1:2	12.5	2.13
6	750	25.4	1:2	12.8	2.02
7	550	19	1:1.5	11.5	5.20
8	650	19	1:1.5	11.8	4.89
9	750	19	1:1.5	12.1	4.55
10	550	25.4	1:1.5	13.3	3.41
11	650	25.4	1:1.5	13.6	3.23
12	750	25.4	1:1.5	13.8	3.11

Table 3.9 tabulates the maximum values of deflection at the pile top and maximum bending moment which could be further used to analyze the results.

The load deflection curve for 600 mm, 700 mm and 800 mm long and 19 mm and 25.4 mm diameter piles which are embedded in clay beds of two different slopes 1:2 and 1:1.5 were plotted and studied. In all the cases the load deflection curves are found to be non-linear. It is observed that as the bed slope increases from 1:2 to 1:1.5, the deflection of the pile top also increases. It is observed to be true for all the diameters and lengths of piles. This may be due to the fact that as the bed slope increases there is considerable reduction in the passive wedge of soil which contribute in resisting the lateral load of piles. Also it can be noted that as the pile diameter increases from 19 mm to 25.4 mm, there is decrease in the deflection of pile top. As the diameter of pile increases there is considerable increase in the moment of resistance of pile and it helps in reducing the deflection of pile top. But as the length increases from 600 mm to 800 mm there is no much change in the deflection of the pile top.

The variation of the bending moment along the length of the pile is plotted for all the twelve cases of model tests and it was observed that the bending moment diagram shows the typical pattern of non-linear variation of bending moment for a long pile. It is observed that the bending moment is zero at the pile top and it increases upto a certain depth and then decreases to zero. The point at which the maximum bending moment acts will be the point of bending failure of the pile at the ultimate load. This point is referred to as the depth of fixity of the pile.

3.7 Observations from the Experimental Investigation

The following observations are made based on the model tests conducted.

3.7.1 Variation of Bending Moment with the Change in Embedment Depth of Pile

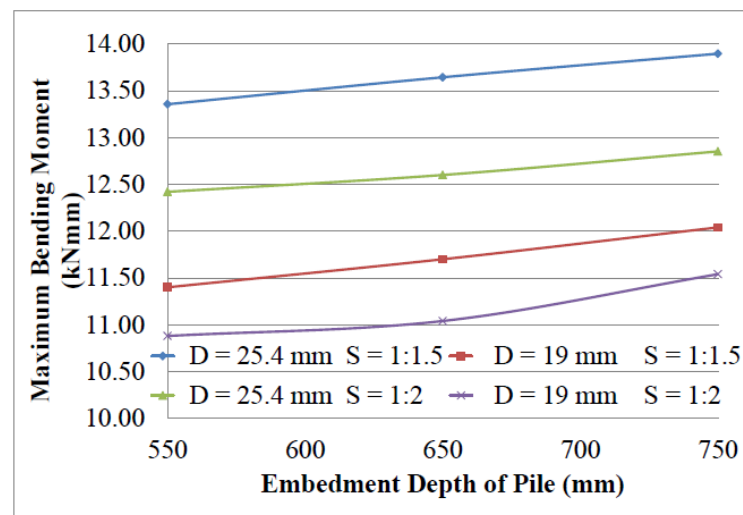


Fig. 3.18 Variation of Bending Moment with the Change in Embedment Depth of Pile

Four groups of curves are plotted to study the variation of maximum bending moment with the change in embedment depth (L_e) of pile as shown in Fig.3.17a – Fig.3.17d. Each group of curve is obtained from three model tests conducted with the embedment depth of pile 550mm, 650 mm and 750mm. In these curves, the diameter (D) of pile is either 25.4mm or 19mm and the bed slope (S) is either 1:1.5 or 1:2. It can be observed from Fig.3.18 that as the embedment depth of pile increases, the maximum bending moment increases

marginally. The increase in bending moment is found to be only around 2 to 4 % for different embedment depths.

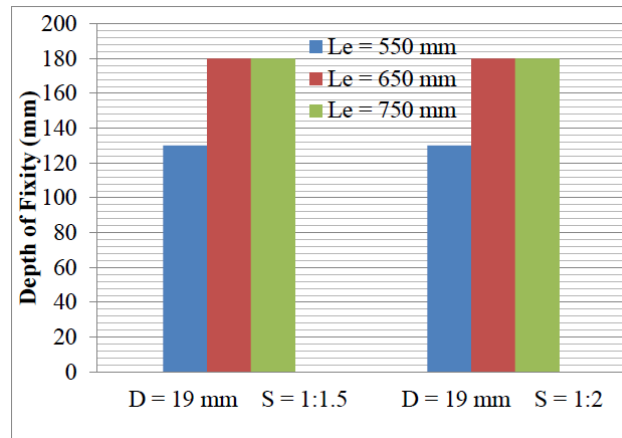


Fig. 3.19 Variation in Depth of fixity with Change in Length of Pile

It can be observed from Fig. 3.19 that beyond an embedment depth of 650mm the depth of fixity almost remains unchanged as the embedment depth of pile increases. Hence the effect of embedment depth of flexible pile is marginal in the case of long piles.

3.7.2 Variation of Bending Moment with the Change in Bed Slope

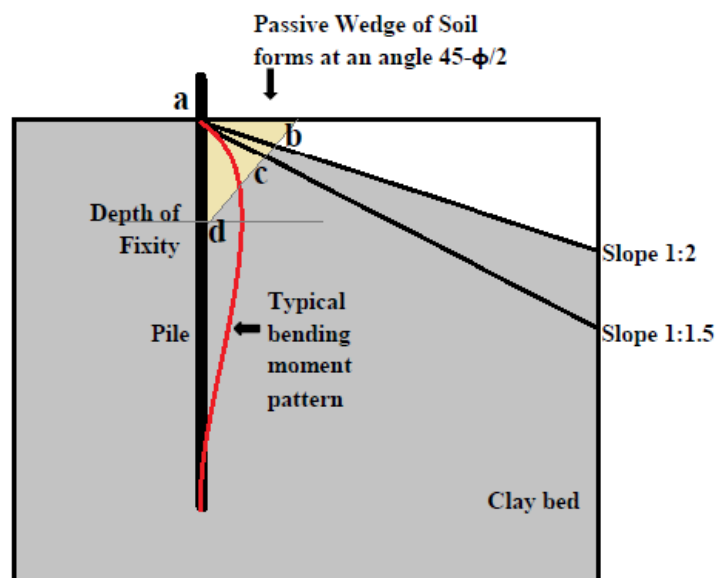


Fig. 3.20 Change in Passive Earth Pressure with Bed Slope

The schematic diagram of the test setup showing different slopes is shown in Fig.3.20. It can be observed from Table 3.9 that as the bed slope increases the maximum bending moment increases, for both diameters of piles. A similar trend was reported by Begum and Muthukkumaran [15]. There is an increase of 7 % to 8 % in the maximum bending moment of pile as the bed slope increases from 1:2 to 1:1.5. Here, the increase in bending moment can be due to the reduction in the passive resistance offered by the soil. As the slope increases from 1:2 to 1:1.5, soil volume generating passive earth pressure decreases from ‘abd’ to ‘acd’ as shown the Fig.3.20.

3.7.3 Variation of Bending Moment with the Change in Diameter of Pile

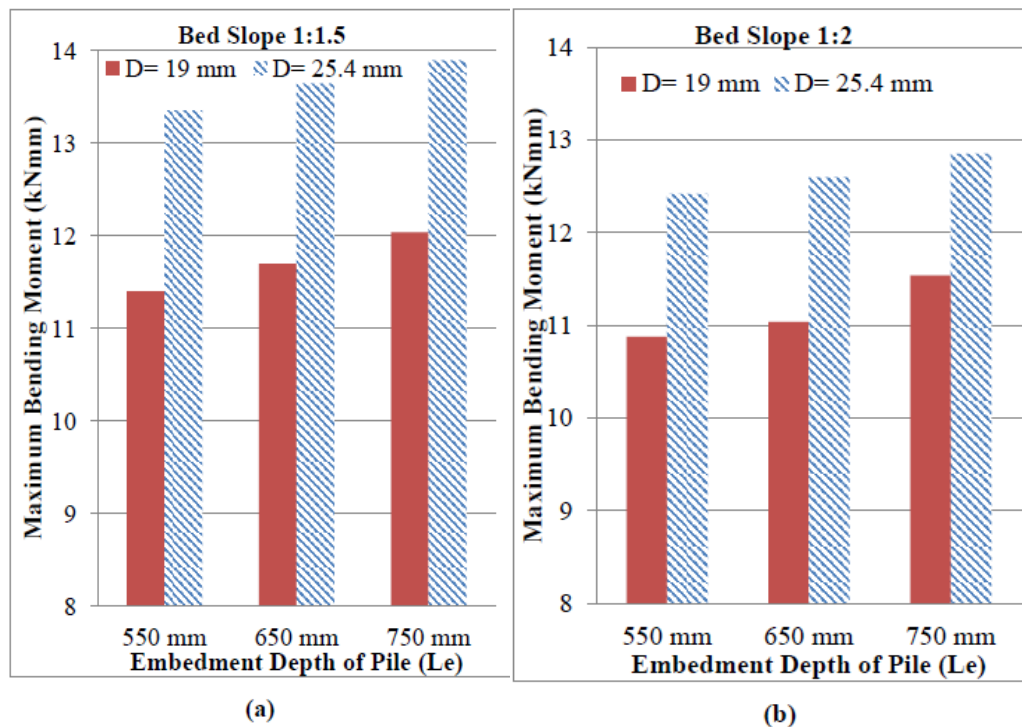


Fig. 3.21 Variation in Bending Moment with Pile Diameter

Based on 12 model tests, the variation of maximum bending moment with the change in diameter of the pile is studied. Each chart in Fig. 3.21 is obtained from six model tests in a particular slope. It is observed that as the diameter of pile increases, the maximum bending moment also increases [79]. It can also be

observed that as the diameter increases from 19 mm to 25.4 mm, there is 13 % increase in maximum bending moment when the bed slope is 1:2 and 15 % increase in bending moment when the bed slope is 1:1.5. The depth of fixity also increases with increase in diameter of the pile. The increase in depth of fixity causes the increase in bending moment of the pile.

Here, when there is an increase in the pile diameter, there will be an increase in the moment of resistance of the pile as per bending equation and it is proportional to section modulus. Hence even though the increase in diameter causes a marginal increase in the bending moment, the considerable increase in moment of resistance will be highly beneficial to carry the lateral loads.

3.8 Summary

The following are the summary of observations from the model Investigations:

- The maximum bending moment increases as the embedment depth of pile, the diameter of pile and bed slope increases.
- There is only a marginal increase in bending moment when the embedment depth of pile increases from 550 mm to 750 mm. Hence a change in embedment depth of pile may not considerably affect the lateral capacity of the pile.
- The bending moment increases considerably when the diameter of the pile increases from 19 mm to 25.4 mm. But since the moment of resistance also increases considerably it will not adversely affect the bending behaviour of the pile.
- The bending moment increases when the slope of soil bed increases from 1:2 to 1:1.5, since the passive resistance of soil decreases due to increase in bed slope.

- The depth of fixity moves down as the embedment depth of pile, the diameter of the pile and bed slope increases.
- For a particular load, deflection is found to be more in a long pile, smaller diameter pile as well as a pile embedded in a steeper bed slope.

.....❧.....

Analytical Investigation

Contents	4.1 <i>Introduction</i>
	4.2 <i>Analytical Formulation</i>
	4.3 <i>Validation of the Formulation</i>
	4.4 <i>Analysis of Model Tests</i>
	4.5 <i>Summary</i>

4.1 Introduction

Classical theories suggested by Reese *et al.* [71] incorporate the influence of soil-structure interaction in the structural behaviour of a laterally loaded pile. The complexity of the formulations necessitates a computer program for the solution of the problem. This chapter is aimed at developing a computer program in MATLAB R2010a, for the analysis of laterally loaded pile. The program is validated with an on-site pile load test suggested by Reese *et al.* The model pile tests discussed in Chapter 3 are also analyzed using the program developed and the results are compared.

4.2 Analytical Formulation

The finite difference method of analysis of the pile is used to calculate the deflection at the top of the pile, bending moment variation along the length of the pile and the depth of fixity of the pile [Reese *et al.*]. Since the method is highly iterative a MATLAB R2010a code is developed and the curves are plotted.

The derivation of the differential equation for the beam column on a foundation given by Hetenyi (1946) is considered for the present formulation. The assumption made is that a bar on an elastic foundation is subjected to horizontal

loading and to a pair of compressive forces P_x acting in the center of gravity of the end cross sections of the bar. If an infinitely small loaded element, bounded by two horizontals a distance dx apart, is cut out of this bar (Fig. 4.1), the equilibrium of moments (ignoring higher-order terms) leads to the equation,

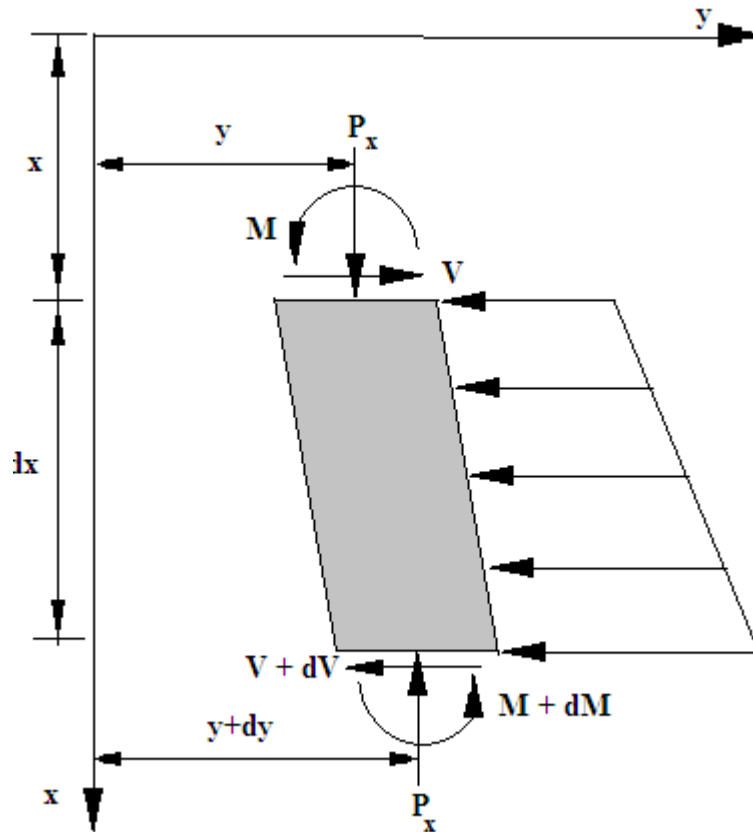


Fig. 4.1 Element of a Beam-Column (Hetenyi *et al.*)

$$(M + dM) - M + P_x dy - V dx = 0 \dots\dots\dots (4.1)$$

Rearranging,

$$\frac{dM}{dx} + P_x \frac{dy}{dx} - V = 0 \dots\dots\dots (4.2)$$

Differentiating with respect to x,

$$\frac{d^2M}{dx^2} + P_x \frac{d^2y}{dx^2} - \frac{dV}{dx} = 0 \dots\dots\dots (4.3)$$

Considering the following identities,

$$\frac{d^2M}{dx^2} = EI \frac{d^4y}{dx^4} \dots\dots\dots (4.4)$$

and

$$\frac{dV}{dx} = p = E_{py}y \dots\dots\dots (4.5)$$

Substituting in Eq.4.1

$$EI \frac{d^4y}{dx^4} + P_x \frac{d^2y}{dx^2} + E_{py}y = 0 \dots\dots\dots (4.6)$$

Where,

P_x = axial load on the pile,

y = lateral deflection of the pile at a point x along the length of the pile.

p = soil reaction per unit length

EI = bending stiffness

E_{py} = Soil Reaction

The assumptions involved in the derivation are,

- 1) The pile is straight and has a uniform cross section.
- 2) The pile has a longitudinal plane of symmetry; loads and reflections lie in that plane.
- 3) The pile material is homogeneous and isotropic.
- 4) The proportional limit of the pile material is not exceeded.
- 5) The modulus of elasticity of the pile material is same in tension and compression.
- 6) Transverse deflection of the pile is small.
- 7) The pile is not subjected to dynamic loading.
- 8) Deflections due to shearing stresses are small.
- 9) To represent a linearly increasing magnitude of soil reaction with depth the following relation is adopted.

$$E_{py} = k_{py}x \dots\dots\dots (4.7)$$

As per the mathematical formulation the derivatives can be written in difference form as follows,

$$\frac{dy}{dx} = \frac{y_{n-1} - y_{n+1}}{2h} \dots\dots\dots (4.8)$$

$$\frac{d^2y}{dx^2} = \frac{y_{n-1} - 2y_n + y_{n+1}}{h^2} \dots\dots\dots (4.9)$$

$$\frac{d^3y}{dx^3} = \frac{-y_{n-2} + 2y_{n-1} - 2y_{n+1} + y_{n+2}}{2h^3} \dots\dots\dots (4.10)$$

$$\frac{d^4y}{dx^4} = \frac{y_{n-2} - 4y_{n-1} + 6y_n - 4y_{n+1} + y_{n+2}}{h^4} \dots\dots\dots (4.11)$$

Using the above expressions and by substituting in Eqn. no.4.6, the differential equation for a pile under lateral loading in difference form is,

Substituting Eqn. no. 4.3 in Eqn.no.4.2,

$$E_p I_p \left(\frac{y_{n-2} - 4y_{n-1} + 6y_n - 4y_{n+1} + y_{n+2}}{h^4} \right) + P_x \left(\frac{y_{n-1} - 2y_n + y_{n+1}}{h^2} \right) + E_{py} y_n = 0 \dots\dots (4.12)$$

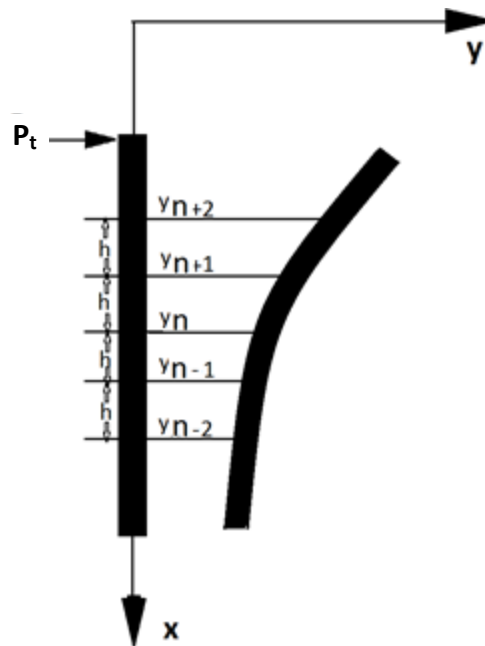


Fig.4.2 Finite Element Discretization of the Pile

4.3 Validation of the Formulation

The validation of the present formulation is done using an example problem suggested by Reese *et al.* [71]. The specifications of the problem are as follows.

A 20 m length steel pipe pile of 380 mm outside diameter and 25mm thickness that is free to rotate is considered for the study. It is subjected to a lateral load of 300 kN to achieve an appropriate level of safety against failure of the pile. The magnitude of the deflection of the pile at the ground line is considered to be critical. Over consolidated clay is assumed to be at the site. The effect of axial load is neglected for the study. Hence the governing equation changes to,

$$E_p I_p \frac{d^4 y}{dx^4} + E_{py} y = 0 \dots\dots\dots (4.13)$$

$$E_p I_p \left(\frac{y_{n-2} - 4y_{n-1} + 6y_n - 4y_{n+1} + y_{n+2}}{h^4} \right) + E_{py} y = 0 \dots\dots\dots (4.14)$$

$$E_p I_p y_{n-2} - 4E_p I_p y_{n-1} + 6E_p I_p y_n - 4E_p I_p y_{n+1} + E_p I_p y_{n+2} + E_{py} h^4 y = 0 \dots (4.15)$$

$$y_{n-2} - 4y_{n-1} + \left[6 + \frac{E_{py} h^4}{E_p I_p} \right] y_n - 4y_{n+1} + y_{n+2} = 0 \dots\dots\dots (4.16)$$

where,

$$E = 2.0 \times 10^8 \text{ kPa}$$

$$I = 4.414 \times 10^{-4} \text{ m}^4$$

There are two boundary conditions each at top and bottom of the pile. The boundary conditions are as follows. At the bottom of the pile, bending moment and displacement are considered to be zero. At the top of the pile, the bending moment is the moment due to the point load applied at a height above the ground level and the shear force is the applied load at the top of the pile

contributes four more differential equations. Thus, for a pile, there exist $(n+4)$ differential equations and $(n+4)$ unknowns, y_{n+2} to y_{n-2} .

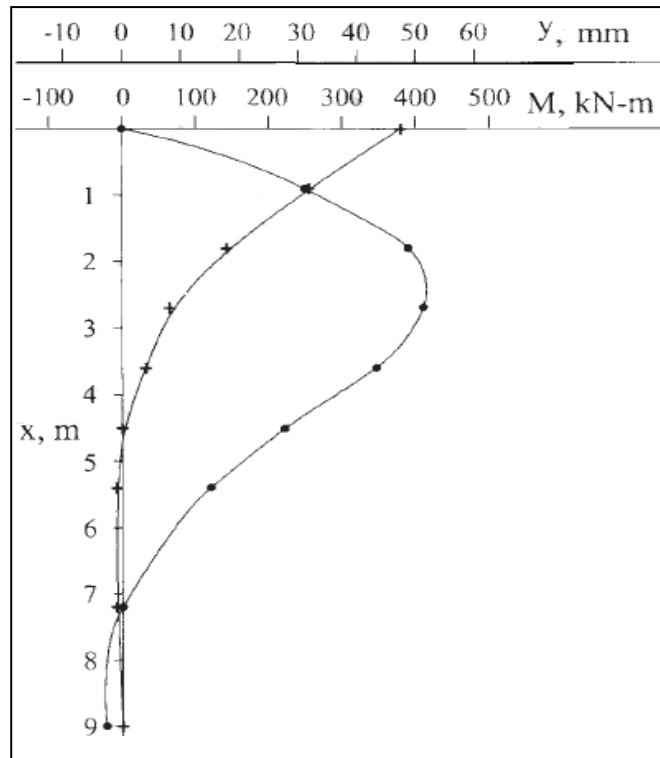


Fig. 4.3 Computed Values of Deflection and Bending Moment of the Validating Problem (Reese *et al.*) [71]

The deflection profile and the bending moment profile along the length of the pile is plotted. As per the reference the maximum deflection at the top of the pile is 47.6 mm, the maximum bending moment is 410 kNm and the depth of fixity is 2.7m from the top of the pile. The corresponding variables are compared with the MATLAB program developed as per Fig.4.4 and Fig.4.5 and the following output is obtained. The maximum deflection at the top of the pile is 47.6436mm, the maximum bending moment is 415.609 kNm and the depth of fixity is 2.47 m from the top of the pile. The MATLAB program developed is included in Appendix-C.

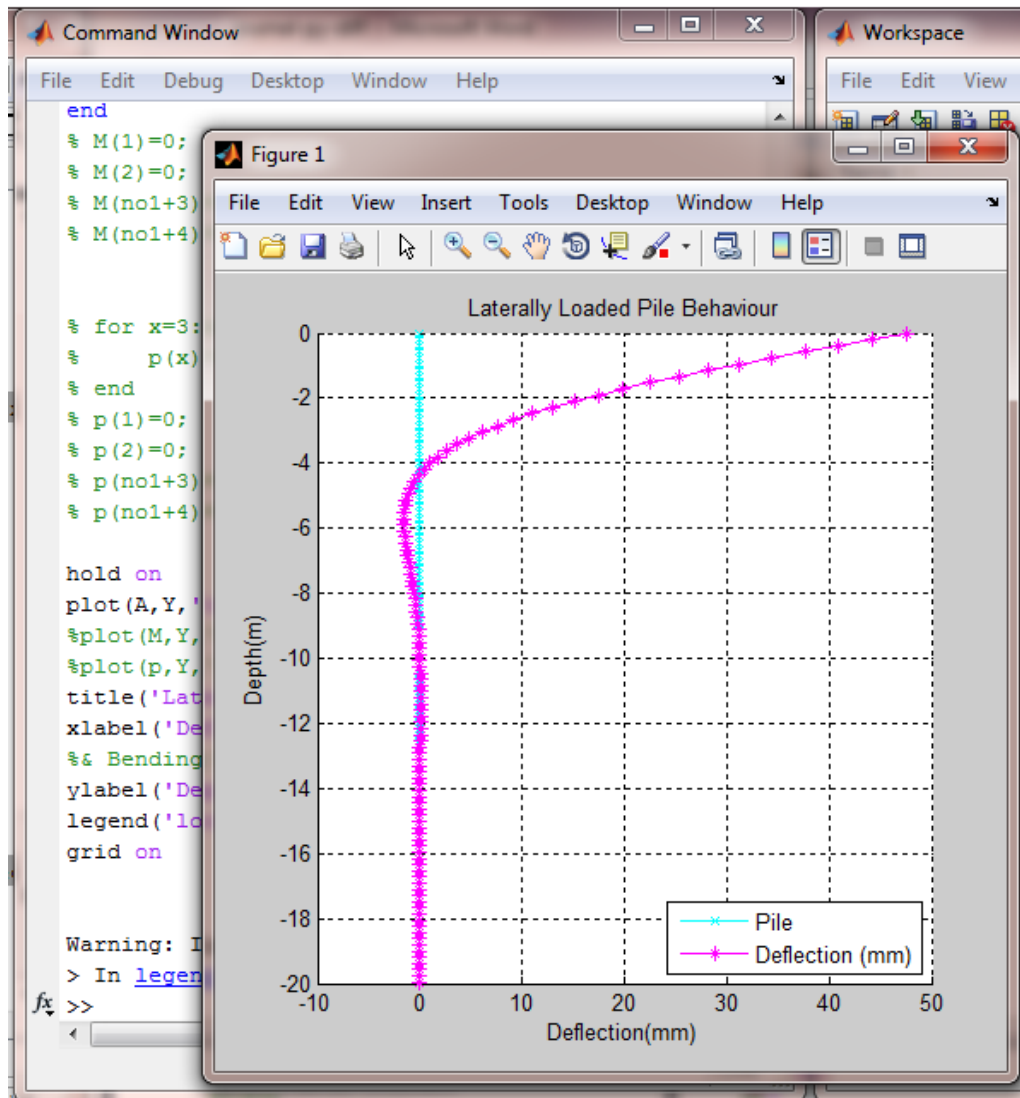


Fig. 4.4 Deflection Variation along the length of the pile

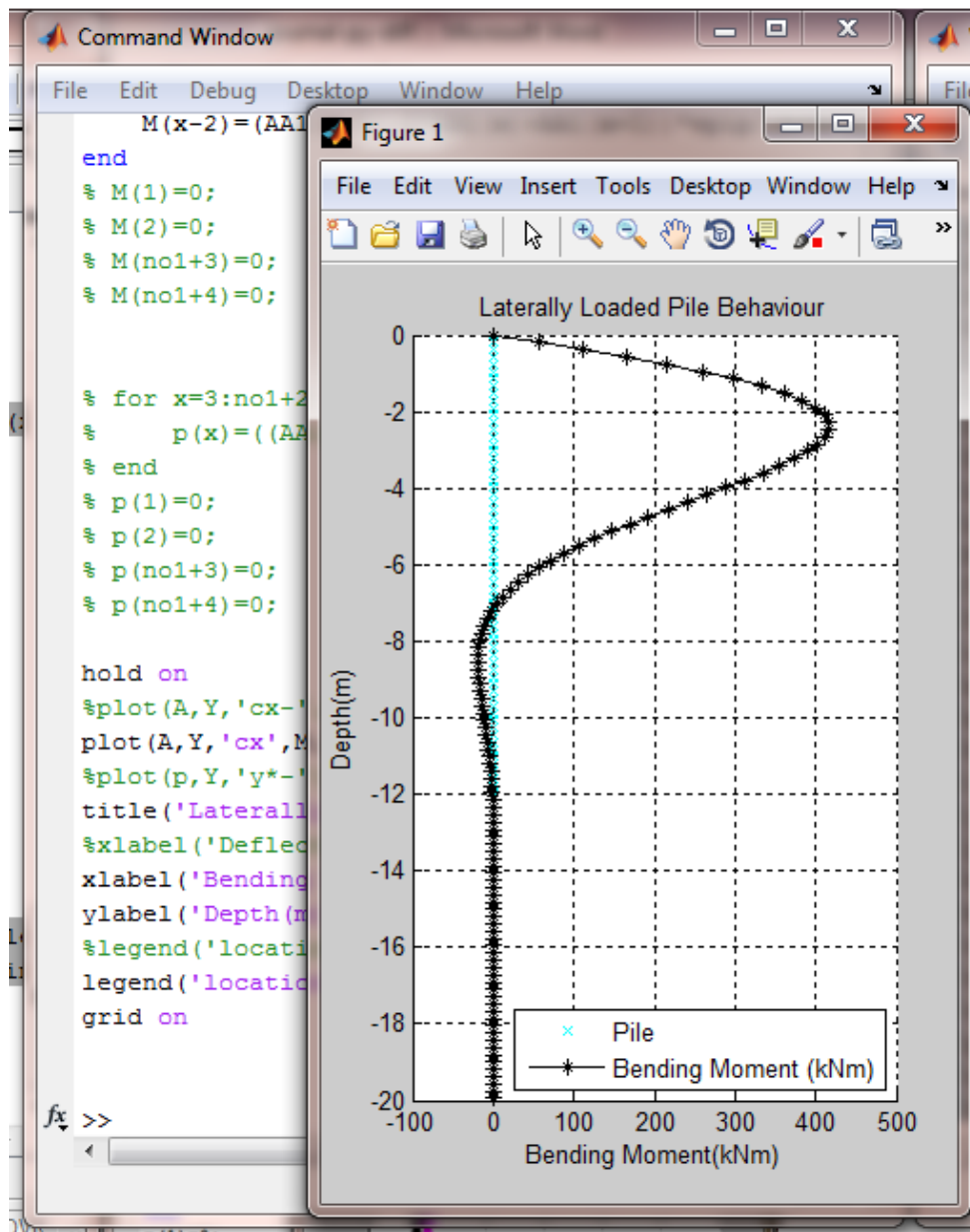


Fig. 4.5 Bending Moment Variation along the length of the pile

4.4 Analysis of Model Tests

The computer program developed and validated for the problem suggested by Reese *et al.* is further used to model the experimental investigation done in Chapter 3.

The experimental investigation includes model study on 25.4 mm and 19 mm diameter hollow aluminium pipe with 1 mm thickness, as the model piles. The length of the pile is varied in the range 600 mm, 700 mm and 800 mm to have a flexible behaviour of pile. The modulus of elasticity of aluminium is adopted to be 70 GPa and the moment of inertia of the model pile is calculated to be 5717 mm⁴ for 25.4 mm pile and 2298 mm⁴ for 19 mm pile.

The un-drained shear strength (C_u) of soil used for the model experiment is obtained from the laboratory tests [Appendix-A] and the sub-grade modulus of soil is calculated based on IS 2911(Part 1/ Sec 2):2010. A co-relation between the un-drained shear strength and soil modulus is obtained based on IS 2911 (Part 1/ Sec 2): 2010, Annex C, Analysis of laterally loaded pile. The recommended values of soil modulus (E_s) for cohesive soil are adopted as per the equation $E_s = \frac{k_1 \times 0.3}{1.5 \times D}$, where D is the diameter of the circular pile and k_1 is the modulus of sub-grade reaction. Soil modulus values for a pile with diameter 1m are tabulated in Table 4.1.

Table 4.1 Recommended Values of soil modulus as per IS 2911 (Part 1/ Section 2) – 2010

Unconfined Compression Strength, q_u kN/m ²	Modulus of Subgrade Reaction, $k_1 \times 10^3$ N/m ³	Soil Modulus, E_s N/m ²
25	4.5	900
50	9.0	1800
100	18.0	3600
200	36.0	7200
400	72.0	14400

Analytical study is performed for all the experimental investigations as in Chapter 3 and a reasonable matching could be obtained in the behaviour of pile (Table 4.2 and Table 4.3). Hence it can be understood that the model investigations were done with reasonable accuracy.

The program developed is also used for a few parametric studies on static and dynamic analysis of piles and the details are included in Appendix-D.1 and Appendix-D.2.1.

Table 4.2 Comparison of Maximum Bending Moment on Pile

Sl.No.	Embedment Depth of Pile (mm)	Diameter of Pile (mm)	Slope of Soil Bed	Maximum Bending Moment (Experimental) (Nm)	Maximum Bending Moment (Analytical) (Nm)
1	550	19	1:2	10.88	13.14
2	650	19	1:2	11.04	13.14
3	750	19	1:2	11.54	13.14
4	550	25.4	1:2	12.42	14.9
5	650	25.4	1:2	12.60	14.99
6	750	25.4	1:2	12.85	14.99
7	550	19	1:1.5	11.40	13.34
8	650	19	1:1.5	11.70	13.35
9	750	19	1:1.5	12.04	13.35
10	550	25.4	1:1.5	13.36	15.1
11	650	25.4	1:1.5	13.64	15.2
12	750	25.4	1:1.5	13.90	15.2

Table 4.3 Comparison of Deflection at Pile Top

Sl.No.	Embedment Depth of Pile (mm)	Diameter of Pile (mm)	Slope of Soil Bed	Maximum Deflection (Experimental) (mm)	Maximum Deflection (Analytical) (mm)
1	550	19	1:2	2.74	3.4
2	650	19	1:2	2.44	3.4
3	750	19	1:2	2.33	3.4
4	550	25.4	1:2	2.35	2.3
5	650	25.4	1:2	2.13	2.28
6	750	25.4	1:2	2.02	2.28
7	550	19	1:1.5	5.20	3.61
8	650	19	1:1.5	4.89	3.61
9	750	19	1:1.5	4.55	3.61
10	550	25.4	1:1.5	3.41	2.45
11	650	25.4	1:1.5	3.23	2.42
12	750	25.4	1:1.5	3.11	2.42

4.5 Summary

- A MATLAB program is developed based on finite difference equation suggested by Reese *et al.* to formulate the behaviour of a single pile-soil system.
- The program is validated with the on-site pile load test suggested by Reese *et al.*
- The model tests conducted in Chapter 3 is also modeled using this program and a reasonable matching between the results ensures that the model tests are well simulated and executed.

.....

Numerical Investigation

Contents	5.1 <i>Introduction</i>
	5.2 <i>Soil-Pile Modeling in PLAXIS-3D</i>
	5.3 <i>Modeling of a Laterally Loaded Single Pile in Sloping Bed</i>
	5.4 <i>Analysis Results of Parametric Study</i>
	5.5 <i>Multivariable Regression Equations</i>
	5.6 <i>Summary</i>

5.1 Introduction

The structural behaviour of laterally loaded pile in sloping clay bed is well established in previous chapters through experimental and analytical investigations. The investigations are further extended in the finite element software, PAXIS-3D to incorporate the influence of bed slopes varying from 0° to 45° . Based on the parametric study multivariable regression equations are developed to highlight the influence of geometry of the pile and the bed slope on the structural behaviour of soil-pile system.

5.2 Soil-Pile Modeling in PLAXIS-3D

PLAXIS 3D is a three dimensional finite element package intended for the analysis of deformation and stability in geotechnical engineering. It deals with various aspects of complex geotechnical structures and construction processes using robust and theoretically sound computational procedures. The soil-pile model created for the present study is validated with available onsite pile load tests mentioned in literatures [Appendix-F]. Proper selection of soil model and pile model are the key factor influencing the analysis results.

5.2.1 Soil-Pile Interaction Modeling Using Mohr-Coulomb Model

The features of various soil models available in literatures were studied [Appendix-E] and it is decided to adopt the elasto-plastic Mohr-Coulomb model for the analysis of the soil pile system in the preset study.

5.2.1.1 Formulation of Mohr-Coulomb Soil Model

Mohr-Coulomb model is a well-known linearly elastic perfectly plastic soil model used as a first approximation of soil behaviour. A constant average stiffness is estimated for the soil layer and hence the computations are relatively fast.

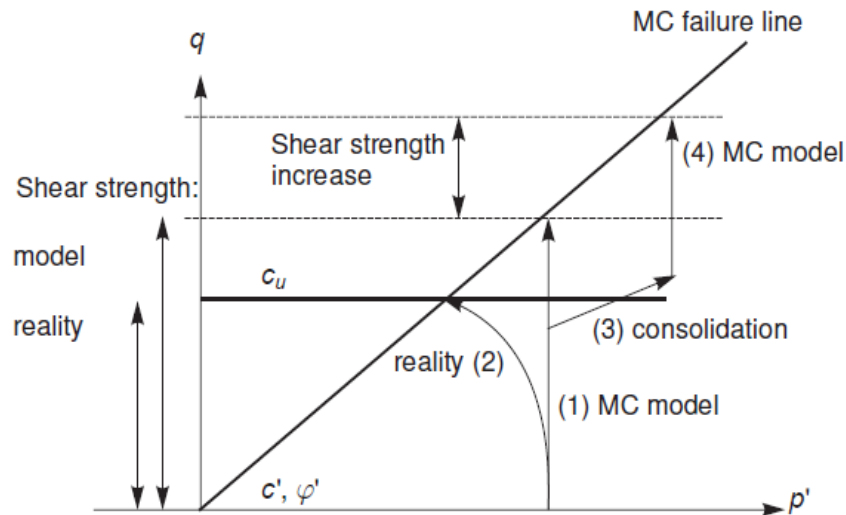


Fig. 5.1 Illustration of Stress Path in Mohr-Coulomb Soil Model [103]

The model will follow an effective stress path where the mean effective stress, p' remains constant upto failure. It is known that especially soft soils, like normally consolidated clays and peat will follow an effective stress path in undrained loading where p' reduces significantly as a result of shear induced pore pressure. As a result the maximum deviatoric stress that can be reached in the model is overestimated in mohr-coulomb model. If at some stress state, soil is consolidated the mean effective stress will increase. Upon further undrained loading with the mohr-coulomb model the observed shear strength will be

increased compared to the previous shear strength, but it is unrealistic in soft soils.

5.2.1.2 Basic Parameters of Mohr-Coulomb Soil Model

Mohr-Coulomb soil model requires five parameters, two stiffness parameters and three strength parameters. The stiffness parameters of the Mohr-Coulomb model are effective young's model (kN/m^2) and effective poisson's ratio. The strength parameters of the model are effective cohesion (kN/m^2), effective friction angle ($^\circ$) and dilatancy angle ($^\circ$).

5.2.2 Soil-Pile Interaction Modeling Using Embedded Pile Element

Pile was modeled using the three node embedded pile in PLAXIS-3D. An embedded pile is a three noded beam element with six degrees of freedom per node that can be placed inside soil volume in any required direction. The element allows deflections due to shearing and bending. The element can also change its length due to axial force. The embedded pile is visualized as line element but the actual volume of the pile is considered for analysis which is inputted to the pile material data set.

The pile head will be free if it is not connected to any other element. The interaction with the soil such as skin resistance and foot resistance are modeled using special interface elements. The special interface elements creates virtual nodes in the soil volume near the beam element nodes and a connection is formed between the three noded beam element nodes and virtual nodes. The beam element representing the pile crosses a ten noded tetrahedron element at any place with an arbitrary orientation. The material parameters of a pile element that distinguishes it from a beam element are the skin resistance and the foot resistance. Skin resistance represents the traction allowed along the skin of the pile and the foot resistance is maximum force allowed at the foot of the pile.

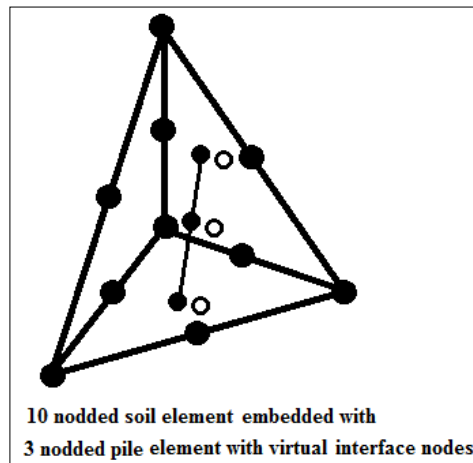


Fig. 5.2 Embedded Pile inside Soil Volume [103]

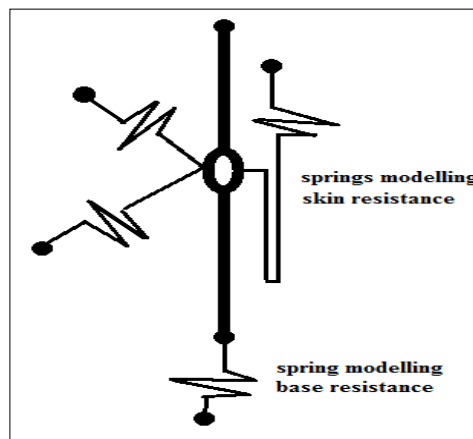


Fig. 5.3 Embedded Pile with Interface [103]

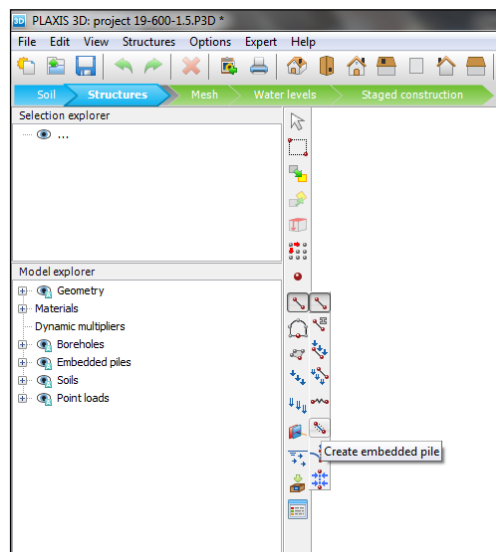


Fig. 5.4 Embedded Pile in PLAXIS-3D

5.3 Modeling of a Laterally Loaded Single Pile in Sloping Bed

A work plane is created with the same dimension as that of the plan of model tank used for the experimental investigation. The units are adopted to be millimeter (mm) for length and Newton (N) for force. Since 1g test method is adopted for the experimental investigation, gravity is considered to be 1g with earth's gravity 9810 N/mm^2 . Weight density of water is considered to be $1\text{e-}5 \text{ N/mm}^3$.

A sloping soil bed is to be created to study the effect of slope on the structural behaviour of laterally loaded piles. A level ground with the known soil properties is to be created first. Then two soil volumes are to be created and deactivated to model the effect of extrusion of pile above the soil volume as well as the slope of the soil bed. The deactivations of the two additional soil volumes are to be done during staged construction.

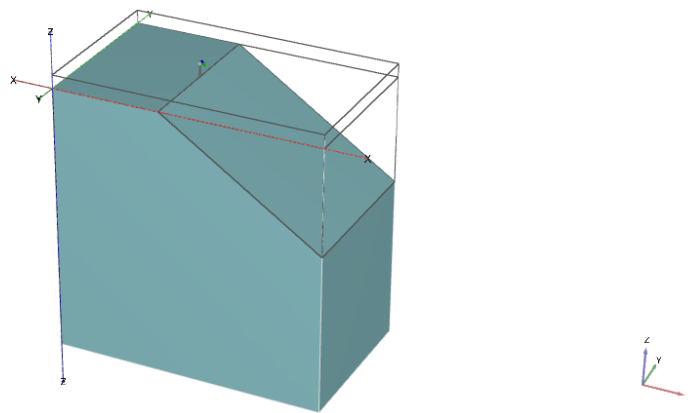


Fig. 5.5 PLAXIS-3D Model of a Single LLP in Sloping Bed

Pile is modeled using the three node embedded pile in PLAXIS-3D. The interaction with the soil such as skin resistance and foot resistance are modeled using special interface elements. Initial phase follows the calculation type, K0 procedure. All the other phases are with calculation type plastic. After the initial phase excavation phase is created where the soil volume to be removed to create the required slope is deactivated. Then in the construction phase, the

embedded pile is activated. Next is the loading phase where a lateral point load of 100 N is applied at the pile top and it is activated. The details of model creation are incorporated in Appendix-G.2.

5.4 Analysis of Results from Parametric Studies

A detailed parametric study has been conducted to study the influence of variation in bed slope, pile diameter and pile length in predicting the depth of fixity, maximum bending moment and the pile top deflection. The details of parameters varied for the analysis is tabulated in Table G.1, Appendix-G.1. The Load-Deflection curves and the bending moment variation along the length of the pile are presented here.

5.4.1 Load-Deflection Curves

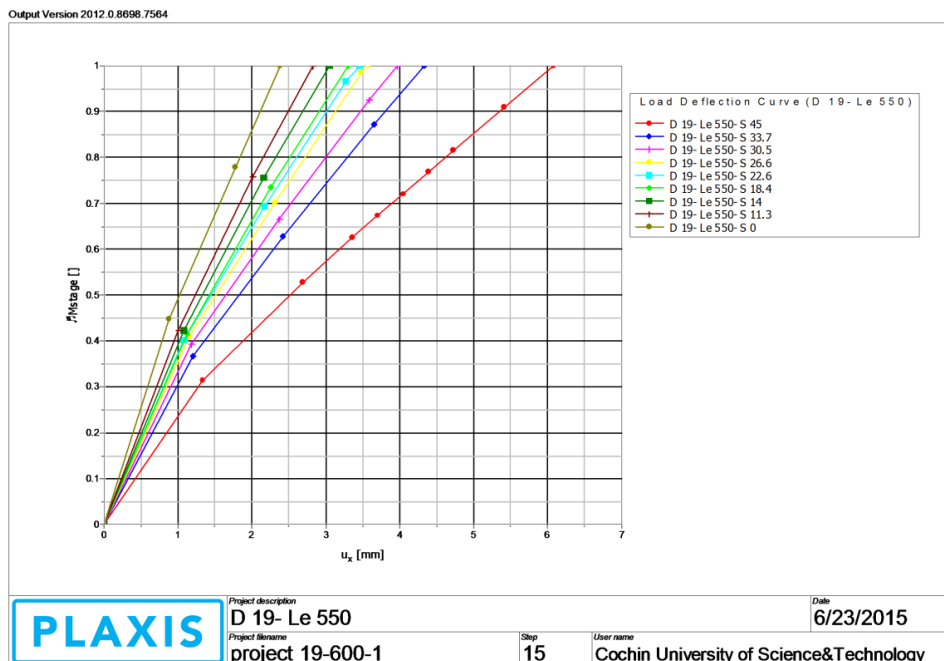


Fig. 5.6.a Load-Deflection Curve for 19 mm Diameter Model Pile with

550 mm Embedment Depth

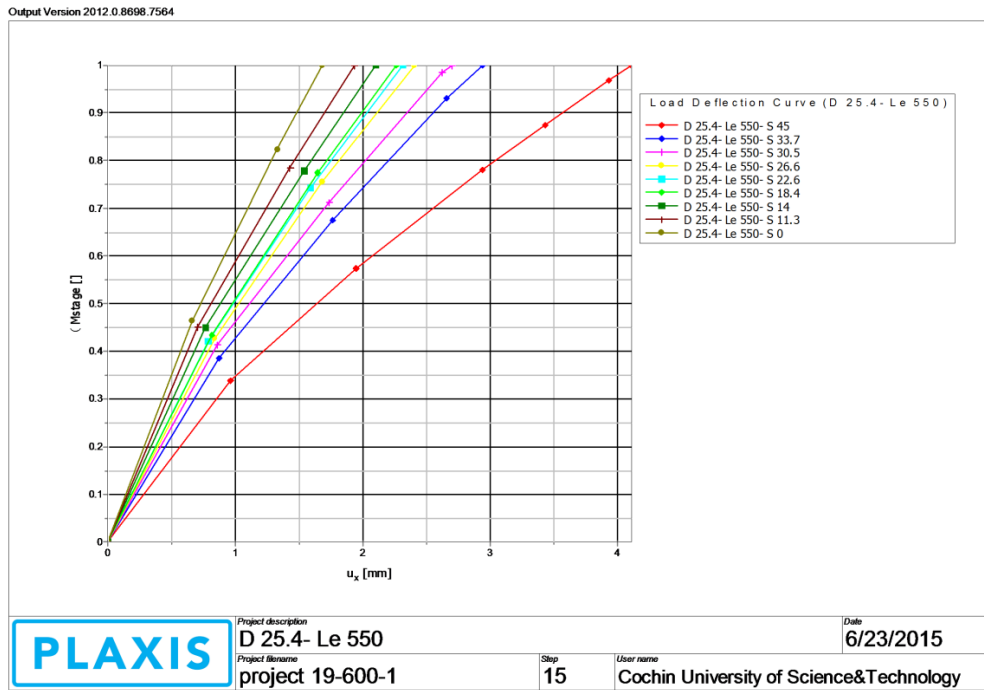


Fig. 5.6.b Load-Deflection Curve for 25.4 mm Diameter Model Pile with 550 mm Embedment Depth

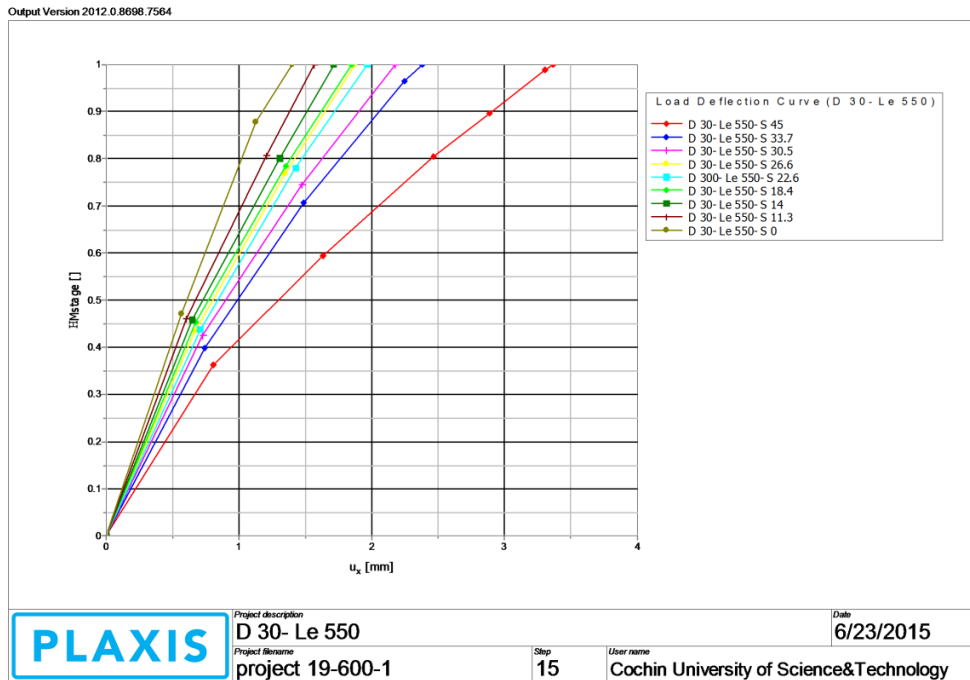


Fig. 5.6.c Load-Deflection Curve for 30 mm Diameter Model Pile with 550 mm Embedment Depth

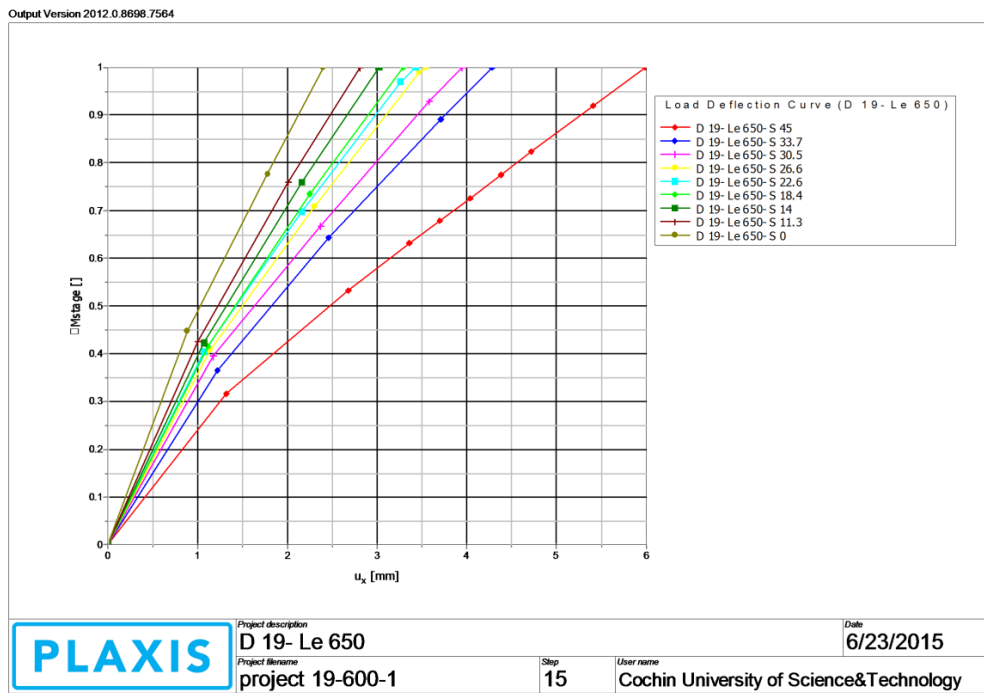


Fig. 5.6.d Load-Deflection Curve for 19 mm Diameter Model Pile with 650 mm Embedment Depth

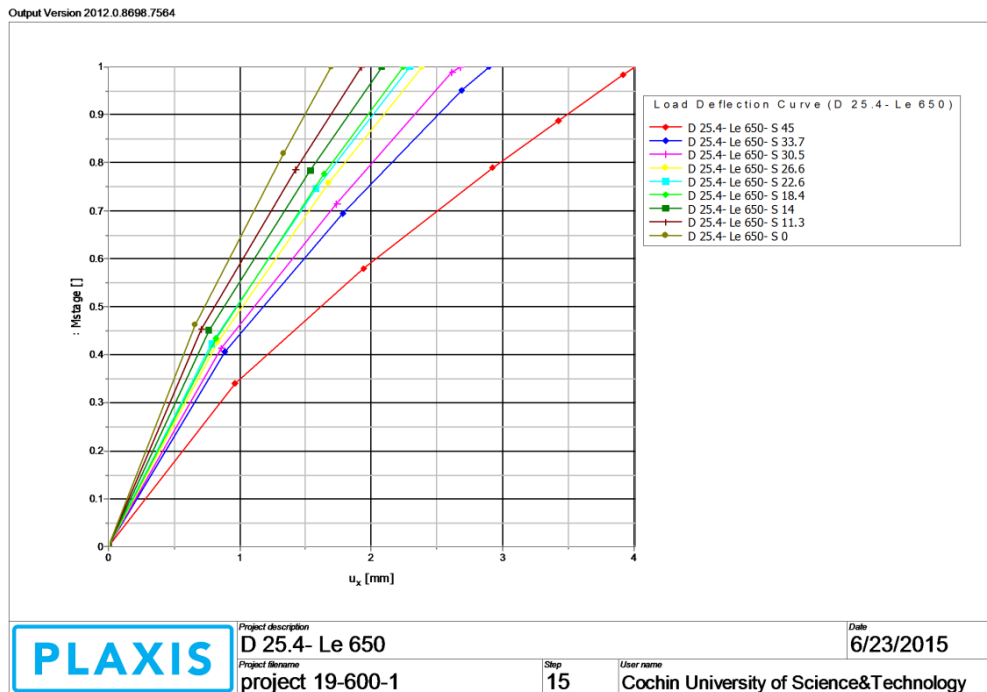


Fig. 5.6.e Load-Deflection Curve for 25.4 mm Diameter Model Pile with 650 mm Embedment Depth

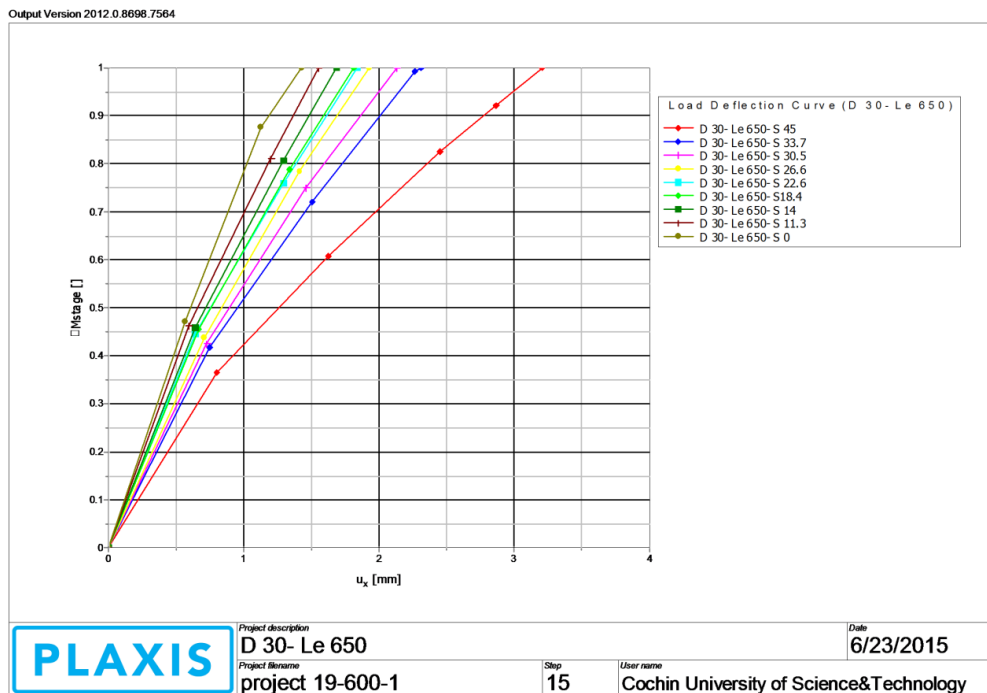


Fig. 5.6.f Load-Deflection Curve for 30 mm Diameter Model Pile with 650 mm Embedment Depth

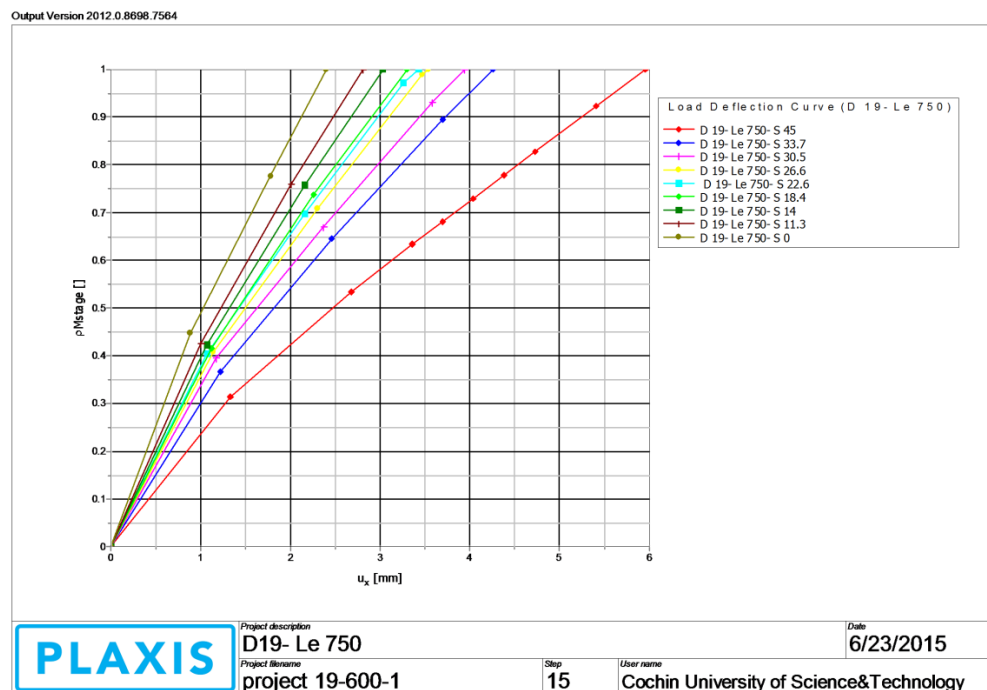


Fig. 5.6.g Load-Deflection Curve for 19 mm Diameter Model Pile with 750 mm Embedment Depth

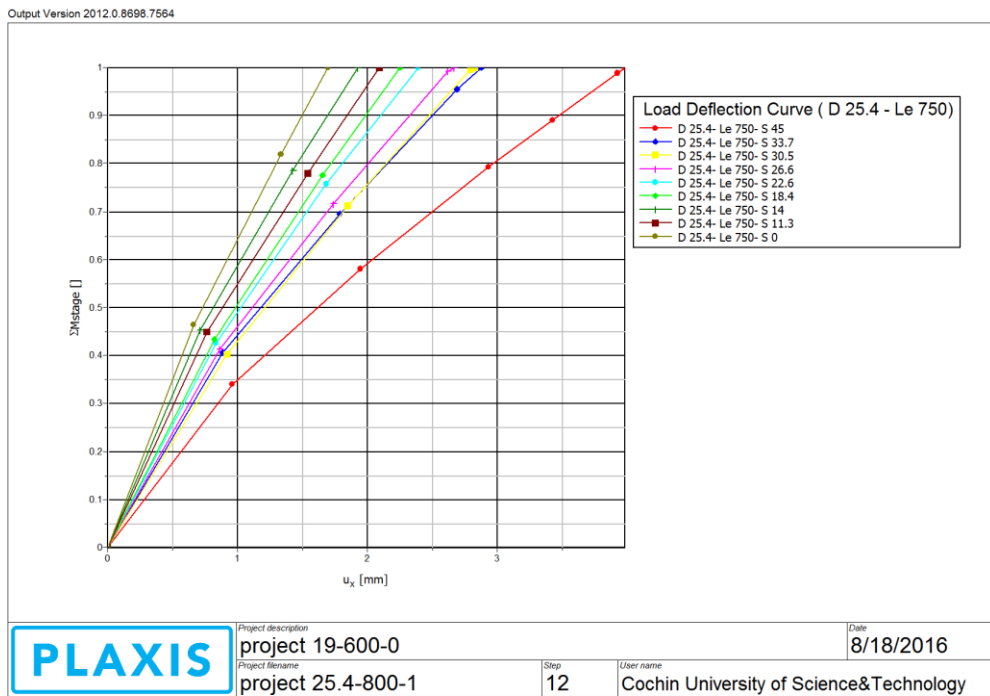


Fig. 5.6.h Load-Deflection Curve for 25.4 mm Diameter Model Pile with 750 mm Embedment Depth

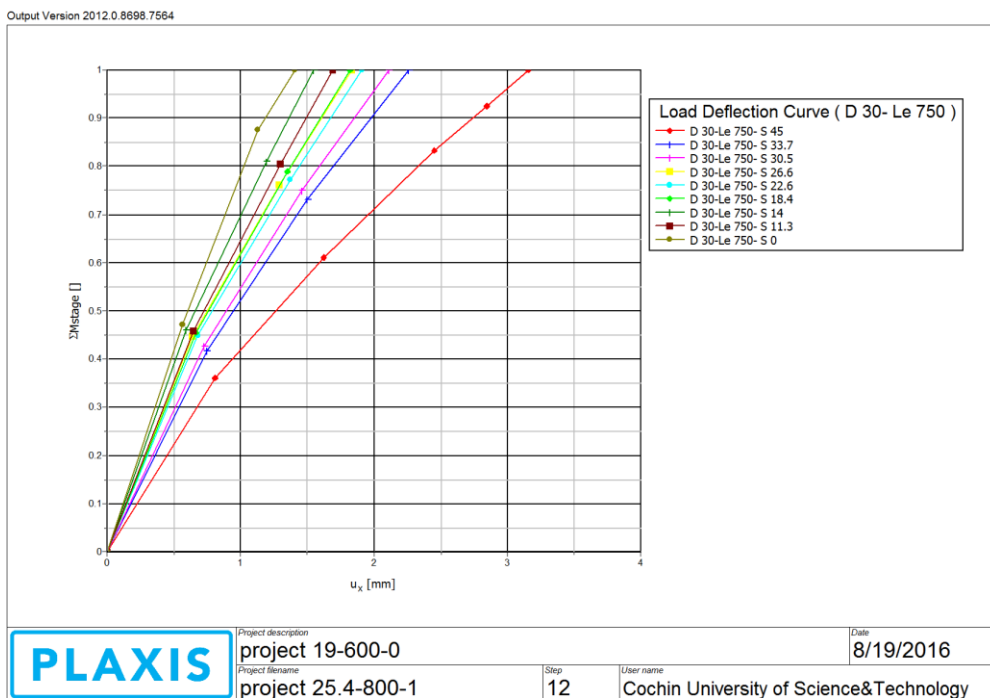


Fig. 5.6.i Load-Deflection Curve for 19 mm Diameter Model Pile with 750 mm Embedment Depth

5.4.2 Bending Moment Diagrams

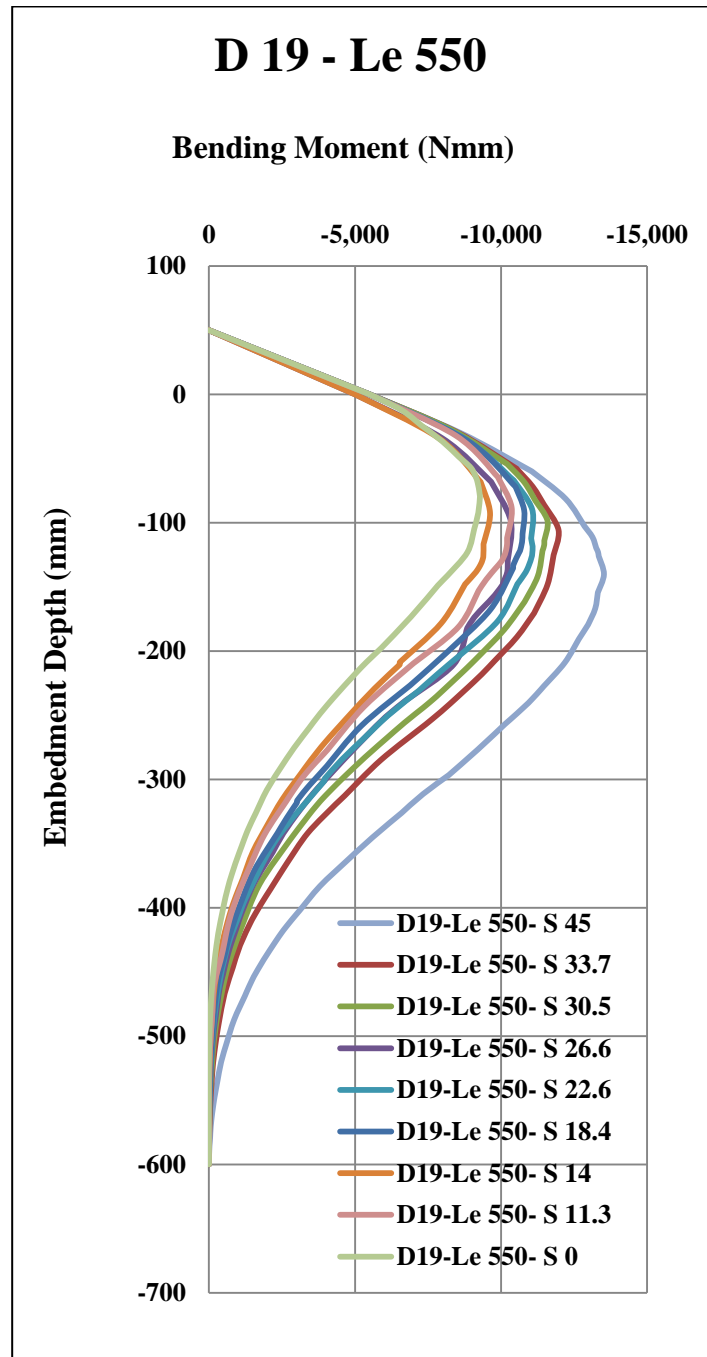


Fig. 5.7.a Bending Moment Diagram for 19 mm Diameter Model Pile with 550 mm Embedment Depth

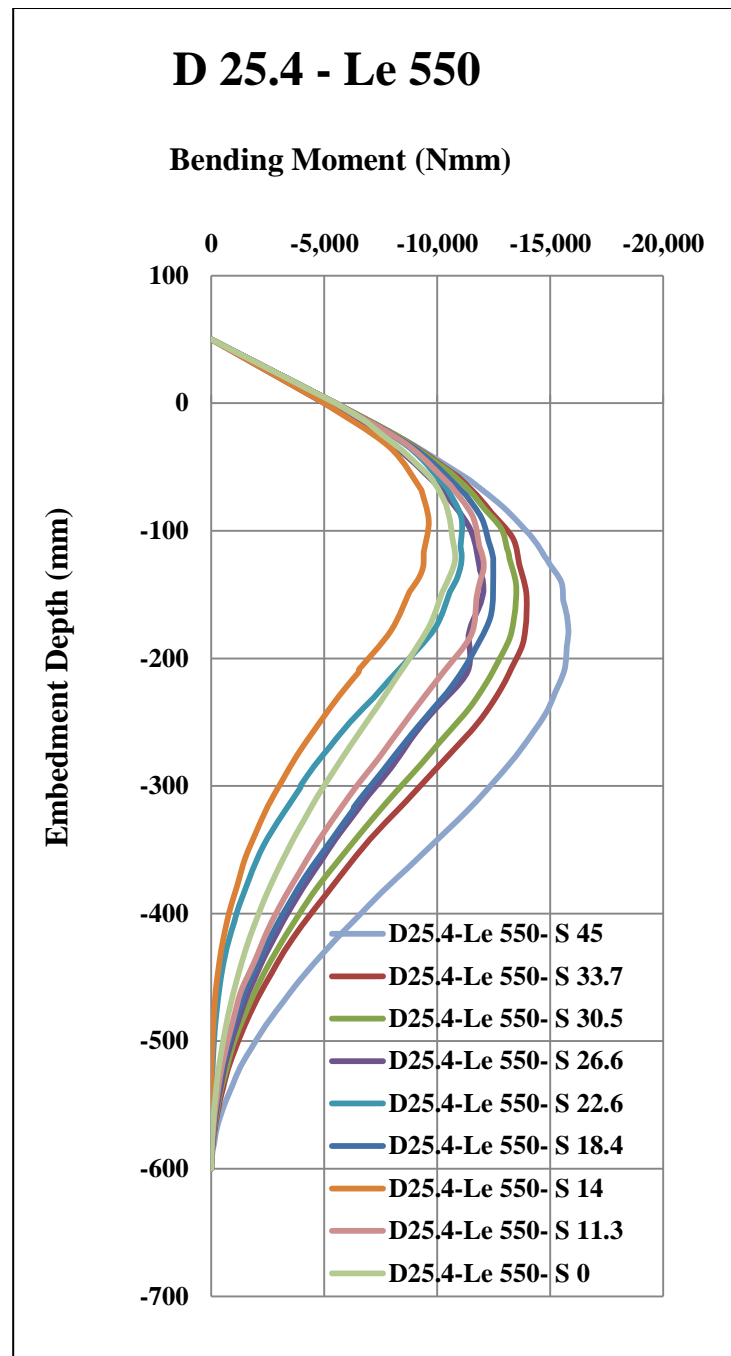


Fig. 5.7.b Bending Moment Diagram for 25.4 mm Diameter Model Pile with 550 mm Embedment Depth

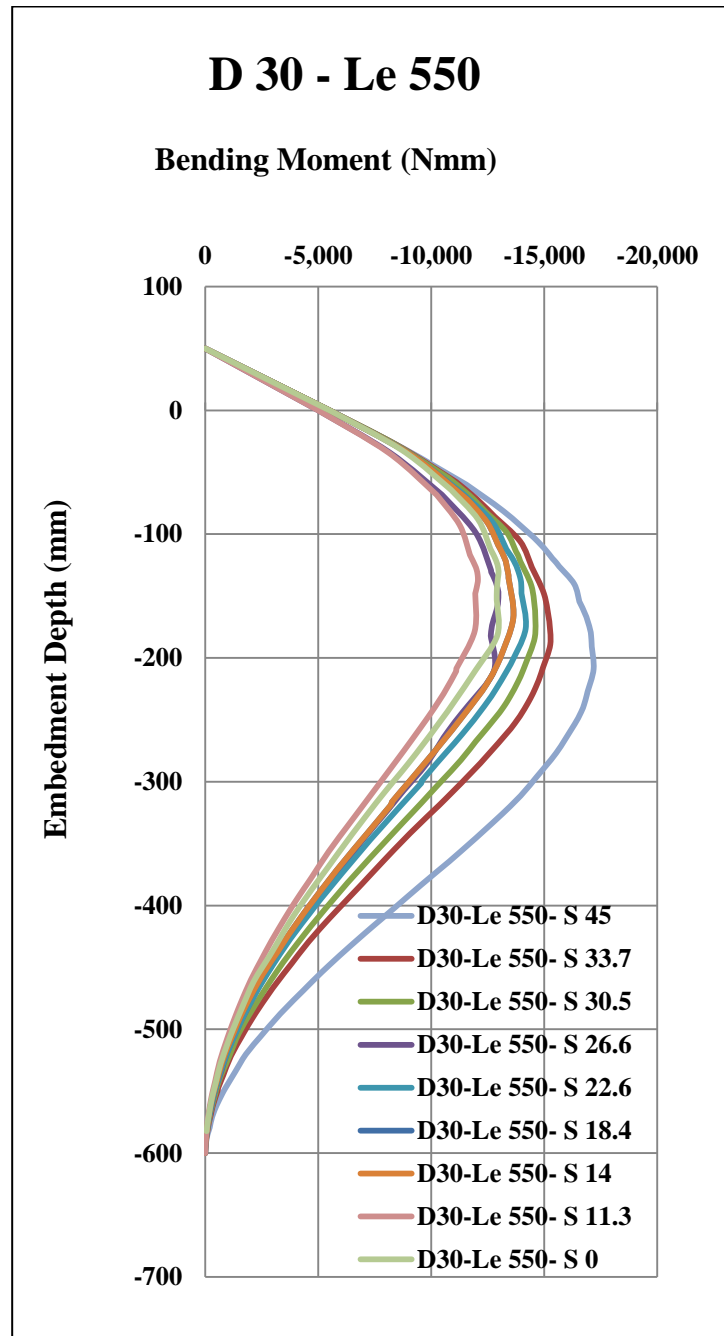


Fig. 5.7.c Bending Moment Diagram for 30 mm Diameter Model Pile with 550 mm Embedment Depth

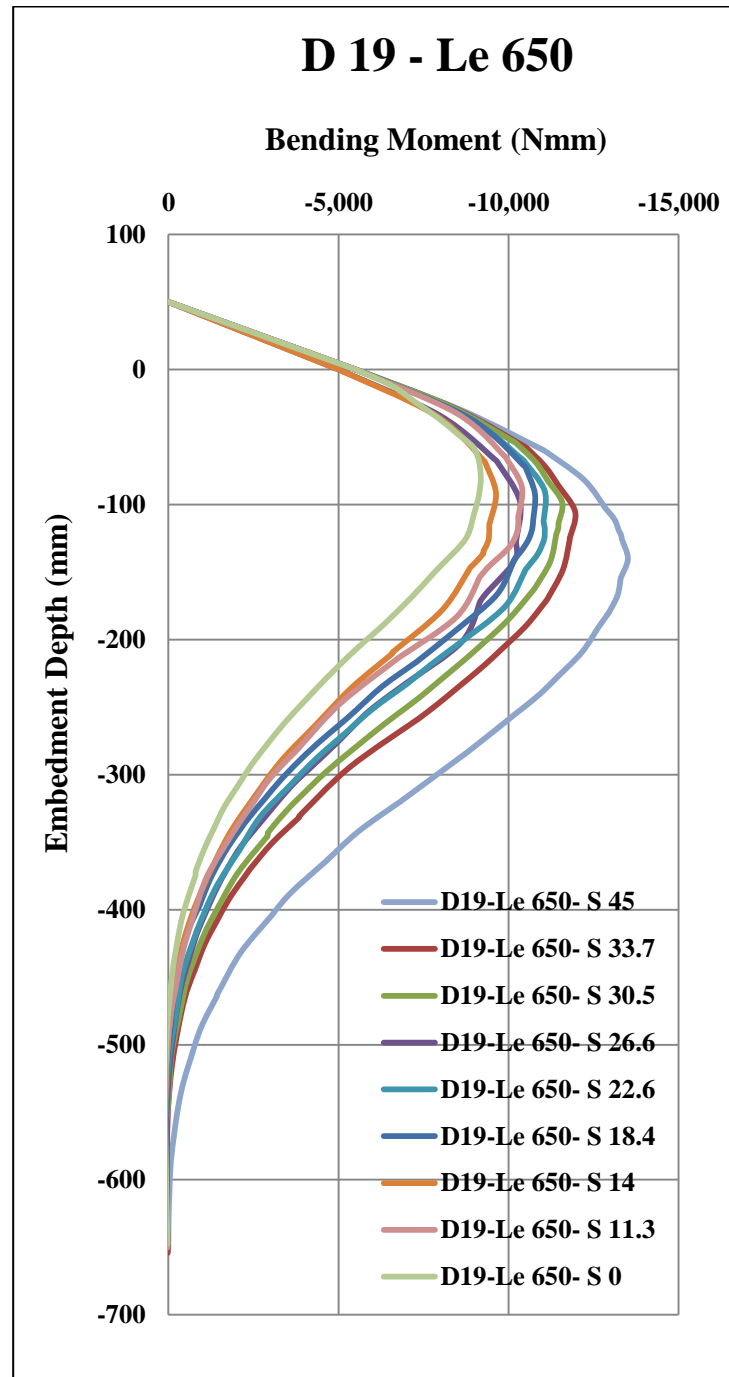


Fig. 5.7.d Bending Moment Diagram for 19 mm Diameter Model Pile with 650 mm Embedment Depth

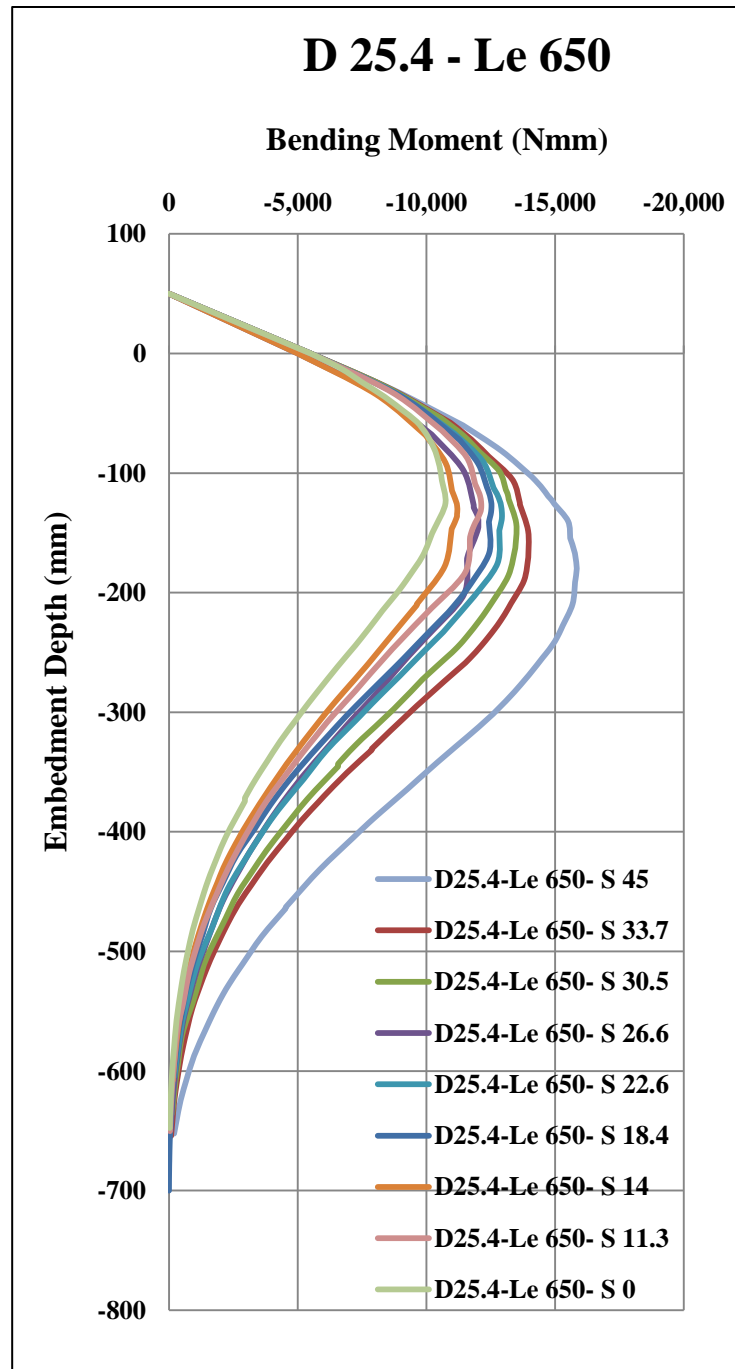


Fig. 5.7.e Bending Moment Diagram for 25.4 mm Diameter Model Pile with 650 mm Embedment Depth

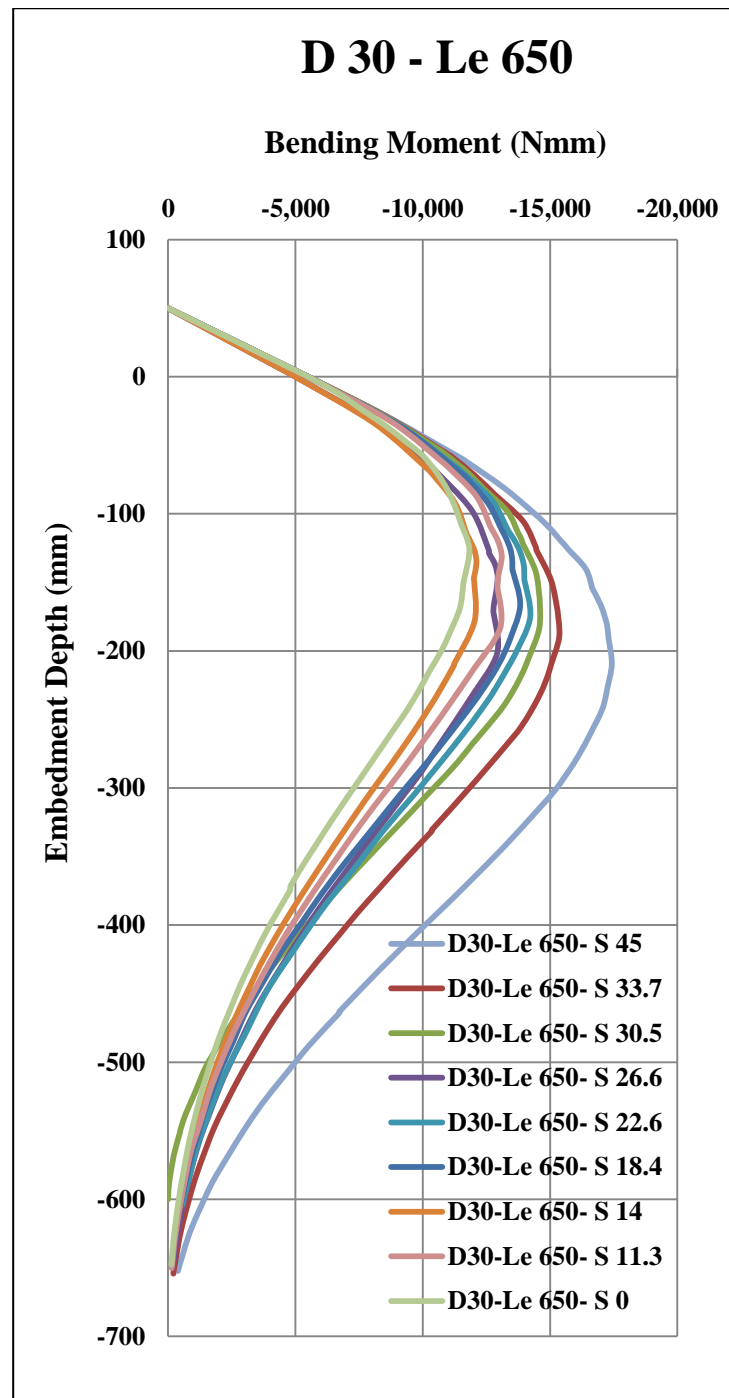


Fig. 5.7.f Bending Moment Diagram for 30 mm Diameter Model Pile with 650 mm Embedment Depth

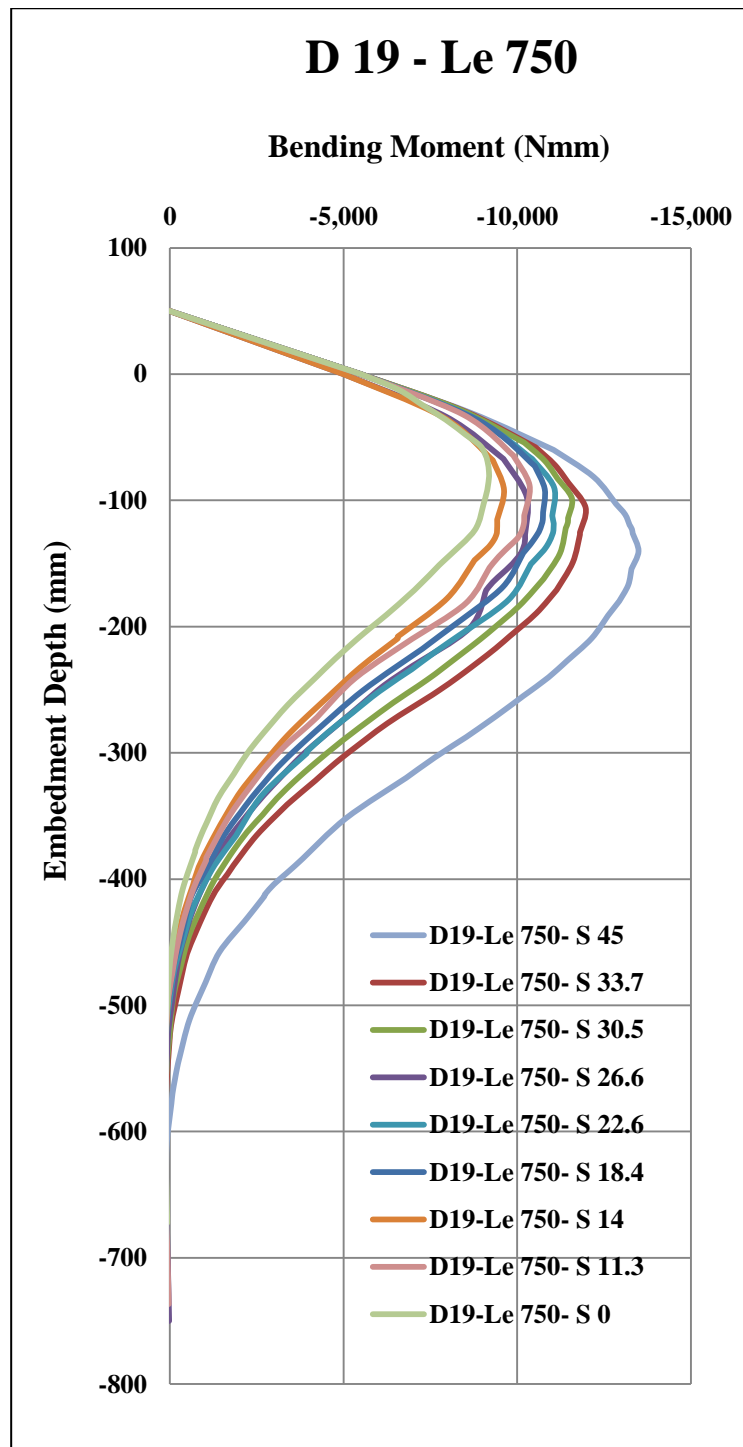


Fig. 5.7.g Bending Moment Diagram for 19 mm Diameter Model Pile with 750 mm Embedment Depth

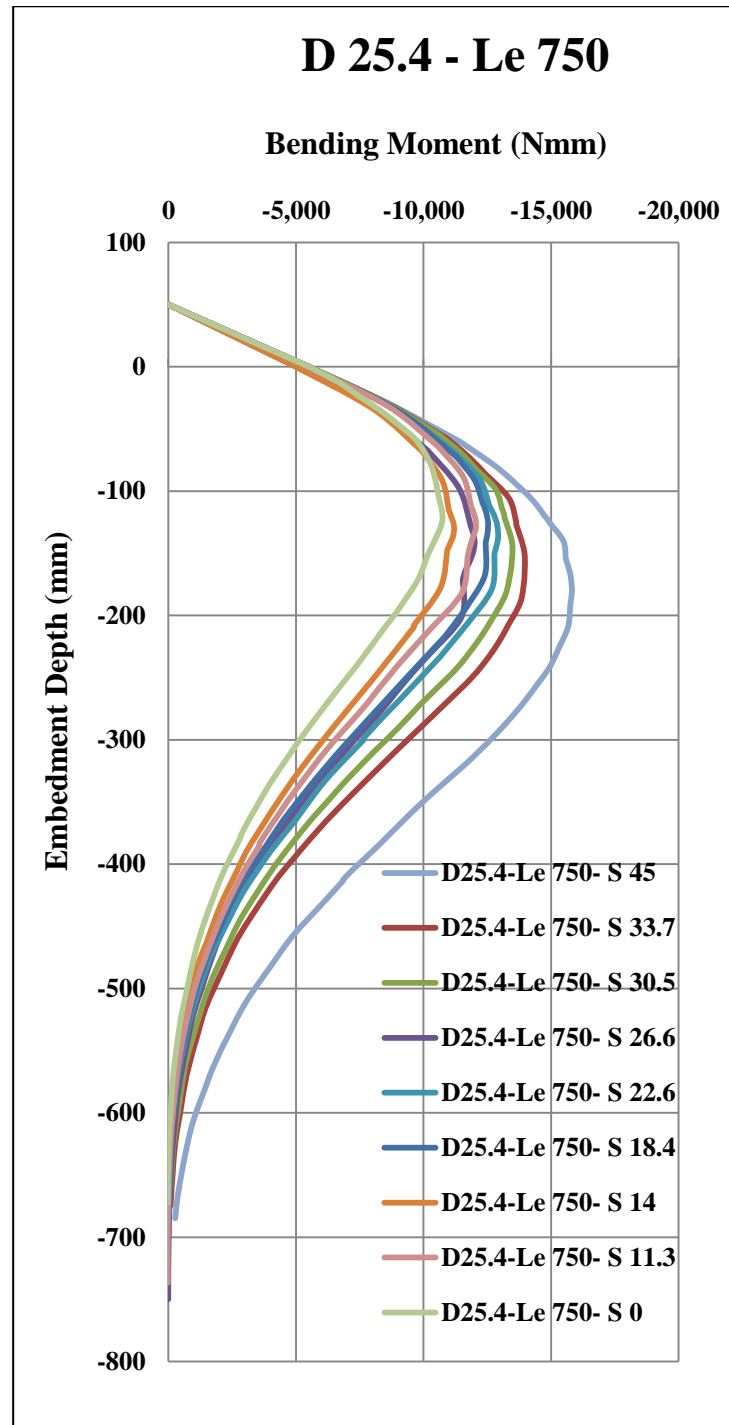


Fig. 5.7.h Bending Moment Diagram for 25.4 mm Diameter Model Pile with 750 mm Embedment Depth

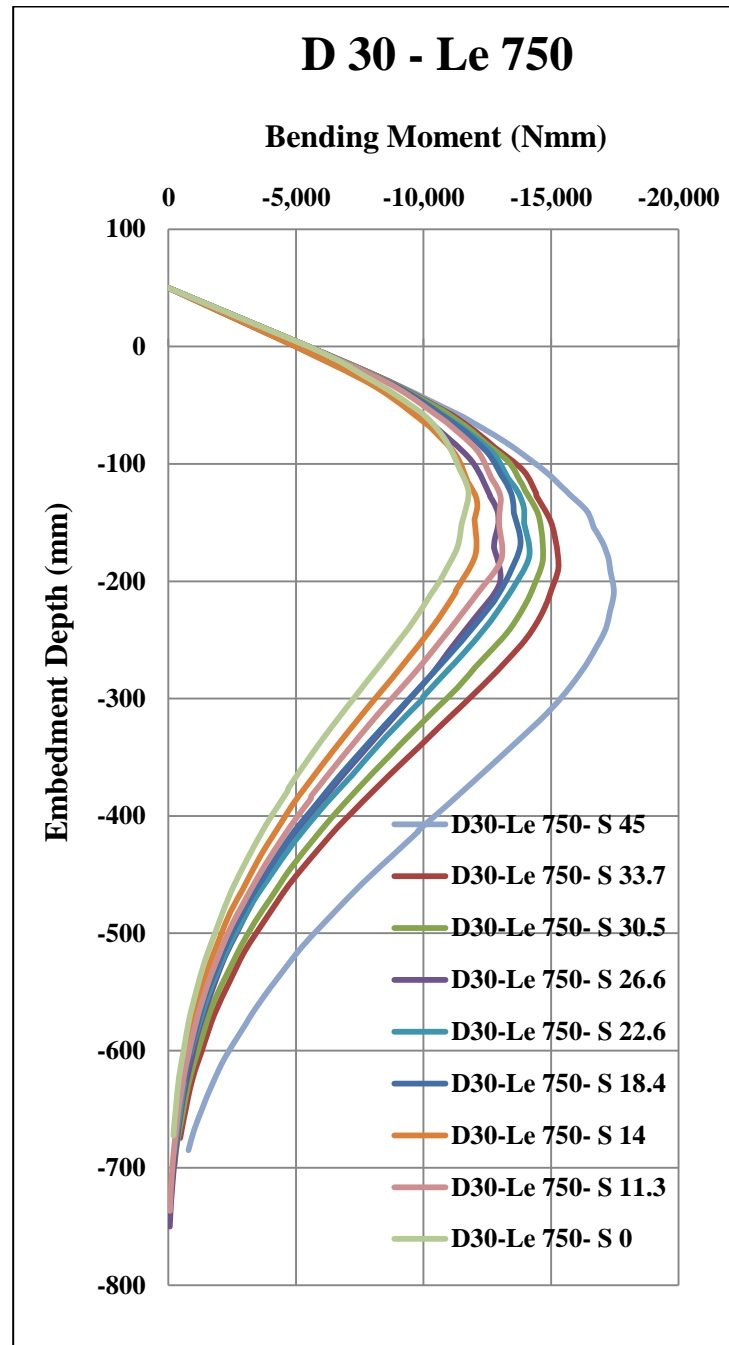


Fig. 5.7.i Bending Moment Diagram for 30 mm Diameter Model Pile with 750 mm Embedment Depth

5.4.3 Tabulated Results

The details of parametric study and the results are grouped and tabulated as follows,

Table 5.1.a Numerical Investigation Results of Model Piles (D=19 mm, L=600 mm)

Diameter of Pile = 19 mm					
Length of Pile = 600 mm					
Sl. No.	S (slope 1 V: S H)	Slope (°)	Maximum Deflection (mm)	Maximum Bending Moment (kNmm)	Depth of Fixity (mm)
1	1	45	6.077	13.522	140.216
2	1.5	33.7	4.327	11.968	105.775
3	1.7	30.5	3.967	11.588	98.396
4	2	26.6	3.453	10.333	98.729
5	2.4	22.6	3.57	11.08	118.419
6	3	18.4	3.304	10.791	90.349
7	4	14	2.819	9.623	92.466
8	5	11.3	3.04	10.361	88.061
9	nil	0	2.385	9.277	79.596

Table 5.1.b Numerical Investigation Results of Model Piles (D=19 mm, L=700 mm)

Diameter of Pile = 19 mm					
Length of Pile = 700 mm					
Sl. No.	S (slope 1 V: S H)	Slope (°)	Maximum Deflection (mm)	Maximum Bending Moment (kNmm)	Depth of Fixity (mm)
1	1	45	5.994	13.51	140.17
2	1.5	33.7	4.283	11.961	105.492
3	1.7	30.5	3.967	11.588	98.396
4	2	26.6	3.432	10.333	97.315
5	2.4	22.6	3.553	11.067	117.391
6	3	18.4	3.288	10.777	92.165
7	4	14	2.81	9.632	91.561
8	5	11.3	3.022	10.392	86.924
9	nil	0	2.403	9.186	82.118

Table 5.1.c Numerical Investigation Results of Model Piles (D=19 mm, L=800 mm)

Diameter of Pile = 19 mm					
Length of Pile = 800 mm					
Sl. No.	S (slope 1 V: S H)	Slope (°)	Maximum Deflection (mm)	Maximum Bending Moment (kNmm)	Depth of Fixity (mm)
1	1	45	5.957	13.491	140.233
2	1.5	33.7	4.263	11.968	105.736
3	1.7	30.5	3.938	11.574	98.431
4	2	26.6	3.428	10.273	97.099
5	2.4	22.6	3.542	11.059	89.604
6	3	18.4	3.3	10.792	91.1
7	4	14	2.806	9.62	91.763
8	5	11.3	3.027	10.355	88.135
9	nil	0	2.398	9.192	80.725

Table 5.1.d Numerical Investigation Results of Model Piles (D=25.4 mm, L=600 mm)

Diameter of Pile = 25.4 mm					
Length of Pile = 600 mm					
Sl. No.	S (slope 1 V: S H)	Slope (°)	Maximum Deflection (mm)	Maximum Bending Moment (kNmm)	Depth of Fixity (mm)
1	1	45	4.102	15.806	179.423
2	1.5	33.7	2.934	13.935	148.19
3	1.7	30.5	2.698	13.484	141.806
4	2	26.6	2.313	12.043	146.735
5	2.4	22.6	2.406	12.949	135.767
6	3	18.4	2.26	12.477	121.807
7	4	14	1.931	11.186	130.689
8	5	11.3	2.101	12.054	124.67
9	nil	0	1.678	10.787	123.037

Table 5.1.e Numerical Investigation Results of Model Piles (D=25.4 mm, L=700 mm)

Diameter of Pile = 25.4 mm					
Length of Pile = 700 mm					
Sl. No.	S (slope 1 V: S H)	Slope (°)	Maximum Deflection (mm)	Maximum Bending Moment (kNmm)	Depth of Fixity (mm)
1	1	45	4.01	15.841	179.809
2	1.5	33.7	2.897	13.957	170.452
3	1.7	30.5	2.678	13.49	142.221
4	2	26.6	2.293	12.018	144.702
5	2.4	22.6	2.392	12.932	133.236
6	3	18.4	2.243	12.526	125.52
7	4	14	1.921	11.203	130.053
8	5	11.3	2.081	12.13	125.922
9	nil	0	1.695	10.741	125.166

Table 5.1.f Numerical Investigation Results of Model Piles (D=25.4 mm, L=800 mm)

Diameter of Pile = 25.4 mm					
Length of Pile = 800 mm					
Sl. No.	S (slope 1 V: S H)	Slope (°)	Maximum Deflection (mm)	Maximum Bending Moment (kNmm)	Depth of Fixity (mm)
1	1	45	3.975	15.825	179.794
2	1.5	33.7	2.874	13.955	170.963
3	1.7	30.5	2.664	13.479	142.112
4	2	26.6	2.821	13.328	152.145
5	2.4	22.6	2.387	12.926	136.348
6	3	18.4	2.251	12.533	127.922
7	4	14	1.919	11.2	129.968
8	5	11.3	2.091	12.056	124.74
9	nil	0	1.693	10.742	123.331

Table 5.1.g Numerical Investigation Results of Model Piles (D=30 mm, L=600 mm)

Diameter of Pile = 30 mm					
Length of Pile = 600 mm					
Sl. No.	S (slope 1 V: S H)	Slope (°)	Maximum Deflection (mm)	Maximum Bending Moment (kNmm)	Depth of Fixity (mm)
1	1	45	3.365	17.18	209.05
2	1.5	33.7	2.382	15.264	189.098
3	1.7	30.5	2.172	14.592	161.716
4	2	26.6	1.873	12.97	146.735
5	2.4	22.6	1.967	14.174	176.421
6	3	18.4	1.848	13.629	167.548
7	4	14	1.57	12.059	134.566
8	5	11.3	1.715	12.978	130.02
9	nil	0	1.402	11.761	123.037

Table 5.1.h Numerical Investigation Results of Model Piles (D=30 mm, L=700 mm)

Diameter of Pile = 30 mm					
Length of Pile = 700 mm					
Sl. No.	S (slope 1 V: S H)	Slope (°)	Maximum Deflection (mm)	Maximum Bending Moment (kNmm)	Depth of Fixity (mm)
1	1	45	3.205	17.426	209.526
2	1.5	33.7	2.313	15.361	189.739
3	1.7	30.5	2.135	14.689	162.578
4	2	26.6	1.837	12.941	145.189
5	2.4	22.6	1.924	14.22	175.527
6	3	18.4	1.817	13.827	166.746
7	4	14	1.55	12.109	135.34
8	5	11.3	1.685	13.105	131.733
9	nil	0	1.426	11.831	125.166

Table 5.1.i Numerical Investigation Results of Model Piles (D=30 mm, L=800 mm)

Diameter of Pile = 30 mm					
Length of Pile = 800 mm					
Sl. No.	S (slope 1 V: S H)	Slope (°)	Maximum Deflection (mm)	Maximum Bending Moment (kNmm)	Depth of Fixity (mm)
1	1	45	3.161	17.46	209.225
2	1.5	33.7	2.264	15.285	189.378
3	1.7	30.5	2.112	14.667	183.579
4	2	26.6	1.831	12.996	201.08
5	2.4	22.6	1.91	14.147	178.671
6	3	18.4	1.821	13.803	168.353
7	4	14	1.548	12.112	135.616
8	5	11.3	1.693	13.034	130.144
9	nil	0	1.408	11.762	123.331

5.5 Multivariable Regression Equations

A multivariable regression analysis (Appendix-I) was also done to develop an equation to predict the variation of maximum deflection and maximum bending moment with the change in bed slope, pile diameter and pile embedment depth.

$$y_{max} = 5.352 + 0.053S - 0.151D - 0.000107L_e \dots\dots\dots (5.1)$$

Where, y_{max} is the maximum deflection at the top of the pile in mm, S is the bed slope with the ground surface in degrees, D and L are the diameter and embedment depth of pile in mm. R^2 corresponding to the regression is 0.88.

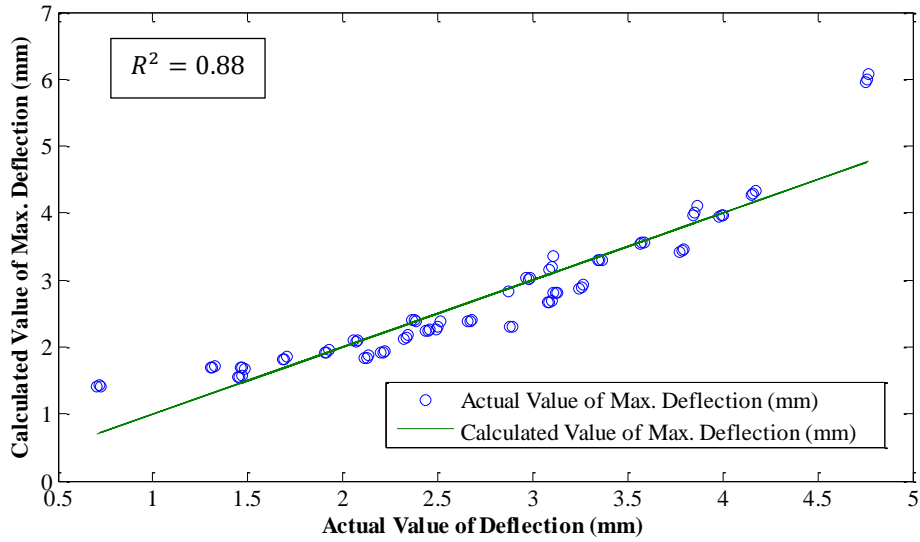


Fig. 5.8 Actual Value of Max. Deflection Vs Calculated Value of Max. Deflection

$$M_{max} = 3.241 + 0.105S + 0.271D + 0.000326L_e \dots\dots\dots (5.2)$$

Where, M_{max} is the maximum bending moment at the depth of fixity of the pile in Newton-meter unit and R^2 corresponding to the regression is 0.90.

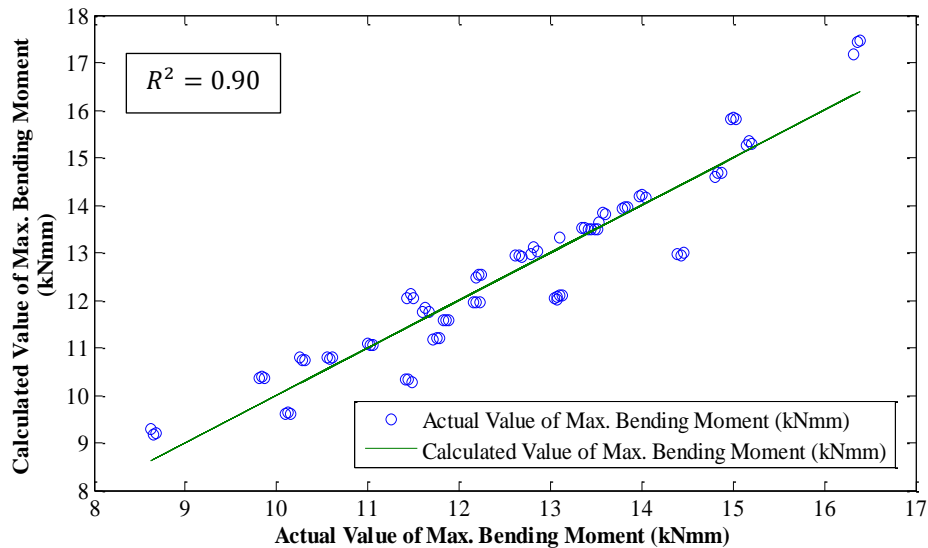


Fig. 5.9 Actual Value of Max. Deflection Vs Calculated Value of Max. Bending Moment

$$D_f = -52.116 + 1.477S + 5.745D + 0.0161L_e \dots\dots\dots (5.3)$$

Where, D_f is the depth at which maximum bending moment is acting in mm and R^2 corresponding to the regression is 0.88.

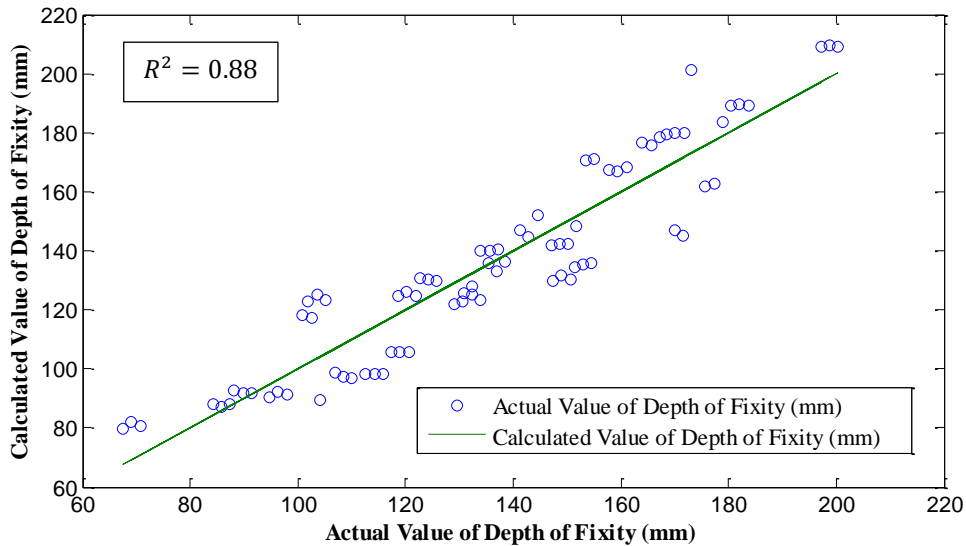


Fig. 5.9 Actual Value of Depth of Fixity Vs Calculated Value of Depth of Fixity

As in the case of static analysis, the change in the properties of soil and pile influences the dynamic response of the soil–pile system and it is clearly established in a parametric study discussed in Appendix-D.2.2.

Equation nos. (5.1), (5.2) and (5.3) can be used to predict the maximum deflection, maximum bending moment and depth of fixity of a single pile embedded at the crest of a slope of the range of values considered in the present study. Variation of depth of fixity as per the suggested equation and the conventional method as per IS code is studied and tabulated as follows. As per IS 2911(Part 1/ Sec 1):2010, cl.6.5.1, the depth of fixity of pile embedded in soft soil is not more than ten times diameter of pile.

Table 5.2 Variation of depth of fixity as per the suggested equation and the conventional method

S°	D (mm)	L (mm)	Df (mm)	10D	% over estimation
0.000	19	600	66.639	190	285
45.000	19	600	133.104	190	143
0.000	30	600	129.834	300	231
45.000	30	600	196.299	300	153
0.000	19	800	69.839	190	272
45.000	19	800	136.304	190	139
0.000	30	800	133.034	300	226
45.000	30	800	199.499	300	150

5.6 Summary

The behaviour of laterally loaded piles was studied using model tests on sloping clay bed in Chapter 3. The results were compared with the numerical analysis results obtained in this chapter. For the numeric analysis, the diameter and the embedment depth of pile were varied along with the bed slope and the structural behaviour of the pile is studied. The following are the observations from the present study:

- The maximum bending moment on the pile increases as the embedment depth of pile, the diameter of pile and bed slope increases.
- The depth of fixity moves down as the embedment depth of pile, the diameter of pile and bed slope increases.
- Based on the parametric studies, equations are developed using multivariable regression to find the magnitudes of maximum deflection, maximum bending moment and depth of fixity in terms of bed slope, the pile diameter and the pile embedment depth.
- These equations can be used to predict the values of the output parameters within the range of input parameters considered for the

study. The parametric study may further extended for different soil conditions and for different loading so that the results could be used for the on-site design of the piles.

From the above observations the following conclusions can be made. The change in embedment depth causes only a marginal increase in depth of fixity and hence the bending moment. Though the change in diameter also causes an increase in depth of fixity and bending moment, considerable increase in the stiffness and moment of resistance will have a positive effect on the load carrying capacity of the pile. Whereas, the increase in top deflection, bending moment and depth of fixity due to the increase in slope can adversely affect the load carrying capacity of the pile. The variation patterns of deflection and bending moment can be predicted using analytical as well as numerical methods. Hence piles embedded in slopes are to be critically analyzed if there is a possibility of change in slope with time.

.....❧.....

Numerical Analysis of Ship Berthing Structure

<i>C</i> <i>o</i> <i>n</i> <i>t</i> <i>e</i> <i>n</i> <i>t</i> <i>s</i>	6.1 <i>Introduction</i>
	6.2 <i>Modeling and Analysis of a Berthing Structure</i>
	6.3 <i>Parameters of Soil and Structure</i>
	6.4 <i>Parametric Study</i>
	6.5 <i>Influence of Pile Diameter on Depth of Fixity</i>
	6.6 <i>Influence of Soil Modulus on Depth of Fixity</i>
	6.7 <i>Influence of Bed Slope on Depth of Fixity</i>
	6.8 <i>Regression Equation to Predict Depth of Fixity</i>
	6.9 <i>Influence of Pile Diameter on Bending Moment</i>
	6.10 <i>Influence of Soil Modulus on Bending Moment</i>
	6.11 <i>Influence of Bed Slope on Bending Moment</i>
	6.12 <i>Regression Equation to Predict Bending Moment</i>
	6.13 <i>Influence of Pile Diameter on Maximum Deflection</i>
	6.14 <i>Influence of Soil Modulus on Maximum Deflection</i>
	6.15 <i>Influence of Bed Slope on Maximum Deflection</i>
	6.16 <i>Regression Equation to Predict Maximum Deflection</i>
	6.17 <i>Summary</i>

6.1 Introduction

Berthing structures are generally constructed in coastal area where the soil will be having soft consistency and the behaviour of a structure is dependent on the stiffness properties of structure as well as the type of soil surrounding the structure. The investigations in previous chapters have established the contributions of influencing parameters in the structural behaviour of a soil-pile system. From the studies it is evident that the pile diameter, soil modulus and the bed slope are the major factors influencing a soil-pile system. Hence in this chapter the influence of the above parameters in the structural behaviour of a

typical frame of a ship berthing structure is studied. Multivariable regression analysis is also done to quantify the contributions of each of the parameters on the depth of fixity of pile, bending moment at the depth of fixity of pile and the deflection of the structure.

6.2 Modeling and Analysis of a Berthing Structure

Based on the literature review a typical dimension is adopted for the analysis of a berthing structure [83, 84, 87, 106]. The soil structure interaction was modeled using the finite element software PLAXIS-3D. Berthing structure was modeled as a frame with girder and pile arrangement as shown in Fig.6.1 and it was embedded in a sloping bed of soil. The girders were modeled as three node beam element. The pile was considered as a three node beam element with an interface that can cross a 10 node tetrahedral soil element at any point in arbitrary orientation [103].

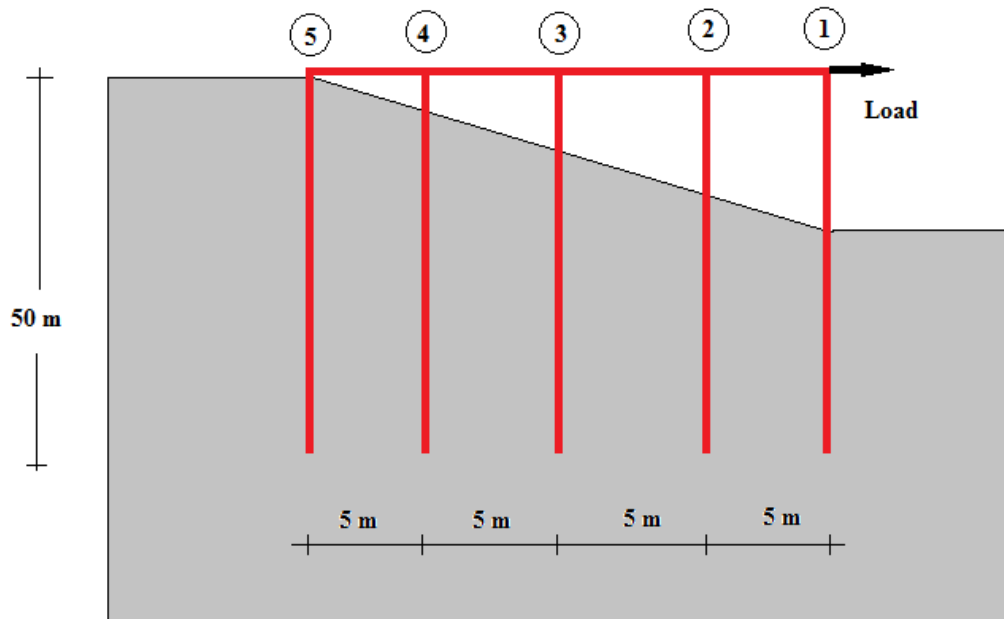


Fig. 6.1 Typical Frame of a Berthing Structure Considered for the Present Study

A lateral load was applied at the beam level to represent a mooring pull of 3000 kN as per cl.5.3, Table 4, IS4651-Part III-1974. The structure was analyzed

and the magnitudes of bending moment acting on piles at the depth of fixity were studied.

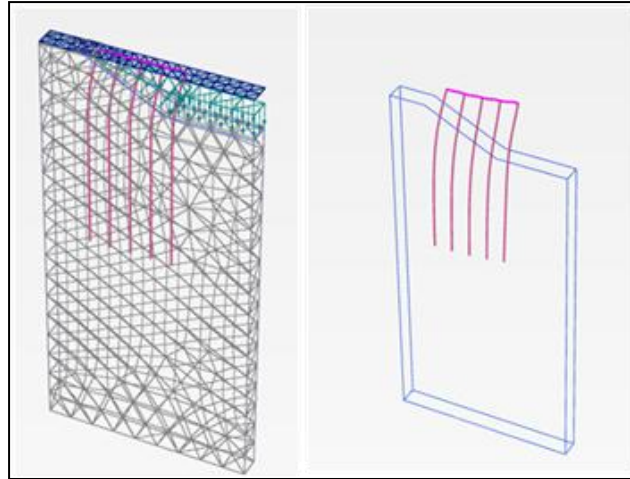


Fig. 6.2 Meshed model and Deflection Pattern of the Typical Berthing Structure Considered

6.3 Parameters of Soil and Structure

Table 6.1 Parameters of Pile and Beam

Sl. No.	Parameter	Name	Magnitude	Unit
1	Pile diameter	D	1 , 1.5, 2	m
2	Pile length	L	50	m
3	Compressive strength of concrete	MIX	35	N/mm ²
4	Young's modulus of concrete	E	30,000,000	kN/m ²
5	Poisson's ratio of concrete	ν_c	0.15	-
6	Unit weight of concrete	γ_c	25	kN/m ³
7	Skin resistance	T_{max}	200	kN/m
8	Base resistance	F_{max}	200	kN/m
9	Cross-sectional area of beam	A_b	0.15	m ²

Table 6.2 Parameters of Soil

Sl. No.	Parameter	Name	Magnitude	Unit
1	Soil Model	Mohr- Coulomb	-	-
2	Saturated unit weight	γ_{sat}	18	kN/m ³
3	Dry unit weight	γ_{unsat}	17	kN/m ³
4	Soil modulus	Es	1000,10,000, 50,000	kN/m ²
5	Cohesion	c	12	kN/m ²
6	Angle of internal friction	ϕ	12	°
7	Poisson's ratio	ν_s	0.3	-
8	Dilatancy angle	ψ	0	°
9	Bed Slope	1 in S (1 vertical in S horizontal)	1 in 2 (26.5°), 1 in 2.22(24.3°), 1 in 2.5 (21.8°), 1 in 2.86 (19.3°), 1 in 3.33 (16.7°), 1 in 4 (14.03°), 1 in 5 (11.3°)	°

6.4 Parametric Study

A parametric study has been conducted to analyze the influence of the parameters involved in the present study; pile diameter soil modulus and bed slope. Bed slope variation was considered with a change in the upper part of the slope (Us) as well as a change in the lower part of the slope (Ls) as shown in Fig. 6.3. The depth of fixity, maximum bending moment and maximum deflection were found to be changing with the change in pile diameter, soil modulus and bed slope. The results are tabulated and are included in Appendix-H.

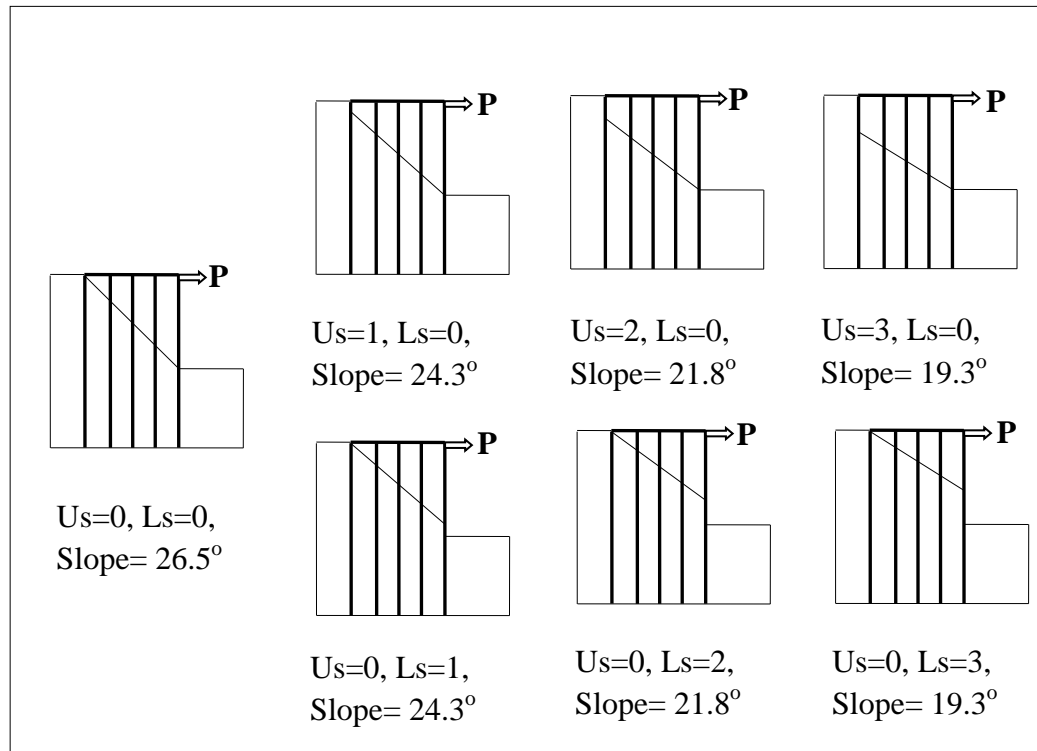


Fig. 6.3 Bed Slope Variation Adopted for Parametric Study

6.5 Influence of Pile Diameter on Depth of Fixity

A particular pattern of depth of fixity variation is observed among the rows of piles as shown in Fig. 6.4. It can be seen that as we move from row5 to row2 the depth of fixity increases. It is due to the reduction in the passive earth pressure due to the presence of bed slope and the shadowing effect due to the presence of another pile in front of the row of pile considered. In row1 there is a decrease in the depth of fixity since there is no shadowing effect for row1 of piles.

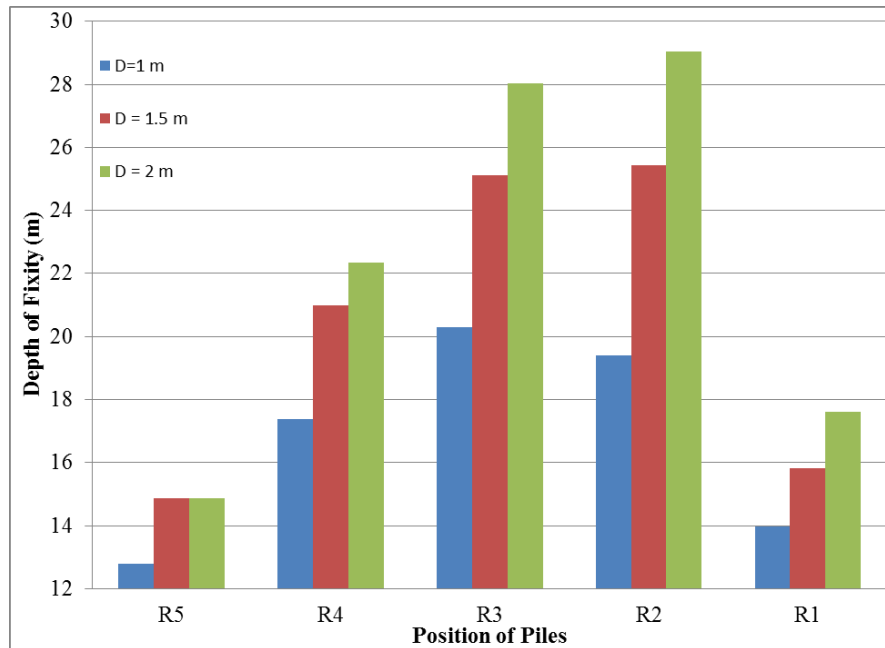


Fig. 6.4 Variation of Depth of Fixity with Diameter of Pile ($E_s = 1000 \text{ kN/m}^2$)

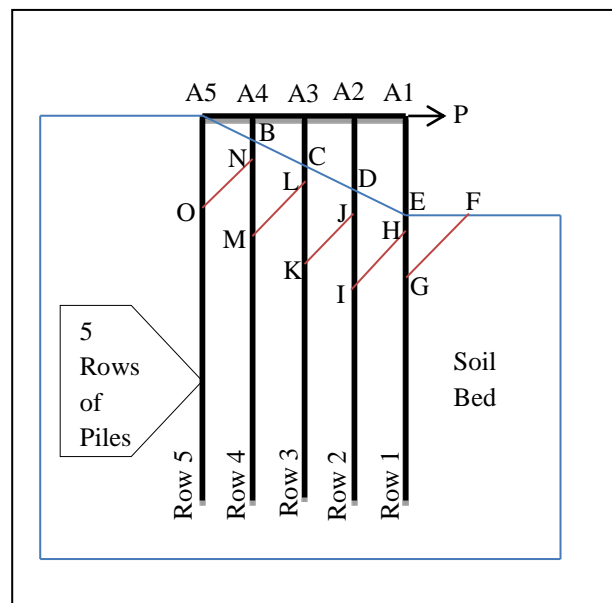


Fig. 6.5 Passive Earth Pressure Acting on Piles in the Berthing Structure

Fig. 6.5 shows the passive earth pressure acting on the piles when lateral load is applied. The areas A5BNO, BCLM, CDJK, DEHI and EFG are the passive earth pressures acting on piles in row5 to row1 respectively. The shadowing effect is also incorporated in the figure. The areas mentioned are equal in magnitude and they resist the lateral force “P” acting at the top of the structure. It is clear from the figure that $A5O < A4M < A3K < A2I$. This increase in depth of fixity is observed in row5 to row2, due to the presence of bed slope which causes a reduction in passive earth pressure acting on the corresponding rows of piles. There is a decrease in depth of fixity in row1 pile since there is no reduction in passive earth pressure acting on row1 pile due to the bed slope as well as shadowing effect.

It can be observed from Fig. 6.4 that the depth of fixity of piles increases with the increase in pile diameter and the same is found to be true for all the soil modulus and pile positions considered for the study. This is due to the fact that as the pile diameter increases the lateral soil pressure on the pile increases and it causes an increase in depth of fixity. When the diameter changes from 1 m to 2 m, it is observed that there is an average of 30 % increase in depth of fixity of the pile in various rows of piles.

6.6 Influence of Soil Modulus on Depth of Fixity

For the parametric study the soil modulus is varied from weak soil ($E_s = 1000 \text{ kN/m}^2$) to stiff soil ($50,000 \text{ kN/m}^2$). From Fig. 6.6 it is evident that as the soil stiffness increases there is around 45% reduction in the depth of fixity of the piles.

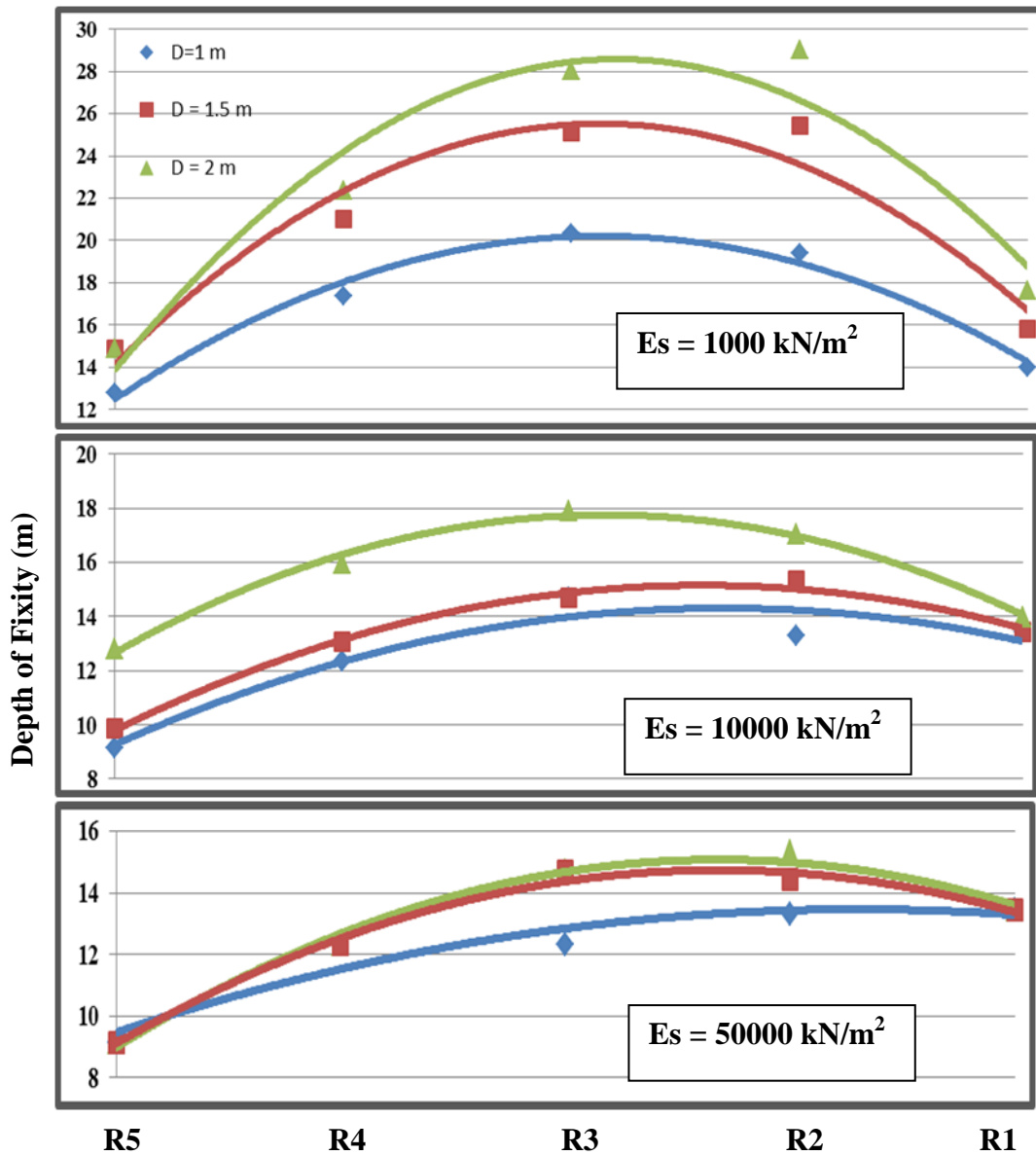


Fig. 6.6 Variation of Depth of Fixity with Soil Modulus

6.7 Influence of Bed Slope on Depth of Fixity

Change in bed slope has two distinct effects as the variation at the upper part of the slope and at the lower part of the slope.

6.7.1 Influence of Soil in the Upper Part of Bed Slope

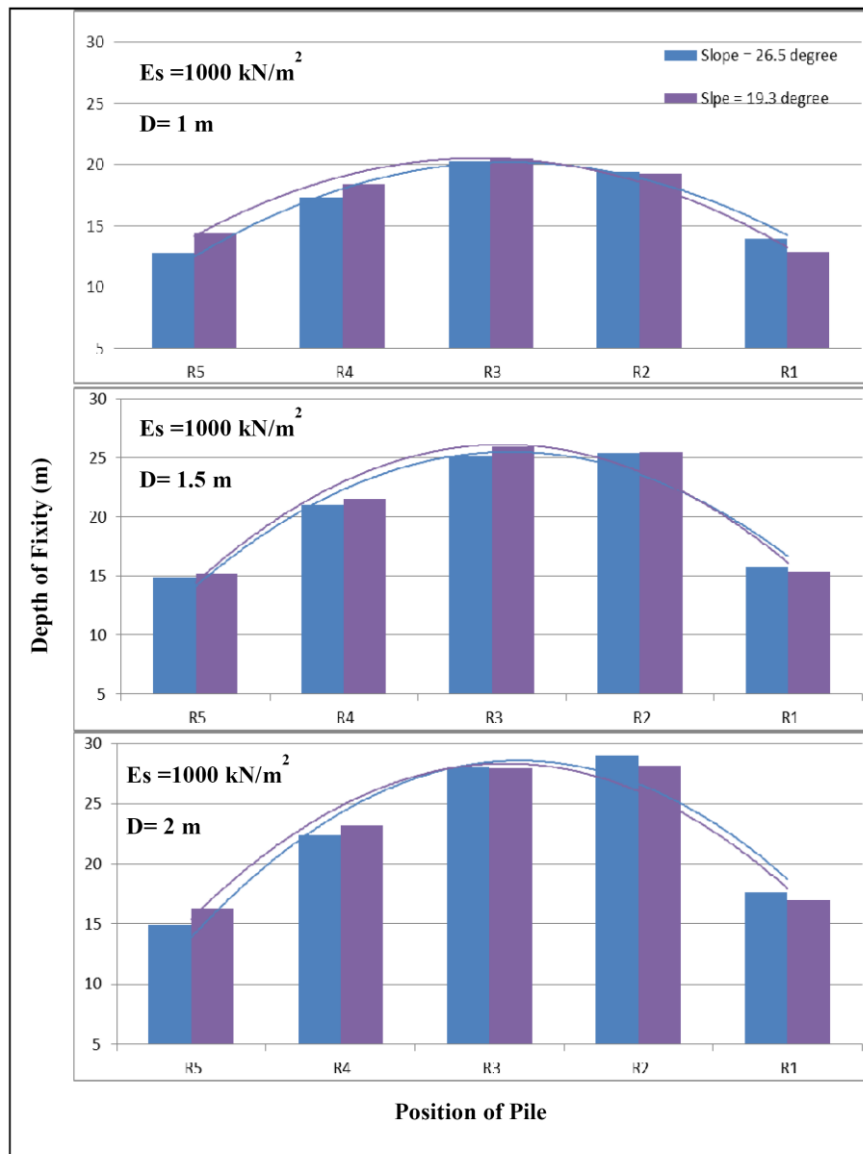


Fig. 6.7 Influence of Soil in the Upper Part of Bed Slope in Depth of Fixity

In this case the bed slope is increased from 19.3° to 26.5° , by adding the soil in the upper part of the bed slope. It can be observed from Fig.6.7 that as the slope increases the depth of fixity increases in row1 and row2 piles. It is due to the fact that an increase in slope is caused due to the addition of soil in the upper part of soil bed which in turn causes lateral soil pressure on the row1 and row2 piles. The depth of fixity decreases with increase of slope in row3, row4 and

row5 piles. It is due to the fact that an increase in slope caused by the addition of soil in the upper part of soil bed helps row3, row4 and row5 piles to get additional volume of passive earth pressure and it causes a decrease in depth of fixity.

6.7.2 Influence of Soil in the Lower Part of Bed Slope

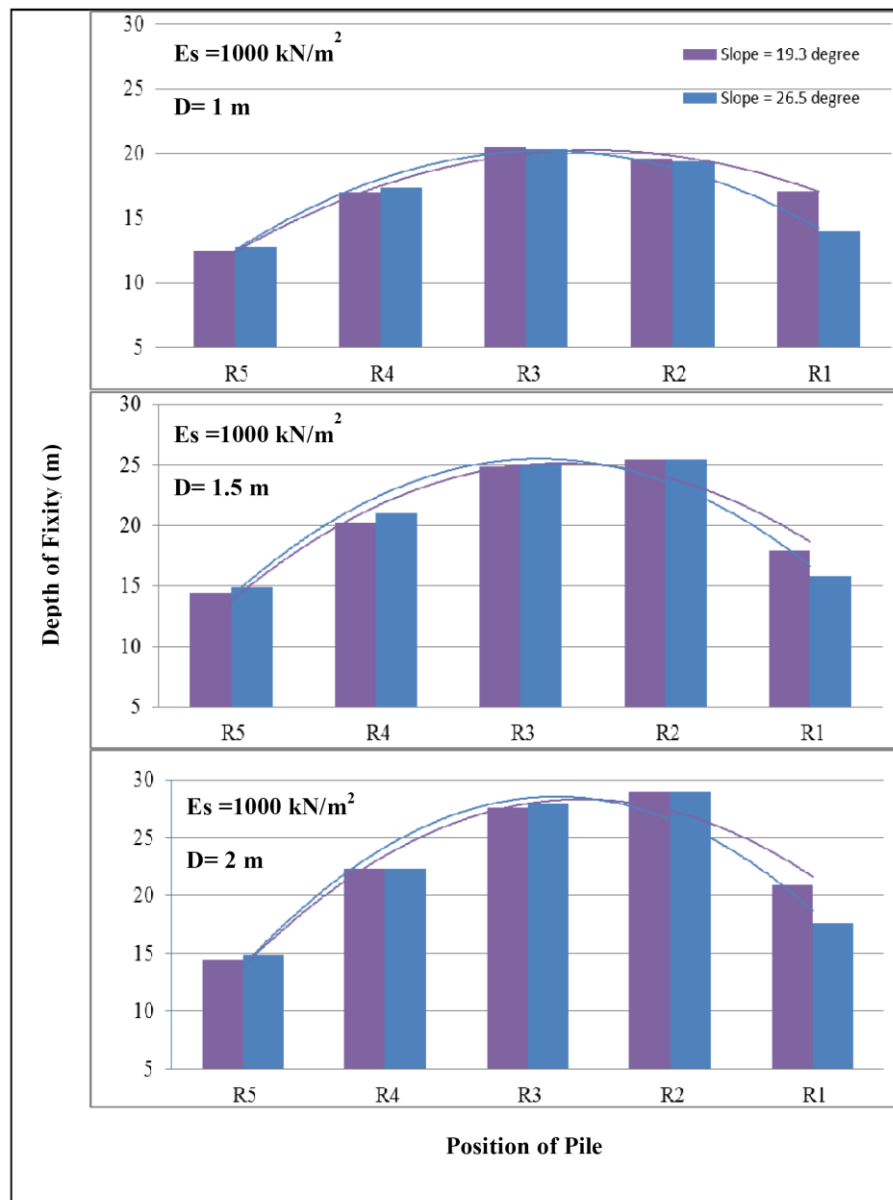


Fig. 6.8 Influence of Soil in the Lower Part of Bed Slope in Depth of Fixity

In this case the bed slope is increased from 19.3° to 26.5° , by removing the soil from the lower part of the bed slope. It can be observed from Fig.6.8 that as the slope increases the depth of fixity decreases in row1 and row2 piles. It is due to the fact that an increase in slope is caused due to the removal of soil from the lower part of soil bed which in turn leads to a reduction in the active earth pressure acting on the pile in row1 and row2 piles. The depth of fixity increases with increase in slope, in row3, row4 and row5 piles. It is due to the fact that, increases in slope caused by the removal of soil from the lower part of soil bed causes an increase in lateral soil pressure on piles at the landside. Hence in row3, row4 and row5 piles the depth of fixity increases.

Hence it can be concluded that bed slope variation influences the depth of fixity in such a way that, whenever soil is removed or added in the bed slope, an unstable bed slope exerts additional lateral loads on piles which causes an increase in depth of fixity.

6.8 Regression Equations to Predict of Depth of Fixity

$$Df1 = 20.54 + 1.60 D - 2.35 \log(Es) + 0.13 \left(\frac{1}{\tan(\theta)} \right) - 0.17 Us - 0.72 Ls \dots\dots (6.1)$$

$$Df2 = 35.94 + 3.98 D - 6.23 \log(Es) + 0.55 \left(\frac{1}{\tan(\theta)} \right) - 0.48 Us - 0.59 Ls \dots\dots (6.2)$$

$$Df3 = 95.3 + 984.1 D + 470.4 \log(Es) - 57.7 \left(\frac{1}{\tan(\theta)} \right) + 119.2 Us - 97.8 Ls \dots\dots (6.3)$$

$$Df4 = 31.34 + 2.87 D - 5.09 \log(Es) - 0.03 \left(\frac{1}{\tan(\theta)} \right) + 0.11 Us - 0.35 Ls \dots\dots (6.4)$$

$$Df5 = 20.36 + 1.82 D - 3.04 \log(Es) - 0.16 \left(\frac{1}{\tan(\theta)} \right) + 0.48 Us - 0.12 Ls \dots\dots (6.5)$$

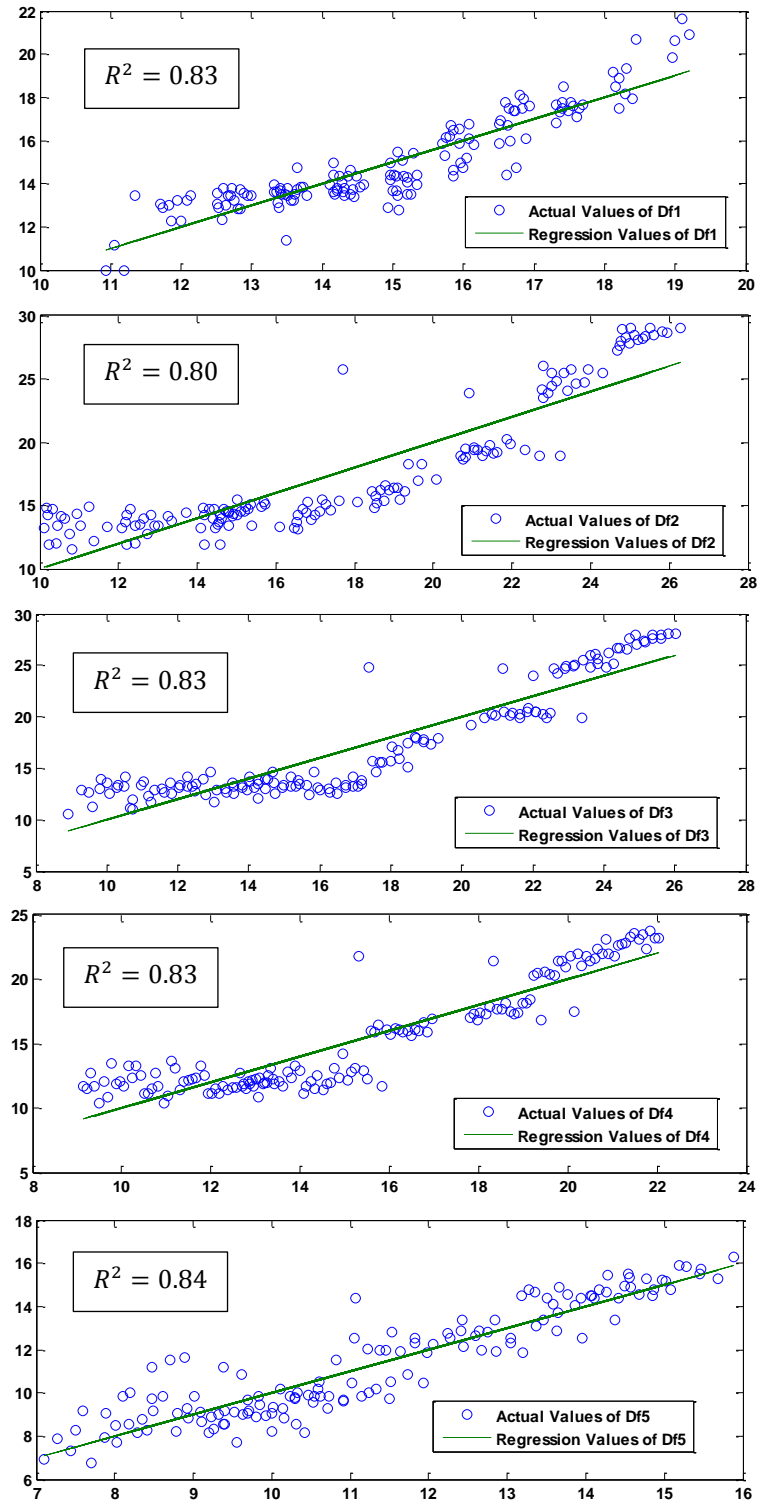


Fig. 6.9 Actual Value of Depth of Fixity Vs Calculated Value of Depth of Fixity

6.9 Influence of Pile Diameter on Bending Moment

A particular pattern of bending moment variation is observed the rows of piles as shown in Fig. 6.10. Row1 pile is subjected to the applied lateral load and hence maximum bending moment is observed there. The influence of load and hence the bending moment decreases in row2 and row3. When it comes to row4 and row5, the soil pressure from the land area causes an additional load and hence the bending moment tends to increase.

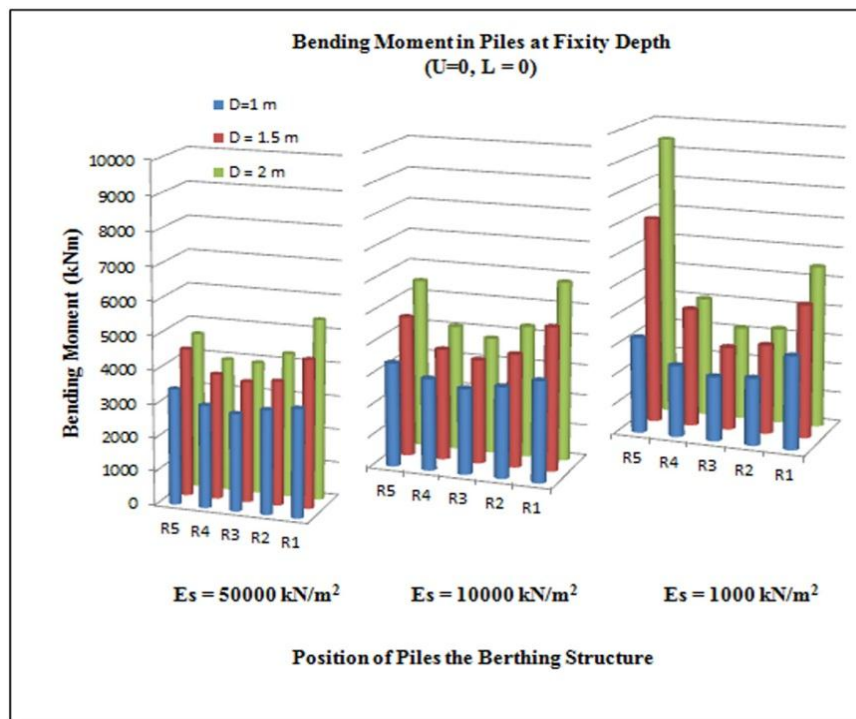


Fig. 6.10 Variation of Bending Moment with Change in Diameter and Soil Modulus

It can be observed from Fig.6.10 that the bending moment in piles increases with the increase in pile diameter and the same is found to be true for all the soil modulus and pile positions considered for the study. This is due to the fact that as the pile diameter increases the lateral soil pressure on the pile increases and which in turn causes an increase in bending moment. The influence of lateral soil pressure is found to be more in higher diameter piles than in lower diameter piles, since the surface area of contact with the soil is more in higher diameter piles

than in lower diameter piles. When the diameter changes from 1 m to 2 m, it is observed that there is an average of 40 % increase in bending moment acting on the pile. It is also noticed that when the soil is very weak ($E_s = 1000 \text{ kN/m}^2$), the increase in bending moment is more than 150 % and it may be due to the failure of bed slope.

6.10 Influence of Soil Modulus on Bending Moment

It is also evident from Fig. 6.10, that bending moment on piles increases with increase in soil modulus. It may be due to the fact that as the soil modulus increases the lateral soil pressure on pile from the land side soil increases considerably and it leads to an increase in bending moment in piles. When the soil modulus increases from 1000 kN/m^2 to $50,000 \text{ kN/m}^2$, it is observed that the bending moment increases around 40 %. It can also be observed in Fig. 6.10 that on the land side of the structure the bending moment on piles increases with decrease in soil modulus. It is due to the fact that the land side soil bed with weaker soil fails and exerts more lateral soil pressure than stiff soil. It causes large lateral load on the piles and hence the bending moment on the land side piles increases. The influence of lateral soil pressure is found to be more in higher diameter piles than in lower diameter piles, since the surface area of contact with the soil is more in higher diameter piles than in lower diameter piles.

6.11 Influence of Bed Slope on Bending Moment

Change in bed slope has two distinct effects as the variation is at the upper part of the slope and at the lower part of the slope. When the soil from the upper part of the slope is removed, the slope decreases but the volume soil supporting the pile also decreases. It adversely affects the soil-pile system. But when the soil is deposited in the lower part of the slope the bed slope decreases and also the volume of soil supporting the pile increases. It benefits the soil-pile system.

6.11.1 Influence of Soil in the Upper Part of the Bed Slope

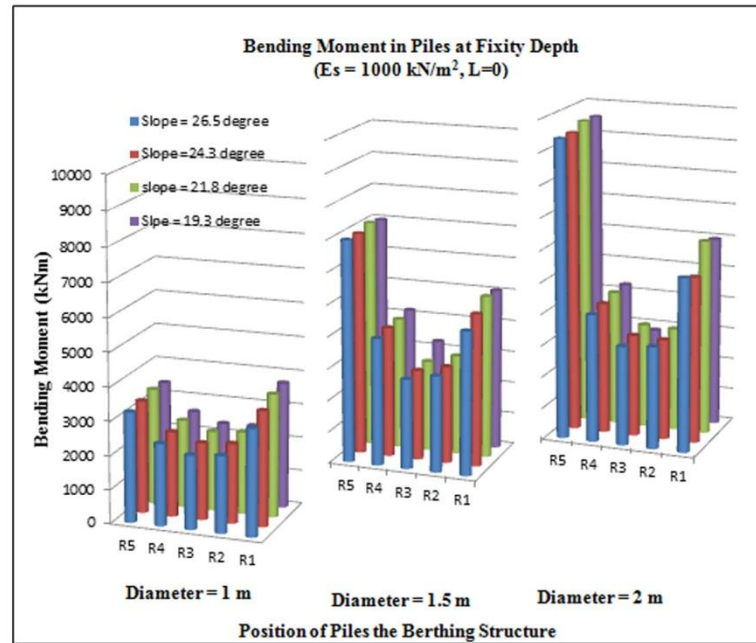


Fig. 6.11 Variation of Bending Moment with Change in Bed Slope by Removing Soil from the Upper Part of the Slope

When the soil from the upper part of the slope is removed, the bed slope decreases as shown in Fig.6.3. The bed slopes corresponding to the removal of soil in the upper part for 0m, 1m, 2m and 3m are 26.5° , 24.3° , 21.8° and 19.3° .

It can be noted from Fig. 6.11 that an increase in slope from 19.3° to 26.5° causes around 3-5 % decrease in bending moment. In this case the removal of soil supporting the pile, from the bed slope causes a decrease in slope and hence it causes an increase in bending moment.

6.11.2 Influence of Soil in the Lower Part of the Bed Slope

From Fig.6.12, it is clear that an increase in slope from 19.3° to 26.5° causes around 3- 5 % increase in bending moment. In this case an increase in slope is caused by the removal of soil supporting the pile, from the bed slope and hence it causes an increase in bending moment.

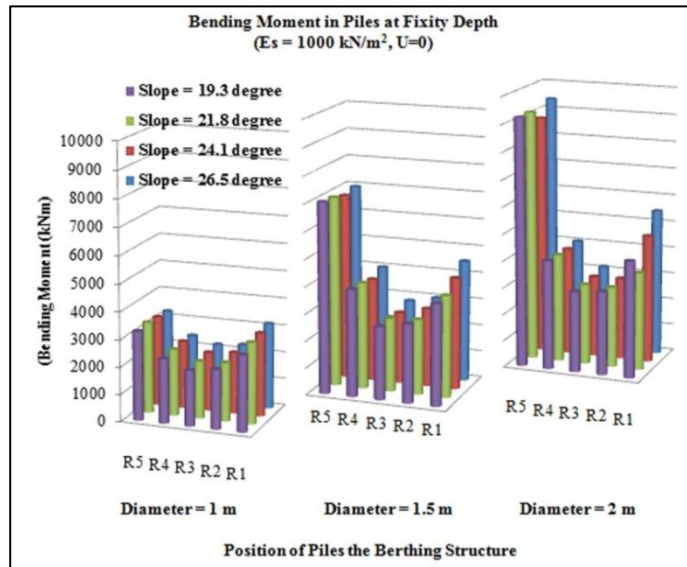


Fig. 6.12 Variation of Bending Moment with Change in Bed Slope by Removing Soil from the Lower Part of the Slope

6.12 Regression Equations to Predict Bending Moment

Multivariable regression analysis is done to predict the magnitude of bending moment in each of the rows. The factors influencing the bending moment are the pile diameter (D), soil modulus (Es), bed slope (S), soil in the upper (Us) and lower (Ls) part of bed slope. A parametric study is conducted by varying all the influencing parameters and 144 tests were conducted. Based on the test results a multivariable regression analysis was conducted and the equations to predict the bending moments in each of the rows are derived as follows.

$$M1 = 1812.3 + 1764.9 D + 8.8 \log(Es) - 67.6 \left(\frac{1}{\tan(\theta)}\right) + 194.9 Us - 247.8 Ls \dots\dots\dots (6)$$

$$M2 = 95.3 + 984.1 D + 470.4 \log(Es) - 57.7 \left(\frac{1}{\tan(\theta)}\right) + 119.2 Us - 97.8 Ls \dots\dots\dots (7)$$

$$M3 = 275.8 + 762.2 D + 413.0 \log(Es) + 36.7 \left(\frac{1}{\tan(\theta)}\right) + 88.2 Us - 88.6 Ls \dots\dots\dots (8)$$

$$M4 = 1855.4 + 1024.9 D + 5.3 \log(Es) - 58.4 \left(\frac{1}{\tan(\theta)}\right) + 77.0 Us - 92.6 Ls \dots\dots\dots (9)$$

$$M5 = 6416.0 + 2834.5 D - 1470.0 \log(Es) + 67.7 \left(\frac{1}{\tan(\theta)}\right) + 42.6 Us - 105.4 Ls \dots\dots\dots (10)$$

With reference to the Fig.6.10, it is clear that the landside piles are having very high values of bending moment due to the failure of the weakest soil considered

in the study. That may be the reason of less values of R^2 for the fourth and fifth row of piles (landside piles).

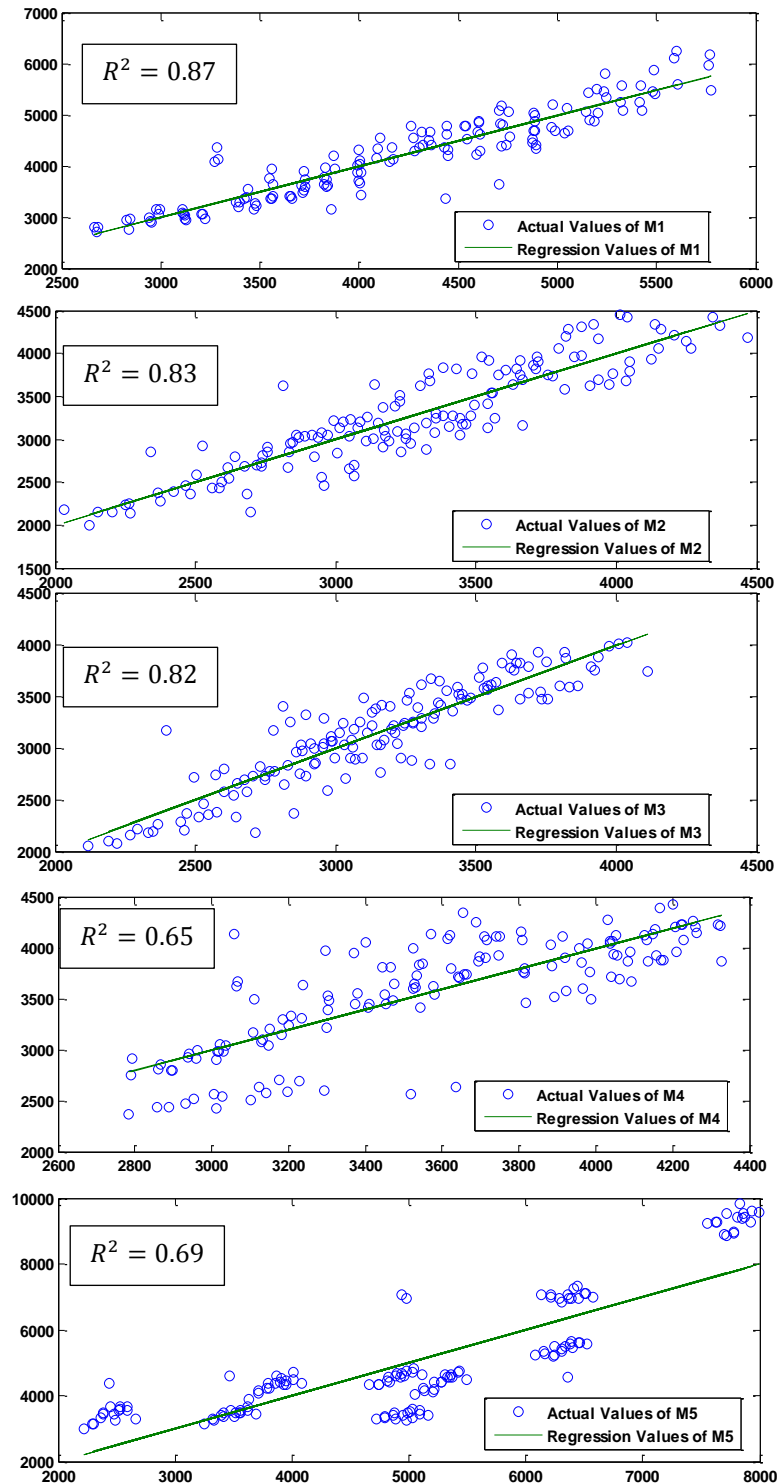


Fig. 6.13 Actual Value of Bending Moment Vs Calculated Value of Bending Moment

6.13 Influence of Pile Diameter on Maximum Deflection

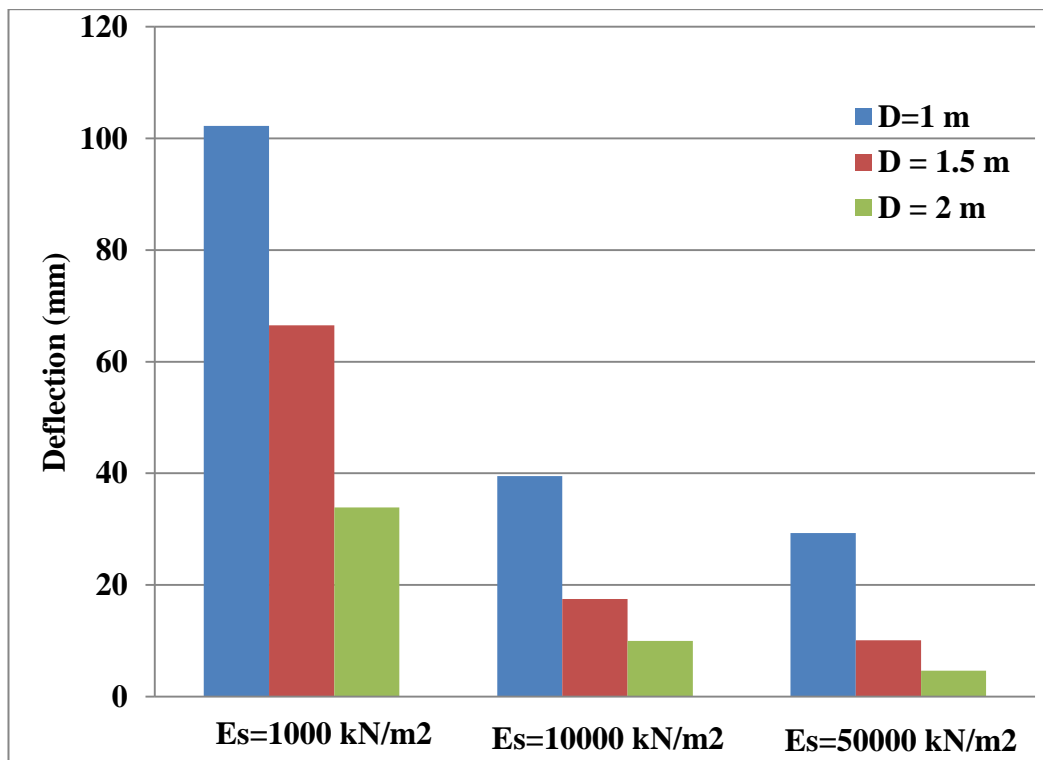


Fig. 6.14 Variation of maximum deflection with pile diameter and soil modulus

It can be seen from Fig. 6.14 that, as the pile diameter increases from 1 m to 2 m there is around 70 % reduction in the deflection of the structure. The reduction in deflection is due to the fact that an increase in pile diameter increases the stiffness of pile and hence it helps the structure to resist the external load acting on it.

6.14 Influence of Soil Modulus on Deflection

It can be seen from Fig. 6.14 that, as the soil modulus increases from 1000 kN/m² to 50000 kN/m², there is around 80 % reduction in the deflection of the structure. The reduction in deflection is due to the fact that an increase in soil modulus increases the stiffness of soil and hence helps the structure to transfer the load to the soil.

6.15 Influence of Bed Slope on Deflection

The bed slope is having a very small influence on the deflection of the frame considered whereas the diameter of the pile and the soil modulus are found to be influencing the deflection of the frame considerably.

6.16 Regression Equation to Predict Deflection

$$Y_{max} = 237.6 - 36.7 D - 37.2 \log(Es) - 0.18 \left(\frac{1}{\tan(\theta)} \right) + 0.86 U_s - 0.38 L_s \dots (11)$$

It is evident from the regression equation that the diameter of the pile and the soil modulus are contributing towards the deflection of the frame. The bed slope is having only a very small influence in the deflection of the frame.

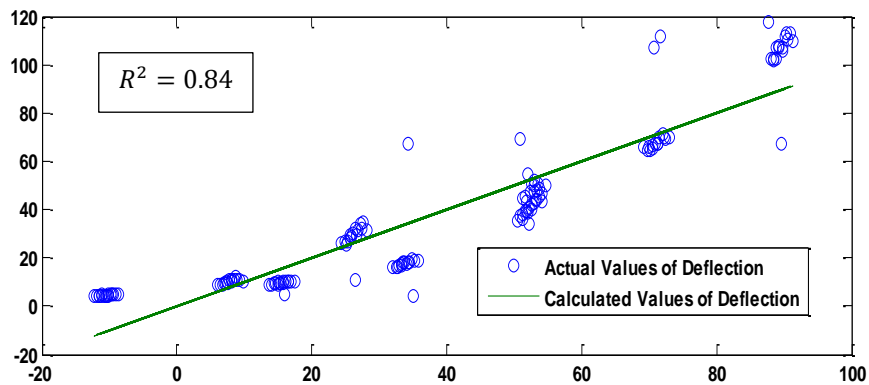


Fig. 6.15 Actual Value Vs Calculated Value of Deflection of the Frame

6.17 Summary

A parametric study has been conducted on a two dimensional berthing structure subjected to lateral load. The influence of different parameters on the variation of depth of fixity, maximum bending moment and deflection were studied and the following conclusions are made.

- An increase in pile diameter from 1 m to 2 m, causes around 30 % increase in depth of fixity of the pile in various rows of piles.
- As the soil stiffness increases from 1000 kN/m² to 50000 kN/m² there is around 45 % reduction in the depth of fixity of piles,

- Bed slope variation influences the depth of fixity in such a way that, if the increase in slope improves the volume of passive wedge, there will be reduction in depth of fixity and vice versa.
- Whenever soil is removed or added in the bed slope, an unstable slope at the shore side exerts additional lateral loads on piles which cause an increase in depth of fixity.
- An increase in pile diameter causes an increase in bending moment on piles. As the diameter of the pile increases from 1 m to 2 m, there is around 40 % increase in maximum bending moment on piles.
- An increase in soil modulus causes an increase in bending moment on piles. When the soil modulus increases from 1000 kN/m² to 50,000 kN/m² there is around 40 % increase in the maximum bending moment on piles.
- Failure of weaker soil bed ($E_s = 1000 \text{ kN/m}^2$) in the landside causes an increase in bending moment on the landside piles.
- The change in bed slope may be due to the soil failure at land side as well as soil deposition at the berthing side of the structure. Change in bed slope has two distinct effects.
- A decrease in bed slope due to the removal of soil from the upper part of soil reduces the volume of soil supporting the pile and hence increases the bending moment acting on the pile.
- A decrease in bed slope due to the addition of soil in the lower part of the bed slope increases the volume of soil supporting the pile and hence decreases the bending moment acting on the piles.
- The position of pile on bed slope considerably influence the magnitude of depth of fixity and bending moment of the pile.

- A weaker soil stratum in the land side causes an increase in maximum bending moment on the landside piles and it demands an abutment wall. Whereas a stiff soil in the land side does not considerably influence the maximum bending moment on landside piles and hence abutment wall is not mandatory under such circumstances.
- Based on the analysis results of the structure under investigation, design charts are developed (Appendix J) to predict the maximum bending movement and the depth of fixity of piles in a berthing structure.

.....❧.....

Summary and Conclusions

Contents	7.1 Summary
	7.2 Conclusions
	7.3 Scope of Future Work

7.1 Summary

Ship berthing structures are heavy concrete structures embedded in weak soil strata in coastal area. They are subjected to significant amount of lateral loads in addition to axial loads. In the present study the influence of soil structure interaction in the structural behaviour of a berthing structure is investigated. A detailed analysis of such laterally loaded pile structures are carried out with the help of model investigations, analytical formulations and numerical investigations on single pile embedded in clayey soil bed. The influence of pile diameter, pile length and bed slope on the structural behaviour of the pile is studied. The numeric analysis has been extended for a typical frame in a berthing structure to study the variation in depth of fixity, maximum bending moment and deflection of pile in the structure with the change in the pile diameter, soil modulus and bed slope.

Based on the literature review it was understood that experimental investigations using model piles are a good option for the study of soil structure interaction analysis of laterally loaded piles, if all the parameters involved in the study could be modeled using the laws of similitude. The Π -terms derived using Buckingham's Pi theorem was used in the present study to simulate the on-site piles.

A set of model tests were conducted on model piles in sloping clay bed subjected to lateral load. Scale factors developed using Buckingham's Π theorem was used to model the pile dimensions corresponding to the selected onsite pile dimensions. The behaviour of the soil pile system was analysed from the load deflection curve as well as the bending moment variation plot. The experiments were repeated for two different diameters of pile, three different embedment depth of pile and two different bed slopes. The experimental results were compared with the program developed using the finite difference formulation of laterally loaded pile by Reese *et al.* [71].

Numerical simulation and analysis using finite element or finite difference methods, considering the influence of soil-structure interaction can also be used for the study of soil-pile system. Proper validation of model created in the numerical software using field data can ensure reliable results. In the present study pile load test data available in literature, for two different sites, were modeled and analysed in PLAXIS-3D to validate the numerical modeling of the soil pile system. Based on the review of literature it was observed that elasto-plastic Mohr-Coulomb soil model can be adopted to represent the clayey soil used in the study. Moreover laboratory model tests conducted were also used to validate the numerical simulation. Further a parametric study conducted was used to develop a set of regression equations to predict the pile top deflection, maximum bending moment and the depth of fixity of the pile.

Based on the results of model tests it was concluded that the diameter of pile and the bed slope were having significant influence in the variation of maximum deflection and maximum bending moment of the pile, whereas the length of the pile was having only a marginal influence on the behaviour of pile. Hence when the study was extended for the analysis of a laterally loaded frame of a typical ship berthing structure, the influence of variation in pile diameter and bed slope on the behaviour of the structure was analysed along with the variation in soil modulus. Here also a set of regression equations were developed, based

on the parametric study to predict the structural behaviour of the berthing structure in terms of maximum bending moment of the pile, depth of fixity of the pile and the deflection of the system considered. The studies revealed that the pile diameter, soil modulus and bed slope are having significant contributions in the structural behaviour of ship berthing structure.

7.2 Conclusions

The major conclusions drawn based on the study are given in the following sections:

7.2.1 Review of Literature

Based on the extensive literature review it was found that the pile stiffness, soil properties, soil profile and gradient, type of loading and analysis type play important roles in predicting the behaviour of a soil-structure system.

7.2.2 Experimental Investigation

The major observations from the laboratory investigations on laterally loaded single pile embedded in sloping clay bed are:

- The maximum bending moment increases as the embedment depth of pile, the diameter of pile and bed slope increases.
- The maximum deflection decreases with increase in embedment depth and diameter of pile. But maximum deflection increases with increase in bed slope.
- There is only a marginal increase of 5 % in maximum bending moment when the embedment depth of model pile increases from 550 mm to 750 mm, whereas the maximum deflection of the pile decreases around 11 % with the increase in embedment depth of pile.
- The maximum bending moment increases on an average of 13 % when the diameter of the pile increases from 19mm to 25.4 mm. But

since flexural rigidity of the pile increases considerably there is a reduction of around 40% in the maximum deflection of the pile.

- The maximum bending moment increases on an average of 7 % when the slope of soil bed increases from 1:2 to 1:1.5, since the passive resistance of soil decreases due to increase in bed slope. An increase in bed slope also causes an increase of 30% in the maximum deflection of pile.
- The increase in maximum bending moment as well as maximum deflection with the increase in bed slope adversely affects the load carrying capacity of pile.

7.2.3 Analytical Investigation

A program developed in MATLAB for the finite element formulation of laterally loaded pile by Reese *et al.* [71] was used to analyse the model piles. The results of the model tests and the analytical solution were found to be in good agreement when the deflection and the bending moment were compared.

7.2.4 Numerical Investigation

- Based on the parametric study of laboratory model pile system in PLAXIS-3D, the following conclusions are made,
 - As the embedment depth of pile increases from 550 mm to 750 mm there is an average of 3 % reduction in maximum deflection, 5 % increase in maximum bending moment and 3 % increase in depth of fixity of pile. Hence the embedment depth is having only a marginal influence in the structural behaviour of a flexible pile.
 - As the pile diameter increases from 19 mm to 30 mm there is an average of around 42 % reduction in maximum deflection, 28 % increase in maximum bending moment and 65 % increase in depth of fixity of pile. The considerable increase in the stiffness of pile with the increase in

pile diameter is having a positive effect in the reduction in deflection of the pile.

- A change in bed slope from horizontal (0°) to 45° causes around 130 % increase in maximum deflection, 50 % increase in maximum bending moment and 75 % increase in depth of fixity of pile. Hence piles embedded in slopes are to be critically analyzed if there is a possibility of change in slope with time.
- The depth of fixity varies in the range of $4D$ to $7D$ when the slope of soil bed increases from horizontal (0°) to 45° .
- The contributions of each of the parameters such as bed slope (S), pile diameter (D) and embedment length of pile (L_e) are well established using the regression equations (5.1) to (5.3) obtained based on the parametric study.

$$M_{max} = 3.241 + 0.105S + 0.271D + 0.000326L_e$$

$$D_f = -52.116 + 1.477S + 5.745D + 0.0161L_e$$

$$y_{max} = 5.352 + 0.053S - 0.151D - 0.000107L_e$$

7.2.5 Numerical Analysis of ship Berthing Structure

- Based on the analysis of a 2D frame in a typical berthing structure it can be concluded that,
 - An increase in pile diameter from 1 m to 2 m, causes an average of around 30 % increase in depth of fixity and 40 % increase in the maximum bending moment on different rows of piles in the frame considered.
 - As the pile diameter increases there is an increase in the contact area between the soil and the surface of pile, which causes an increase in the active earth pressure acting on the piles and it causes an increase in depth of fixity and maximum bending moment on piles.

- As the soil modulus increases from 1000 kN/m^2 to 50000 kN/m^2 , there is an average reduction of 45% in the depth of fixity of piles, a decrease of 150% in maximum bending movement on landside piles and an increase of 40% increase in maximum bending moment on other piles.
- The increase in soil modulus causes an increase in maximum bending moment on piles other than land side piles. It may be due to the increase in the active earth pressure acting on the piles with the increase in soil modulus.
- The increase in soil modulus causes increase in maximum bending moment of piles. It is due to the increase in the active earth pressure acting on the piles with the increase in soil modulus.
- As the position of pile changes from crest of the bed slope towards the bottom of the slope it is observed that the depth of fixity increases so as to get the required volume of passive wedge of soil to support the laterally loaded pile.
- The maximum bending moment on piles decreases as we move away from the berthing side of the frame considered. But the additional soil pressure on the land side piles increases the maximum bending moment acting on them.
- The failure of weaker soil bed ($E_s = 1000 \text{ kN/m}^2$) in the landside also causes an increase in bending moment on the landside piles.
- The bed slope is having a very small influence on the deflection of the frame considered whereas the diameter of the pile and the soil modulus are found to be influencing the deflection of the frame considerably.
- Bed slope variation influences the depth of fixity in such a way that, if there is a failure of bed slope at the land side, there will be a reduction in passive earth pressure and hence it will increase the depth of fixity and maximum bending moment on piles.

- When soil is deposited at the bottom of the bed slope an unstable slope will be created and it exerts additional lateral loads on piles which causes an increase in depth of fixity as well as maximum bending moment of piles.
- A weaker soil stratum in the land side causes an increase in maximum bending moment on the landside piles and it demands an abutment wall. Whereas a stiff soil in the land side does not considerably influence the maximum bending moment on landside piles and hence abutment wall is not mandatory under such circumstances.

7.2.6 Multivariable Regression Equations

A set of regression equations are developed to predict the maximum bending moment, depth of fixity and maximum deflection, for a single pile in sloping clay bed as well as for a typical frame of a berthing structure. These equations can be used to predict the values of the output parameters within the range of input parameters considered for the study. The contribution of each of the parameters in the regression equation is a clear indication of the influence of input parameters in predicting the output parameters.

It can be concluded based on the present study that laterally loaded piles in sloping soil bed needs to be critically analysed by incorporating the changes in the behaviour of passive and active wedge of soil surrounding it with the changes in bed slope as well as the soil properties. Also it is evident from the present study of laterally loaded single pile as well as a frame of berthing structure that pile embedded at the crest of the slope are always vulnerable to failure due to the influence of bed slope and soil properties. The detailed analysis of such structures in the present study and the regression equations developed based on the parametric study will help to assess the influence of bed slope, soil properties and pile stiffness in the structural behaviour of a laterally loaded pile in sloping bed of soil.

7.3 Scope of Future Work

The present study could be extended for,

- The studies may be conducted for pile groups with varying number of piles as well as varying orientations of pile groups subjected to lateral load.
- The studies can be extended to the changes in the behaviour of piles with the changes in the bed soil properties other than soil modulus.
- The change in the behaviour of pile with the change in pile material and inclined (raker) piles can also be investigated.
- Studies on prototype piles may yield a better understanding about the structural behaviour of single pile as well as group piles.

.....❧.....

References

- [1] Abbas J M, Chik Z (2010) Influence of Group Configuration on the Lateral Pile Group Response Subjected to Lateral Load, *Electronic Journal of Geotechnical Engineering*, 15(G)
- [2] Abbas J M, Chik Z H, Taha M R (2008) Single Pile Simulation and Analysis Subjected to Lateral load, *Electronic Journal of Geotechnical Engineering*, 13(E), 1-15
- [3] Abdelhacine Gouasmia, Abdelhamid Belkhiri, Allaeddine Athmani (2015) Dynamic Soil-Structure Interaction Analysis of Reinforced Concrete Buildings. *World Academy of Science, Engineering and Technology, International Journal of Civil, Environmental, Structural, Construction and Architectural Engineering*; Vol:9, No:7
- [4] Anuj Chandiwala, “Fem Modeling for Piled Raft Foundation in Sand”, *International Journal of Civil Engineering & Technology (IJCIET)*, Volume 4, Issue 6, 2013, pp. 239 - 251, ISSN Print: 0976 – 6308, ISSN Online:0976 – 6316
- [5] Ashour M, Noris G, Pilling P (2002) Strain Wedge Model Capability of Analyzing Behaviour of Laterally Loaded Isolated Piles, Drilled Shafts and Pile Groups, *Journal of Bridge Engineering*, 7(4), 245-254
- [6] Ashour M, Norris G (2000) Modelling Lateral Soil-Pile Response Based on Soil-Pile Interaction, *Journal of Geotechnical and Geoenvironmental Engineering*, 126(5), 420-428
- [7] Aslan Sadeghi Hokmabadi (2014) Effect of Dynamic Soil-Pile-Structure Interaction on Seismic Response of Mid-Rise Moment Resisting Frames. A thesis of Doctor of Philosophy, Faculty of Engineering and Information Technology, University of Technology Sydney (UTS)
- [8] Avaei A, Ghotbi A R, Aryafar M (2008) Investigation of Pile- Soil Interaction Subjected to Lateral Loads in Layered Soils, *American Journal of Engineering and Applied Sciences*, 1(1), 76-81
- [9] Ayothiraman R, Boominathan A (2004) Flexural Behaviour of Single Piles in Clay Under Lateral Excitation, 13th World Conference on Earthquake Engineering

- [10] Ayothiraman R, Boominathan A (2013) Depth of Fixity of Piles in clay Under Dynamic Lateral Load, *Geotechnical and Geological Engineering*, 31, 447-461
- [11] Babaei A (2011) Numerical Investigation of Axial Bearing Capacity of Piles Embedded in Sloping Ground, *International Journal of the Physical Science*, 6(33), 7589-7603
- [12] Badry P, Satyam N (2016) An Efficient approach for assessing the seismic soil structure interaction effect for the asymmetrical pile group. *Innovative Infrastructure Solutions journal*, Springer. DOI: 10.1007/s41062-016-0003-1
- [13] Banerjee (2002) Inelastic Soil-Pile-Structure Interaction under Static Loading, *International Symposium on Structural and Earthquake Engineering*, 394-401
- [14] Begum A, Muthukkumaran K (2008) Numerical modeling for Laterally Loaded Piles on a Sloping Ground, *The 12th international conference of International Association for Computer Methods and advances in Geomechanics*, 1-6 Oct2008, 3368-3375
- [15] Beegum, N. and Muthukkumaran, K.(2009) Experimental investigation on single model pile in sloping ground under lateral load, *Intl. Journal of Geotechnical Engineering*, Volume 3 Issue 1 , pp. 133-146
- [16] Blaney G W, O'Neill M W (1986) Analysis of Dynamic Laterally Loaded Pile in Clay, *Journal of Geotechnical Engineering*, 112(9), 827-840
- [17] Boominathan A, Ayothiraman R (2007) An Experimental study on Static and Dynamic Bending Behaviour of Piles in Soft Clay, *Geotechnical and Geological Engineering*, 25, 177-189
- [18] Boulanger R W, Curras C J, Kutter B L, Wilson D W, Abghari A (1999), *Seismic Soil-Pile-Structure Interaction Experiments and Analysis*, *Journal of Geotechnical and Geoenvironmental Engineering*
- [19] Broms B.B (1964), *Lateral Resistance of Piles in Cohesive Soils*, *J. Soil Mechanics and Found. Div., ASCE*, 90(2), 309-326
- [20] Brown D A, Hidden S A, Zhang S (1994) Determination of P-Y Curves Using Inclinator Data, *Geotechnical Testing Journal*, 17(2), 150-158
- [21] Chandrasekaran S S, Boominathan A, Dodagoudar G R (2010) Group Interaction Effects on Laterally Loaded Piles in Clay, *Journal of Geotechnical and Geoenvironmental Engineering*, 136(4), 573-582

-
- [22] Chandrasekaran S S, Boominathan A, Dodagouder G R (2008) Cyclic Lateral Response of Model Pile Groups in Clay, The 12th International Conference of International Association for Computer Methods and Advances in Geomechanics
- [23] Charles W W, Zhang L M (2001) Three Dimensional Analysis of Performance of Laterally Loaded Sleeved Piles in Sloping Ground, *Journal of Geotechnical and Geoenvironmental Engineering*, 127(6)
- [24] Chik Z H, Abbas J M, Taha M R, Shafique Q S M (2009) Lateral Behaviour of Single Pile Cohesionless Soil Subjected to Both Vertical and Horizontal Loads, *European Journal of Scientific Research*, 29(2)
- [25] Chore A S, Ingle R K, Sawant V A (2012) Parametric study of Laterally Loaded Pile Groups using Simplified F.E.Models, *Coupled Systems Mechanics*, 1(1), 1-7
- [26] Chore H S, Ingle R K, Sawant V A (2012) Non-linear Analysis of pile groups subjected to lateral loads using p-y curves, *Interaction and Multiscale Mechanics*, 5(1), 57-73
- [27] Conte E, Troncone A, Vena M (2013) Nonlinear Three Dimensional Analysis of Reinforced Concrete Piles Subjected to Horizontal Loading, 49, 123-133
- [28] Cox W R, Dixon D A, Murphy B S (1984) Lateral Load Tests on 25.4 mm (1 in.) Diameter Piles in Very Soft Clay in Side-by-Side and In-Line Groups, *Laterally Loaded Deep Foundations: Analysis and Performance*, ASTM STP835, American Society for Testing and Materials, 122-139
- [29] Deepak R, Gandhi S R (2004), Improvement of Lateral Capacity of Pile due to Compaction of Surrounding Soil, *Indian Geotechnical Conference 2004*, 382-385
- [30] Duggal S.K. (2011) *Earthquake Resistant Design of Structures*. Oxford University Press
- [31] Duncan M J, Evans Jr. L T, Ooi P S K (1994) Lateral Load Analysis of Single Piles and Drilled Shafts, *Journal of Geotechnical Engineering*, 120(5), 1018-1033
- [32] Gabr M A, Orden R H (1990) Lateral Analysis of Piers Constructed on slopes, *Journal of Geotechnical Engineering*, 116(12), 1831-1850

-
- [33] Gandhi S R, Selvam (1994) Model Tests on Pile Group under Lateral Loads, 228-233
- [34] Gandhi S R, Selvam S (1997) Group Effect on Driven Piles Under Lateral Load, *Journal of Geotechnical and Geoenvironmental Engineering*, 123(8), 702-709
- [35] Gandhi S R, Suresh P K, Raju V S (1988) Lateral Load Tests on Large Diameter Bored Pile and Analysis, *Indian Geotechnical Conference*, Vol.1, 373-377
- [36] Gao M, Chin D B, Ma M Y, Sun R G (1986) A Field Investigation and Analysis of a Large Pipe Pile Under Static and Dynamic Lateral Loading, *Marine Geotechnology and Nearshore/ Offshore Structures*, ASTM STP 923, American Society for Testing and Materials, 306-328
- [37] Georgiadis K, Georgiadis M (2010), Undrained Lateral Pile response in sloping Ground, *Journal of Geotechnical and Geoenvironmental Engineering*, 136(11), 1489-1500
- [38] Georgiadis K, Georgiadis M (2012) Development of p-y curve for undrained response of piles near slopes, *computers and Geotechnics*, 40, 53-61
- [39] Gleser S M (1984) Generalized Behaviour of Laterally Loaded Vertical Piles, *Laterally Loaded Deep Foundations: Analysis and Performance*, ASTM STP 835, American Society for Testing and Materials, 72-96
- [40] Godbole P N, Viladkar M N, Noorzaei J (1990) Nonlinear Soil Structure Interaction Analysis using Coupled Finite Elements, *Computers and Structures*, 36(6), 1089-1096
- [41] Gokul K M, Sathyanarayanan D, Subha I P, Muthukkumaran K (2009) Behaviour of an Open Type Berthing Structure under Earthquake Condition- a Numerical Approach, *Indian Geotechnical Conference-2009*, 553-557
- [42] Guangling He, Jie Li (2008) Seismic Response of Superstructure on Soft Soil Considering Soil-Pile-Structure Interaction. *The 14th World Conference on Earthquake Engineering*, Beijing, China; October 12-17
- [43] Hajjalilue-Bonab, M., Sojoudi, Y., and Puppala, A. (2013) Study of Strain Wedge Parameters for Laterally Loaded Piles”, *Int. J. Geomech.*, 13(2), 143–152

- [44] Haldar S, Babu S G L (2008) Effect of Soil Spatial Variability on the response of Laterally Loaded Pile in Undrained Clay, *Computers and Geotechnics*, 35, 537-547
- [45] Hokmabadi A.S., Fatahi B., Samali B. (2013) Seismic Response of Superstructure on Soft Soil Considering Soil-Pile-Structure Interaction. *Proceedings of the 18th International Conference on Soil Mechanics and Geotechnical Engineering, Paris* ; PP 547-550
- [46] Hooman Torabi, Mohammad T. Rayhani (2014) Three dimensional Finite Element modeling of seismic soil–structure interaction in soft soil. *Computers and Geotechnics*; 60, 9–19
- [47] Horwath J S (1984) Simplified Elastic Continuum Applied to the Laterally Loaded Pile Problem- Part 1: Theory, *Laterally Loaded Deep Foundations: Analysis and Performance*, ASTM STP 835, American Society for Testing and Materials, 112-121
- [48] Ilyas T, Leung C F, Chow Y K, Budi S S (2004) Centrifuge Model Study of Laterally Loaded Pile Groups in Clay, *Journal of Geotechnical and Geoenvironmental Engineering*, 130(1), 274-283
- [49] IS 2911 (Part 1/ Section 2) – 2010, Design and Construction of Pile Foundations - Code of Practice, Part 1-Concrete Piles, Section 2- Bored Cast In-situ Concrete Piles
- [50] Ismael N F (1998) Lateral Loading tests on Bored Piles in Cemented Sand. *Proceedings of the Third International Geotechnical Seminar on Deep Foundation on Bored and Auger Piles, Ghent, Belgium, 19-21 October*, pp: 137-144
- [51] John P. Wolf (1985) *Dynamic Soil-Structure Interaction*. Prentice Hall Inc
- [52] Karthigeyan S V, Ramakrishna V G S T, Rajagopal K (2006) Influence of vertical Load on the lateral response of Piles in Sand, *Computers and Geotechnics*, 33, 121-131
- [53] Kasinathan Muthukkumaran and Ranganathan Sundaravadivelu, Numerical Modeling of Dredging Effect on Berthing Structure, *ActaGeotechnica*, 2: 249-259.
- [54] Kausel E (2010) Early History of Soil Structure Interaction, *Soil Dynamics and Earthquake Engineering*

- [55] Kim B T, Kim N K, Lee W J, Kim Y S (2004) Experimental Load-transfer Curves of Laterally Loaded Piles in Nak-Dong River Sand, *Journal of Geotechnical and Geoenvironmental Engineering*, 130(4), 416-425
- [56] Kim B T, Kim Y S (1999) Back Analysis for Prediction and Behaviour of Laterally Loaded Single Piles in Sand, *KSCE Journal of Civil Engineering*, 3(3), 273-288
- [57] Kim Y, Jeong S (2011) Analysis of Soil Resistance on Laterally Loaded Piles based on 3D Soil-Pile Interaction, *Computers and Geotechnics*, 38, 248-257
- [58] Kim Y, Jeong S, Lee S (2011) Wedge Failure Analysis of Soil Resistance on Laterally Loaded Piles in Clay, *Journal of Geotechnical and Geoenvironmental Engineering*, 137(7), 678-694
- [59] Kishida A, Takewaki I (2007) Analysis of Earthquake Energy Input in Soil-pile-structure System with Uncertain Soil Parameter, *An International Journal of Advances in Structural Engineering*, Vol.10, No.3, pp229-244
- [60] Kishida A, Takewaki I (2010) Response spectrum method for kinematic soil-pile interaction analysis, *Advances in Structural Engineering*, Vol.13, No.1, pp181-197
- [61] Kishore N Y, Rao N S, Mani J S (2009) The Behaviour of Laterally Loaded Piles Subjected to Scour in Marine Environment, *KSCE Journal of Civil Engineering*, 13(6), 403-406
- [62] Kishore N Y, Rao N S, Mani J S (2008) Influence of the Scour on Laterally Loaded Piles, *The 12th International Conference of International Association for Computer Methods and Advances in Geomechanics*
- [63] Kojima K, Fujita K, Takewaki I (2014) Unified analysis of kinematic and inertial earthquake pile responses via single-input response spectrum method. *Soil Dynamics and Earthquake Engineering*, Vol.63, pp36-55
- [64] Kok, S T (2009), A Review of Basic Soil Constitutive Models for Geotechnical Application, *Electronic Journal of Geotechnical Engineering*, 2009
- [65] Kolesoglu M. K. and S. M. Springman (2011), Analytical and 3D Numerical Modelling of Full Height Bridge Abutments Constructed on Pile Foundations Through Soft Soil, *Computers and Geotechnics*, Vol.38, pp. 934-948

- [66] Landriani L (2007) Laterally Loaded Model Pile Analysis Regarding the Influence of Soil Saturation and Matric Suction in a Clay Soil, *McNair Research Journal*, 3, 25-32
- [67] Lane P A, Griffiths D V (2000) Assessment of Stability of Slopes Under Drawdown Conditions, *Journal of Geotechnical and Geoenvironmental Engineering*, 126(5), 443-450
- [68] Lee J, Prezzi M, Salgado R (2011) Experimental Investigation of the Combined Load Response of Model Piles Driven in Sand, *Geotechnical Testing Journal*, 34(6)
- [69] Li R, Gong J (2008) Analysis of Laterally Loaded Pile in Layered Soil, *Electronic Journal of Geotechnical Engineering*, 13(J)
- [70] Lin, H., Ni, L., Suleiman, M., and Raich, A. (2015) Interaction between Laterally Loaded Pile and Surrounding Soil, *J. Geotech.Geoenviron.Eng.*, 141(4), 04014119
- [71] Lymon C. Reese, William M. Isenhower and Shin Tower Wang, *Analysis and Design of Shallow and Deep foundations*, John Wiley and Sons Inc., 2006
- [72] Maheshwari B K, Watanabe H (2005) Dynamic Analysis of Pile Foundations: Effects of Material Nonlinearity of Soil, *Electronic Journal of Geotechnical Engineering*, 10€
- [73] Martin G R, Chen C Y (2005) Response of Piles Due to Lateral Slope Movement, *Computers and Structures*, 83, 588-598
- [74] MATLAB R2010a, (2010), (computer software), The Math Works Inc., Natick, Massachusetts
- [75] Mazurenko L V, Shvartsman D A (1967) Calculation of Single Piles for Lateral Loads, *Fundamenty I Mekhaniks Gruntov*, 2, 35-38
- [76] Mironov V V (1971) Method of Analysis for Laterally Loaded Pile, *Foundation Engineering*, 3, 15-17
- [77] Moayed Z, Judi A, Rabe B K (2008) Lateral Bearing Capacity of Piles in Cohesive Soils Based on Soil's Failure Strength Control, *Electronic Journal of Geotechnical Engineering*, 13(D), 1-11
- [78] Mohammed, A. Gabr and Roy, H. Orden. (1990) Lateral Analysis of Piers Constructed on Slopes, *Journal of Geotechnical Engineering*, 116(12), 1831-1850

- [79] Mohamed, Y. E. A., Nour Eldaim, Y. E. A., Abdelwahab A. E. (2013) Laboratory model tests on laterally loaded piles in plastic clay, *Intl. Journal of Geotechnical Engineering*, Volume 7, pp. 241-250
- [80] Mostofi A, Bargi K (2011) Analytical and Numerical Evaluation of Flexible Response of Floating Piers to ship Berthing Impact, *International Journal of Civil and Structural Engineering*, 2(1), 249- 259
- [81] Mostofi A, Bargi K (2012) New Concept in Analysis of Floating Piers for Ship Berthing Impact, *Marine Structures*, 25, 58-70
- [82] Murugan M, Natarajan C Muthukkumaran K(2011) Behaviour of Laterally Loaded Piles in Cohesionless Soils, *International Journal of Earthscience and Engineering*, 4(6), 104-106
- [83] Muthukkumaran K, Sundaravadivelu R (2007) Numerical Modeling of Dredging Effect on Berthing Structure, *Acta Geotechnica*, 2, 249-259
- [84] Muthukkumaran K, Sundaravadivelu R, Gandhi S R (2004) Effect of Sloping Ground on Single Pile Load Deflection Behaviour under Lateral Soil Movement, 13th World Conference on Earthquake Engineering
- [85] Muthukkumaran K, Gokul Krishnan M. (2012) Three Dimensional Analysis of Piles on Sloping Ground subjected to passive Load Induced by Surcharge, *Intl. Journal of Engineering and Technology Innovation*, 2(1), 31-47
- [86] Muthukkumaran, K. (2014) Effect of Slope and Loading Direction on Laterally Loaded Piles in Cohesionless Soil, *Int. J. Geomech.*, 14(1), 1–7
- [87] Muthukkumaran K, Sundaravadivelu R, Gandhi S R (2004) Monitoring Lateral Deflections of a Berthing Structure During Dredging- A Case Study, *Fifth International Conference on Case Histories in Geotechnical Engineering*, New York, 13-17 April 2004
- [88] Muthukkumaran K, Sundaravadivelu R, Gandhi S R (2007) Effect of Dredging and Axial Load on Berthing Structure, *International Journal of Geoengineering Case Histories*, 1(2), 73-88
- [89] Mylonakis G, Gazetas G (1999) Lateral Vibration and Internal Forces of Grouped Piles in Layered Soil, *Journal of Geotechnical and Geoenvironmental Engineering*, 125(1), 16-25

- [90] Naemeh Naghavi, Mohammad Hassan Baziar (2008) Parametric Study of the Response of Single Pile Under Lateral Loading At The Pile Head. Iran Sixth International Conference on Case Histories in Geotechnical Engineering Missouri University of Science and Technology, Scholars' Mine; Aug 11-16
- [91] Nainan P Kurian, K.S.Beena and Krishna Kumar (1997), Settlement of reinforced sand in foundations, Journal of Geotechnical and Geoenvironmental Engineering
- [92] NarasimhaRao S., V. G. S. T. Ramakrishna and G. BalaramaRaju, Behaviour of Pile Supported Dolphins in Marine Clay Under Lateral Loading, Journal of Geotechnical Engineering, Vol. (122), Issue.(8), pp. 607-612.
- [93] Nath U K, Hazarika P J (2012) Lateral Resistance of Pile Cap – An Experimental Investigation, International Journal of Geotechnical Engineering, 7(3), 266-272
- [94] NathU. K. andHazarika, P. J. (2013) Parametric study of pile cap lateral resistance: finite element analysis, Intl. Journal of Geotechnical Engineering, Volume 7 Issue, pp. 273-281
- [95] Okada T, Fujita K, Takewaki I (2016) Robustness evaluation of seismic pile response considering uncertainty mechanism of soil properties. Innovative Infrastructure Solutions journal, Springer. DOI: 10.1007/s41062-016-0009-8
- [96] Oortmerssen G V, Pinkster J A, Boom V D H J J(1986) Computer Simulation of Moored Ship Behaviour, Journal of Waterway, Port, coastal and Ocean Engineering, 112(2), 296-308
- [97] Osman, A. and Randolph, M. (2012) Analytical Solution for the Consolidation around a Laterally Loaded Pile, Int. J. Geomech., 12(3), 199–208
- [98] Peralta P. and M. Achmus (2010) An Experimental Investigation of Piles in Sand Subjected to Lateral Cyclic Loads, Physical Modelling in Geotechnics. Proceedings of the 7th International Conference on Physical Modelling in Geotechnics, 28th June - 1st 401 July 2010, Zurich, Switzerland
- [99] Pandian N S, Nagraj T S, Babu S G L (1991) Effects of Drying on the Engineering Behaviour of Cochin Marine Clays, Geotechnique, 41(1), 143-147

- [100] Patra N R, Pise P J (2001) Ultimate Lateral Resistance of Pile Groups in Sand, *Journal of Geotechnical and Geoenvironmental Engineering*, 127(6), 481-487
- [101] Phanikanth V S, Choudhury D, Reddy R G (2010) Behaviour of Fixed Head Single Pile in Cohesionless Soil Under Lateral Loads, *Electronic Journal of Geotechnical Engineering*, 15(M), 1243-1262
- [102] Phanikanth V S, Choudhury D, Reddy R G (2010) Response of Single Pile under Lateral Loads in Cohesionless Soils, *Electronic Journal of Geotechnical Engineering*, 15(H), 813-830
- [103] PLAXIS 3D, (computer software), Plaxisbv , P.O. Box 572, 2600 AN Delft, The Netherlands
- [104] Poulos H.G and Davis E.H (1980), *Pile Foundation Analysis and Design*, John Wiley and SonsInc, Newyork,N.Y
- [105] Premalatha P V, Muthukkumaran K, Jayabalan P (2011) Behaviour of Piles Supported Berthing Structure under Lateral Loads, 2011 Pan-AmCGS Geotechnical Conference
- [106] Premalatha P. V., K. Muthukumaran and P. Jeyabalan (2009), Analysing the Optimum Length of Tie Rod Anchor for a Berthing Structure, *Indian Geotechnical Conference*, Guntur, India, pp. 127-130.
- [107] Premalatha P. V., K. Muthukumaran and P. Jayabalan (2011), Distribution of Lateral Load Among the Piles of a Berthing Structure, *International Journal of Earth Sciences and Engineering*, Vol. (4), Issue (6), pp.1129-1138.
- [108] Pyke R, Beikae M (1984) A new Solution for the Resistance of Single Piles to Lateral Loading, *Laterally Loaded Deep Foundations: Analysis and Performance*, ASTM STP 835, American Society for Testing and Materials, 3-20
- [109] Rahman M, Alim A, Chowdhury A S (2003), Investigation of Lateral Load Resistance of Laterally Loaded Pile in Sandy Soil, *Deep Foundations and Auger Pile*, 209- 215
- [110] Rahul Sawant, Dr. M. N. Bajad (2015) A review on: The influence of soil conditions on the seismic forces in RC buildings. *Int. Journal of Engineering Research and Applications* www.ijera.com ISSN: 2248-9622, Vol. 5, Issue 6, (Part - 5); June. pp.81-87

- [111] Rani, S. and Prashant, A. (2014) Estimation of the Linear Spring Constant for a Laterally Loaded Monopile Embedded in Nonlinear Soil”, *Int. J. Geomech.*, 412 10.1061/(ASCE)GM.1943-5622.0000441 , 04014090
- [112] Rao N S, Ramakrishna V G S T, Rao M B (1998) Influence of Rigidity on Laterally Loaded Pile Groups in Marine Clay, *Journal of Geotechnical and Geoenvironmental Engineering*, 124(6),542-549
- [113] Rao N S, Ramakrishna V G S T, Raju G B (1996) Behaviour of Pile Supported Dolphins in Marine Clay under Lateral Loading, *Journal of Geotechnical Engineering*, 122(8), 607-612
- [114] Reddy N P C, Rao D P, Dora Y L (1992) Clay Minerology of Innershelf Sediments off Cochin, West Coast of India, *Indian Journal of Marine Sciences*, 21, 152-154
- [115] Reese L C, Cox W R (1969) Soil Behaviour from analysis of Tests of Un-instrumented Piles under Lateral Loading, *Performance of Deep Foundations*, ASTM STP 444, American Society for Testing and Materials, 160-176
- [116] Reese L.C, Cox W.R and Koop. F. D (1974), Analysis of Laterally Loaded Piles in Sand, *Proc. 5th Annual Offshore Technology Conf.*, Paper No.OTC 2080 473-485
- [117] Reese L C, Wang S T (1986) Method of Analysis of Piles under Lateral Loading, *Marine Geotechnology and Nearshore/ Offshore Structures*, ASTM STP 923, American Society for Testing and Materials, 199-211
- [118] Reese L C, Wright S G, Aurora R P (1984) Analysis of a Pile Group Under Lateral Loading, ASTM STP 835, American Society for Testing and Materials, 56-71
- [119] Reese, Lymon C, William M. Isenhower, Shin-Tower Wang (2006).*Analysis and design of shallow and deep foundations*, John Wiley and Sons Inc.
- [120] Richard Jay Keiter (1999), *Structural Assessment of Pile Supported Piers*, Masters Thesis Report, Massachusetts Institute of Technology
- [121] Roberto O. Cudmani (2004) Numerical Study of the Soil-Structure Interaction During Strong Earthquakes. 13th World Conference On Earthquake Engineering, Vancouver, B.C., Canada; August 1-6, Paper No. 2959

- [122] Rollins K M, Gerber T M, Lane J D, Ashford S A (2005) Lateral Resistance of a Full Scale Pile Group in Liquefied Sand, *Journal of Geotechnical and Geoenvironmental Engineering*, 131(1), 115- 125
- [123] Rollins K M, Lane J D, Gerber T M (2005) Measured and Computed Lateral Response of a Pile Group in Sand, *Journal of Geotechnical and Geoenvironmental Engineering*, 131 No. 1, 103-114
- [124] Rollins K M, Peterson K T, Weaver T J (1998), Lateral Load Behaviour of Full Scale Pile Group in Clay, *Journal of Geotechnical and Geoenvironmental Engineering*, 124(6), 468-478
- [125] Rollins K M, Sparks A (2002) Lateral resistance of Full Scale Pile Cap with Gravel Backfill, *Journal of Geotechnical and Geoenvironmental Engineering*, 128(9), 711-723
- [126] Ruesta P F, Townsend F C (1997) Evaluation of Laterally Loaded Pile Group at Roosevelt Bridge, *Journal of Geotechnical and Geoenvironmental Engineering*, 123(12), 1153-1161
- [127] Salini U, Girish M S (2009) Lateral Capacity of Model Piles on Cohesionless Soil, *Electronic Journal of Geotechnical engineering*, 14(P)
- [128] Sanchez M, Roesset J M (2013) Evaluation of Models for Laterally Loaded Piles, *Computers and Geotechnics*, 48, 316-320
- [129] Sawant V A, Shukla S K (2012) Finite Element Analysis for Laterally Loaded Piles in Sloping Ground, *Coupled Systems Mechanics*, 1(1), 59-78
- [130] Sawant V A, Shukla S K (2012) Three Dimensional Finite Element Analysis of Laterally Loaded Piles in Sloping Ground, *Indian Geotechnical Journal*, 42(4), 278-286
- [131] Sawwaf M EI (2008) Lateral Behaviour of Vertical Pile Group embedded in Stabilized Earth Slope, *Journal of Geotechnical and Geoenvironmental Engineering*, 134(7), 1015-1020
- [132] Selvadurai, A. P. S. (1979). *Elastic Analysis of Soil Foundation Interaction*, Elsevier Scientific Publishing Company
- [133] Sekhar Chandra Dutta, Rana Roy (2002), A critical review on idealization and modelling for interaction among soil-foundation-structure system, *Computers and Structures*, 80(2002), 1579-1594

- [134] Sivapriya A V, Gandhi S R (2013) Experimental and Numerical Study on Pile Behaviour Under Lateral Load in Clayey Slope, *Indian Geotechnical Journal*, 43(1), 105-114
- [135] Sivapriya S V, Gandhi S R (2011) Behaviour of Single Pile in Sloping Ground Under Static Lateral Load, *Proceedings of Indian Geotechnical Conference*, 199-202
- [136] Steven L. Kramer (2014) *Geotechnical Earthquake Engineering*. Pearson Education Inc.
- [137] Soltani A (2008) A FEM Model to Investigate the Lateral Behaviour of Cylindrical Piles in Saturated Clay, *Electronic Journal of Geotechnical Engineering*, 15(D), 373 - 384
- [138] Sundaravadivelu R, Gandhi S R, Natarajan R, Thilakavathy G (2000) Design of Slipway facility for Repair and Maintenance of Port Crafts, 4th International Conference on Coasts, Ports & Marine Structures
- [139] Tafreshi M S N (2008) Uncouple Nonlinear Modeling of Seismic Soil-Pile-Superstructure Interaction in Soft Clay, *International Journal of Civil engineering*, 6(4), 275-283
- [140] Takewaki I (2005) Frequency Domain Analysis of Earthquake Input Energy to Structure-Pile Systems, *Engineering Structures*, Vol.27, No.4, pp549-563
- [141] Takewaki I, Kishida A (2005) Efficient Analysis of Pile-group Effect on Seismic Stiffness and Strength Design of Buildings, *Soil Dynamics and Earthquake Engineering*, Vol.25, No.5, pp355-367
- [142] Ti K S, Bujang B K, Saw G S (2009) A Review of Basic Constitutive Models for Geotechnical Application, *Electronic Journal of Geotechnical Engineering*, 14(J)
- [143] Tomlinson, M.J. (1994) *Pile Design and Construction Practice*, Fourth Edition, E & FN Spon, an imprint of Chapman & Hall, 2-6 Boundary Row, London SE1 8HN, UK. Trenter, N.A. (2001). *Earth Works: A Guide*, Thomas Telford.
- [144] Van der Molen W, Lighterigen H (2003) Behaviour of a Moored LNG Ship in SwellWaves, *Journal of Waterway, Port, Coastal and Ocean engineering*, 129(1), 15-21

- [145] Van Oortmerssen G., J. A. Pinkster and H. J. J. Van Den Boom (1986), Computer Simulation of Moored Ship Behaviour, *Journal of Waterway, Port, Coastal, Ocean Engineering*, 112: 296-308
- [146] Vasani, P. C, Interactive Analysis Models for Soil and Structures, *Structural Engineering Forum of India*
- [147] Wai, F C, Atef F.S (1982), *Constitutive Equations for Engineering Materials*, John Wiley & Sons, New York
- [148] William T. Thomson, *Theory of Vibrations with Applications*, Pearson Education, Eighth Impression, 2008
- [149] Wei W B, Cheng Y M (2009) Strength reduction analysis for slope reinforced with one row of piles, *Computers and Geotechnics*, 36, 1176-1185
- [150] Y. El-Mossallamy (1999). Load-settlement behaviour of large diameter bored piles in over-consolidated clay. *Proceeding of the 7th. International Symposium on Numerical Models in Geotechnical Engineering*, Graz, Austria, September 1999, pp. 443-450
- [151] Zadeh N G, Kalantari B (2011) Performance of Single Pile Under Vertical and Lateral Load in Sand, Clay and Layered Soil, *Electronic Journal of Geotechnical Engineering*, 16(K), 1131-1146
- [152] Zhang L, McVay M C, Lai P (1999) Numerical Analysis of Laterally Loaded 3X3 to 7X3 Pile Groups in Sands, *Journal of Geotechnical and Geoenvironmental Engineering*, 125(11), 936-946
- [153] Zhang, L., Zhao, M., and Zou, X. (2015) Behavior of Laterally Loaded Piles in Multilayered Soils, *Int. J. Geomech.*, 15(2), 06014017
- [154] Zhu H, Chang M F P E (2002) Load Transfer Curves along Bored Piles Considering Modulus Degradation, *Journal of Geotechnical and Geoenvironmental Engineering*, 128(9), 764-774



Experimental Investigation of Soil Sample

A.1 Atterberg Limits (IS: 2720 (Part 5) – 1985)

Liquid Limit, LL= 45

Plastic Limit, PL= 30

Natural Moisture Content, nmc = 39

$$\text{Consistency Index, } I_c = \frac{(LL-nmc)}{(LL-PL)} = \frac{(45-39)}{(45-30)} = 0.4$$

A.2 Unconfined Compression Testing (IS: 2720 (Part 10) – 1991)



Fig. A.1 UCC Apparatus

$$\text{Stress, } q_u = \frac{\text{Load}}{\text{Area}} = \frac{(\text{Proving Ring Reading} \times \text{Proving Ring Constant})}{\left(\frac{A_0 L_0}{(L_0 - \Delta L)} \right)}$$

$$= \frac{[70 \times 2.34]}{\left[\frac{(\pi/4 \times 3.8^2) \times 7.5}{7.5 - (7.5 - 6.8)} \right]} = 13.101 \text{ N/cm}^2 = \mathbf{131.01 \text{ kN/m}^2}$$

$$\text{Undrained shear strength} = \frac{\mathbf{131.01}}{2} = 65.505 \text{ kN/m}^2$$

A.3 Compaction Test (IS: 2720 (Part 7) – 1980)



Fig. A.2 Compaction Testing Apparatus

Density of the soil used in the experiment is obtained from compaction test as

$$1.778 \text{ g/cc} = \mathbf{17.78 \text{ kN/m}^3}$$

A.4 Direct Shear Test (IS: 2720 (Part 13) – 1986)



Fig. A.3 Direct Shear Test

Direct shear test was conducted on the collected soil sample and the cohesion is obtained to be 23.4 kN/m^2 and angle of friction is $\tan^{-1}(0.424) = 22.9^\circ$

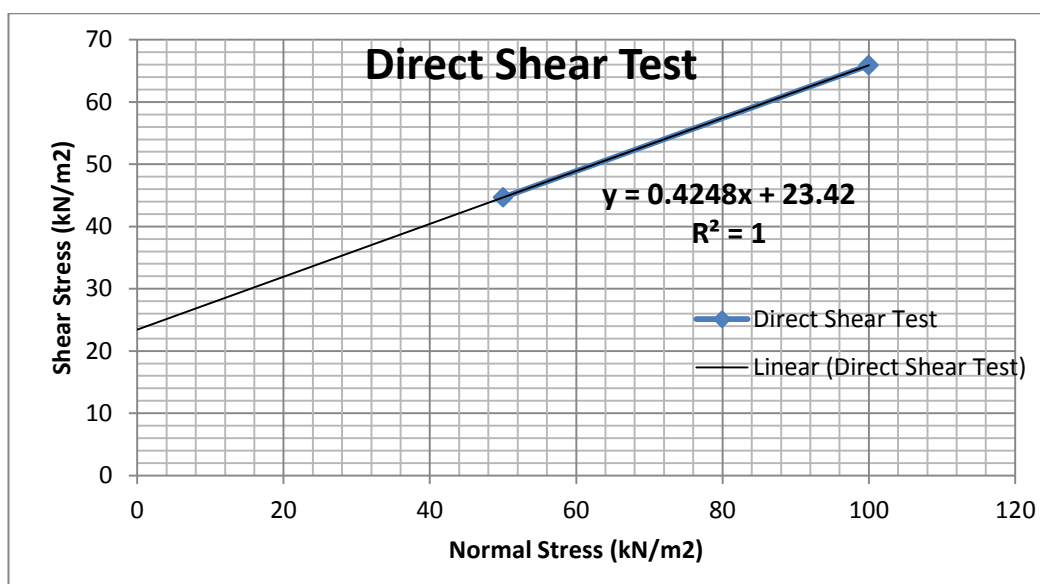


Fig. A.4 Direct Shear Test

A.5 Specific Gravity (IS: 2720 (Part III/Sec 2) – 1980)



Fig. A.5 Pycnometer used to test specific gravity of soil

Table B.1 Specific Gravity Test

Weights measured	Weight (g)
Pycnometer + cap	33.37
Pycnometer + oven dried soil sample	55.61
Pycnometer + ovedried soil sample + water	95.88
Pycnometer + water	82.27
Weight of dry soil, W_s	$55.61 - 33.37 = 22.24$
Weight of water, W_2	$82.27 - 33.37 = 48.90$
Weight of ovedried soil sample+ water, W_1	$95.88 - 33.37 = 62.51$

Specific gravity of soil sample is, $G = \frac{W_s}{W_s + (W_2 - W_1)} = 2.577$

Appendix B

Model Tests

B.1 Calibration Curve

B.1.1 Calibration of 19 mm Diameter Model Pile

Table B.1 Bending Test on 19 mm Diameter Model Pile

Load, W (N)	Strain ($10e-6$ mm/mm)	Bending Moment, $\frac{WLe}{4}$ (Nmm)
0.00	0	0
0.74	7	178.752
2.12	24	508.032
3.49	45	837.312
4.88	63	1171.296
6.27	71	1505.28

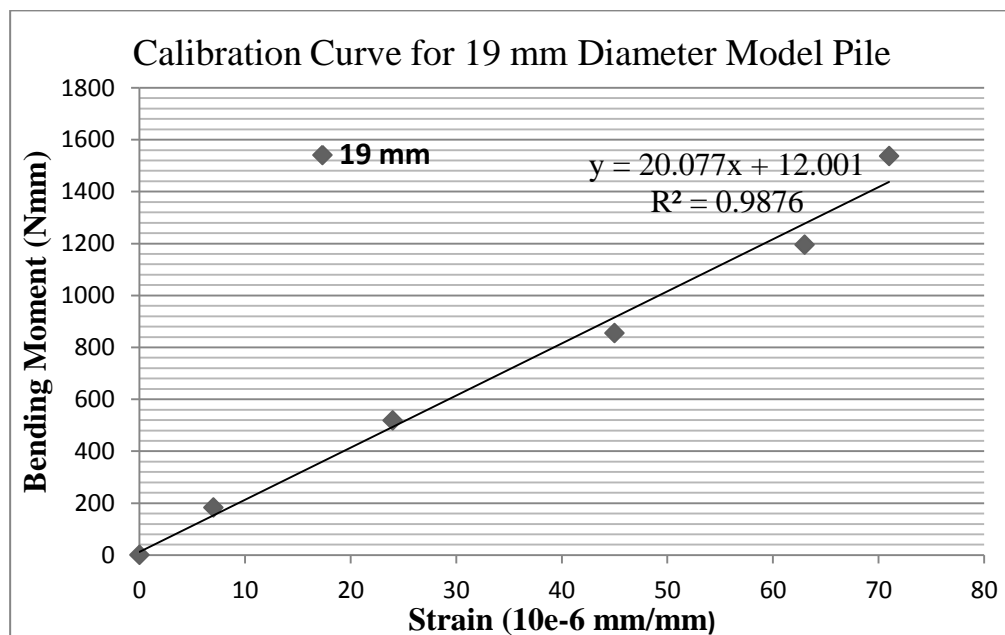


Fig. B.1 Calibration Curve for 19 mm Diameter Model Pile

B.1.2 Calibration of 25.4 mm Diameter Model Pile

Table B.2 Bending Test on 25.4 mm Diameter Model Pile

Load, W (N)	Strain ($10e-6$ mm/mm)	Bending Moment, $\frac{WLe}{4}$ (Nmm)
0.00	0	0
0.74	2	178.752
2.12	14	508.032
3.49	25	837.312
4.88	33	1171.296
6.27	39	1505.28

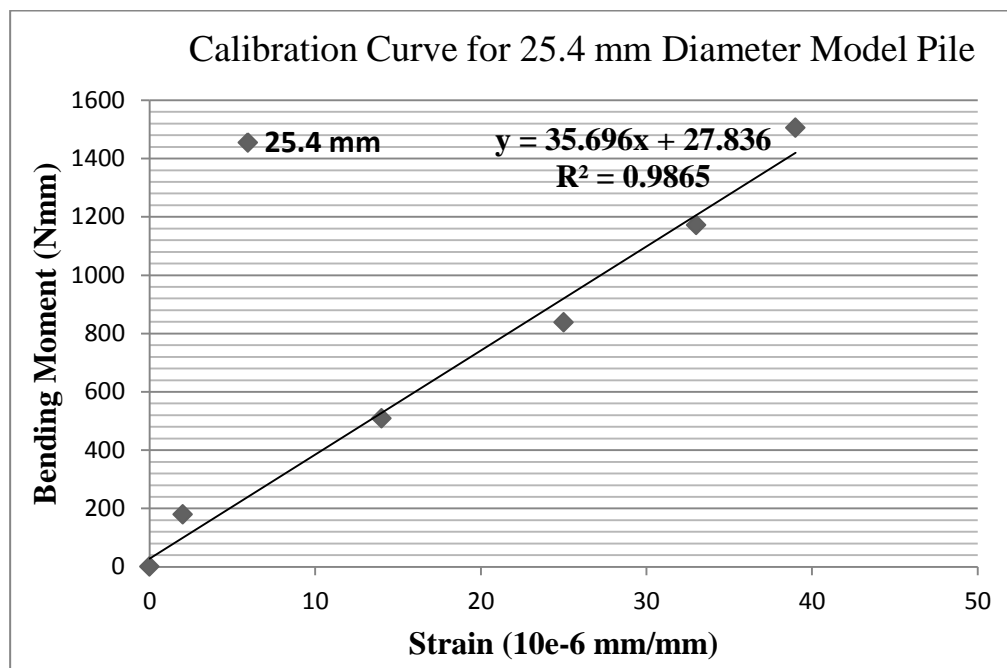


Fig. B.2 Calibration Curve for 25.4 mm Diameter Model Pile

B.2 Bending Moments in Model Piles

Table B.2 Strain Gauge Readings and Bending Moments in Model Piles

Pile Length : 600 mm
 Pile Diameter : 25.4 mm
 Bed Slope : 1:1.5

Position of Strain Gauge from GL (mm)	Initial Strain Gauge Reading	Final Strain Gauge Reading	Strain (X10-6 mm/mm)	Bending Moment (kNmm)
0	2	2	0	0.0
-180	10	381	371	13.3
-230	8	68	60	2.2
-400	15	15	0	0.0

Pile Length : 700 mm
 Pile Diameter : 25.4 mm
 Bed Slope : 1:1.5

Position of Strain Gauge from GL (mm)	Initial Strain Gauge Reading	Final Strain Gauge Reading	Strain (X10-6 mm/mm)	Bending Moment (kNmm)
0	7	7	0	0.0
-180	32	411	379	13.6
-400	32	137	105	3.8
-600	-54	7	61	2.2

Pile Length : 800 mm
 Pile Diameter : 25.4 mm
 Bed Slope : 1:1.5

Position of Strain Gauge from GL (mm)	Initial Strain Gauge Reading	Final Strain Gauge Reading	Strain (X10-6 mm/mm)	Bending Moment (kNmm)
0	7	7	0	0.0
-180	32	411	379	13.6
-400	32	137	105	3.8
-600	-54	7	61	2.2
-800	5	-2	-7	-0.2

Pile Length : 600 mm
 Pile Diameter : 19 mm
 Bed Slope : 1:1.5

Position of Strain Gauge from GL (mm)	Initial Strain Gauge Reading	Final Strain Gauge Reading	Strain (X10-6 mm/mm)	Bending Moment (kNmm)
0	-12	-12	0	0.0
-130	-176	394	570	11.5
-180	-207	-91	116	2.3
-400	-168	-124	44	0.9
-600	-32	-32	0	0.0

Pile Length : 700 mm
 Pile Diameter : 19 mm
 Bed Slope : 1:1.5

Position of Strain Gauge from GL (mm)	Initial Strain Gauge Reading	Final Strain Gauge Reading	Strain (X10-6 mm/mm)	Bending Moment (kNmm)
0	23	23	0	0.0
-80	-349	-161	188	3.8
-180	-807	-222	585	11.8
-400	65	65	0	0.0
-600	528	538	10	0.2

Pile Length : 800 mm
 Pile Diameter : 19 mm
 Bed Slope : 1:1.5

Position of Strain Gauge from GL (mm)	Initial Strain Gauge Reading	Final Strain Gauge Reading	Strain (X10-6 mm/mm)	Bending Moment (kNmm)
0	33	33	0	0
-180	-1344	-742	602	12.1
-400	-1416	-1341	75	1.5
-800	0	0	0	0

Pile Length : 600 mm
 Pile Diameter : 25.4 mm
 Bed Slope : 1:2

Position of Strain Gauge from GL (mm)	Initial Strain Gauge Reading	Final Strain Gauge Reading	Strain (X10-6 mm/mm)	Bending Moment (kNmm)
0	54	54	0	0.0
-80	-4272	-4400	128	4.6
-180	-4340	-4685	345	12.3
-400	-687	-687	0	0.0

Pile Length : 700 mm
 Pile Diameter : 25.4 mm
 Bed Slope : 1:2

Position of Strain Gauge from GL (mm)	Initial Strain Gauge Reading	Final Strain Gauge Reading	Strain (X10-6 mm/mm)	Bending Moment (kNmm)
0	2	2	0	0.0
-130	-4	183	187	6.7
-180	32	382	350	12.5
-400	-4	112	116	4.2
-600	-3	-9	-6	-0.2

Pile Length : 800 mm
 Pile Diameter : 25.4 mm
 Bed Slope : 1:2

Position of Strain Gauge from GL (mm)	Initial Strain Gauge Reading	Final Strain Gauge Reading	Strain (X10-6 mm/mm)	Bending Moment (kNmm)
0	116	116	0	0.0
-130	-292	-120	172	6.2
-180	-458	-101	357	12.8
-400	-287	-227	60	2.2
-800	-294	-312	-18	-0.6

Pile Length : 600 mm
 Pile Diameter : 19 mm
 Bed Slope : 1:2

Position of Strain Gauge from GL (m)	Initial Strain Gauge Reading	Final Strain Gauge Reading	Strain (X10-6 mm/mm)	Bending Moment (kNmm)
0	7	7	0	0.0
-130	45	589	544	10.9
-230	-9	-130	-121	-2.4
-400	-13	-127	-114	-2.3

Pile Length : 700 mm
 Pile Diameter : 19 mm
 Bed Slope : 1:2

Position of Strain Gauge from GL (mm)	Initial Strain Gauge Reading	Final Strain Gauge Reading	Strain (X10-6 mm/mm)	Bending Moment (kNmm)
0	121	121	0	0.0
-180	-230	322	552	11.1
-400	-257	-124	133	2.7

Pile Length : 800 mm
 Pile Diameter : 19 mm
 Bed Slope : 1:2

Position of Strain Gauge from GL (mm)	Initial Strain Gauge Reading	Final Strain Gauge Reading	Strain (X10-6 mm/mm)	Bending Moment (kNmm)
0	0	0	0	0.0
-180	0	577	577	11.6
-400	36	100	64	1.3
-800	11	11	0	0.0

B3. Load and Deflection of Model Tests

Table B.3.1 Load- Deflection Details Model Pile with Diameter = 25.4 mm and Bed Slope = 1:1.5

Load (kg) P	Deflection (mm)		
	L = 600 mm	L = 700 mm	L = 800 mm
0	0	0	0
10	0.08	0.06	0.01
20	0.2	0.33	0.23
30	0.39	0.6	0.5
40	0.75	0.9	0.89
50	0.98	1.05	1.15
60	1.3	1.4	1.23
70	1.8	1.67	1.42
80	2.25	2.1	1.73
90	2.73	2.69	2.46
100	3.41	3.23	3.11

Table B.3.2 Load- Deflection Details Model Pile with Diameter = 1.9 mm and Bed Slope = 1:1.5

Load (kg) P	Deflection (mm)		
	600 mm	700 mm	800 mm
0	0	0	0
10	0.15	0.13	0.08
20	0.74	0.25	0.32
30	1.21	0.78	0.62
40	1.63	1.21	0.93
50	2.11	1.77	1.3
60	2.69	2.27	1.7
70	3.32	2.9	2.13
80	3.95	3.44	2.9
90	4.67	4.24	3.99
100	5.2	4.89	4.55

Table B.3.3 Load- Deflection Details Model Pile with Diameter = 25.4 mm and Bed Slope = 1:2

Load (kg) P	Deflection (mm)		
	600 mm	700 mm	800 mm
0	0	0	0
10	0.14	0.1	0.03
20	0.39	0.23	0.1
30	0.62	0.34	0.21
40	0.78	0.61	0.47
50	0.99	0.91	0.94
60	1.13	1.06	0.94
70	1.31	1.2	1
80	1.67	1.6	1.43
90	1.99	1.96	1.9
100	2.35	2.13	2.02

Table B.3.4 Load- Deflection Details Model Pile with Diameter = 25.4 mm and Bed Slope = 1:1.5

Load (kg) P	Deflection (mm)		
	600	700	800
0	0	0	0
10	0.19	0.12	0.09
20	0.5	0.31	0.33
30	0.95	0.55	0.35
40	1.18	0.85	0.7
50	1.5	1.05	1.02
60	1.9	1.51	1.26
70	2.44	1.93	1.71
80	3.1	2.3	2.32
90	3.62	3.2	2.83
100	4.5	4.32	4.15

Appendix C**MATLAB Coding for the Analysis of Single Pile****C.1 Static Analysis of Single Pile**

```
clear;

clc;

Load=300;

digits(30);format long;

Length=20000;

ii=1;

% input variables

% 'Load' is the applied load

% 'Length' is the pile length

% 'Dia' is the pile diameter

% 'kpy' is the soil modulus parameter

% 'ep' is the young's modulus of pile

% 'ip' is the moment of inertia of pile

% output variables

% 'ZD' is the depth of fixity

% 'YY' is the pile top deflection

% 'MM' is the bending moment

for Load=50:50:300

    for Dia=200:100:600
```

```

for kpy=0.000005:0.000005:.000025

    % Dia=380;

    XX(ii,1)=1;

    XX(ii,2)=Dia;

    XX(ii,3)=kpy;

    XX(ii,4)=Load;

    ep=200;

    ip=((power(Dia,4)-power((Dia-50),4))*(22/7))/64;

    epip=ep*ip;

    no1=(Length)/(Dia/2);

    no=ceil(no1);

    h=Dia/2;

    z(1)=1;z(2)=-4;z(4)=-4;z(5)=1;

    T=power((epip/kpy),(1/5));

    epy(no)=0;

    c(no)=6;

    for i=no-1:-1:1

        epy(i)=epy(i+1)+kpy*h;

        c(i)=6+epy(i)*h*h*h*h/epip;

    end

    for i=1:no+4

        for j=1:no+4

```

```

        D(i,j)= 0;
    end
end
for i=1:no+4
    B(i)=0;
end
%B.C2 @top
D(no+4,no)=1;
D(no+4,no+1)=-2;
D(no+4,no+3)=2;D(no+4,no+4)=-1;
B(no+4)=(Load*2*h*h*h/(epip));
%B/C1 @top
D(no+3,no+1)=1;D(no+3,no+2)=-2;D(no+3,no+3)=1;
%B.C1 @bottom
D(no+1,2)=1;D(no+1,3)=-2;D(no+1,4)=1;
%B.C2 @bottom
D(no+2,1)=1;D(no+2,2)=-2;D(no+2,4)=2;D(no+2,5)=-1;
for i=1:no
    j=i;
    for p=1:5
        if p==3
            D(i,j)=c(i);
        else

```

```

        D(i,j)= z(p);
    end
    j=j+1;
end
end
DD=D;
for i=1:no+4
    for j=1:no+4
        if(j<i)
            if(D(i,j) ~= 0)
                k=j;
                m=D(i,k)/D(k,k);
                for j1=j:no+4
                    D(i,j1)= D(i,j1)-(m*D(k,j1));
                end
                B(i)=B(i)-(B(k)*m);
            end
        end
    end
end
end
no1=no;
for i=no+4:-1:1
    for j=i:-1:i

```

```

        if(D(i,j)~=0)
            C(i)=B(i)/D(i,j);
            for k=1:no+4
                B(k)=B(k)-D(k,j)*C(i);
            end
            no=no-1;
        end
    end
end
for x=1:no1+4
    Y(x)=-(x-1)*Dia/2000;
    A(x)=0;
end
for x=1:no1+4
    AA(no1+5-x)=C(x);
end
for x=no1+2:-1:3
    M(x)=(AA(x-1)-2*AA(x)+AA(x+1))*epip/(h*h*1000);
end
M(1)=0;
M(2)=0;
M(no1+3)=0;
M(no1+4)=0;

```

```

    for i=1:no1+4
        if M(i)==max(M)
            zd=i;
        end
    end

    end

    ZD(ii)=(zd-3)*h;
    YY(ii)=AA(3);
    MM(ii)=max(M);
    ii=ii+1;

    % hold on
    % plot(A,Y,'cx-',AA,Y,'m*-');
    % plot(M,Y,'k*-');
    % title('Laterally Loaded Pile Behaviour')
    % xlabel('Deflection(mm) & Bending Moment(kNm)')
    % ylabel('Depth(m)')
    % legend('location','SouthEast','Pile', 'Deflection (mm)','Bending
    %Moment (kNm)');
    % grid on

    end

end

end

MM=MM';
YY=YY';

```

```

ZD=ZD';

% A=XX'*XX;

% K=(XX'*XX)^-1;

% B=K*XX'*MM;

% B

% M=XX*B;

% E=MM-M;

% MaxErr=max(abs(MM-M))

% plot(XX*B,MM,'o',XX*B,M,'-')

% title('Analysis of Bending Moment (M)')

% xlabel('Actual Values of M')

% ylabel('Calculated Values of M')

% legend('location','SouthEast','Actual Values', 'Calculated Values')

% mu=mean(MM);

% SST=sum((MM-mu).^2);

% SSE=sum((M-MM).^2);

% r2=1-SSE/SST

% A=XX'*XX;

% K=(XX'*XX)^-1;

% B=K*XX'*YY;

% B

% M=XX*B;

% E=YY-M;

```

```

% MaxErr=max(abs(YY-M))
% plot(XX*B,YY,'o',XX*B,M,'-')
% title('Analysis of Top Deflection (y)')
% xlabel('Actual Values of y')
% ylabel('Calculated Values of y')
% legend('location','SouthEast','Actual Values', 'Calculated VAlues')
% mu=mean(YY);
% SST=sum((YY-mu).^2);
% SSE=sum((M-YY).^2);
% r2=1-SSE/SST
A=XX'*XX;
K=(XX'*XX)^-1;
B=K*XX'*ZD;
B
M=XX*B;
E=ZD-M;
MaxErr=max(abs(ZD-M))
plot(XX*B,ZD,'o',XX*B,M,'-')
    title('Analysis of Depth of Fixity (Zd)')
    xlabel('Actual Values of Zd')
    ylabel('Calculated Values of Zd')
    legend('location','SouthEast','Actual Values', 'Calculated VAlues')
mu=mean(ZD);
SST=sum((ZD-mu).^2);
SSE=sum((M-ZD).^2);
r2=1-SSE/SST

```

C.2 Calculation of Natural Frequency of Single Pile

```

clear;
clc;
digits(30);
format long;
Length=40.000;
ii=1;
for Load=1000000:50:1000000
    for Dia=1.5000:.100:1.5000
        %Relation Between qu and E :- A. P. S. Selvadurai
        % Elastic Analysis of Soil Foundation Interaction,pp 423
        %Subgrade Modulus :- IS 2911(Part 1/ Sec 2) : 2010, ANNEX C
        kpy=48000000;B=Dia;
        K=kpy*0.3/(1.5*B);
        for kpy=K:5000000:K
            Ht=3.000;
            Mt=Load*Ht;
            mass=200000;
            Px=mass*9.8;
            ep=30000000000;
            ip=(power(Dia,4)*(22/7))/64;
            epip=ep*ip;
            no1=(Length)/(Dia/2);
            no=ceil(no1);
            h=Dia/2;
            z(1)=1;z(2)=-4;z(4)=-4;z(5)=1;
            T=power((epip/kpy),(1/5));
            epy(no)=0;
            c(no)=6;
            for i=no-1:-1:1

```



```

        epy(i)=epy(i+1)+kpy*h;
        c(i)=6+epy(i)*h*h*h*h/epip;
    end
    for i=1:no+4
        for j=1:no+4
            D(i,j)= 0;
        end
    end
    end
    for i=1:no+4
        B(i)=0;
    end
    end

    %B.C2 @top
    D(no+4,no)=1;
    D(no+4,no+1)=(-2+(Px*h*h/epip));
    D(no+4,no+3)=(2-(Px*h*h/epip));
    D(no+4,no+4)=-1;
    %D(no+4,no)=1;
    %D(no+4,no+1)=(-2);
    %D(no+4,no+3)=(2);D(no+4,no+4)=-1;
    B(no+4)=(Load*2*h*h*h/(epip));
    %B/C1 @top
    D(no+3,no+1)=1;D(no+3,no+2)=-2;D(no+3,no+3)=1;
    B(no+3)=(Mt*h*h/(epip));
    %B.C1 @bottom
    D(no+1,2)=1;D(no+1,3)=-2;D(no+1,4)=1;
    %B.C2 @bottom
    D(no+2,1)=1;D(no+2,2)=-2;D(no+2,4)=2;D(no+2,5)=-1;
    for i=1:no
        j=i;

```

```

for p=1:5
    if p==3
        D(i,j)=c(i);
    else
        D(i,j)= z(p);
    end
    j=j+1;
end
end
DD=D;
for i=1:no+4
    for j=1:no+4
        if(j<i)
            if(D(i,j) ~= 0)
                k=j;
                m=D(i,k)/D(k,k);
                for j1=j:no+4
                    D(i,j1)= D(i,j1)-(m*D(k,j1));
                end
                B(i)=B(i)-(B(k)*m);
            end
        end
    end
end
end
no1=no;
for i=no+4:-1:1
    for j=i:-1:i
        if(D(i,j)~=0)
            C(i)=B(i)/D(i,j);
            for k=1:no+4

```

```

                                B(k)=B(k)-D(k,j)*C(i);
                                end
                                no=no-1;
                                end
                                end
                                end

for x=1:no1+4
    Y(x)=-(x-1)*Dia/2000;
    A(x)=0;
end
for x=1:no1+4
    AA(no1+5-x)=C(x);
end
for x=no1+2:-1:3
    M(x)=(AA(x-1)-2*AA(x)+AA(x+1))*epip/(h*h*1000);
end
M(1)=0;
M(2)=0;
M(no1+3)=0;
M(no1+4)=0;
for i=1:no1+4
    if M(i)==max(M)
        zd=i;
    end
end

Ymax=AA(3)
Mmax=max(M)
for i=3:no1+2

```

```

        Mo(i-2)=M(i);
        Yo(i-2)=(i-2)*(Dia/2000);
    end

    ZD(ii)=(zd-3)*h;
    YY(ii)=AA(3);
    MM(ii)=max(M);
    ii=ii+1;
    % hold on
    %plot(A,Y,'cx-',AA,Y,'m*-');
    % plot(Mo,-Yo,'k*-');
    % title('Laterally Loaded Pile Behaviour')
    % xlabel('Deflection(mm) & Bending Moment(kNm)')
    % ylabel('Depth(m)')
    % legend('location','SouthEast','Pile', 'Deflection (mm)','Bending
    %Moment (kNm)');
    % grid on
end
end
end

Df=ZD
%DYNAMIC ANALYSIS
%constants
g=9.8;
pi=(22/7);
Ec= 30000000000;
rc=25000;

```

%pile & mass system

% variables

mass=200000;% mass @top of pile

%mass=204081;

%Dia=1.5;%Diameter of pile

%Ht=3;%Height of pile above the ground level

L=Df+Ht;%L=Total effective length of pile, Df=Depth of fixity from static analysis

%L=Df+Ht+1;

%SSI Effect-1

%L changes due to SSI

%L increases as the soil stiffness decreases

% natural frequency of the system

$A_p = \pi * \text{power}(\text{Dia}, 2) / 4;$

$I_p = \pi * \text{power}(\text{Dia}, 4) / 64;$

$M_p = \rho c * A_p * L / g;$

$k_p = (\text{power}(3.515, 2) * E_c * I_p) / (\text{power}(L, 3));$

$k_m = (3 * E_c * I_p) / (\text{power}(L, 3));$

$k = 1 / ((1 / k_p) + (1 / k_m));$

$w_p^2 = (k_p / M_p);$

$w_m^2 = (k_m / \text{mass});$

% William T. Thomson, Theory of Vibrations with Applications, pp 281
 $w_0 = \sqrt{1/((1/w_p^2) + (1/w_m^2))}$; % w_0 = natural frequency of the pile mass system

$f_n = w_0 / (2 * (22/7))$

% dynamic load
 $w = 2 * (22/7) * 3.3$;
 % $A_0 = 1$;
 $A_0 = 1000$;
 % SSI Effect-2
 % A_0 changes as the input wave travels through the soil
 % - A_0 increases at natural frequencies
 % - A_0 decreases due to damping
 % Damping-----1. Material damping (prop to Damping Ratio)
 % 2. Radiation damping (prop to $1/z$)

% Damping Ratio
 $DR = 0.05$;
 % S. K. Duggal, Earthquake Resistant Design of Structures
 % pp64, Damping Ratio for Concrete Building = 5%

$\beta = w/w_0$;

$A = (A_0/k) * (1/\sqrt{(1 - \beta * \beta)^2 + 4 * DR.^2 * \beta.^2})$;
 $\phi = \text{atan}(-2 * DR * \beta / (1 - \beta * \beta))$;
 $w_d = w_0 * \sqrt{1 - DR.^2}$;
 $i = 1$;
 % keep the increment of t = time period of system i.e. $t_i = 1/(w_0/2 * \pi)$
 for $t = 0 : .05 : 5$

```

%applied force
f(i)=A0*sin(w*t);

%transient motion

ut(i)=(A0/k)*(1/(((1-beta*beta).^2)+((2*DR*beta).^2)))*(exp(-
1*DR*w0*t))*((w/wd)*(beta.^2+2*(DR.^2)-
1)*sin(wd*t))+2*DR*beta*cos(wd*t));
%steady motion
us(i)=(A0/k)*(1/((1-beta*beta).^2+(2*DR*beta).^2))*((1-beta.^2)*sin(w*t)-
2*DR*beta*cos(w*t));

%total displacement
%u(i)=A*sin(w*t+(phi));
u(i)=ut(i)+us(i);
tt(i)=t;
i=i+1;
end
hold on

%plot(tt,f,'R');
plot(tt,u,'B');

%plot(tt,ut,'Y');
%plot(tt,us,'G');

*****

```

Appendix D

Parametric Study based on Analytical and Numerical Investigation

D.1 Parametric Study of Static Analysis

A MATLAB code has been developed (APPENDIX-C) for the static analysis of a single pile. It is used for the parametric study of the laterally loaded pile by considering the diameter of the pile and the subgrade modulus of soil as independent parameters. The diameter was varied from 200mm to 600mm which keeps the pile in the long pile category. The subgrade modulus of soil was varied from $5e-6$ kN/mm² to $25e-6$ kN/mm². The variation of deflection at the top of the pile (y), maximum bending moment (M) and the depth of fixity (D_f) are studied and the corresponding equations are developed using multivariable regression analysis.

$$y = 40.925 - 0.067467 * Dia - 9.29235 * 10e5 * kpy + 0.01089 * Load,$$

$$R^2 = 0.7960 \dots\dots\dots (D.1)$$

$$M = 87.604 - 0.33939 * Dia - 3.210026 * 10e6 * kpy + 1.1606 * Load,$$

$$R^2 = 0.9710 \dots\dots\dots (D.2)$$

$$D_f = 1075.0 + 3.31 * Dia - 2.78 * 10e7 * kpy,$$

$$R^2 = 0.9655 \dots\dots\dots (D.3)$$

A correlation coefficient of 0.79 to 0.97 is obtained from all the developed equations. The above equations enables predicting the analysis results of laterally loaded piles.

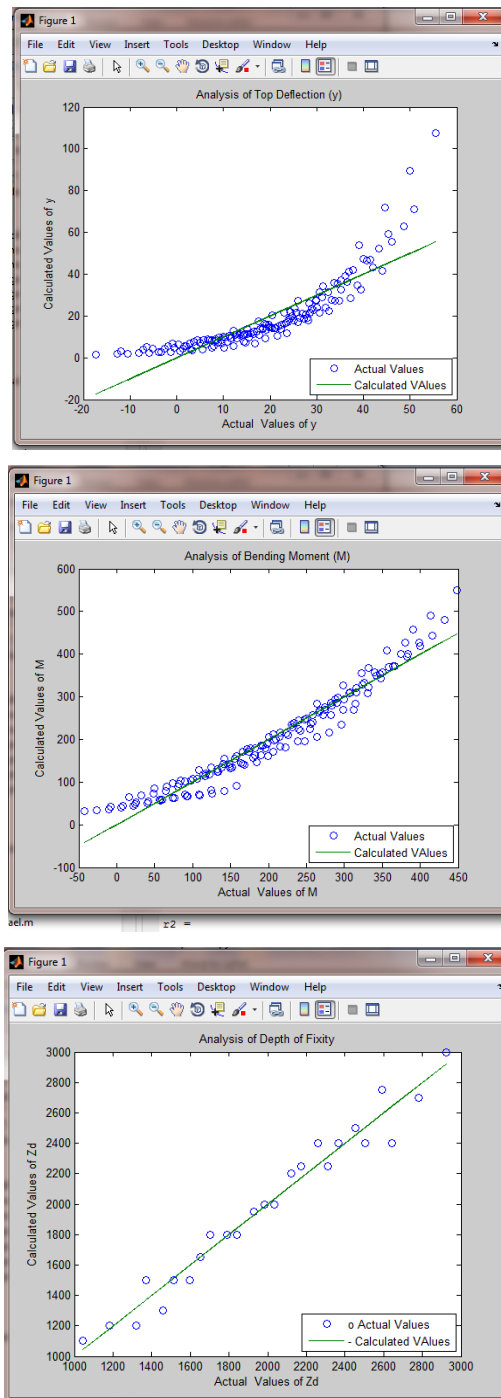


Fig. D.1 Regression Analysis of Parametric Study

D.2 Parametric Study on Dynamic Analysis of Single Pile

Two parametric studies conducted to study the influence of soil structure interaction on the dynamic behaviour of a laterally loaded pile is discussed here.

D.2.1 The Influence of SSI on the Natural Frequency of Single Pile

A MATLAB program has been developed for the analysis of laterally loaded single pile in sloping bed of soil (Chapter 4). It is used to calculate the maximum bending moment and deflection of the pile. From the analysis it is clear that for a particular pile, as the bed slope increases there is an increase in maximum bending moment and pile top deflection. The increase in maximum bending moment is due to the increase in depth of fixity of the pile with the increase in bed slope. An increase in depth of fixity causes reduction in stiffness of pile which in turn causes changes in the natural frequency and dynamic behaviour of the pile.

The natural frequency of a structure depends on the stiffness and mass of the structure. When the soil pile system is considered for the dynamic analysis, the length of pile is considered to be the sum of the height (h) of the pile above the ground level and the depth of fixity (D_f) below the ground level.

The equation to calculate the circular natural frequency (ω) of the pile, considering the mass (m), Young's modulus (E), moment of inertia (I) and length (l) of the pile is, [148]

$$\omega^2 = 3.515^2 \left(\frac{EI}{ml^3} \right) \dots\dots\dots (D.4)$$

The natural frequency is,

$$f_n = \frac{\omega}{2\pi} \dots\dots\dots (D.5)$$

Concrete circular piles are considered for this study with modulus of concrete $E = 3e9 \text{ N/m}^2$ and density of concrete $\rho = 2500 \text{ kg/m}^3$. The cross sectional area $A = \frac{\pi D^2}{4}$, the mass $m = \rho Al$, $I = \frac{\pi D^4}{64}$ and $l = (h + D_f)$. The natural frequency of a soil-pile system with the pile head in level with the ground (h=0) is calculated with as,

$$f_n = \left[\frac{3.515}{8\pi} \sqrt{\frac{E}{\rho}} \right] \frac{D}{D_f^2} \dots \dots \dots (D.6)$$

Hence, the natural frequency of the soil-pile system varies with diameter of the pile (D) and the depth of fixity (D_f) as in equation no.(D.6)

$$f_n = [153.15] \frac{D}{D_f^2} \dots \dots \dots (D.7)$$

Hence a change in bed slope causes a change in depth of fixity of pile which in turn influences the natural frequency of the pile.

A parametric study has been conducted with the soil modulus ranging from 500 N/m² to 40000 N/m² and the diameter of the pile was varied from 0.5 m to 2.0 m. The range of soil modulus has been considered as per IS2911 (part-1/ sec-2)-2010, as listed in Table 4.2. This study can be used to predict the variation of the depth of fixity of the system. The variation of depth of fixity with the soil modulus and the diameter of the pile was plotted and studied using surface fitting and multiple regression analysis.

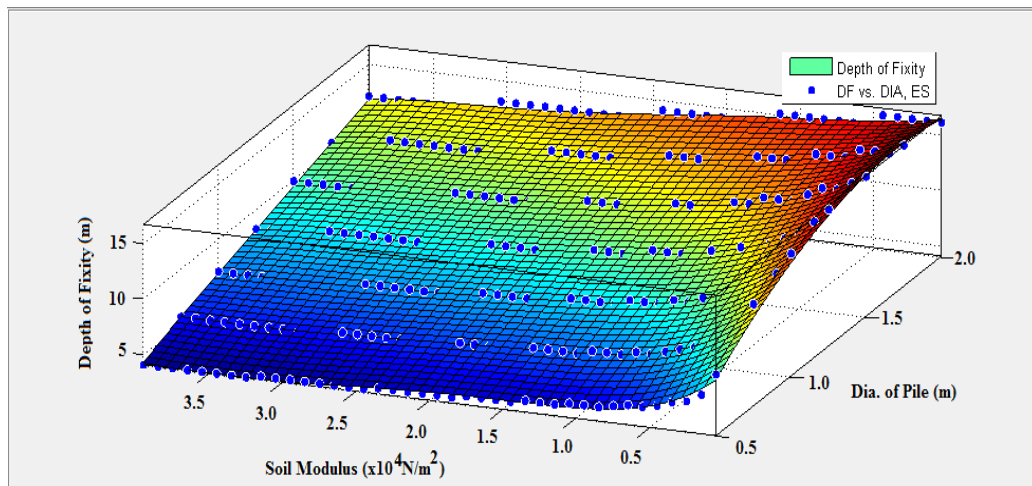


Fig. D.2 Variation in Depth of Fixity with Soil Modulus and Diameter of Pile

From Fig.D.2 it is clear that, the depth of fixity increases with the increase in diameter of pile and the reduction in the soil modulus. The variation

of depth of fixity is predicted using multivariable regression analysis with $R^2=0.94$ as,

$$D_f = 4.81 + 5.89D - 1.22e^{-4}Es \dots\dots\dots (D.8)$$

Where, D is the diameter of the pile in metre and Es is the soil modulus..

The parametric study is now extended to calculate the natural frequency of the soil-pile system using equation no.D.7. The expected non-linear variation of natural frequency of the pile with variation in Es and D is plotted using surface fitting curve in Fig. D.3. It was extended to multivariable regression analysis and an equation is predicted, with $R^2= 0.84$ to represent the natural frequency of the pile.

$$f_n = 2.65 - 1.14D + 5.14e^{-5}Es \dots\dots\dots (D.9)$$

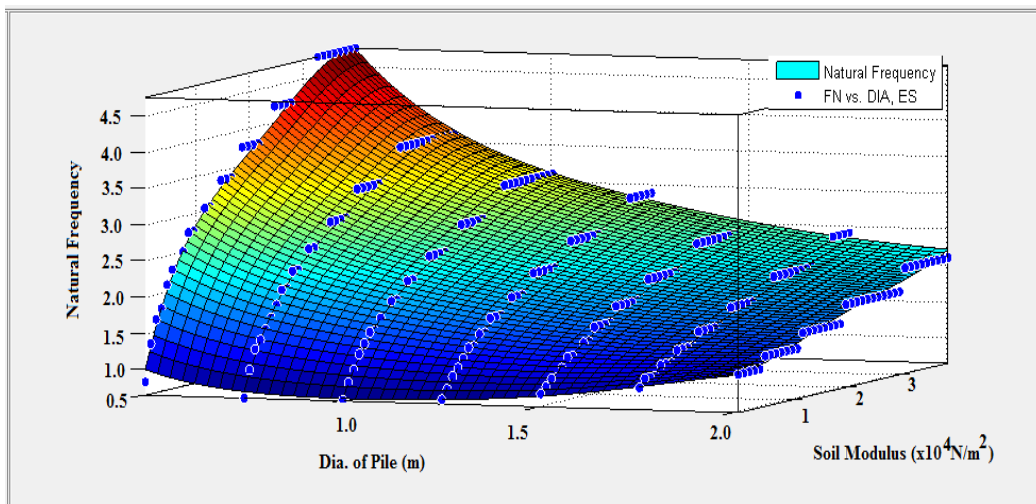


Fig. D.3 Variation in Natural Frequency with Soil Modulus and Diameter of Pile

If the predominant frequency of the dynamic loading happens to be same as the natural frequency of the soil-pile system, there is a possibility of changing the natural frequency of the system by adjusting the diameter of the pile as suggested by the equation no.D.9. A detailed study on soil-pile interaction analysis is necessary for the satisfactory design and performance

of pile foundations, especially for low rise structures and for structures embedded in soft soil.

D.2.2 The Influence of SSI on the Dynamic Response of Single Pile

The influence of bed slope variation in the depth of fixity of pile and the natural frequency of pile are studied in the previous section. In this section the influence of pile diameter, pile head projection, mass at pile top and soil modulus on the dynamic response of the pile are studied. Dynamic response of soil structure interaction is characterized by plotting frequency ratio and stiffness ratio curves as suggested by Wolf *et al.* [51].

D.2.2.1 Description of the present study

Numerical analysis of the present problem was performed using the finite element software PLAXIS-3D. Assuming elasto-plastic behaviour of soil, Mohr-Coulomb soil model was adopted to model the soil characteristics in which the soil has a linear elastic relationship until failure and plastic deformation beyond that. The pile was modeled as an embedded pile which includes the pile model with the interface element. A linear skin resistance was applied at the pile soil interface. In PLAXIS-3D, the pile was modeled as embedded pile which is a three node beam element with an interface and soil as a 10 node tetrahedron element. A medium meshing was adopted and it creates around 30000 soil elements. A mesh refinement of 'very fine' was also tried. Even though the execution time was more the results were almost same when compared with that of medium mesh refinement. Hence a medium mesh refinement is adopted for the present study. Standard fixities were adopted at the boundary which fixes the bottom in all directions and the vertical sides in horizontal directions.

Table D.1 Material properties of soil

Properties	Soil
Model	Mohr-Coulomb
Type	Drained
γ_{unsat}	17 kN/m ³
γ_{sat}	18 kN/m ³
E_s	1000 – 200000 kN/m ²

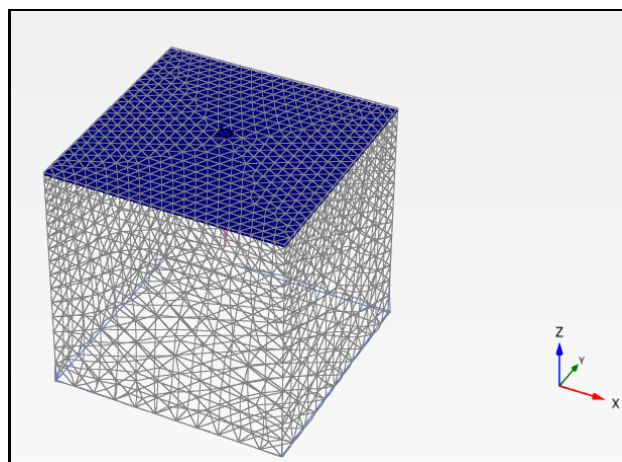
Table D.2 Material properties of pile

Properties	Pile
Model	Embedded Pile
Type	Massive circular pile
γ_c	25kN/m ³
E	30000000 kN/m ²

A soil volume of 50m X 50m X 100m was created with a pile having 50m embedment length and was dynamically analysed for a SHM. The natural frequency and dynamic response of the structure was found out by varying the following parameters. The shear wave velocity of the soil was varied by varying the young's modulus of soil to represent the very soft soil to rock. The analysis consisted of four phases, including the initial phase, excavation phase, construction phase and loading phase. The soil volume was introduced in the initial phase. The soil volume below the pile head upto the ground level was deactivated in the excavation phase. The pile and the pile cap were modeled and activated in the construction phase. The self-weight of the structural elements were considered in the analysis during the construction phase. The excitation force was applied in the loading phase.

Table D.3 Parameters Analyzed

Parameter	variation adopted for parametric study
Es	1000kN/m ² , 10000 kN/m ² , 50000 kN/m ² , 200000 kN/m ²
D	1 m, 1.3 m, 1.5 m
h	3 m, 6 m, 9 m
m	2 T, 4 T, 6 T, 12 T

**Fig.D.9 PLAXIS-3D Model for Dynamic analysis**

D.2.2.2 Structural behaviour of soil-pile system

The structural behaviour of soil pile system was studied by analyzing the results of the parametric study. Considering different parameters as mentioned in Table D.3, all together 144 analyses were conducted for the parametric study. Analyses were repeated for different sets of soil modulus, pile head projection, pile diameter and mass at pile top by changing only one parameter at a time and keeping all other parameters constant. The typical results are discussed herein corresponding to the variation of each parameter.

D.2.2.3 Influence of pile diameter

The pile diameters adopted for the study are 1 m, 1.3 m and 1.5 m. It can be observed from Fig.D.10 that an increase in pile diameter causes a decrease in

pile head displacement. Such behaviour is due to the increase in the stiffness of pile as the pile diameter increases.

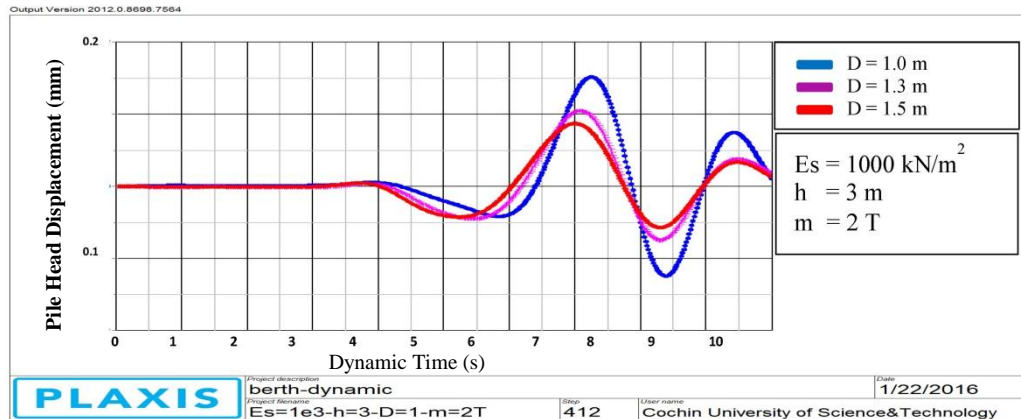


Fig. D.10 Variation of pile head displacement with variation in diameter of pile

D.2.2.4 Influence of pile head projection above the ground level

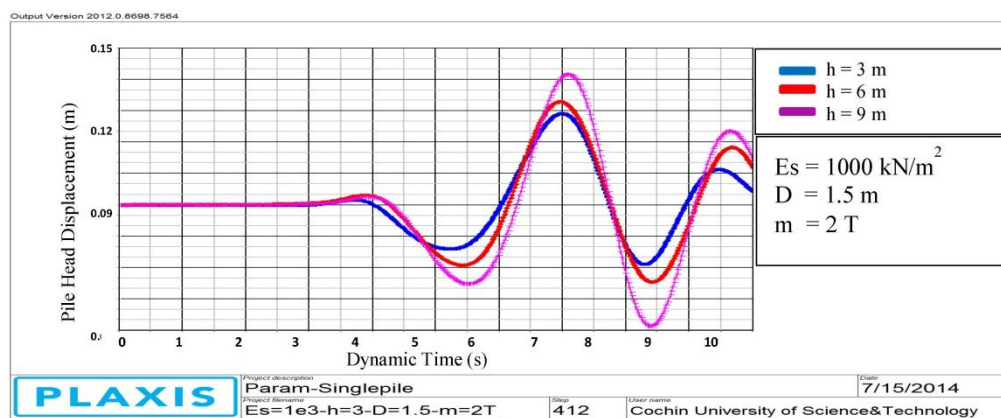


Fig. D.11 Variation of pile head displacement with variation in pile head projection

Pile head projection above the ground level was varied from 3 m, 6 m and 9 m. It can be observed in Fig. D.11 that as the pile head projection increases the pile head displacement also increases. It can be concluded that an increase in the unsupported length causes an increase in the pile head displacement.

D.2.2.5 Influence of mass at the pile top on the structural response

The mass at the pile head was varied from 2T, 4T, 6T and 12 T. It can be observed from Fig. D.12 that increase in the mass at the pile head causes a decrease in the pile head displacement. This behaviour is due to the increase in the inertia of the system due to the increase in the mass at the pile top.

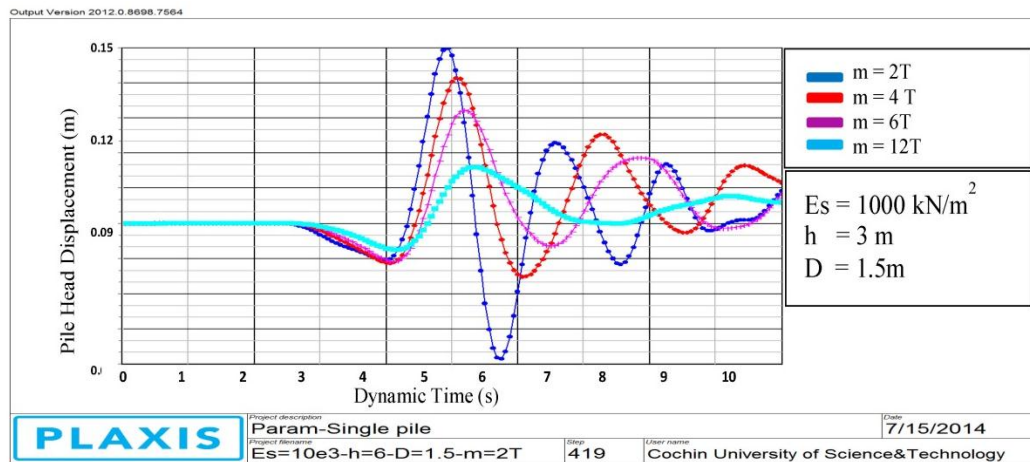


Fig. D.12 Variation of pile head displacement with variation in mass at the pile top

D.2.2.6 Influence of soil modulus on the structural response

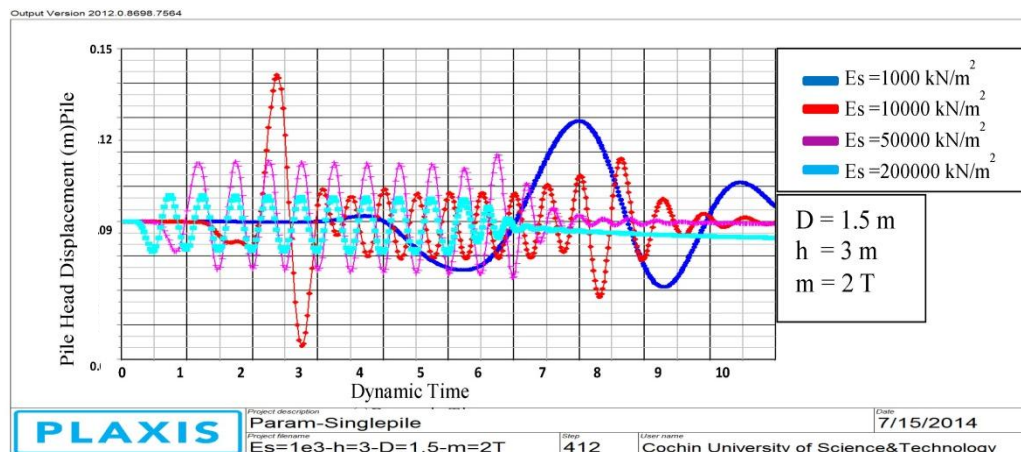


Fig. D.13 Variation of pile head displacement with variation in soil modulus

Soil modulus was varied from very soft consistency (1000 kN/m^2) to rock (200000 kN/m^2). It can be observed from Fig. D.13 that soil-pile system with higher values of soil modulus (rock) is found to produce less deflection to the

pile head compared to a soil with lower values of soil modulus (soft soil). It is also observed from Fig. D.13 that in soft soil, excitation reaches the pile top slowly compared to rock. It is due to the fact that shear wave velocity is proportional to the soil modulus [10]. Hence in a soft soil profile the exciting force travel slowly and hence pile head displacement initiates only at later time compared to a rock profile.

D.2.2.7 Analysis of Interaction among Parameters

The parameters investigated in the present study are pile diameter (D), pile head projection above the ground level (h), mass at the pile top (m) and the soil modulus (E_s). The natural frequency of the SDOF system ($\hat{\omega}$) and the fixed base natural frequency of the pile (ω_s) are obtained from the parametric study. Shear wave velocity of soil (V_s) is calculated from soil modulus. To analyse the interaction among the parameters, the dimensionless quantities such as frequency ratio ($\hat{\omega}/\omega_s$), stiffness ratio (ratio of stiffness of the structure to that of the soil, $\omega_s h/V_s$), slenderness ratio (h/D) and mass ratio ($m/\gamma_{\text{sat}} D^3$) are calculated and the curves are plotted as suggested by Wolf [51].

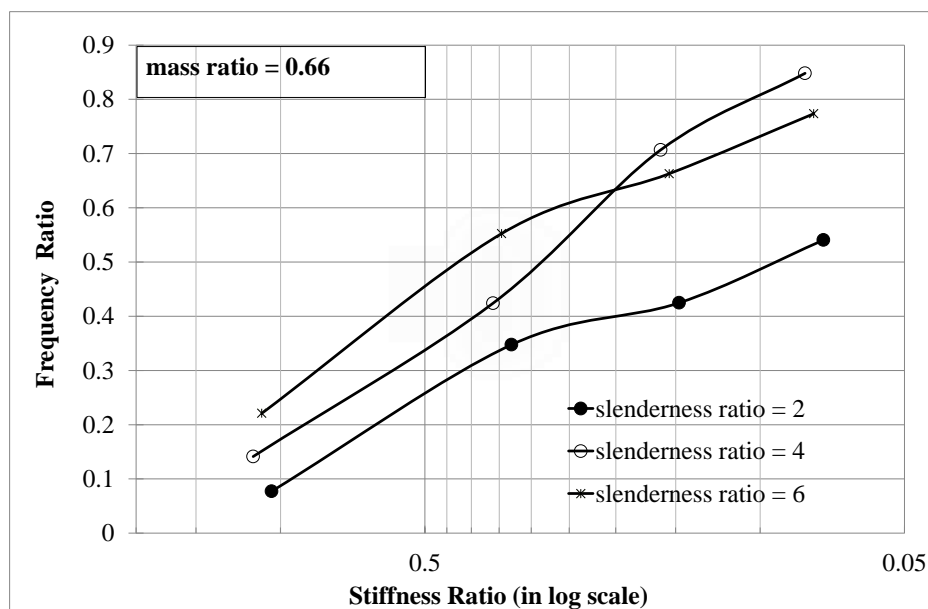


Fig. D.14 Frequency ratio Vs stiffness ratio curve for different slenderness ratio

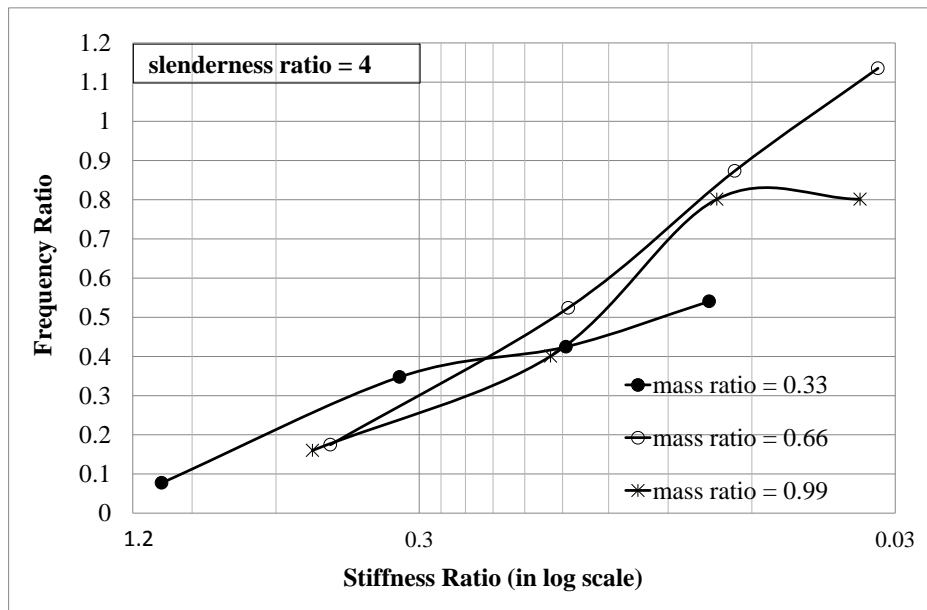


Fig. D.15 Frequency ratio Vs stiffness ratio curve for different mass ratio

Frequency ratio can be considered as an indicator of the soil pile interaction since it is the ratio of the natural frequency of the soil pile system to that of pile alone which is fixed at the base. Hence the behaviour of the soil pile interaction with different soil properties, represented by stiffness ratio can be studied by examining the Fig. 5.35 and Fig. 5.36 for different slenderness ratio and mass ratio respectively.

It can be observed from the figures that as the slenderness ratio increases the frequency ratio decreases in general. The stiffness ratio which is inversely proportional to the shear wave velocity of the soil increases as the soil modulus decreases. A similar trend can be observed for any slenderness ratio and mass ratio of the system studied. Hence it is concluded that as the soil becomes softer the natural frequency of the system comes down and there is a possibility of resonance with the excitation force.

A SDOF system embedded in soil subjected to harmonic loading applied at a depth within the soil mass has been investigated. The analysis was conducted

by varying the diameter of the pile, pile head projection, mass at pile head and the soil modulus. The study leads to the following conclusions,

- Displacement of the pile head can be decreased by increasing the pile diameter, decreasing the pile head projection or by increasing the mass at the pile head.
- The stiffer soil can again decrease the displacement at the pile head.
- As expected the excitation travels faster in a stiffer soil and in a softer soil it reaches the pile head only at a later time.
- Dynamic response of soil structure interaction can be effectively characterized by frequency ratio and stiffness ratio. Special care on the above parameters should be given when a stiff structure is founded on a soft flexible soil.

Appendix E

Review on Soil Constitutive Models

E.1 Soil Constitutive Models

The complexity in the behavior of soils has led to the development of many models of soil based on the classical theories of elasticity, plasticity and visco-elasticity for the analysis of Soil-Structure interaction problems. The elastic property of the soil is represented using a spring, the plastic property of the soil is represented using a slider and the viscous property of the soil is represented using a dashpot.

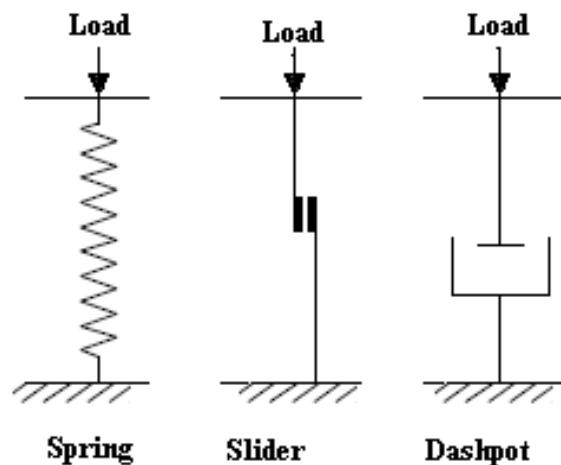


Fig. E.1 Basic components of soil models[64]

E.2 Elastic Models

In this type of model, soil behaviour which exhibit purely elastic characteristic is considered. The simplest type of idealized soil response is to assume the behaviour of supporting soil medium as a linear elastic continuum. Here the deformations are assumed as linear and reversible. Extensive research has been done to obtain exact and approximate solutions of these models so that

they can be used in soil-structure interaction problems. The basic elastic models are Winkler model and Continuum model.

E.2.1 Winkler Model

In Winkler model soil is assumed as a system of identical but mutually independent, closely spaced, discrete, linearly elastic springs. The characteristic features of this representation of soil medium are the discontinuous behaviour of the surface displacement. According to this idealization, deformation of the soil medium due to the applied load is confined to the loaded region only. The surface displacement of the soil medium at every point is directly proportional to the stress applied to it at that point and completely independent of the stresses or displacements at other or even immediately neighbouring point of the soil-structure interface. Fig.5.2 shows the physical representation of Winkler model of soil-structure interface.[2]

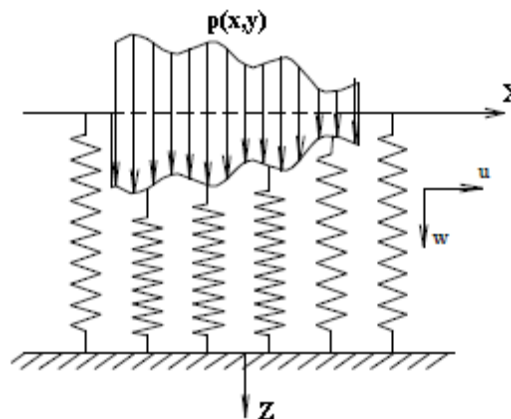


Fig. E.2 Winkler Model [146]

The response function for the Winkler model is,

$$p(x,y) = k w(x,y) \dots \dots \dots (E.1)$$

where, $p(x,y)$ is the applied stress at a point, $w(x,y)$ is the deflection at that point and k is the sub grade modulus with units of stress per unit length.

In this model displacement occurs immediately under the loaded area and outside the region the displacements are zero. Applicability of Winkler model is limited to such soil media which possesses cohesion or transmissibility of applied forces.

E.2.2 Elastic Continuum Model

In elastic continuum model the continuous behaviour of soil is idealized as three dimensional continuous elastic solid. In this case the soil surface deflections due to loading will occur under and around the loaded region.

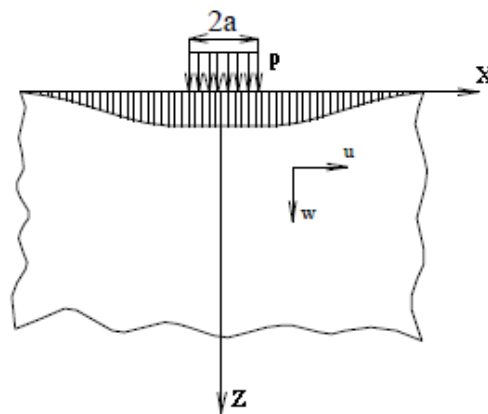


Fig. E.3 Elastic Continuum Model [146]

The above figure shows the typical surface displacement profile of a soil medium subjected to a uniform load 'p' of radius 'a'. The distribution of displacements and stresses in such media remain continuous under the action of external force system. In this case some continuous function is assumed to represent the behaviour of soil medium.

In continuum idealization, soil is assumed to be semi infinite and isotropic for the sake of simplicity. However, the effect of soil layering and anisotropy may be conveniently accounted for in the analysis.

This approach provides much more information on the stresses and deformations within soil mass than Winkler model. However this idealization has a major drawback of inaccuracy in reactions calculated at the peripheries of

the foundation. It has also been found that, for soil in reality, the surface displacements away from the loaded region decreased more rapidly than what is predicted by this approach.

E.3 Elastic-plastic Models

In soil-structure interaction analysis, nonlinear behaviour of soil mass is often modelled in the form of an elasto-plastic element. Here deformations occur linearly and proportional to the applied stress up to a certain stress level. This behaviour may be represented by an ideal reversible spring.

E.3.1 Mohr-Coulomb Model

It is an elastic-perfectly plastic model. The set of parameters adopted to represent the model are: young's modulus, poisson's ratio, friction angle, cohesion and the dilatancy angle[3]. For each sublayer a linear variation of the young's modulus has been assumed. As the model does not allow changing the soil stiffness within the strain level, a reduced static stiffness has been adopted during the preliminary construction stage.

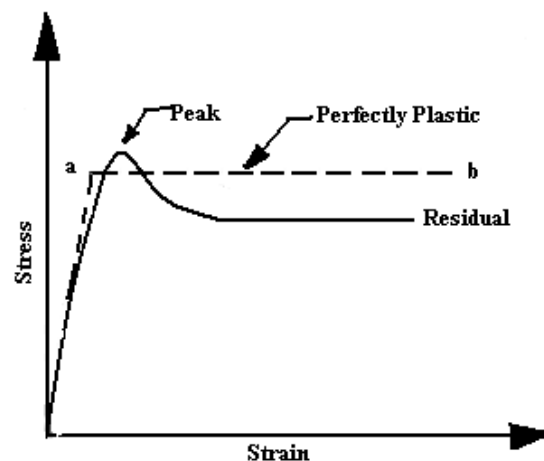


Fig. E.4 Elastic-Perfectly Plastic Assumption of Mohr-Coulomb Model [147]

Mohr-Coulomb model is a simple model applicable to three dimensional stresses with only two strength parameters to describe the plastic behaviour. Researchers have indicated by means of triaxial test that stress combinations

causing failure in real soil samples agree quite well with the hexagonal shape of failure contour. This model is applicable to analyse the stability of dams, slopes, embankments and shallow foundations.

E.3.2 St.Venant's Model

St.Venant's model is formed when an elastic element is connected in series with a plastic element. Use of such a single element generally shows an abrupt transition from elastic to plastic state. The use of large number of St.Venant's units in parallel represents the Elasto-Plastic behaviour of soil more accurately.

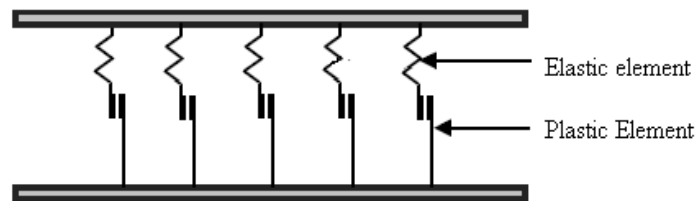


Fig.E.5 St.Venant's Elasto-Plastic Unit [147]

Use of a number of springs helps to facilitate the simulation of the gradual transition of soil strain from elastic to plastic zone. The following expression may be used in terms of strain modulai for elastic and plastic strains respectively.

$$\epsilon_{ep} = M_e \sigma + M_p \log[\sigma / (\sigma_u - \sigma)] \dots\dots\dots (E.2)$$

Where M_e is the elastic strain modulus of soil, M_p is the plastic strain modulus of soil and σ_u is the ultimate load that can sustain. Conceptually, the above mechanical model may appear to be useful enough. But the problem occurs in the proper adjustment of such springs at the base of the structure.

E.3 Viscoelastic Models

The real deformation characteristics of fine grained soil media under the application of any load are always time dependant to some extend depending on the permeability of soil media. Loading applied to a saturated layer of clay, at the

first instance, causes an increase in pressure in the pore water of soil. With time the pore water pressure will dissipate resulting in progressive increase of effective stress in soil skeleton. This leads to time dependent settlement of foundation. Here are numerous instances of rheological processes in the foundation leading to large and non-uniform settlement.

The mechanical models represent the rheological properties of the soil skeleton by a combination of elastic, viscous and plastic elements. These models are generally formed by a combination of springs and dashpots in series. Displacement of retaining walls and the instability of slopes are two classical examples apart from the time dependent settlement of framed structures. Various models are available to describe the rheological properties of clayey soils.

E.3.1 Generalized Maxwell's Model

It is the most general form of the linear model for viscoelasticity. In this model a spring and a dashpot are connected in series and subjected to loading. For better results a number of such arrangements in parallel may be used.

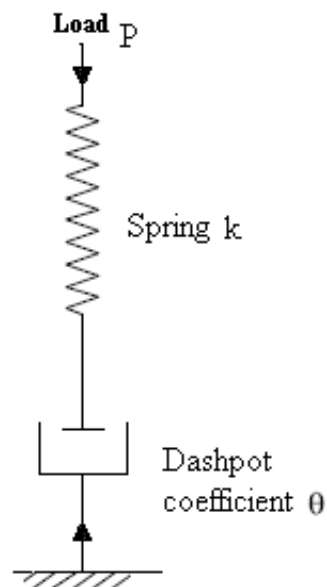


Fig. E.6 Generalized Maxwell Model [147]

E.3.2 Kelvin's Model

It is a viscoelastic model having the properties of elasticity and viscosity. It is named after the British physicist and engineer William Thomson, 1st Baron Kelvin. It can be represented by a purely viscous damper and purely elastic spring connected in parallel as shown in Fig. E.7 [4].

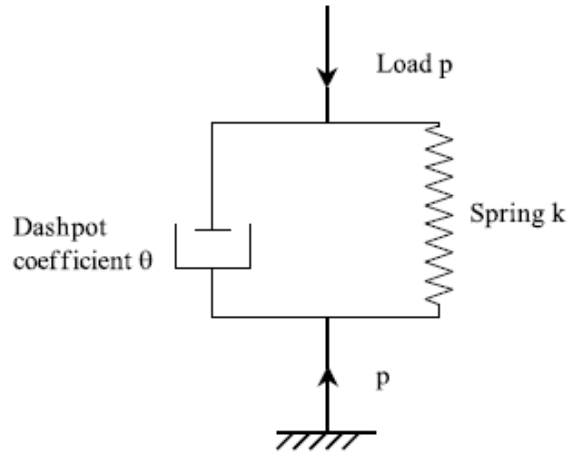


Fig. E.7 Kelvin Model [133]

Since the two components of the model are arranged in parallel, the strains in each component are identical:

$$\varepsilon_{total} = \varepsilon_D = \varepsilon_S \dots\dots\dots(E.3)$$

Where ε_D is the strain the dashpot and ε_S is aht strain the spring. Similarly, the total stress will be the sum of the stress in each component.

$$\sigma_{Total} = \sigma_D + \sigma_S \dots\dots\dots(E.4)$$

From these equations we get that in a Kelvin model, stress σ , strain ε and their rates of change with respect to time t are governed by equations of the form:

$$\sigma(t) = E \varepsilon(t) + \eta [d\varepsilon(t)/dt] \dots\dots\dots(E.5)$$

where, E is a modulus of elasticity and η is the viscosity. The equation can be applied either to the shear stress or normal stress of a material.

E.4 Interface Elements

Interface elements are numerical entities used in finite element technique for modeling geometric discontinuities that are present in some boundaries of structures. An interface element should be able to account for the relative motion along the interface and thus to accurately simulate the deformations and physical behavior of geomaterials. In finite element analysis of civil engineering structures a large variety of applications for interface elements is present. Interface elements can be used to model soil-structure interaction effect in a pile foundation surrounded by soil media.

In numerical practice two types of interface elements are used. The first class of elements contains the continuous interface elements (line, plane and shell interfaces). It is a reduction from a classical volume finite element (thin layer interface element) and the second class of elements contains the nodal or point interface elements, which to a certain extent are identical to spring elements. It is also called a surface element which is a zero thickness joint element.

E.4.1 Zero-thickness Interface Element

It was developed by Goodman et al. in 1968. In this element the nodes at the contact surface are separated and some normal and tangential springs are used to connect them. Later, however, rheological elements were used in the form of springs and dashpots operating between the nodes of the interface elements.

These rectangular elements possess four nodes and eight degrees of freedom as shown in fig.5.8.

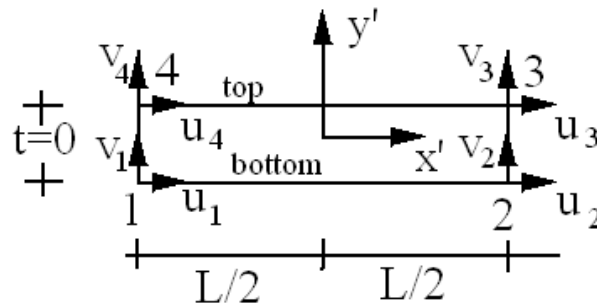


Fig. E.8 Goodman's Interface Element [91]

E.4.2 Thin Interface Element

It was suggested by Desai and Nagaraj. In this element it is assumed that only a thin element of the weaker material at the contact undergoes a highly localized shear strain along the contact surface. The formulation of this element fits well in the context of finite element method and can easily be used to include the nonlinearity and/or plasticity of the behavior of material and yield more realistic results.

E.4.3 Line interface Element

This special isoparametric element has been developed (Beena 1994) with a view to represent the friction between soil and reinforcement. The geometry of the present element is such that it is a line with four nodes. The element has four nodes and zero thickness as assumed by Goodman *et. al.*, a linear variation of displacement along the length of the element is assumed. Relative displacement between the top and bottom nodes is taken as the corresponding strain in the element[5].

E.5 Discussions on Soil Models

The review of the different categories of the soil models as applied in the soil-structure interaction analysis leads to the following inferences.

- 1) The effect of soil-structure interaction is to be considered for the accurate estimate of the design force quantities. To obtain the same

realistic and simplified modelling of the soil-structure system is absolutely necessary.

- 2) Winkler hypothesis yields reasonable performance and it is very easy to exercise. So for practical purpose this idealization may be used.
- 3) The clayey soil having low permeability possesses time dependent behaviour under sustained loading, in such time dependent process of soil-structure interaction, critical condition may occur at any time during the process in some situation. Under such circumstances, modelling soil as viscoelastic medium can only provide the crucial input for the design.
- 4) For a particular problem which uses Kochi marine clay as the soil medium one of the suggestion for modelling is to use the Winkler model to start with and any one of the viscoelastic model or elastoplastic model to do the detailed soil-structure analysis.

Appendix F

Validation of the Plaxis-3D Numerical Model

F.1 Numerical Validation of PLAXIS-3D Model using Pile Load Test on Axially Loaded Pile

F.1.1 Details of Pile Load Test

An onsite pile load test at El-Mossallamy, Germany [150] has been analyzed for the validation of numerical model created in PLAXIS-3D. The load test investigated the load-settlement behaviour of a single pile. Figure F.1 gives the layout of the pile load test arrangement. The upper 4.5 m subsoil consist of silt (loam) followed by tertiary sediments down to great depths. These tertiary sediments are stiff plastic clay similar to the so-called Frankfurt clay, with a varying degree of over-consolidation. The groundwater table is about 3.5 m below the ground surface. The considered pile has a diameter of 1.3 m and a length of 9.5 m. It is located completely in the over-consolidated clay.

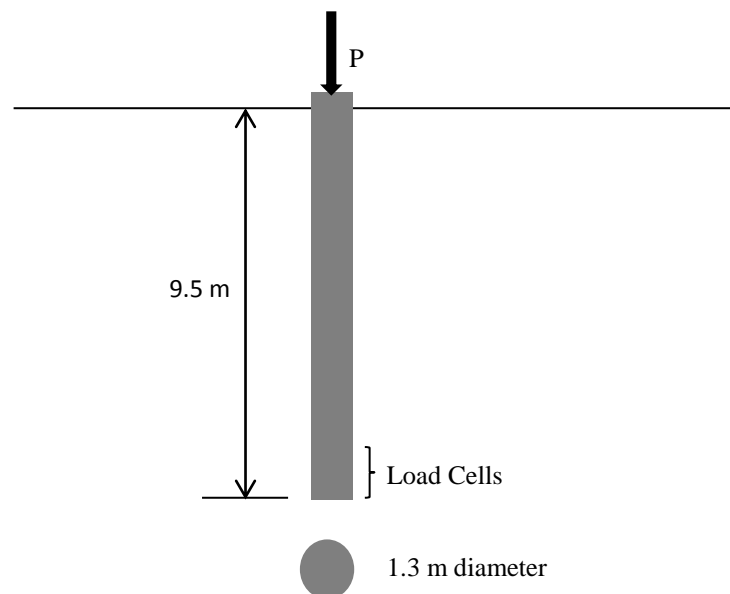


Fig. F.1 Layout of the Pile Load Test

The loading system consists of two hydraulic jacks working against a reaction beam. The loads were applied in increments and maintained constant until

the settlement rate was negligible. Both the applied loads and the corresponding displacements at the tested pile head were measured.

F.1.2 Modeling the Soil- Pile System

A soil volume of 50 m X50 m X16 m was considered for modeling the site. The required soil parameters were determined based on literature (see Table F.1). The concrete pile was modelled as a non-porous linear elastic material with Young's modulus $E = 3 \times 10^7$ kN/m², Poisson ratio $\nu = 0.2$ and unit weight $\gamma = 24$ kN/m³.

Table F.1 Model Parameters for Different Soil Data Sets

Sl.No.	Parameter	Nomenclature	OC Clay	Unit
1	Material Model	Model	HS	-
2	Type of Material Behaviour	Drained	Drained	-
3	Unsaturated soil weight	γ_{unsat}	20	kN/m ³
4	Saturated soil weight	γ_{sat}	20	kN/m ³
5	Secant Stiffness	E_{50}^{ref}	4.5×10^4	kN/m ²
6	Oedometer stiffness	$E_{\text{oed}}^{\text{ref}}$	2.715×10^4	kN/m ²
7	Unloading reloading stiffness	$E_{\text{ur}}^{\text{ref}}$	9×10^4	kN/m ²
8	Power	m	1	-
9	Unloading reloading poisson ratio	ν_{ur}	0.2	-
10	Cohesion	c'	20	kN/m ²
11	Friction angle	ϕ'	20	°
12	Dilatancy angle	ψ	0	°
13	Lateral earth pressure coefficient for normal consolidation	K_0^{nc}	0.658	-
14	Lateral earth pressure coefficient	K_0	0.8	-
15	Over-consolidation ratio	OCR	1	-
16	Pre-overburden pressure	POP	50	kN/m ²
17	Interface reduction factor	R_{inter}	1.0	-

Pile was modeled using the three node embedded pile in PLAXIS-3D. An embedded pile is a three noded beam element with six degrees of freedom per node that can be placed inside soil volume in any required direction. The element allows deflections due to shearing and bending. The element can also change its length due to axial force. The embedded pile is visualized as line element but the actual volume of the pile is considered for analysis which is inputted to the pile material data set.

Table F.2. Material Properties of Embedded Pile

Sl.No.	Parameter	Nomenclature	Magnitude	Unit
1	Young's modulus	E	3×10^7	kN/m ²
2	Weight	γ	5	kN/m ³
3	Properties type	<i>Type</i>	Massive circular pile	-
4	Diameter	ϕ	1.3	m
5	Cross sectional area	A	1.327	m ²
6	Moment of inertia against bending around the third axis	I_3	0.140	m ⁴
7	Moment of inertia against bending around the second axis	I_2	0.140	m ⁴
8	Moment of inertia against oblique bending	I_{23}	0	m ⁴
9	Skin friction distribution	<i>Type</i>	Linear	-
10	Maximum traction allowed at the top of the embedded pile	$T_{topmax.}$	19.18	kN/m
11	Maximum traction allowed at the bottom of the embedded pile	$T_{bottommax.}$	383.56	kN/m
12	Base resistance	F_{max}	1320	kN

F.1.3 Staged Construction

The analysis was done in three phases such as initial phase, construction phase and loading phase. The soil volume alone will be active in initial phase. Initial phase follows the calculation type, K0 procedure. All the other phases are with calculation type plastic. Construction phase activates the pile element and loading phase activates each of the loads applied. In the present problem the load deflection curve of the pile load test was available. From that curve the maximum load was noted as 3250 kN. The load was applied at the top of the pile and the analysis was done.

F.1.4 Comparison of Results

PLAXIS-3D curve manager is used to plot the load settlement curve of the present analysis and is shown in Fig.F.2. The load settlement curve available

from the literature [150] and the curve obtained from the present study are plotted together using plot digitizer as shown in Fig. F.2. It was observed that both the experimental and numerical results are in good agreement. Hence it can be concluded that the software is capable of incorporating the non-linear soil structure interaction effect.

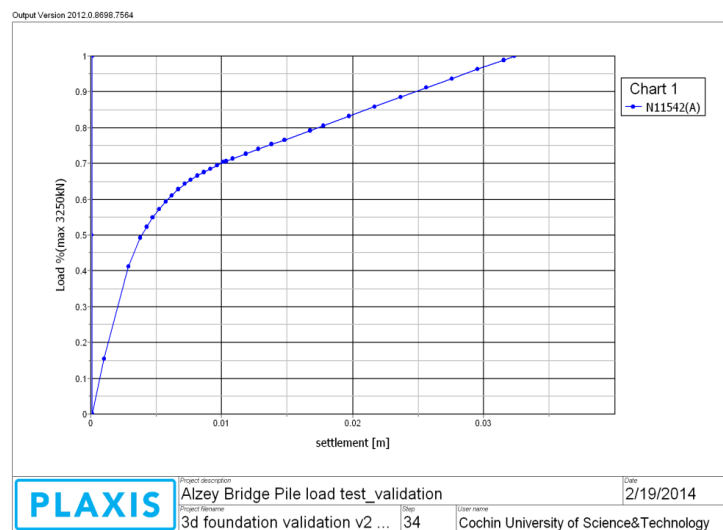


Fig. F.2 Plaxis 3D Curve Manager Output

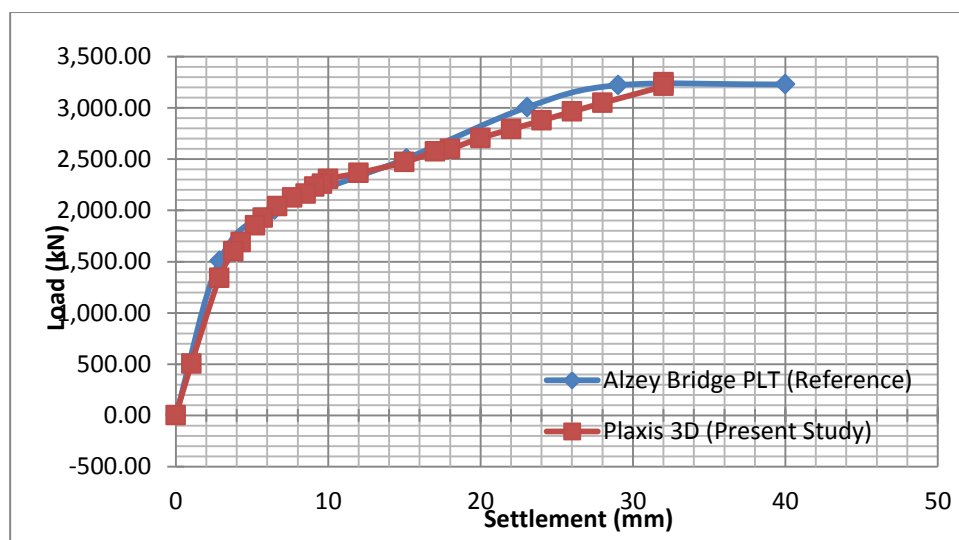


Fig. F.3 Comparison of the Alzey Bridge PLT results in Plaxis 3D models with measured results.

F.2 Numerical Validation of PLAXIS-3D Model using Pile Load Test on Laterally Loaded Pile

A pile load test conducted by Ismael *et al.* [50] has been modeled and studied. The pile was 0.3 m in diameter and had a length of 5 m situated in Kuwait. The surface soil was found to a depth of 3.5 m and was characterized as having both component of shear strength, c and ϕ . The soil profile consisted of a medium dense cemented silty sand layer to a depth 3 m. This was underlain by medium dense to very dense silty sand with cemented lumps to the bottom of the borehole. All properties of soil are listed in Table F.3. Ground water was not encountered within the depth of the borehole. In conclusion, the comparison between the PLAXIS 3D simulation and the reported lateral data is shown in Fig.F.4 and Fig.F.5. The piles were deflecting not in the same magnitude at the field test due to the variability of soil properties. Also the numerical simulation is reasonably accurate for the problem of laterally loaded piles and pile-soil interaction over a wide range of deformation for 5 m piles.

Table F.3 Geotechnical Properties of the Soil Layers and the Pile

Parameter	Nomenclature	medium dense cemented silty sand layer	Medium dense to very dense silty sand with cemented lumps	Pile	Unit
Unsaturated soil weight	γ_{unsat}	18	19	25	kN/m ³
Saturated soil weight	γ_{sat}	18	19	-	kN/m ³
Young's modulus	E	1.30E+04	1.30E+04	2E+09	kPa
Poisson's constant	ν	0.3	0.3	0.15	-
Cohesion	c	20	1	-	kPa
Friction angle	ϕ	35	45	-	-

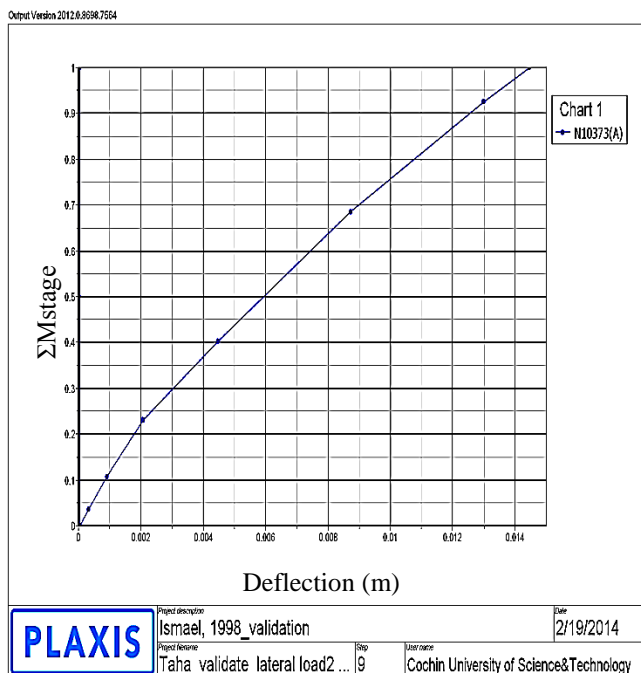


Fig. F.4 PLAXIS 3D Output

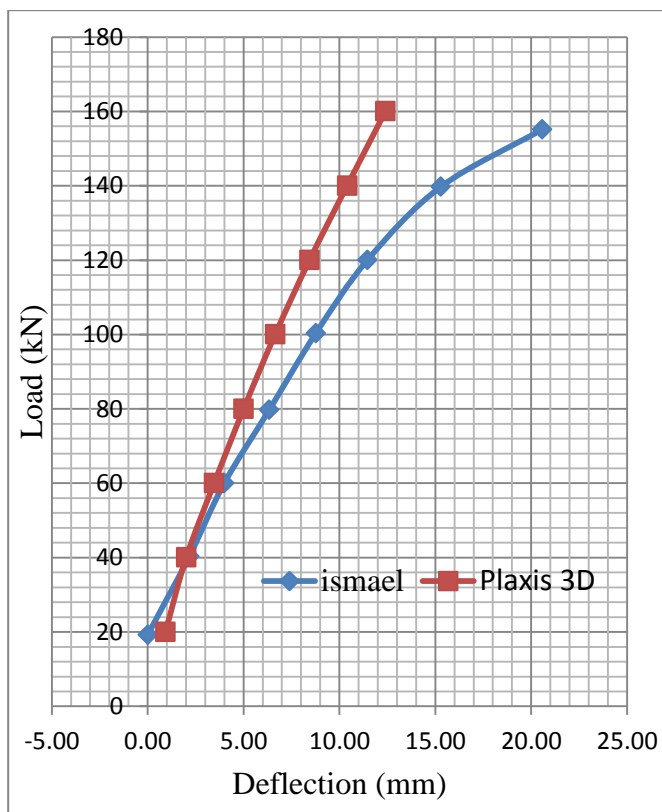


Fig. F.5 Comparison of PLAXIS 3D with Field Test

Plaxis 3D curve manager is used to plot the load deflection curve of the present analysis and is shown in Fig.F.4. The load deflection curve available from the literature [50] and the curve obtained from the present study are plotted together using plot digitizer as shown in Fig.F.5. It was observed that both the experimental and numerical results are comparable, especially in the working range of loads. Hence it can be concluded that the software is capable of incorporating the non-linear soil structure interaction effect.

Appendix G

Parametric Study of a Single Pile Using PLAXIS 3D

G.1 List of Experiments

Table G.1 Details of Numerical Test on Single Model Pile

Sl.No.	Length of Model Pile (mm)	Diameter of Model Pile (mm)	Slope of Soil Bed
1	600	19	No slope
2	600	19	1:5
3	600	19	1:4
4	600	19	1:3
5	600	19	1:2.4
6	600	19	1:2
7	600	19	1:1.7
8	600	19	1:1.5
9	600	19	1:1
10	600	25.4	No slope
11	600	25.4	1:5
12	600	25.4	1:4
13	600	25.4	1:3
14	600	25.4	1:2.4
15	600	25.4	1:2
16	600	25.4	1:1.7
17	600	25.4	1:1.5
18	600	25.4	1:1
19	600	30	No slope
20	600	30	1:5
21	600	30	1:4
22	600	30	1:3

23	600	30	1:2.4
24	600	30	1:2
25	600	30	1:1.7
26	600	30	1:1.5
27	600	30	1:1
28	700	19	No slope
29	700	19	1:5
30	700	19	1:4
31	700	19	1:3
32	700	19	1:2.4
33	700	19	1:2
34	700	19	1:1.7
35	700	19	1:1.5
36	700	19	1:1
37	700	25.4	No slope
38	700	25.4	1:5
39	700	25.4	1:4
40	700	25.4	1:3
41	700	25.4	1:2.4
42	700	25.4	1:2
43	700	25.4	1:1.7
44	700	25.4	1:1.5
45	700	25.4	1:1
46	700	30	No slope
47	700	30	1:5
48	700	30	1:4
49	700	30	1:3
50	700	30	1:2.4
51	700	30	1:2
52	700	30	1:1.7

53	700	30	1:1.5
54	700	30	1:1
55	800	19	No slope
56	800	19	1:5
57	800	19	1:4
58	800	19	1:3
59	800	19	1:2.4
60	800	19	1:2
61	800	19	1:1.7
62	800	19	1:1.5
63	800	19	1:1
64	800	25.4	No slope
65	800	25.4	1:5
66	800	25.4	1:4
67	800	25.4	1:3
68	800	25.4	1:2.4
69	800	25.4	1:2
70	800	25.4	1:1.7
71	800	25.4	1:1.5
72	800	25.4	1:1
73	800	30	No slope
74	800	30	1:5
75	800	30	1:4
76	800	30	1:3
77	800	30	1:2.4
78	800	30	1:2
79	800	30	1:1.7
80	800	30	1:1.5
81	800	30	1:1

G.2 Modeling of a Single Pile

G.2.1 Work Plane

A work plane was created with the same dimension as that of the plan of model tank used for the experimental investigation. The units adopted were millimeter (mm) for length and Newton (N) for force.

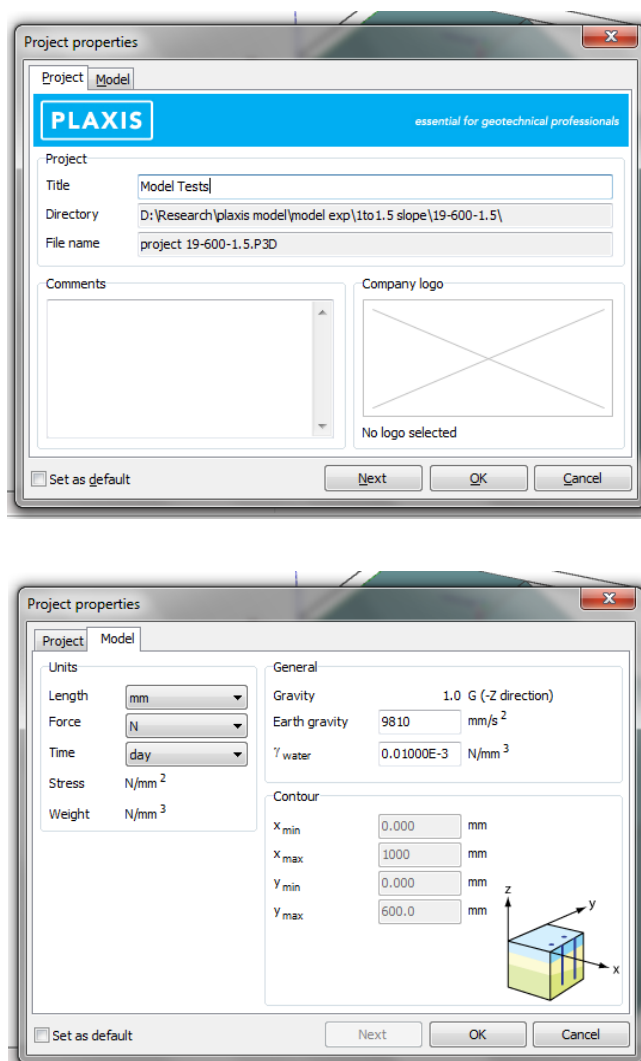


Fig. G.1 Work Plane Creation

Since 1G test method was adopted for the experimental investigation, gravity is considered to be 1G with earth's gravity 9810 mm/s². Density of water is considered to be 1e-5 N/mm³.

G.2.2 Bore Hole

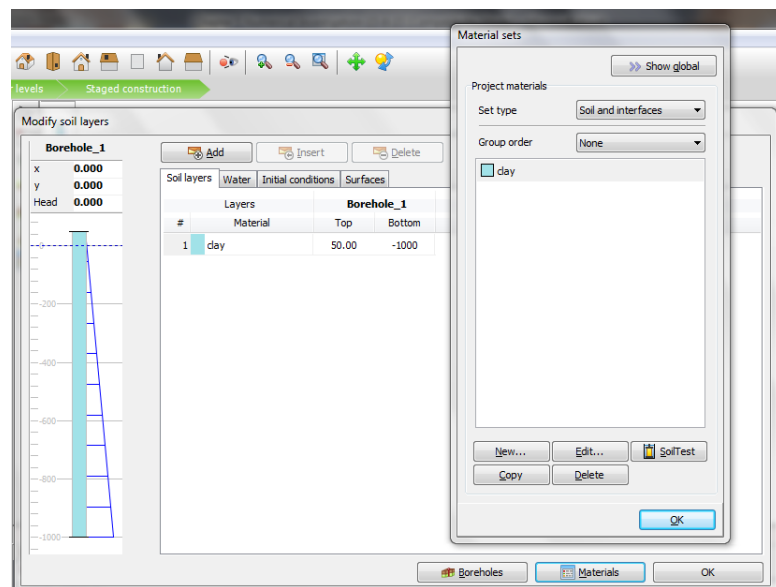
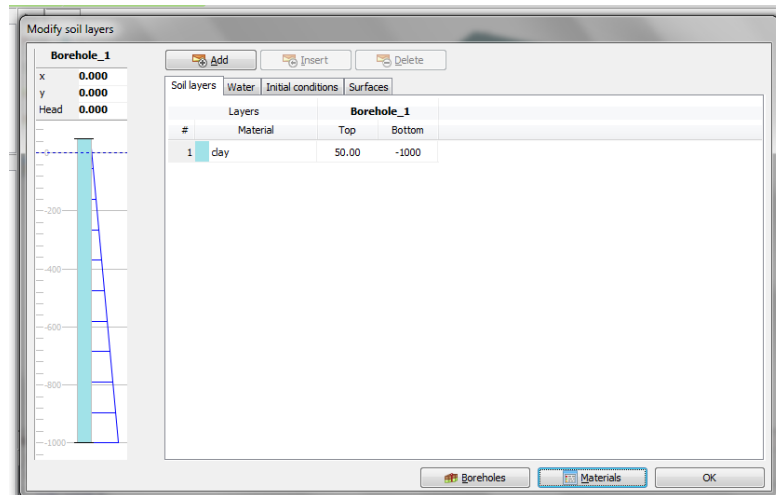


Fig. G.2 Borehole Details

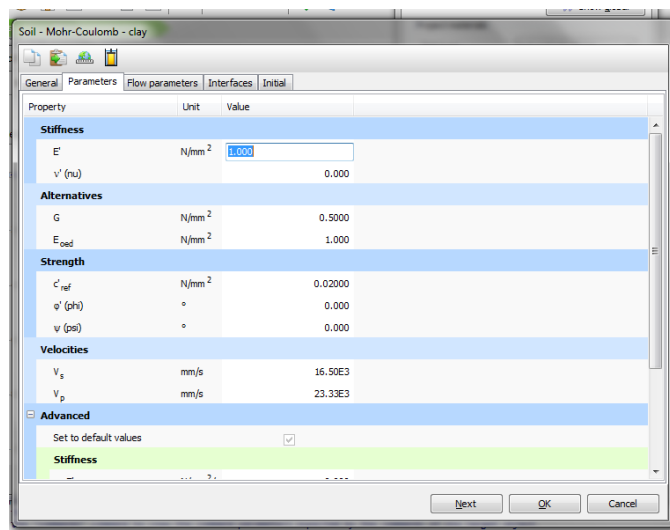
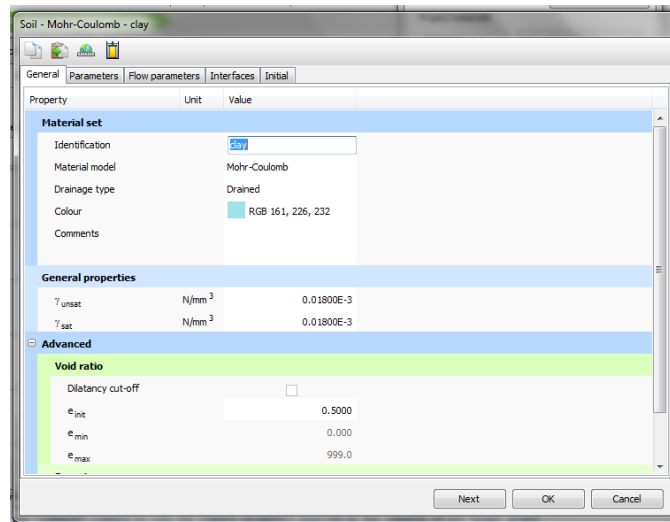


Fig. G.3 Soil Properties

G.5.2.3 Sloping Clay Bed

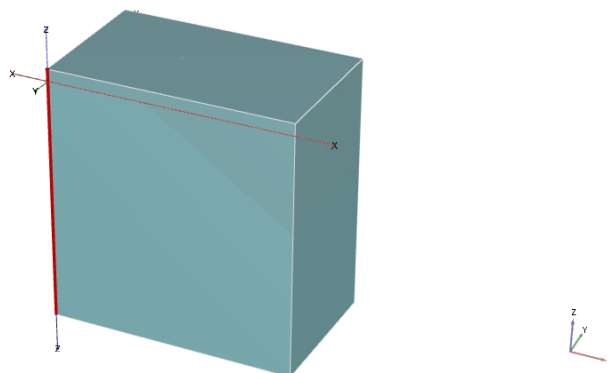


Fig. G.4 Initial Soil Volume

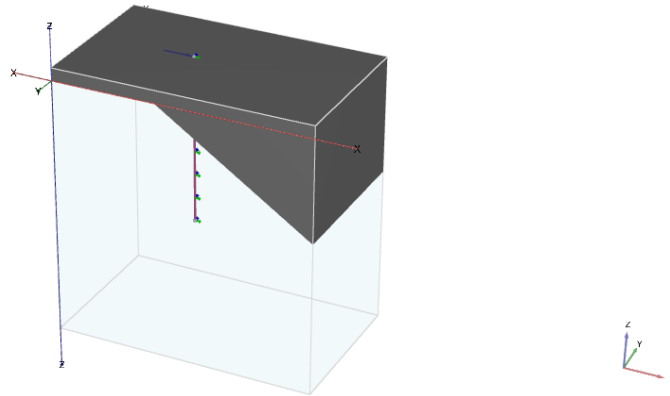


Fig. G.5 Soil Volumes to be Deactivated

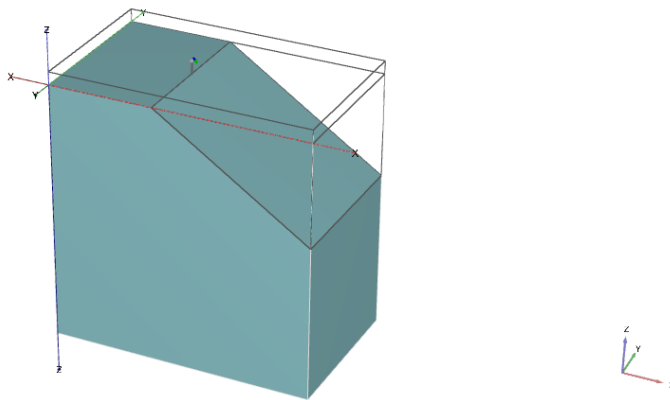


Fig. G.6 Soil Volume after incorporating the Bed Slope

A sloping soil bed is to be created to study the effect of slope on the structural behaviour of laterally loaded piles. A level ground with the known soil properties was to be created first. Then two soil volumes are to be created and deactivated to model the effect of extrusion of pile above the soil volume as well as the slope of the soil bed. The deactivations of the two additional soil volumes were done during staged construction.

G.2.4 Embedded Pile

Pile is modeled using the three node embedded pile in PLAXIS-3D [103]. An embedded pile is a three noded beam element with six degrees of freedom per node that can be placed inside soil volume in any required direction.

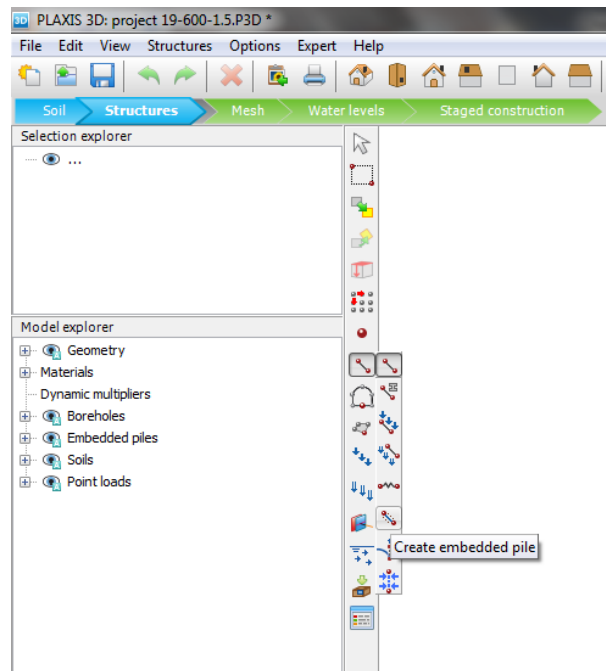


Fig. G.7 Embedded Pile Option in PLAXIS-3D

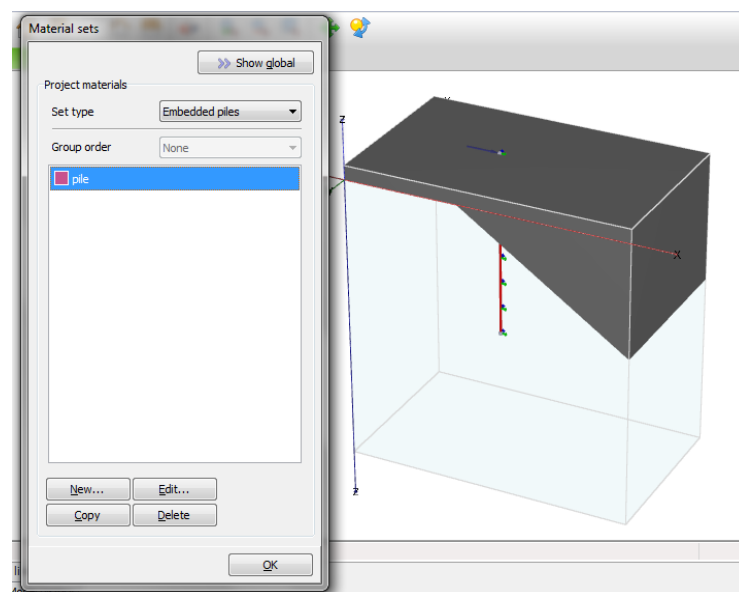


Fig. G.8 Embedded Pile in PLAXIS-3D Model

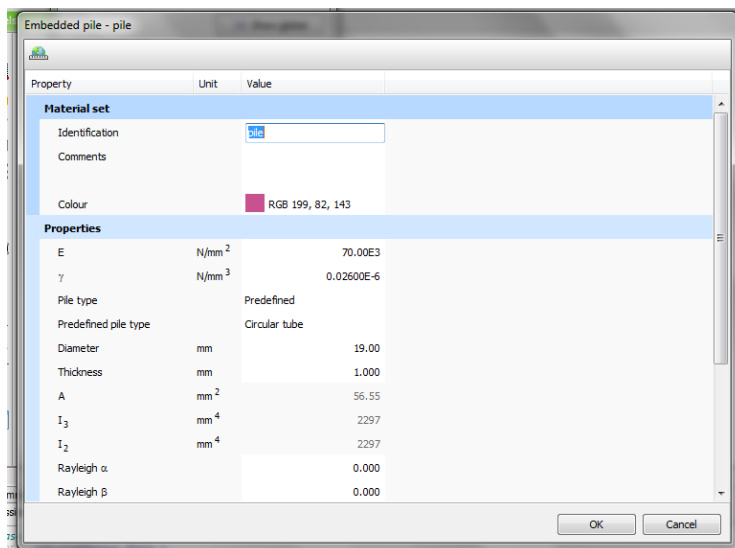


Fig. G.9 Assigning the Material Properties to Embedded Pile

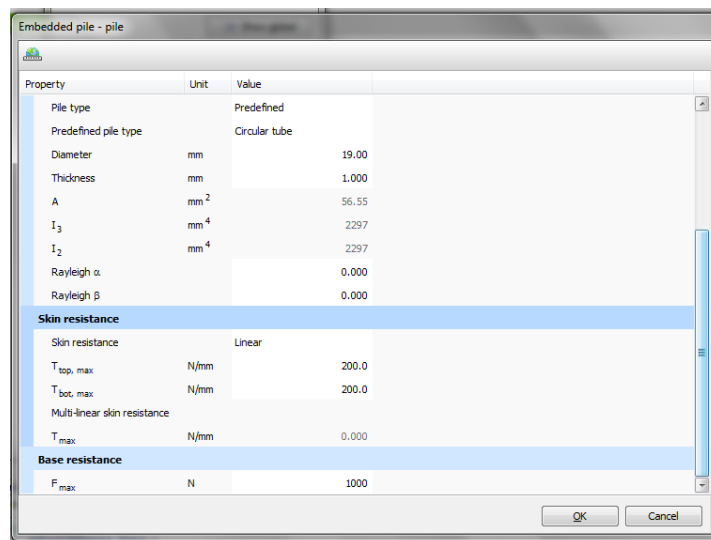


Fig. G.10 Assigning the Sectional Properties to Embedded Pile

G.2.5 Mesh Generation

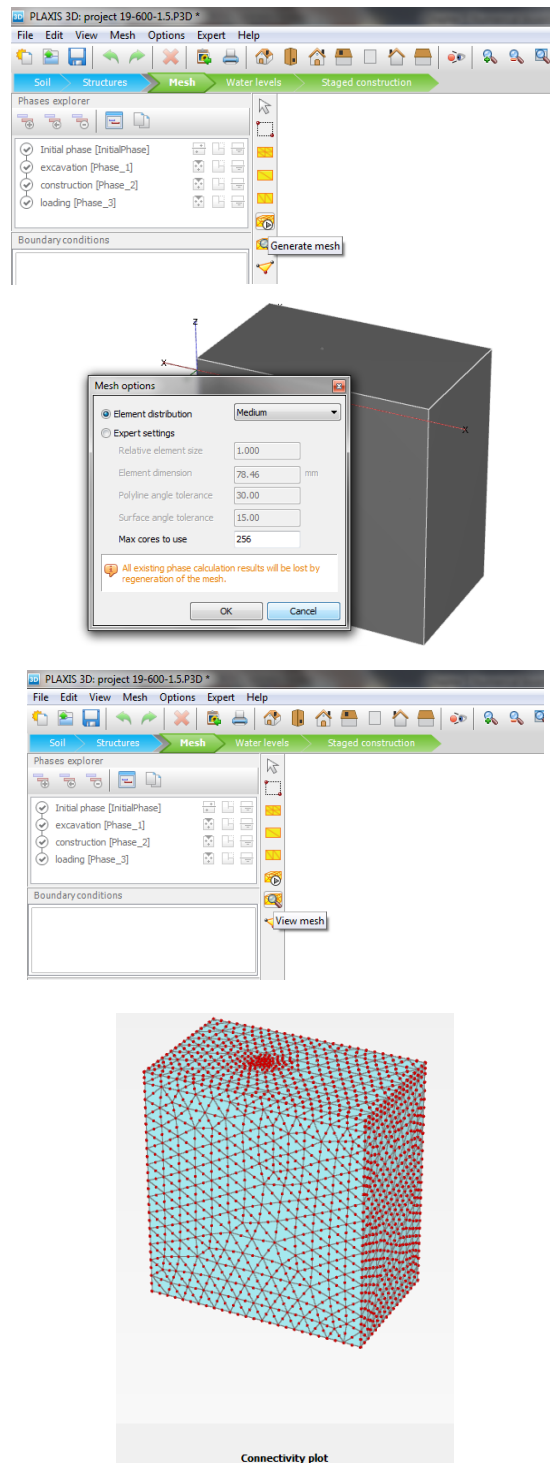


Fig. G.11 Meshing the Model

G.2.6 Loads

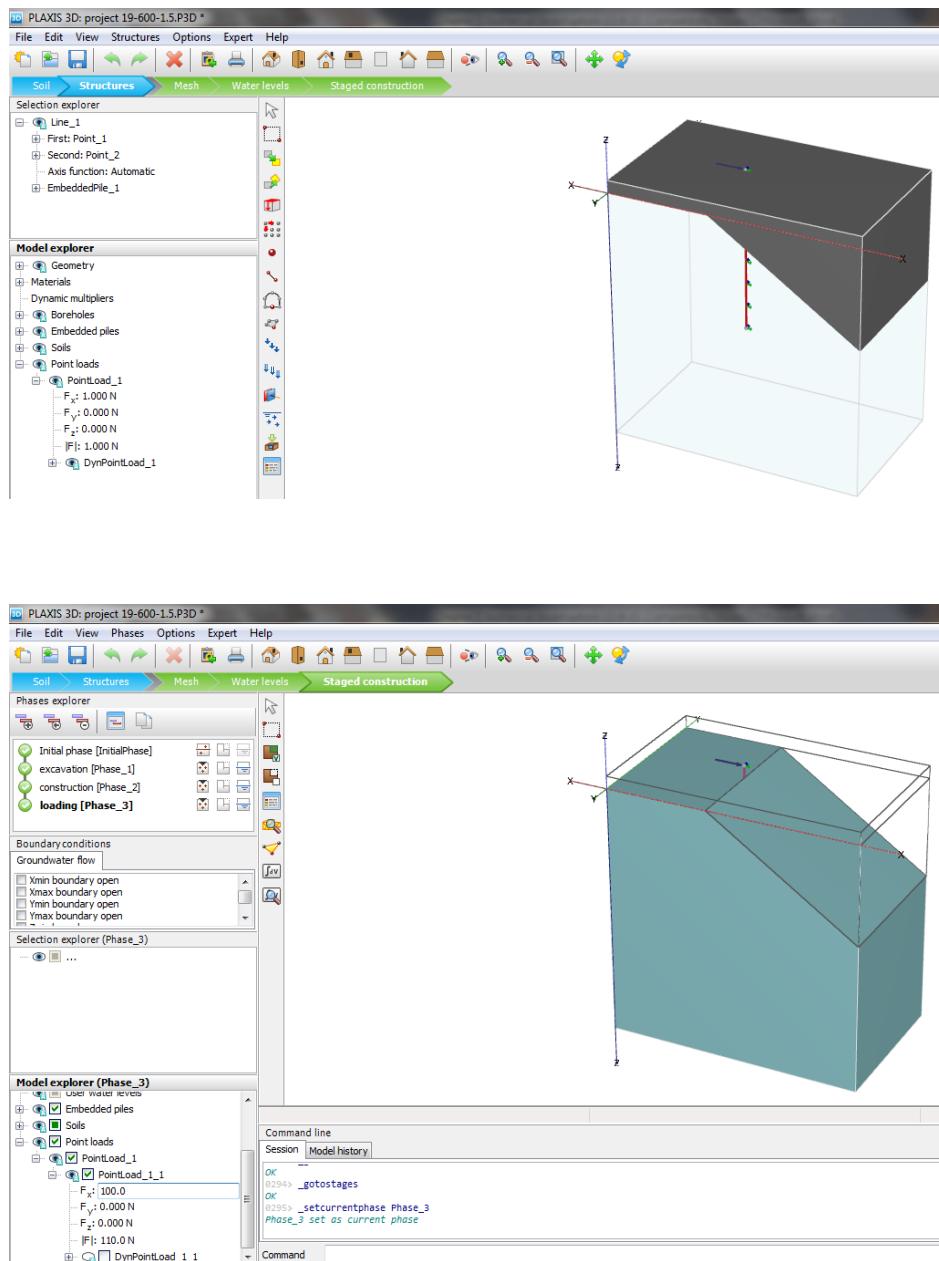


Fig. G.12 Application of Point Load

G.2.7 Boundary Conditions

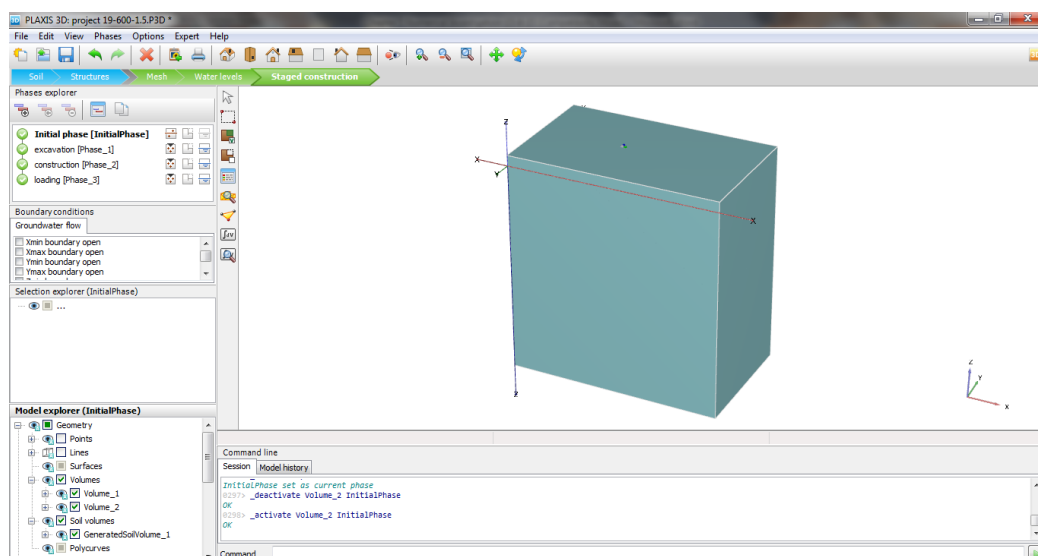


Fig.G.13 Initial Phase

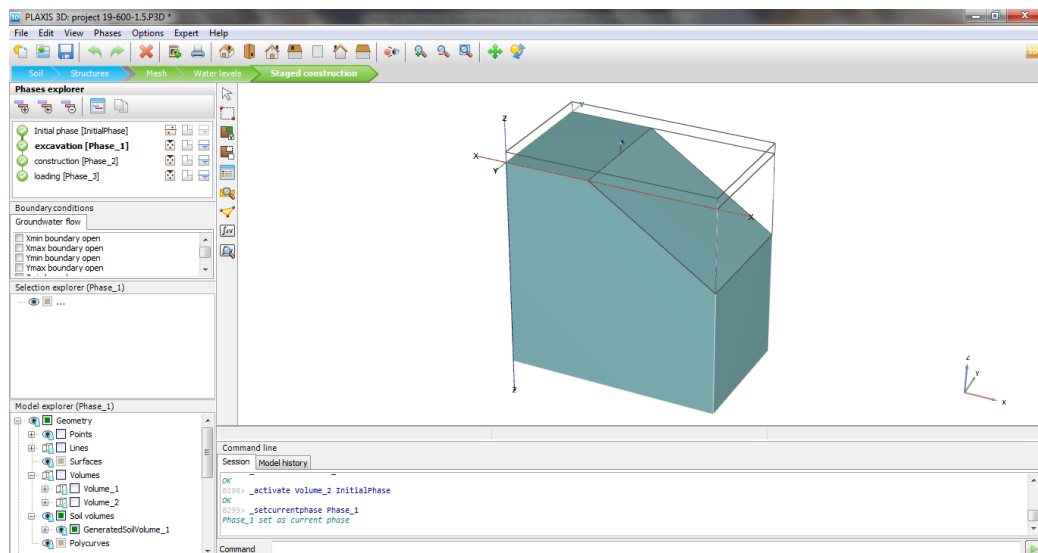


Fig.G.14 Excavation Phase (Phase_1)

G.2.8 Staged Construction

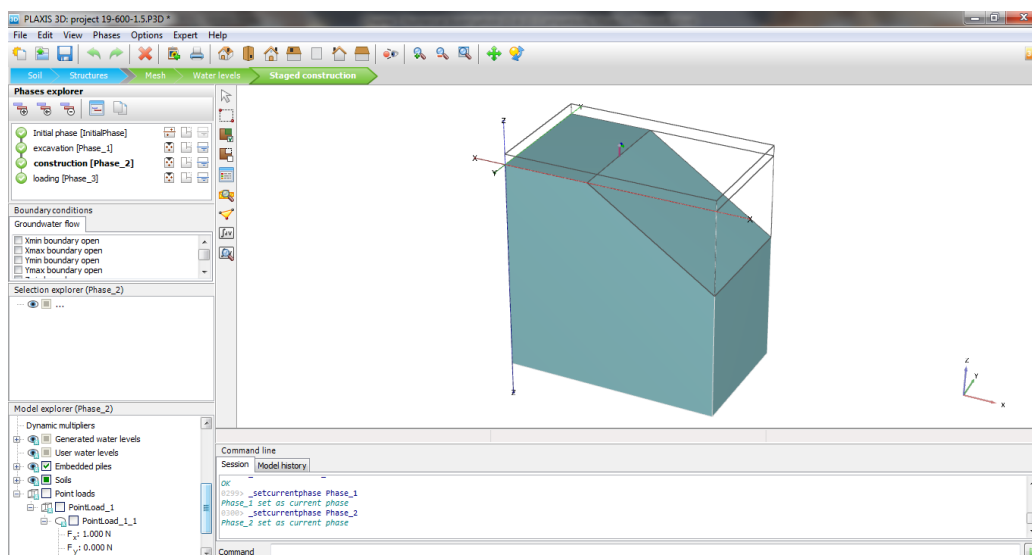


Fig.G.15 Construction Phase (Phase_2)

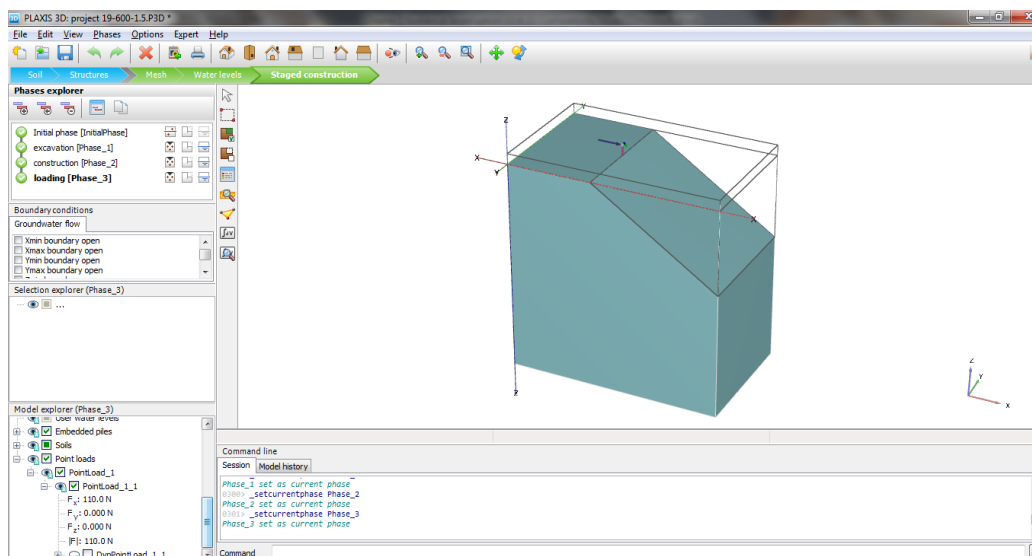


Fig.G.16 Loading Phase (Phase_3)

Initial phase follows the calculation type, K0 procedure. All the other phases are with calculation type plastic.

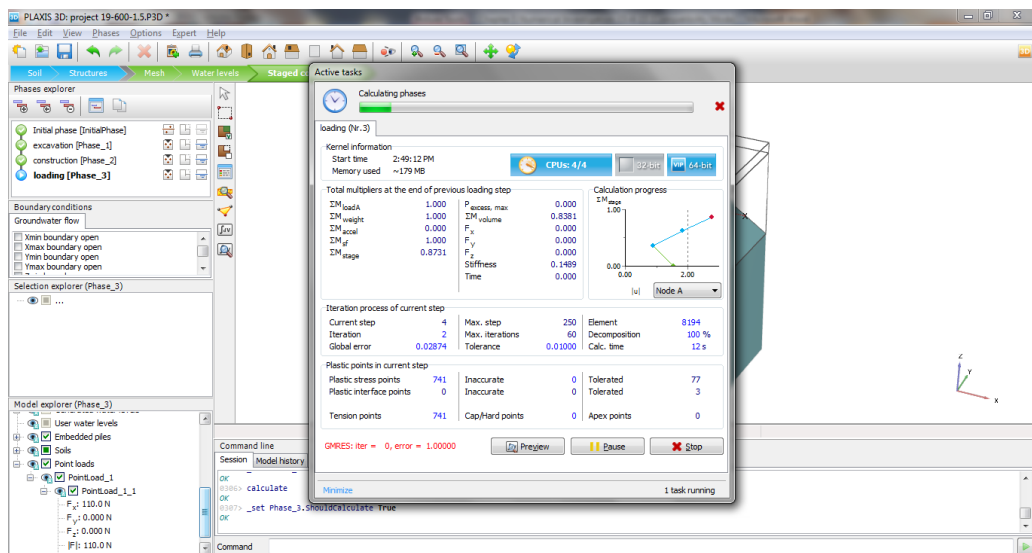
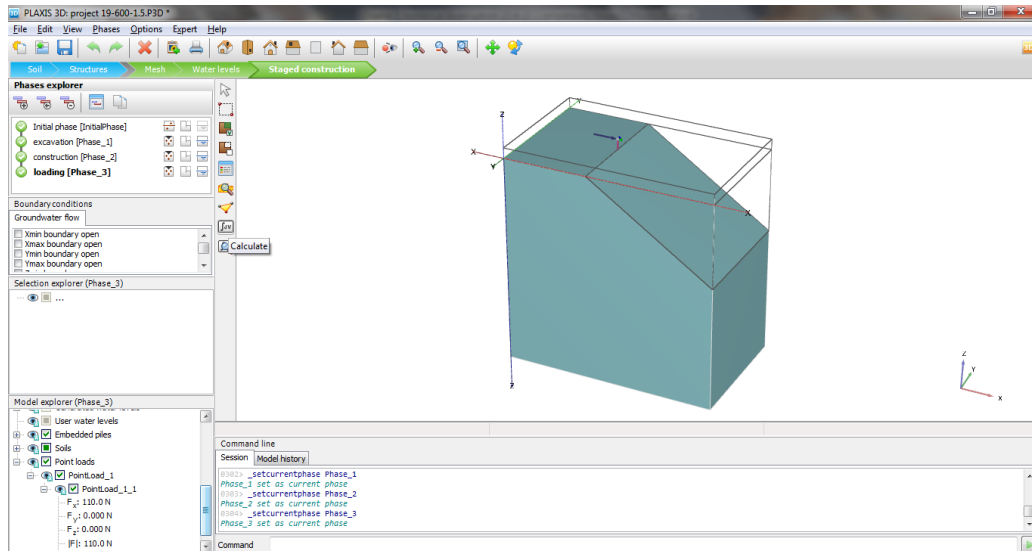


Fig.G.17 Analysis Phase

Appendix H

Parametric Study of Berthing Structure

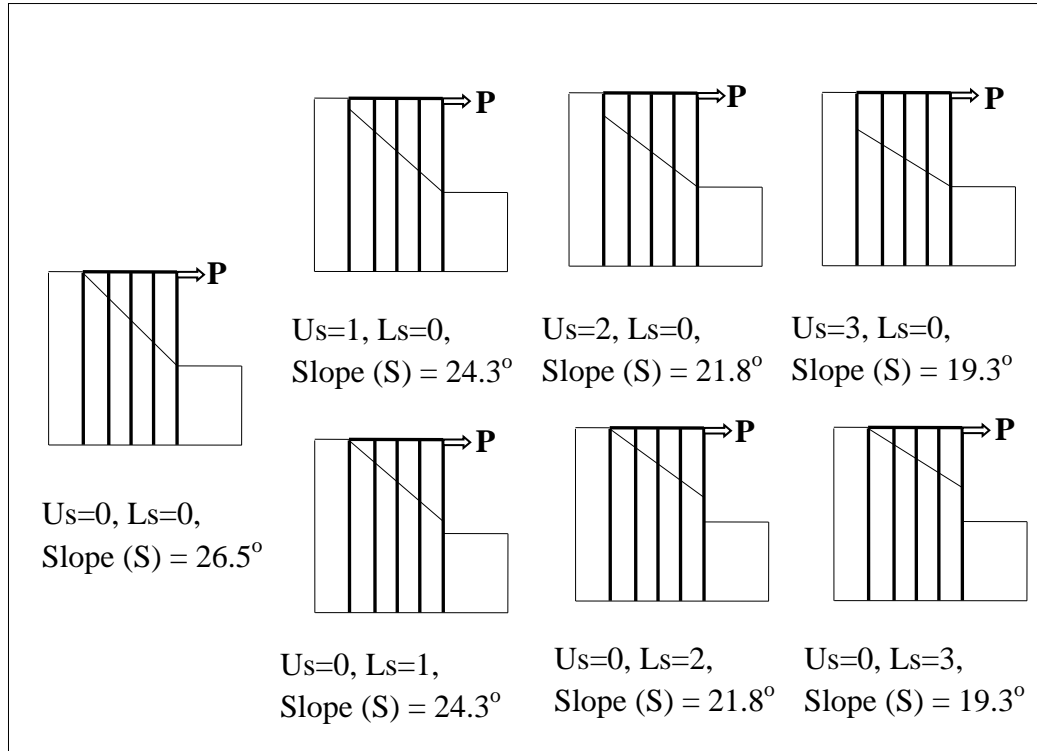


Fig.H.1 Details of Parameters Varied in the Study

Table H.1 Details of Maximum Bending Moment in Piles

Sl.No.	U_s (m)	L_s (m)	D (m)	E_s (kN/m ²)	S (°)	M_1 (kNm)	M_2 (kNm)	M_3 (kNm)	M_4 (kNm)	M_5 (kNm)
1	0	0	1	1.00E+03	26.6	3152.22	2272.31	2187.55	2429.38	3257.08
2	0	0	1	1.00E+04	26.6	3276.52	2964.15	2777.73	2982.82	3375.77
3	0	0	1	5.00E+04	26.6	3235.98	3106.17	2899.78	3055.64	3447.60
4	0	0	1.5	1.00E+03	26.6	4511.46	3026.61	2826.10	4006.69	6970.39
5	0	0	1.5	1.00E+04	26.6	4669.67	3685.27	3388.11	3619.17	4567.03
6	0	0	1.5	5.00E+04	26.6	4419.76	3698.72	3598.28	3732.61	4401.77
7	0	0	2	1.00E+03	26.6	5473.79	3238.41	3145.71	4046.45	9403.94
8	0	0	2	1.00E+04	26.6	5817.34	4285.57	3786.11	4073.53	5480.93

9	0	0	2	5.00E+04	26.6	5363.43	4282.28	3929.38	3943.72	4637.69
10	0	1	1	1.00E+03	24.2	3063.12	2251.02	2155.49	2472.48	3292.13
11	0	1	1	1.00E+04	24.2	3054.35	2685.34	2579.07	2923.34	3346.81
12	0	1	1	5.00E+04	24.2	2968.78	2567.76	2595.27	2966.93	3491.50
13	0	1	1.5	1.00E+03	24.2	4151.41	2910.51	2655.52	3813.04	6856.69
14	0	1	1.5	1.00E+04	24.2	4350.69	3439.79	3183.82	3546.18	4417.00
15	0	1	1.5	5.00E+04	24.2	4563.35	3539.92	3334.85	3456.28	4210.20
16	0	1	2	1.00E+03	24.2	4774.75	3067.28	3034.80	4007.09	8868.23
17	0	1	2	1.00E+04	24.2	5216.80	3953.66	3472.50	3860.97	5247.78
18	0	1	2	5.00E+04	24.2	4687.20	3792.33	3472.02	3603.36	4174.50
19	0	2	1	1.00E+03	21.8	2987.06	2149.01	2104.62	2439.00	3337.21
20	0	2	1	1.00E+04	21.8	2919.10	2551.34	2578.10	2816.31	3270.86
21	0	2	1	5.00E+04	21.8	2910.51	2552.53	2726.79	2860.44	3131.50
22	0	2	1.5	1.00E+03	21.8	3780.18	2794.34	2737.46	3951.10	7007.21
23	0	2	1.5	1.00E+04	21.8	3973.93	3261.26	3113.25	3450.06	4328.00
24	0	2	1.5	5.00E+04	21.8	3745.71	3240.00	3258.56	3563.13	4136.34
25	0	2	2	1.00E+03	21.8	3653.85	3008.34	3016.09	4039.19	9254.33
26	0	2	2	1.00E+04	21.8	4848.08	3804.80	3439.47	3832.90	5272.68
27	0	2	2	5.00E+04	21.8	4384.03	3695.60	3473.47	3529.77	4151.97
28	0	3	1	1.00E+03	19.3	2800.65	2178.48	2048.26	2368.54	3273.23
29	0	3	1	1.00E+04	19.3	2705.15	2581.62	2456.76	2748.77	3132.16
30	0	3	1	5.00E+04	19.3	2795.74	2675.72	2651.38	2919.03	3005.46
31	0	3	1.5	1.00E+03	19.3	3768.66	2924.34	2722.47	3978.60	7060.14
32	0	3	1.5	1.00E+04	19.3	3944.25	3222.71	3050.73	3391.51	4335.35
33	0	3	1.5	5.00E+04	19.3	3645.24	3184.92	3187.81	3491.38	3901.15
34	0	3	2	1.00E+03	19.3	4363.66	3132.69	3029.79	4081.47	9248.06
35	0	3	2	1.00E+04	19.3	4789.02	3765.09	3393.38	3799.30	5234.84
36	0	3	2	5.00E+04	19.3	4216.02	3582.33	3368.59	3468.23	4048.51
37	1	0	1	1.00E+03	24.2	3411.44	2356.78	2280.77	2510.74	3333.35
38	1	0	1	1.00E+04	24.2	3417.15	3082.46	2958.66	3169.92	3475.39
39	1	0	1	5.00E+04	24.2	3373.99	3130.45	3035.40	3501.47	3585.03
40	1	0	1.5	1.00E+03	24.2	4794.21	3048.39	2839.41	4096.94	6962.84
41	1	0	1.5	1.00E+04	24.2	4794.21	3048.39	3219.79	4134.08	6962.84
42	1	0	1.5	5.00E+04	24.2	4539.48	3730.62	3587.79	3804.30	4349.47

43	1	0	2	1.00E+03	24.2	5249.42	3179.76	3219.79	4134.08	9402.14
44	1	0	2	1.00E+04	24.2	5587.51	4167.52	3775.88	4083.97	5468.08
45	1	0	2	5.00E+04	24.2	5084.45	4058.35	3798.70	3871.38	4573.48
46	1	1	1	1.00E+03	21.8	3289.99	2379.36	2266.38	2546.50	3405.09
47	1	1	1	1.00E+04	21.8	3198.71	2946.85	2781.14	2991.65	3556.56
48	1	1	1	5.00E+04	21.8	3302.73	2912.95	2890.93	3043.18	3662.68
49	1	1	1.5	1.00E+03	21.8	4794.21	3048.39	2697.95	3836.08	6962.84
50	1	1	1.5	1.00E+04	21.8	4548.87	3759.88	3420.50	3420.50	4688.60
51	1	1	1.5	5.00E+04	21.8	4305.52	3743.20	3526.92	3853.39	4590.55
52	1	1	2	1.00E+03	21.8	5080.98	3074.00	3219.79	4134.08	8945.94
53	1	1	2	1.00E+04	21.8	5442.34	4195.61	3601.29	3935.90	5356.64
54	1	1	2	5.00E+04	21.8	4908.06	4053.90	3597.13	3695.73	4395.51
55	1	2	1	1.00E+03	19.3	3095.23	2232.47	2213.89	2514.28	3413.67
56	1	2	1	1.00E+04	19.3	3044.66	2697.45	2732.57	2921.64	3407.11
57	1	2	1	5.00E+04	19.3	2943.60	2655.61	2902.05	2999.78	3345.19
58	1	2	1.5	1.00E+03	19.3	3890.10	2804.91	2693.14	3813.52	6955.02
59	1	2	1.5	1.00E+04	19.3	4110.84	3381.38	3250.51	3484.51	4435.81
60	1	2	1.5	5.00E+04	19.3	3883.53	3413.30	3423.68	3655.22	4239.26
61	1	2	2	1.00E+03	19.3	4456.80	2847.48	3075.66	4050.01	8902.19
62	1	2	2	1.00E+04	19.3	4883.77	3862.61	3471.56	3775.64	5212.43
63	1	2	2	5.00E+04	19.3	4409.29	3684.10	3472.24	3499.03	4108.94
64	1	3	1	1.00E+03	16.7	2940.67	1999.32	2075.38	2435.35	3348.91
65	1	3	1	1.00E+04	16.7	2754.70	2498.84	2539.35	2796.13	3295.78
66	1	3	1	5.00E+04	16.7	2978.82	2794.46	2852.60	2795.67	3150.93
67	1	3	1.5	1.00E+03	16.7	3632.56	2673.78	2798.75	4063.67	7056.29
68	1	3	1.5	1.00E+04	16.7	3914.72	3207.21	3148.53	3421.64	4351.57
69	1	3	1.5	5.00E+04	16.7	3611.96	3270.57	3207.92	3455.13	4057.11
70	1	3	2	1.00E+03	16.7	4229.91	2984.04	3063.57	4121.33	9285.76
71	1	3	2	1.00E+04	16.7	4876.06	3753.82	3555.16	3914.92	5353.46
72	1	3	2	5.00E+04	16.7	4300.68	3626.19	3530.40	3588.18	4238.16
73	2	0	1	1.00E+03	21.8	3644.24	2433.32	2353.37	2594.74	3431.65
74	2	0	1	1.00E+04	21.8	3605.85	3233.51	3042.87	3242.06	3645.37
75	2	0	1	5.00E+04	21.8	3614.66	3279.46	3245.29	3334.10	3647.70
76	2	0	1.5	1.00E+03	21.8	5103.44	3134.24	2860.32	4118.15	7094.99

77	2	0	1.5	1.00E+04	21.8	5195.95	3921.27	3672.73	3911.20	4809.19
78	2	0	1.5	5.00E+04	21.8	4818.38	3973.33	3907.37	4080.36	4721.16
79	2	0	2	1.00E+03	21.8	6130.51	3251.28	3287.66	4238.11	9594.99
80	2	0	2	1.00E+04	21.8	6261.73	4425.48	3938.84	4231.94	5615.61
81	2	0	2	5.00E+04	21.8	5618.00	4324.27	4017.51	4089.38	4736.56
82	2	1	1	1.00E+03	19.3	3376.78	2460.55	2363.69	2638.51	3504.20
83	2	1	1	1.00E+04	19.3	3377.41	3020.54	2972.01	3075.53	3479.08
84	2	1	1	5.00E+04	19.3	3405.92	2951.06	3081.32	3106.60	3568.11
85	2	1	1.5	1.00E+03	19.3	3376.78	2460.55	2363.69	2638.51	3504.20
86	2	1	1.5	1.00E+04	19.3	4617.40	3819.26	3532.46	3725.93	4590.27
87	2	1	1.5	5.00E+04	19.3	4333.82	3750.70	3621.93	3714.09	4325.43
88	2	1	2	1.00E+03	19.3	5267.01	3171.74	2906.52	4143.69	9396.25
89	2	1	2	1.00E+04	19.3	5580.33	4332.87	3825.00	4187.45	5586.55
90	2	1	2	5.00E+04	19.3	5085.93	4139.59	3881.58	3939.24	4553.43
91	2	2	1	1.00E+03	16.7	4092.68	2854.14	3172.59	4148.51	7066.74
92	2	2	1	1.00E+04	16.7	4377.46	3622.96	3411.61	3631.63	4609.51
93	2	2	1	5.00E+04	16.7	4138.73	3637.93	3491.03	3676.98	4376.77
94	2	2	1.5	1.00E+03	16.7	4092.68	2854.14	3172.59	4148.51	7066.74
95	2	2	1.5	1.00E+04	16.7	4377.46	3622.96	3411.61	3631.63	4609.51
96	2	2	1.5	5.00E+04	16.7	4138.73	3637.93	3491.03	3551.12	4376.77
97	2	2	2	1.00E+03	16.7	4663.05	2886.41	2767.93	3875.41	8985.32
98	2	2	2	1.00E+04	16.7	5140.16	4062.99	3635.84	3963.16	5430.14
99	2	2	2	5.00E+04	16.7	4692.94	3931.69	3609.61	3672.08	4393.90
100	2	3	1	1.00E+03	14.0	3146.26	2152.28	2185.40	2562.22	3487.63
101	2	3	1	1.00E+04	14.0	3071.38	2679.91	2726.18	2910.30	3483.28
102	2	3	1	5.00E+04	14.0	3145.81	2839.06	2703.65	2984.09	3427.59
103	2	3	1.5	1.00E+03	14.0	3146.26	2152.28	2185.40	2562.22	3487.63
104	2	3	1.5	1.00E+04	14.0	4207.67	3365.30	3343.59	3605.06	4575.24
105	2	3	1.5	5.00E+04	14.0	3953.15	3402.53	3357.64	3651.69	4384.19
106	2	3	2	1.00E+03	14.0	4427.53	2972.64	2907.78	4278.24	9549.02
107	2	3	2	1.00E+04	14.0	5082.13	3920.85	3683.75	4071.00	5503.51
108	2	3	2	5.00E+04	14.0	4582.06	3769.90	3609.80	3720.50	4417.92
109	3	0	1	1.00E+03	19.3	3725.90	2357.79	2333.67	2606.52	3388.35
110	3	0	1	1.00E+04	19.3	3659.40	3187.48	3006.22	3219.79	3436.29

111	3	0	1	5.00E+04	19.3	3429.95	3278.16	3293.23	3534.91	3303.45
112	3	0	1.5	1.00E+03	19.3	5051.49	3040.37	3247.84	4169.18	6993.64
113	3	0	1.5	1.00E+04	19.3	4998.37	3824.10	3520.11	3766.92	4619.77
114	3	0	1.5	5.00E+04	19.3	4346.62	3639.04	3546.60	3761.25	4361.84
115	3	0	2	1.00E+03	19.3	5973.53	3163.24	2842.88	4242.85	9565.57
116	3	0	2	1.00E+04	19.3	6189.77	4337.63	3875.81	4230.65	5575.11
117	3	0	2	5.00E+04	19.3	5501.02	4178.83	3750.26	3874.23	4491.93
118	3	1	1	1.00E+03	16.7	3488.28	2432.57	2384.31	2698.71	3546.81
119	3	1	1	1.00E+04	16.7	3528.39	3199.35	3064.61	3311.81	3557.62
120	3	1	1	5.00E+04	16.7	3744.57	3300.63	3242.10	3643.07	3569.34
121	3	1	1.5	1.00E+03	16.7	4678.89	3040.44	3286.00	4114.80	7101.49
122	3	1	1.5	1.00E+04	16.7	4862.10	3961.82	3655.28	3932.47	4727.29
123	3	1	1.5	5.00E+04	16.7	4627.23	3962.56	3824.15	4121.97	4471.37
124	3	1	2	1.00E+03	16.7	5471.05	3126.36	2842.85	4276.07	9265.46
125	3	1	2	1.00E+04	16.7	5888.49	4453.39	3840.41	4214.80	5599.57
126	3	1	2	5.00E+04	16.7	5420.98	4418.22	4031.38	4159.76	4691.63
127	3	2	1	1.00E+03	14.0	3368.82	2389.56	2333.16	2701.18	3594.02
128	3	2	1	1.00E+04	14.0	3400.82	3032.52	2995.96	3145.30	3545.44
129	3	2	1	5.00E+04	14.0	3561.54	3097.40	3151.08	3297.82	3681.89
130	3	2	1.5	1.00E+03	14.0	4375.12	3053.29	3331.46	4259.99	7338.08
131	3	2	1.5	1.00E+04	14.0	4679.61	3831.30	3612.25	3875.96	4745.17
132	3	2	1.5	5.00E+04	14.0	4423.50	3819.33	3827.28	3918.23	4461.94
133	3	2	2	1.00E+03	14.0	4886.43	3147.58	2879.78	4441.30	9533.00
134	3	2	2	1.00E+04	14.0	5505.51	4308.99	3795.06	4208.86	5629.34
135	3	2	2	5.00E+04	14.0	5052.55	4213.02	3989.52	3970.44	4644.51
136	3	3	1	1.00E+03	11.3	3153.31	2138.48	2206.26	2581.99	3484.41
137	3	3	1	1.00E+04	11.3	3070.41	2726.80	2754.93	3045.66	3489.36
138	3	3	1	5.00E+04	11.3	2963.17	2698.43	3030.61	3208.75	3260.40
139	3	3	1.5	1.00E+03	11.3	4027.86	2849.40	3258.28	4355.53	7262.90
140	3	3	1.5	1.00E+04	11.3	4319.61	3517.28	3461.63	3751.43	4654.42
141	3	3	1.5	5.00E+04	11.3	4036.81	3544.36	3570.18	3751.73	4523.87
142	3	3	2	1.00E+03	11.3	4529.06	3006.38	3039.87	4403.39	9820.37
143	3	3	2	1.00E+04	11.3	4691.02	3910.98	3758.52	3890.11	4568.37
144	3	3	2	5.00E+04	11.3	4691.02	3910.98	3758.52	3890.11	4568.37

Table H.2 Details of Depth of Fixity and Deflection in Piles

No.	Us (m)	Ls (m)	D (m)	Es (kN/m ²)	S (°)	Df1 (m)	Df2 (m)	Df3 (m)	Df4 (m)	Df5 (m)	y _{max} (mm)
1	0	0	1	1.00E+03	26.55	13.981	19.406	20.309	17.371	12.801	102.23
2	0	0	1	1.00E+04	26.55	13.435	13.291	14.688	12.329	9.157	39.51
3	0	0	1	5.00E+04	26.55	13.435	13.291	12.342	12.329	9.157	29.28
4	0	0	1.5	1.00E+03	26.55	15.818	25.432	25.111	20.99	14.88	66.50
5	0	0	1.5	1.00E+04	26.55	13.435	15.314	14.688	13.083	9.863	17.50
6	0	0	1.5	5.00E+04	26.55	13.435	14.416	14.688	12.329	9.157	10.10
7	0	0	2	1.00E+03	26.55	17.607	29.035	28.042	22.358	14.88	33.90
8	0	0	2	1.00E+04	26.55	13.981	17.051	17.907	15.95	12.801	9.97
9	0	0	2	5.00E+04	26.55	13.435	15.314	14.688	12.329	9.157	4.65
10	0	1	1	1.00E+03	24.22	16.112	20.266	20.515	17.692	12.638	102.55
11	0	1	1	1.00E+04	24.22	13.832	14.888	13.812	11.913	7.72	38.11
12	0	1	1	5.00E+04	24.22	13.232	14.888	11.904	11.913	7.332	26.76
13	0	1	1.5	1.00E+03	24.22	16.112	24.72	25.627	20.914	14.397	64.30
14	0	1	1.5	1.00E+04	24.22	13.832	15.378	13.812	12.369	9.902	16.70
15	0	1	1.5	5.00E+04	24.22	13.536	14.137	12.824	11.391	8.772	9.30
16	0	1	2	1.00E+03	24.22	17.649	28.738	27.901	23.238	14.397	43.30
17	0	1	2	1.00E+04	24.22	14.429	17.001	17.556	15.901	11.963	9.49
18	0	1	2	5.00E+04	24.22	13.832	14.888	13.812	11.913	8.34	4.16
19	0	2	1	1.00E+03	21.79	17.469	19.802	20.244	17.321	13.14	102.40
20	0	2	1	1.00E+04	21.79	14.339	14.523	13.376	10.842	8.568	37.22
21	0	2	1	5.00E+04	21.79	13.741	11.562	13.376	10.39	7.895	26.98
22	0	2	1.5	1.00E+03	21.79	17.469	24.044	25.505	20.391	14.659	64.80
23	0	2	1.5	1.00E+04	21.79	15.423	15.473	13.376	11.427	8.568	16.30
24	0	2	1.5	5.00E+04	21.79	13.741	14.274	13.376	10.39	8.568	8.90
25	0	2	2	1.00E+03	21.79	20.682	28.35	27.285	21.765	14.659	44.92
26	0	2	2	1.00E+04	21.79	16.734	15.473	17.424	16.104	12.04	9.16
27	0	2	2	5.00E+04	21.79	13.741	14.523	13.376	11.427	9.093	4.07
28	0	3	1	1.00E+03	19.28	17.096	19.59	20.523	17.029	12.526	118.00
29	0	3	1	1.00E+04	19.28	13.497	13.441	13.903	11.691	8.875	35.36
30	0	3	1	5.00E+04	19.28	13.497	13.441	13.903	11.691	6.941	26.03
31	0	3	1.5	1.00E+03	19.28	17.934	25.481	24.884	20.238	14.476	65.80

32	0	3	1.5	1.00E+04	19.28	15.173	15.269	12.642	11.691	9.267	16.40
33	0	3	1.5	5.00E+04	19.28	13.497	13.441	12.642	11.122	8.483	8.70
34	0	3	2	1.00E+03	19.28	20.894	29.029	27.588	22.342	14.476	69.34
35	0	3	2	1.00E+04	19.28	17.934	16.56	17.077	15.971	12.526	9.07
36	0	3	2	5.00E+04	19.28	13.497	14.717	12.642	11.122	9.267	3.98
37	1	0	1	1.00E+03	24.22	14.07	19.859	20.281	18.095	11.869	105.90
38	1	0	1	1.00E+04	24.22	12.853	15.138	13.323	13.267	8.817	41.88
39	1	0	1	5.00E+04	24.22	10	12.158	13.323	13.267	7.737	31.86
40	1	0	1.5	1.00E+03	24.22	14.731	25.751	24.843	21.792	14.393	67.39
41	1	0	1.5	1.00E+04	24.22	14.731	25.751	24.843	21.792	14.393	67.39
42	1	0	1.5	5.00E+04	24.22	12.296	13.745	13.934	13.267	8.817	10.69
43	1	0	2	1.00E+03	24.22	18.088	28.627	28.126	23.733	15.15	47.02
44	1	0	2	1.00E+04	24.22	13.41	18.287	17.371	16.673	11.869	9.94
45	1	0	2	5.00E+04	24.22	12.853	15.138	13.934	11.978	9.459	4.53
46	1	1	1	1.00E+03	21.79	15.883	19.157	20.844	18.127	12.321	107.6
47	1	1	1	1.00E+04	21.79	13.225	14.751	14.186	12.042	8.233	41.00
48	1	1	1	5.00E+04	21.79	13.225	14.377	14.186	12.042	7.941	30.40
49	1	1	1.5	1.00E+03	21.79	14.731	25.751	24.843	21.792	14.393	67.40
50	1	1	1.5	1.00E+04	21.79	14.642	15.126	14.186	14.186	9.672	18.20
51	1	1	1.5	5.00E+04	21.79	13.225	13.41	14.186	12.042	8.233	10.80
52	1	1	2	1.00E+03	21.79	17.626	28.982	27.652	23.554	14.505	50.58
53	1	1	2	1.00E+04	21.79	14.306	16.131	17.866	16.023	12.321	9.42
54	1	1	2	5.00E+04	21.79	13.225	14.377	13.74	12.042	9.672	4.29
55	1	2	1	1.00E+03	19.28	17.377	19.404	20.335	17.867	11.897	107.10
56	1	2	1	1.00E+04	19.28	14.365	14.17	12.569	11.825	9.847	39.33
57	1	2	1	5.00E+04	19.28	13.77	14.17	12.569	12.06	6.762	28.43
58	1	2	1.5	1.00E+03	19.28	17.788	24.802	24.996	20.313	14.556	65.50
59	1	2	1.5	1.00E+04	19.28	14.365	13.834	12.569	11.825	9.847	16.70
60	1	2	1.5	5.00E+04	19.28	13.77	13.497	12.569	10.91	9.847	9.30
61	1	2	2	1.00E+03	19.28	19.355	28.418	27.074	22.592	14.556	54.62
62	1	2	2	1.00E+04	19.28	14.96	16.213	15.937	15.673	11.897	9.01
63	1	2	2	5.00E+04	19.28	13.77	13.497	12.569	11.59	9.118	3.96
64	1	3	1	1.00E+03	16.69	17.354	19.486	20.149	17.303	11.988	101.93
65	1	3	1	1.00E+04	16.69	15.077	11.902	12.072	11.485	8.993	35.96

66	1	3	1	5.00E+04	16.69	11.388	11.902	11.282	11.485	8.268	25.55
67	1	3	1.5	1.00E+03	16.69	18.173	26.072	24.245	20.499	14.13	65.70
68	1	3	1.5	1.00E+04	16.69	16.525	13.162	12.861	12.062	9.818	16.40
69	1	3	1.5	5.00E+04	16.69	13.628	11.902	12.861	11.485	8.268	8.70
70	1	3	2	1.00E+03	16.69	21.636	28.955	26.632	21.95	14.926	45.56
71	1	3	2	1.00E+04	16.69	17.354	15.22	15.581	15.903	11.988	9.41
72	1	3	2	5.00E+04	16.69	12.775	11.902	12.861	11.485	8.993	4.12
73	2	0	1	1.00E+03	21.79	13.451	19.214	20.473	18.123	12.853	110.19
74	2	0	1	1.00E+04	21.79	13.451	13.376	13.52	12.853	10.173	43.79
75	2	0	1	5.00E+04	21.79	11.137	13.376	10.984	12.482	9.753	32.12
76	2	0	1.5	1.00E+03	21.79	14.628	24.62	25.164	21.411	15.485	69.60
77	2	0	1.5	1.00E+04	21.79	13.451	14.613	13.52	12.853	9.753	4.30
78	2	0	1.5	5.00E+04	21.79	12.273	13.376	13.52	12.482	8.558	11.00
79	2	0	2	1.00E+03	21.79	15.953	28.504	27.658	23.21	15.485	48.79
80	2	0	2	1.00E+04	21.79	13.451	18.25	17.783	15.912	12.853	10.37
81	2	0	2	5.00E+04	21.79	13.451	15.435	13.52	12.482	9.753	5.01
82	2	1	1	1.00E+03	19.28	16.681	18.884	19.843	17.451	13.395	111.50
83	2	1	1	1.00E+04	19.28	13.532	14.269	13.14	11.66	8.152	42.88
84	2	1	1	5.00E+04	19.28	13.025	13.935	13.14	11.66	8.152	31.29
85	2	1	1.5	1.00E+03	19.28	16.681	18.884	19.843	17.451	13.395	111.5
86	2	1	1.5	1.00E+04	19.28	14.039	14.269	13.14	12.19	10.152	18.00
87	2	1	1.5	5.00E+04	19.28	13.025	13.935	13.14	12.19	8.152	11.10
88	2	1	2	1.00E+03	19.28	18.518	28.041	27.398	23.129	15.832	47.75
89	2	1	2	1.00E+04	19.28	15.464	16.392	15.084	15.617	12.775	10.15
90	2	1	2	5.00E+04	19.28	13.532	13.935	13.14	12.19	10.152	4.76
91	2	2	1	1.00E+03	16.69	17.781	23.892	24.628	21.439	14.773	67.18
92	2	2	1	1.00E+04	16.69	14.353	14.693	13.025	11.965	9.821	17.73
93	2	2	1	5.00E+04	16.69	13.806	14.693	13.025	10.885	9.821	10.78
94	2	2	1.5	1.00E+03	16.69	17.781	23.892	24.628	21.439	14.773	67.20
95	2	2	1.5	1.00E+04	16.69	14.353	14.693	13.025	11.965	9.821	17.70
96	2	2	1.5	5.00E+04	16.69	13.806	14.693	13.025	13.659	9.821	10.80
97	2	2	2	1.00E+03	16.69	18.9	28.236	26.56	22.708	14.773	50.13
98	2	2	2	1.00E+04	16.69	14.353	16.261	15.662	16.125	12.272	9.44
99	2	2	2	5.00E+04	16.69	13.806	14.693	13.025	11.585	8.938	4.26

100	2	3	1	1.00E+03	14.03	17.488	18.905	19.897	16.827	12.548	106.87
101	2	3	1	1.00E+04	14.03	13.683	13.216	12.932	11.829	9.062	39.05
102	2	3	1	5.00E+04	14.03	13.683	13.216	12.932	12.688	9.062	28.50
103	2	3	1.5	1.00E+03	14.03	17.488	18.905	19.897	16.827	12.548	106.8
104	2	3	1.5	1.00E+04	14.03	16.475	13.216	12.368	11.49	9.619	18.10
105	2	3	1.5	5.00E+04	14.03	13.683	13.216	13.751	12.688	9.062	9.60
106	2	3	2	1.00E+03	14.03	20.626	27.284	26.233	23.045	14.773	47.4
107	2	3	2	1.00E+04	14.03	17.488	16.158	15.656	16.404	12.548	9.82
108	2	3	2	5.00E+04	14.03	13.683	13.216	12.368	11.151	9.062	4.48
109	3	0	1	1.00E+03	19.28	12.913	19.304	20.49	18.403	14.499	109.40
110	3	0	1	1.00E+04	19.28	12.309	14.494	13.238	11.132	10.465	43.49
111	3	0	1	5.00E+04	19.28	10	12.731	13.238	11.132	11.628	31.71
112	3	0	1.5	1.00E+03	19.28	15.315	25.505	25.939	21.56	15.22	69.70
113	3	0	1.5	1.00E+04	19.28	12.913	14.494	13.238	12.264	10.465	18.60
114	3	0	1.5	5.00E+04	19.28	12.913	12.731	13.238	11.132	8.896	10.20
115	3	0	2	1.00E+03	19.28	16.952	28.14	27.899	23.19	16.305	49.74
116	3	0	2	1.00E+04	19.28	13.517	16.43	18.028	16.913	13.376	10.51
117	3	0	2	5.00E+04	19.28	12.913	14.494	14.198	12.264	9.302	4.69
118	3	1	1	1.00E+03	16.69	15.849	19.378	20.077	17.296	14.028	112.90
119	3	1	1	1.00E+04	16.69	13.626	14.433	13.6	12.801	11.518	45.25
120	3	1	1	5.00E+04	16.69	13.06	12.034	13.6	13.314	11.518	35.03
121	3	1	1.5	1.00E+03	16.69	15.849	24.432	24.952	22.007	15.278	69.10
122	3	1	1.5	1.00E+04	16.69	13.626	14.433	13.6	12.801	10.837	18.80
123	3	1	1.5	5.00E+04	16.69	13.06	12.034	13.6	12.288	10.837	10.90
124	3	1	2	1.00E+03	16.69	16.795	27.765	27.937	23.489	15.278	46.94
125	3	1	2	1.00E+04	16.69	14.193	15.355	16.724	16.058	12.892	10.14
126	3	1	2	5.00E+04	16.69	13.626	13.986	13.6	12.288	9.553	4.82
127	3	2	1	1.00E+03	14.03	16.73	18.877	20.273	17.691	13.684	113.2
128	3	2	1	1.00E+04	14.03	14.976	14.286	13.149	13.093	10.497	44.09
129	3	2	1	5.00E+04	14.03	13.536	14.286	12.653	13.456	11.179	34.12
130	3	2	1.5	1.00E+03	14.03	17.646	23.51	24.64	21.443	15.345	71.30
131	3	2	1.5	1.00E+04	14.03	14.976	14.286	13.149	13.093	10.497	19.20
132	3	2	1.5	5.00E+04	14.03	13.974	14.286	11.696	13.093	11.179	12.00
133	3	2	2	1.00E+03	14.03	19.145	28.005	26.726	22.763	15.704	50.85

134	3	2	2	1.00E+04	14.03	16.135	15.771	15.583	16.121	13.399	10.24
135	3	2	2	5.00E+04	14.03	13.974	14.286	11.696	12.731	9.772	4.93
136	3	3	1	1.00E+03	11.31	17.328	18.62	19.238	17.354	13.078	107.30
137	3	3	1	1.00E+04	11.31	14.408	13.661	13.206	11.685	10.018	39.76
138	3	3	1	5.00E+04	11.31	13.096	14.808	10.497	11.685	10.018	29.42
139	3	3	1.5	1.00E+03	11.31	18.504	24.163	24.007	20.545	15.426	69.6
140	3	3	1.5	1.00E+04	11.31	16.175	13.661	13.206	12.561	10.018	17.90
141	3	3	1.5	5.00E+04	11.31	14.408	13.661	11.15	11.685	8.688	10.10
142	3	3	2	1.00E+03	11.31	19.852	27.643	26.051	21.943	15.907	51.96
143	3	3	2	1.00E+04	11.31	14.408	14.808	13.206	11.685	9.353	4.58
144	3	3	2	5.00E+04	11.31	14.408	14.808	13.206	11.685	9.353	4.58

Appendix I

Multivariable Regression Analysis

I.1 Regression Analysis

Regression Analysis is a statistical tool used to estimate the relationships among variables. There are many methods for modeling and analyzing several variables, focusing on the relationship between a dependent variable and one or more independent variables.

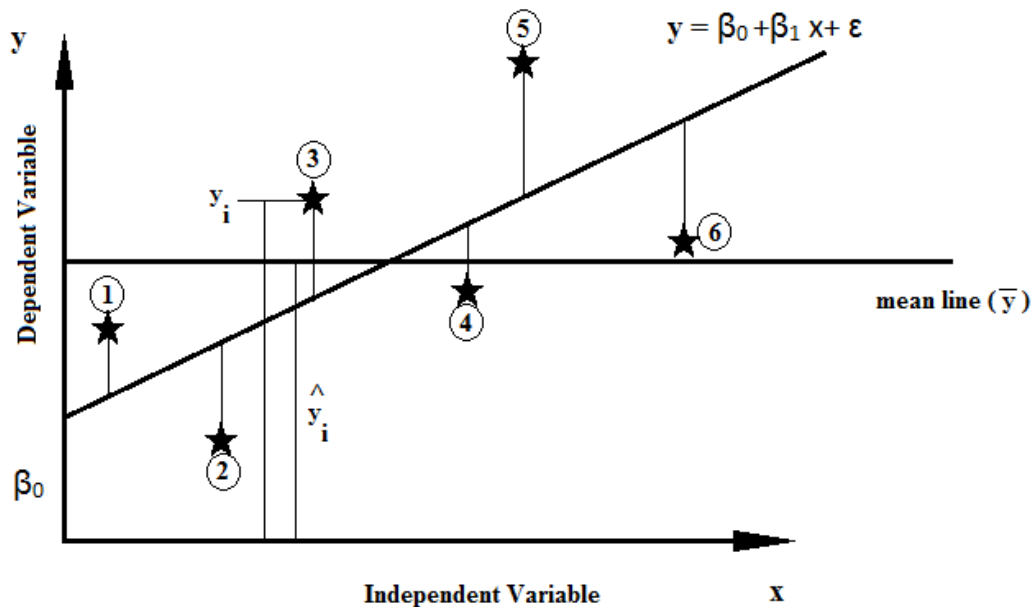


Fig.G.1 Graphical Representation of Regression

The proportion of total variation, $R^2 = 1 - \frac{SSE}{SST}$

$$SSE = \sum (y_i - \hat{y}_i)^2$$

$$SST = \sum (y_i - \bar{y})^2$$

$$y = \beta_0 + \beta_1 x + \epsilon$$

As the number of independent variables increases the relationship between the dependent variable and the 'k' independent variables becomes,

$$y = \beta_0 + \beta_1x_1 + \beta_2x_2 + \beta_3x_3 + \dots + \beta_kx_k + \varepsilon$$

I.2 Multivariable Regression Analysis

$$\begin{Bmatrix} y_1 \\ y_2 \\ \vdots \\ y_n \end{Bmatrix} = \begin{bmatrix} 1 & x_{12} & \dots & x_{1k} \\ 1 & x_{22} & \dots & x_{2k} \\ \vdots & \vdots & \ddots & \vdots \\ 1 & x_{n2} & \dots & x_{nk} \end{bmatrix} \begin{Bmatrix} \beta_1 \\ \beta_2 \\ \vdots \\ \beta_n \end{Bmatrix} + \begin{Bmatrix} \varepsilon_1 \\ \varepsilon_2 \\ \vdots \\ \varepsilon_n \end{Bmatrix}$$

$$Y = X\beta$$

$$X^T Y = X^T X\beta$$

Hence,

$$\beta = (X^T X)^{-1} X^T Y$$

I.3 MATLAB Coding

Consider the existing matrices [X] , [Y] and [\beta],

$$M = X\beta;$$

$$B = ((X' * X)^{-1}) * X' * Y$$

$$MU = \text{mean}(Y);$$

$$SST = \text{sum}((Y - MU).^2);$$

$$SSE = \text{sum}((M - Y).^2);$$

$$R2 = 1 - \left(\frac{SSE}{SST}\right)$$

$$\text{MaxErr} = \text{max}(\text{abs}(Y - M))$$

$$\text{plot}(X * B, Y, 'o', X * B, M, '-')$$

Appendix J

Design Chart for the Analysis of Ship Berthing Structure

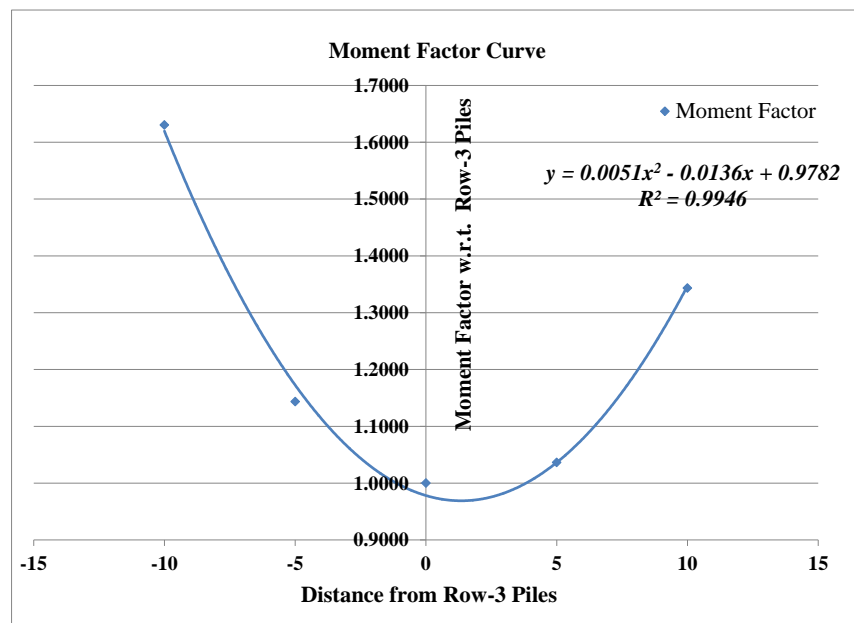
A. Design Charts for Bending Moment Based on the Numerical Analysis of Ship Berthing Structure

Numerical analysis of ship berthing structures are carried out as explained in Chapter 6. The values obtained in the parametric study are tabulated in Appendix-H and is used to develop design charts to calculate the bending moment acting on middle row (R3) of pile.

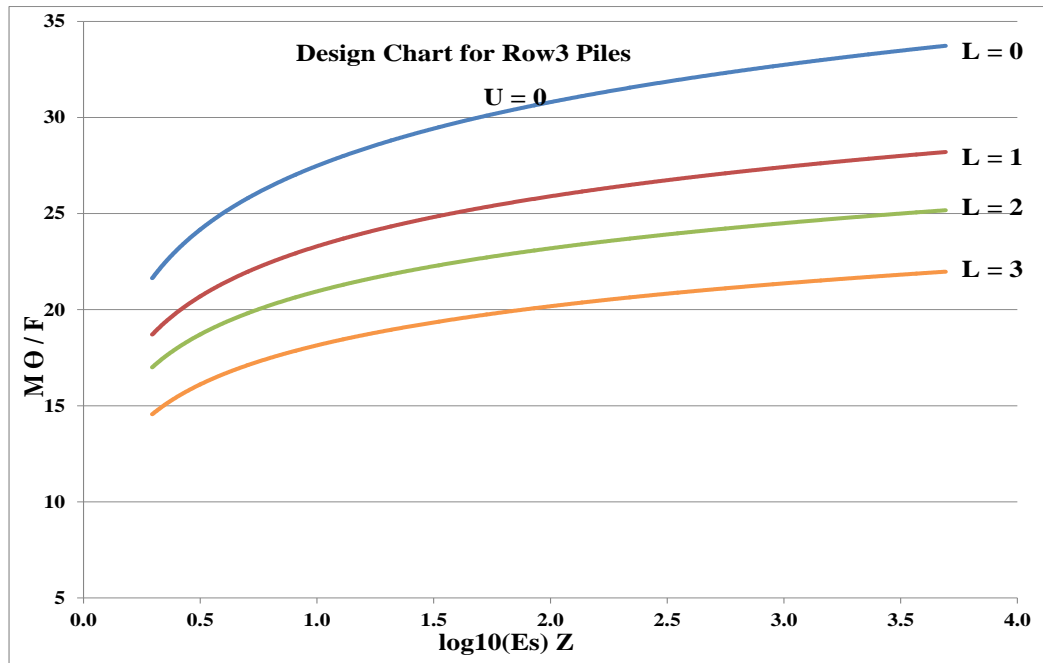
A parabolic variation of bending moment is observed among the different rows of piles and row-3 piles are always at the vertex of the parabola with minimum values of bending moment. Hence design charts are developed for row-3 pile and the value of bending moment thus obtained is multiplied with the moment factor for each row to obtain the bending moment of that row.

Moment Factor for each row

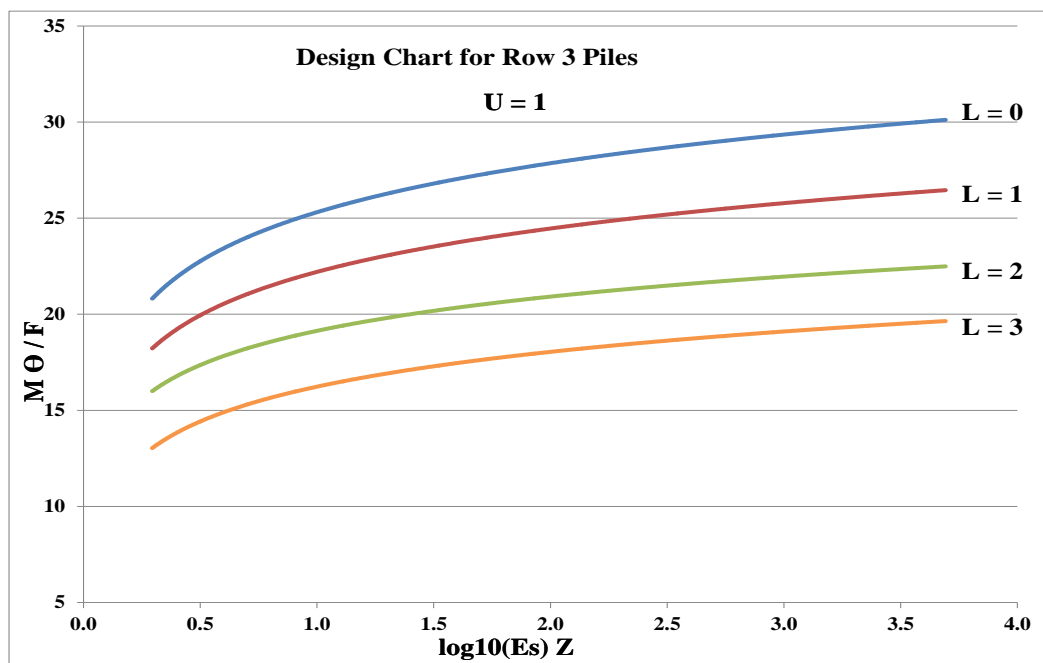
$$\text{M.F.} = 0.0051x^2 - 0.0136x + 0.9782, R^2 = 0.9946$$



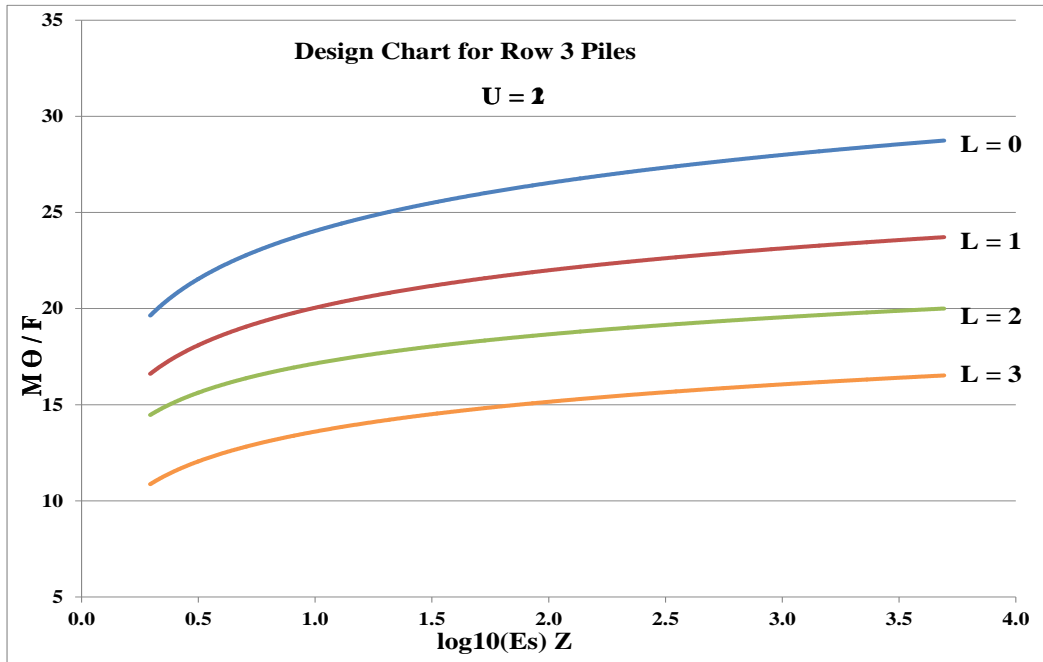
Design Chart A1



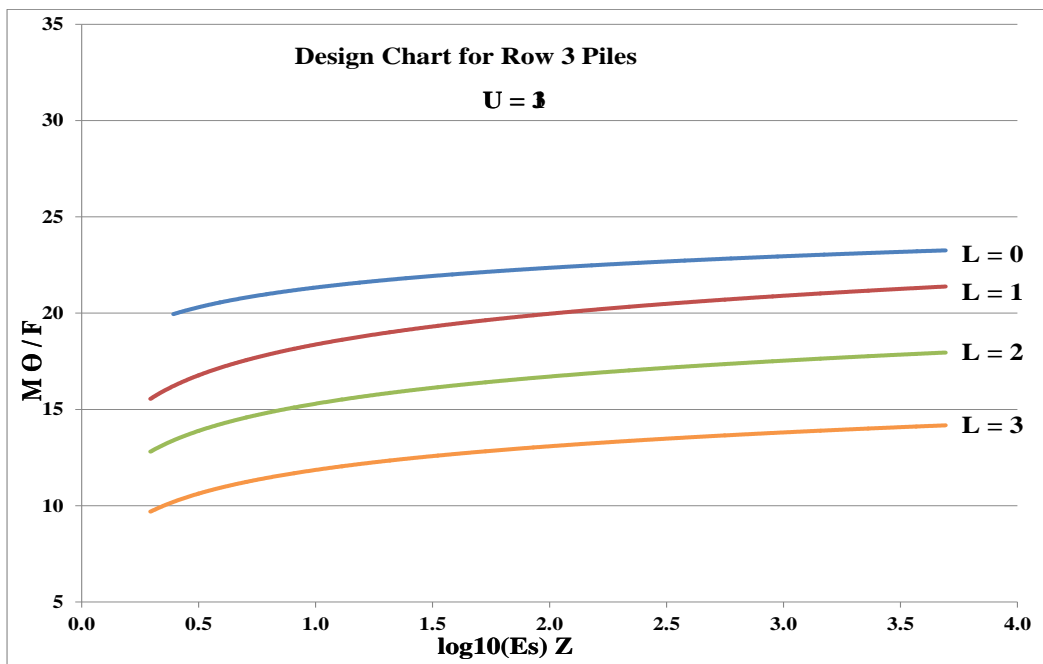
Design Chart A2



Design Chart A3



Design Chart A4



Sample Calculation:

Input Parameters:

$$E_s = 1000 \text{ kN/m}^2$$

$$D = 1 \text{ m}$$

$$F = 3000 \text{ kN}$$

$$U = 0 \text{ m}$$

$$L = 2 \text{ m}$$

Based on the above values,

$$Z = 0.098214$$

$$\Theta = 21.8^\circ$$

$$\log_{10}(E_s) = 3$$

Then the design chart selected is,

Design Chart A1

Intermediate Parameters calculated for the design chart is:

$$\text{Parameter on } x - \text{axis: } \log_{10}(E_s)Z = 0.295$$

Based on the parameter on x-axis, the parameter on y-axis is obtained as;

$$\text{Parameter on } y - \text{axis: } \frac{M\Theta}{F} = 16$$

Hence the bending moment acting on row 3 pile is,

$$M = \frac{16 \cdot 3000}{21.8} = 2201.835 \text{ kNm}$$

Considering the moment factor for each row, design bending moments are,

Sl. No.	Row No.	Distance from R3 x (m)	Moment Factor	Bending Moment (kNm)
1	R1	10	1.3522	2912.42
2	R2	5	1.0377	2235.03
3	R3	0	0.9782	2153.83
4	R4	-5	1.1737	2527.96
5	R5	-10	1.6242	3498.26

Comparing the calculated bending moments with the actual bending moments obtained from the numerical analysis;

Sl. No.	Row No.	Actual Bending Moment (Appendix-H) (kNm)	Calculated Bending Moment (kNm)	Percentage Variation (%)
1	R1	2987.06	2912.42	2.5
2	R2	2149.01	2235.03	4.0
3	R3	2104.62	2153.83	2.3
4	R4	2439.00	2527.96	3.6
5	R5	3337.21	3498.26	4.8

B. Design Charts for Depth of Fixity Based on the Numerical Analysis of Ship Berthing Structure

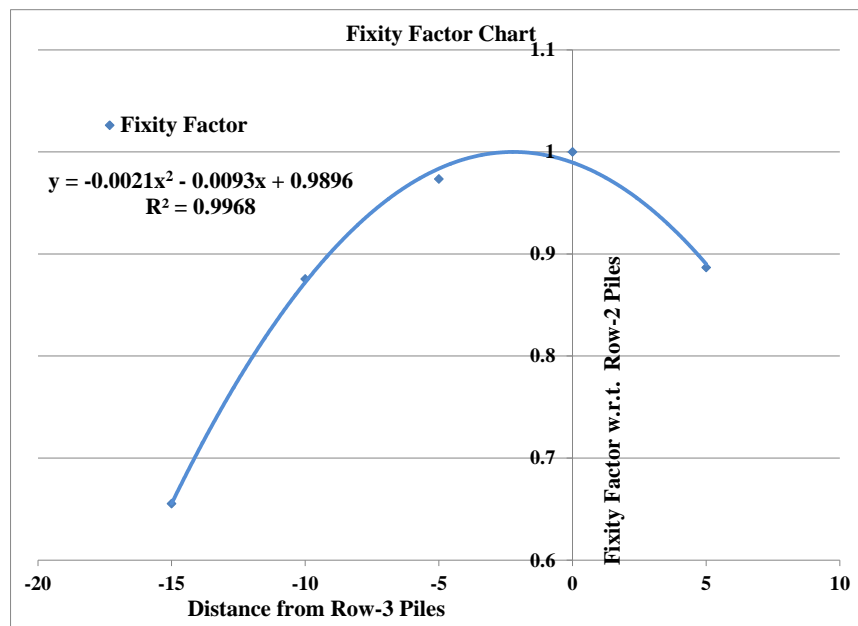
Numerical analysis of ship berthing structures are carried out as explained in Chapter 6. The values obtained in the parametric study are tabulated in Appendix-H and is used to develop design charts to calculate the depth of fixity acting on second row (R2) of pile.

A parabolic variation of depth of fixity is observed among the different rows of piles and row-2 piles are always at the vertex of the parabola with maximum valued of depth of fixity. Hence design charts are developed for row-2 pile and the value of depth of fixity thus obtained is multiplied with the fixity factor for each row to obtain the depth of fixity of that row.

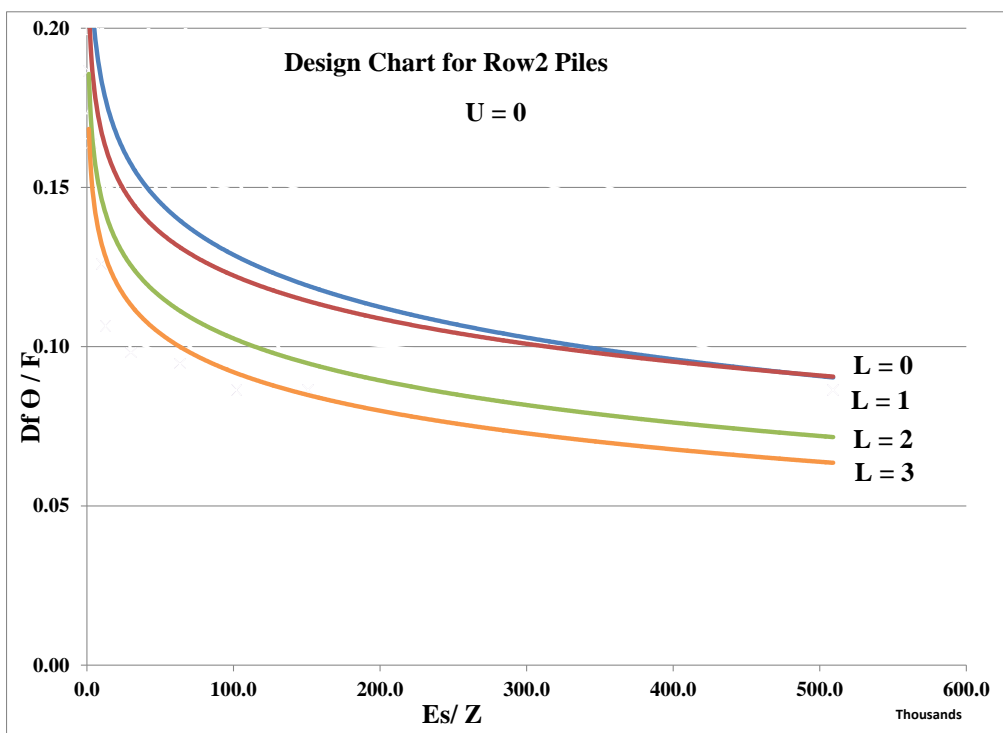
Fixity Factor for each Row

$$F.F. = -0.0021x^2 - 0.0093x + 0.9896$$

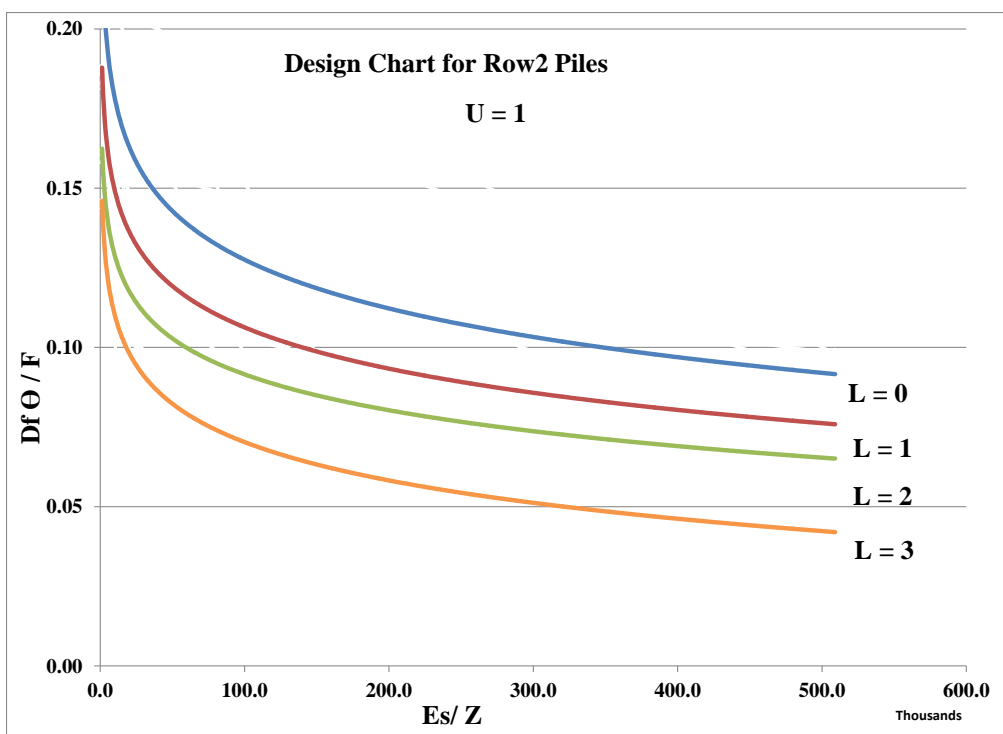
$$R^2 = 0.9968$$



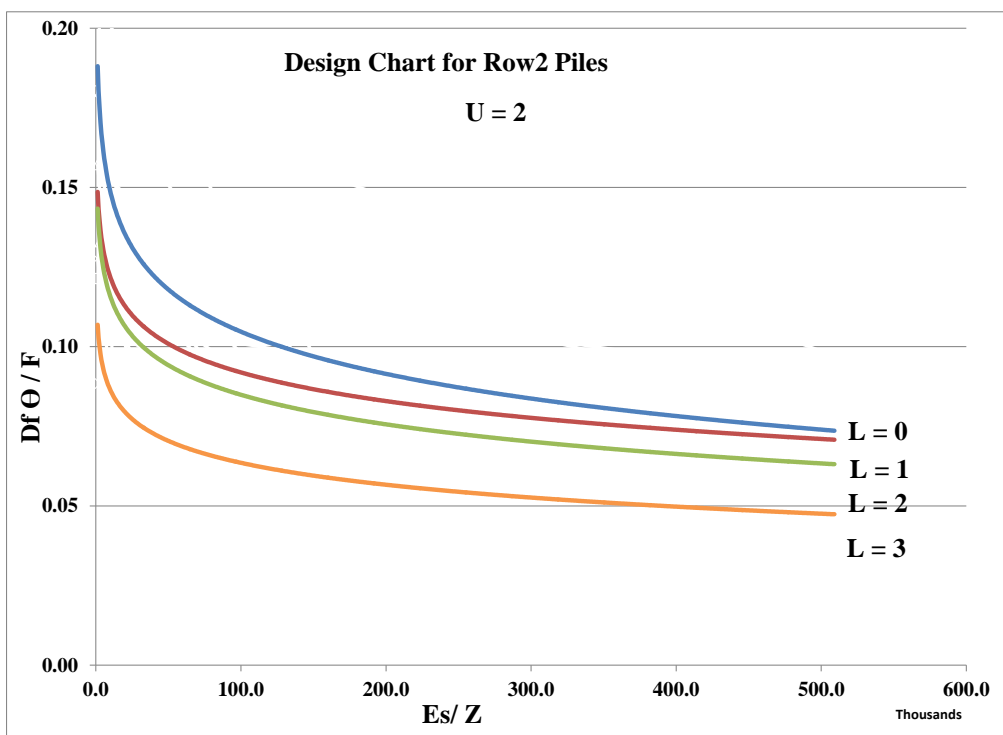
Design Chart B1



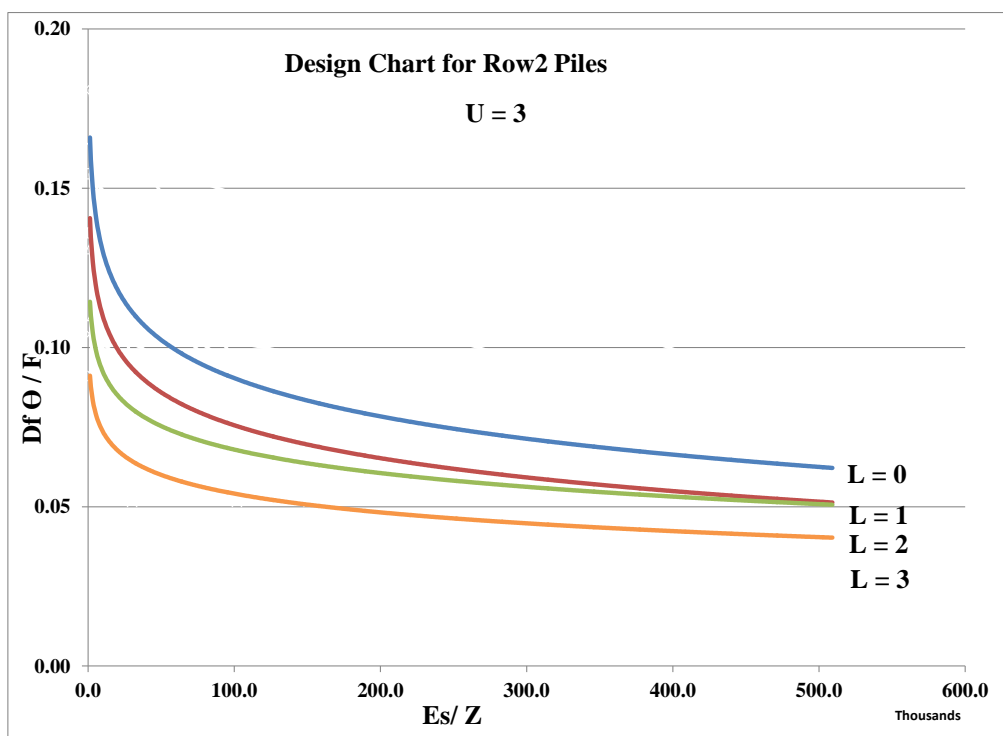
Design Chart B2



Design Chart B3



Design Chart B4



Sample Calculation:

Input Parameters:

$$E_s = 1000 \text{ kN/m}^2$$

$$D = 1 \text{ m}$$

$$F = 3000 \text{ kN}$$

$$U = 0 \text{ m}$$

$$L = 2 \text{ m}$$

Based on the above values,

$$Z = 0.098214$$

$$\Theta = 21.8^\circ$$

Then the design chart selected is,

Design Chart B1

Intermediate Parameters calculated for the design chart is:

$$\text{Parameter on } x - \text{axis: } \frac{(E_s)}{Z} = \frac{1000}{0.098214} = 10182$$

Based on the parameter on x-axis, the parameter on y-axis is obtained as;

$$\text{Parameter on } y - \text{axis: } \frac{M\theta}{F} = 0.16$$

Hence the bending moment acting on row 3 pile is,

$$Df = \frac{0.15 \cdot 3000}{21.8} = 20.64 \text{ m}$$

Considering the moment factor for each row, design bending moments are,

Sl. No.	Row No.	Distance from R3 x (m)	Fixity Factor	Depth of Fixity (m)
1	R1	5	0.8906	18.38198
2	R2	0	0.9896	20.42534
3	R3	-5	0.9836	20.3015
4	R4	-10	0.8726	18.01046
5	R5	-15	0.6566	13.55222

Comparing the calculated bending moments with the actual bending moments obtained from the numerical analysis;

Sl. No.	Row No.	Actual Bending Moment (Appendix-H) (kNm)	Calculated Bending Moment (kNm)	Percentage Variation (%)
1	R1	17.47	18.38	5.21
2	R2	19.80	20.43	3.17
3	R3	20.24	20.3	0.28
4	R4	17.32	18.01	3.98
5	R5	13.14	13.55	3.12

.....

Publications Related to the Work

- [1] Kavitha P. E., Narayanan K. P., Beena K. S., A Review of Soil Constitutive Models for Soil Structure Interaction Analysis, Proceedings of Indian Geotechnical Conference, CUSAT Kochi, Dec. 15-17, 2011.
- [2] Kavitha P. E., Beena K. S., Narayanan K. P., Structural Significance of Soil-Structure Interaction Analysis on Laterally Loaded Piles, Proceedings of National Conference on Innovations in Civil Engineering, Karukutty, 2012.
- [3] Kavitha P. E., Beena K. S., Narayanan K. P., Experimental Investigation of Laterally Loaded Pile in Sloping Ground Embedded in Clay, Proceedings of Indian Geotechnical Conference, IIT Delhi, Dec. 13-15, 2012.
- [4] Kavitha P. E., Beena K. S., Narayanan K. P., Analytical Study on Soil-Pile Interaction Effect in the Variation of Natural Frequency of a Single Pile, International Journal of Civil Engineering and Technology, Vol.5, Issue.12, pp 226-229.
- [5] Kavitha P. E., Beena K. S., Narayanan K. P., A review on soil–structure interaction analysis of laterally loaded piles, Innovative Infrastructure Solutions,1(1), 1-15, Springer, DOI: 10.1007/s41062-016-0015-x.
- [6] Kavitha P. E., Beena K. S., Narayanan K. P., Numerical Investigations on the Influence of Soil Structure Interaction in the Dynamic Response of SDOF System, Procedia Technology, Elsevier, Manuscript ID-RAEREST-CE-121. (accepted).
- [7] Beena K. S., Kavitha P.E., Narayanan K. P., Behaviour of Laterally Loaded Model Pile in Sloping Clay Bed, International Journal of Geomechanics, ASCE, Manuscript ID- GMENG-1682. (communicated).
- [8] Kavitha P. E., Beena K. S., Narayanan K. P., Influence of Soil Structure Interaction in the Structural Behaviour of a Berthing Structure in Sloping Ground, Journal of The Institution of Engineers (India): Series A, Springer, Manuscript ID –IEIA–D–16- 00134 (communicated).

Curriculum Vitae

Kavitha P. E.
60/1724
Purakat House
Kathrikadavu, Kaloor,
Kochi-682017
09446986225
pe_kavitha@yahoo.com



Personal Data

Date of Birth: 01 March 1978
Gender: Female
Religion and Caste: Christian Latin Catholic
Name of Husband: Dr. Shajan P.X.

Education

Sl. No.	Name of the Qualifying Examination	Institution/ University	Year of Passing	Aggregate Percentage of Marks
1	SSLC	Our Ladies Convent Girls High School, Thoppumpady	1993	90 %
2	Pre-Degree	St.Tresa's College, Ernakulam / M.G. University	1995	81 %
3	BTech.	Govt. Engg. College, Thrissur / Calicut University	1999	72.5 %
4	MCA	Indira Gandhi National Open University	2006	65 %
5	MTech.	Department of Ship Technology / Cochin University of Science and Technology	2007	7.95 CGPA

Employment History

Associate Professor (Non-Cadre)

*Sree Narayana Gurukulam College of Engineering, Kadayiruppu
(Joined as Lecturer on 30th October 2006 and continuing till date)*

Convener of National Conferences TRACE-2013 and TRACE-2014

Department Convener of International Conference ICETEM'2016

Published 12 papers in National and International Conferences and Journals.

Apprentice Trainee

*Cochin Port Trust, Willingdon Island
(Dec 1999 – Dec 2000)*

Worked as trainee at

BOT Bridge Construction Site at Thoppumpady

BTP Ship Berthing Structure Extension at Willingdon Island

An Office Building Site at Fire Station, Willingdon Island

Published Papers

- [1] Kavitha P.E., Narayanan K. P., Beena K. S., A Review of Soil Constitutive Models for Soil Structure Interaction Analysis, Proceedings of Indian Geotechnical Conference, CUSAT, Kochi, Dec. 15-17, 2011.
- [2] Kavitha P.E., Beena K. S., Narayanan K. P., Structural Significance of Soil-Structure Interaction Analysis on Laterally Loaded Piles, Proceedings of National Conference on Innovations in Civil Engineering, SCMS, Karukutty, 2012.
- [3] Kavitha P.E., Beena K. S., Narayanan K. P., Experimental Investigation of Laterally Loaded Pile in Sloping Ground Embedded in Clay, Proceedings of Indian Geotechnical Conference, IIT - Delhi, Dec. 13-15, 2012.
- [4] Kavitha P.E., Beena K. S., Narayanan K. P., Analytical Study on Soil-Pile Interaction Effect in the Variation of Natural Frequency of a Single Pile, International Journal of Civil Engineering and Technology, Vol.5, Issue.12, pp 226-229.
- [5] Kavitha P.E., Beena K. S., Narayanan K. P., A review on soil–structure interaction analysis of laterally loaded piles, Innovative Infrastructure Solutions,1(1), 1-15, Springer, DOI: 10.1007/s41062-016-0015-x.

Kavitha P. E.

